DENDRIMERS FOR IMAGING AND MOLECULAR SIEVING

BY

STUART ALEXANDER MCNELLES, B.Sc

A THESIS

SUBMITTED TO THE SCHOOL OF GRADUATE STUDIES

OF MCMASTER UNIVERSITY

IN PARTIAL FULFILMENT OF THE REQUIREMENTS

FOR THE DEGREE OF

DOCTOR OF PHILOSOPHY

IN CHEMISTRY

Doctor of Philosophy
(Chemistry)

McMaster University
Hamilton, Ontario, Canada

Title:	DENDRIMERS FOR IMAGING AND MOLECULAR SIEVING
Author:	STUART ALEXANDER MCNELLES, B.Sc. (University of Ontario Institute of Technology)
Supervisor:	Professor Alex Adronov
Number of Pages:	xviii, 247

Abstract

The Enhanced Permeability and Retention (EPR) effect has seen considerable exploration by many researchers since it's discovery by Maeda *et al* in 1985. Polymers and nanoparticles with a long blood residence half-life can accumulate in some tumour tissues, allowing for the delivery of either diagnostic or therapeutic payloads.

We have contributed to this field by the development of methodology to prepare radiolabeled dendrimers which are suitable for EPR effect accumulation with a variety of peripheral functionalities. The first of these was a ^{99m}Tc-labeled fifth generation dendron which was peripherally functionalized with low molecular weight poly(ethylene glycol) chains, which was observed to accumulate in xenograft mouse tumours over the course of 6 hours. This work led to the development of improved synthetic means for the preparation of high generation dendrimers with complex peripheral functionality, which hinged on the use of the Strain Promoted Alkyne-Azide Cycloaddition reaction to give high generation dendrimers by a convergent approach. This resulted in the facile preparation of dendrimers with challenging peripheral functionality in reaction times as short as 5 minutes. This SPAAC based convergent synthesis approach was used to prepare ^{99m}Tc labeled sulfobetaine and carboxybetaine dendrons of the sixth generation, and these compounds were found to have a size greater than the renal clearance threshold of ~ 5 nm, though it was found that labeling with $[^{99m}Tc(CO)_3]^+$ was not possible without extensive degradation of the zwitterionic dendrimers. Finally, the dendritic architecture explored for imaging was adapted for use in shielding an enzyme from macromolecules while retaining activity against the native small molecule substrate, and we found that conjugation of high-

generation bis-MPA dendrons to α-chymotrypsin was an effective way to eliminate enzyme activity against macromolecules while preserving efficacy against small substrates, indicating this approach may be an effective way to shield proteins from the immune system without interfering with their desired function.

This work illustrates the ability to radiolabel polyester dendrimers for tumour imaging through the EPR effect. In addition, it has demonstrated that polymer architecture has a large impact on the properties of polymer-protein conjugates and gives evidence of unique properties that are imparted by the conjugation of high-generation dendrimers onto a protein.

Acknowledgements

Over the past six years, numerous people have had a profound impact on my Ph.D. First among them is without a doubt my supervisor, Professor Alex Adronov. His limitless advice, support, and mentorship has had a profound effect on the scientist that I have become, and for that I will always be grateful.

I would also like to thank my committee members, Professor John Valliant and Professor Harald Stöver for their interest and assistance throughout my time at McMaster. From using lab space, getting advice, or even just talking science with you, I have learned a great deal from both of you.

Along the way, I have also had the opportunity to collaborate with a number of people, including Sabrina Hodgson, Darryl Fong, Kelvin Li, Samantha Ros, Victoria Marando, Julia Pantaleo, and Giancarlo Da-Re. I have learned a great deal from all of you, and I have been fortunate for the opportunity to work alongside you. I would also like to thank the members of the Valliant group past and present who have helped me with radiochemistry, particularly Aimen Zlitni and Reza Yazdani who taught me how to work with ^{99m}Tc.

I would also like to thank the members of the Adronov group for their friendship and camaraderie over the years, without which this PhD would have certainly been an unbearable slog. I want to especially thank Ryan, Nicole, Sabrina, Vlad, Darryl, Jimbo, Kelvin, and Victoria for advice, conversations, and listening to my rambling stories. I had

always heard stories from my father about how the friendships he made in graduate school were some of the most valuable and enduring, and now I understand why.

To my parents who have supported me and encouraged me throughout my life, I could never thank you enough. Dad, you inspired me to be inquisitive about the world and see the joy of figuring things out. Mom, you have always been supportive and understanding throughout all these years and helped me in every way you could. Thank you both.

Lastly, I would like to thank Anam. I'll never be able to tell you how much you have meant to me for all these years. You are an incessant source of joy, love, and support throughout our time together. You take care of me during the lows and make the highs higher than I ever could have imagined. I still don't understand how a person can make me as happy as you do, but I am extremely grateful for it. I look forward to everything to come as long as you are with me Little Bear.

List of Abbreviations

ALL	Acute Lymphoblastic Leukemia
α-CT	α-Chymotrypsin
ATRP	Atom Transfer Radical Polymerization
AU	Absorbance Units
Bis-MPA	2,2-bis(hydroxymethyl)propionic acid
Boc	*tert*-Butyloxycarbamate
BSA	Bovine Seum Albumin
Cbz	Carboxybenzyl carbamate
CDI	N,N'-carbonyldiimidazole
CRP	Controlled Radical Polymerization
CT	Computed Tomography
DBCO	Dibenzoazacyclooctyne
DBU	1,8-Diazabicyclo[5.4.0]undec-7-ene
DCM	Dichloromethane
DIBAC	Dibenzoazacyclooctyne
DLS	Dynamic Light Scattering
DMEM	Dulbecco's Minimum Essential Media
DMF	Dimethylformamide
DMSO	Dimethylsulfoxide
DNA	Deoxyribonucleic acid
DPA	Dipicolylamine
DRIFTS	Diffuse Reflectance Infrared Fourier Transfer Spectroscopy
EDC-HCl	1-Ethyl-3-(3-dimethylaminopropyl)carbodiimide
EPR	Enhanced Permeability and Retention Effect
ESI-MS	Electrospray Ionization Mass Spectrometry
EtOAc	Ethyl Acetate
FBS	Fetal Bovine Serum
FDA	Food and Drug Administration

FPE	Fluoride Promoted Esterification
FPLC	Fast Protein Liquid Chromatography
FTIR	Fourier Transform Infrared Spectroscopy
G-CSF	Granulocyte Colony Stimulating Factor
HPLC	High Pressure Liquid Chromatograohy
HPMA	Hydroxypropyl Methacrylamide
ID/g	Injected Dose per Gram
MALDI-MS	Matrix Assisted Laser Desorption Ionization Mass Spectrometry
Matrigel-DPBS	Matrigel Dulbecco's Phosphate Buffered Saline
M_n	Number Average Molecular Weight
mPEG	Polyethylene Glycol Monomethyl Ether
MRI	Magnetic Resonance Imaging
M_w	Weight Average Molecular Weight
MWCO	Molecular Weight Cutoff
NHS	*N*-hydroxysuccinimide
NMR	Nuclear Magnetic Resonance Spectroscopy
PAMAM	Poly(amidoamine)
pCB	Poly(carboxybetaine)
PDA	Photodiode Array Detector
PEG	Polyethylene Glycol
PEOZ	Poly(2-ethyl-2-oxazoline)
PET	Positron Emission Tomography
POEGMA	Poly(oligoethyleneglycol) methacrylate
POZ	Polyoxazoline
PPI	Poly(propylene imine)
pSB	Poly(sulfobetaine)
*p*TSe	*para*-Toluene Sulfonyl Ethanol
PVP	Poly(vinyl pyrrolidone)
PyBOP	benzotriazol-1-yl-oxytripyrrolidinophosphonium

RAFT	Reversible Addition Fragmentation Chain Transfer
SEC	Size Exclusion Chromatography
SPAAC	Strain Promoted Azide-Alkyne Cycloaddition
SPECT	Single Photon Emission Computed Tomography
SPF	Specific Pathogen Free
TCO	*Trans*-Cyclooctene
TEG	Triethylene Glycol
TFA	Trifluoroacetic Acid
THF	Tetrahydrofuran
TLC	Thin Layer Chromatography
UV	Ultraviolet

List of Tables

List of Figures

List of Schemes

Contents

1 Introduction

1.1 Introduction to polymer architectures

Polymer chemistry as a discipline is dedicated to advancing the synthesis, characterization and understanding of polymers and macromolecules. Polymers are macromolecules that are formed by the linking of many smaller subunits known as monomers. Due to the vast array of available monomers, there is enormous variety in the structure and function of their resulting polymers. The composition of the polymer in terms of its constituent monomers plays a major role in determining its resulting properties. Polymerization of simple olefins transforms gaseous starting materials into convenient structural plastics for consumer applications. The polymerization of dicarboxylic acids can result in polyesters or polyamides, which are used for wide ranging applications from consumer plastics, fabrics, and high-performance engineering grade materials. Apart from synthetic macromolecules, nature makes extraordinary use of polymers with a wide array of functions such as energy storage, structural reinforcement, and the encoding of genetic information. It is precisely this diversity in function and properties that makes polymer chemistry such a compelling and impactful field of research.

One common challenge polymers face in specialized applications is their dispersity of molecular weights. As a consequence of their synthetic preparation, most polymers have a broad range of chains with different molecular weights. Molecular weight can have a profound impact on the properties of a polymer for a given application (strength, glass

transition temperature, viscosity), and thus the careful control of this molecular weight is of great interest to polymer chemists. While numerous molecular weight averages have been described, the number average molecular weight (M_n) and weight averaged molecular weight (M_w) are the most commonly used, and these are defined in Equation 1 and 2 below.

$$M_n = \frac{\sum M_i N_i}{\sum N_i} \tag{1}$$

$$M_w = \frac{\sum M_i^2 N_i}{\sum M_i N_i} \tag{2}$$

M_n can be simply calculated by measuring and summing the molecular weight of all the chains in a sample and dividing this by the number of chains. M_w is calculated by summing weight fractions, but due to the squaring of the molecular weight term, higher molecular weight components in a sample have a much larger impact on the molecular weight than they do for M_n. The determination of M_w is often important for predicting the properties of a polymer, as having a small fraction of high molecular weight components in a polymer sample can have substantial effects on the bulk properties. The ratio of these two molecular weights (M_w/M_n) is referred to as dispersity, denoted with the symbol Đ. Typically, dispersity ranges from 1 (for uniform molecular weight compounds such as proteins) to 3 (for uncontrolled polymerization), though this is by no means an upper bound.

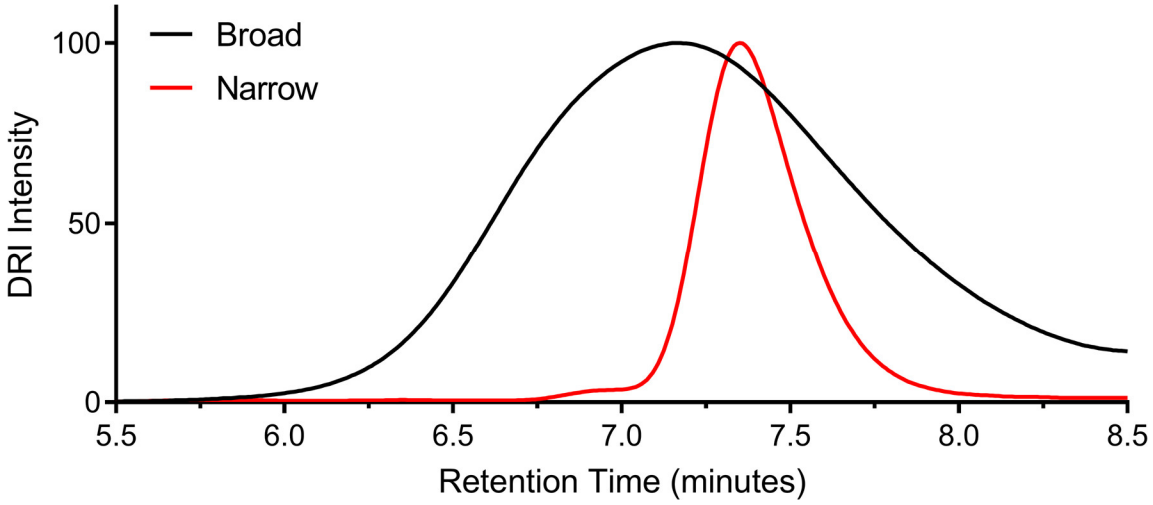

Figure 1.1. Narrow vs. Broad dispersity polymers by Gel Permeation Chromatography. Dispersity of the broad and narrow polymer are 2 and 1.02, respectively

A second critical aspect of polymer chemistry lays in the control of polymer architecture. Numerous examples of distinct polymer architectures exist, which include but are not limited to linear, cyclic, branched, hyperbranched, graft, block, star, and dendritic polymers (Figure 1.2). In each case, the function and properties of otherwise similar polymers can be substantially different because of the overall structural architecture. This thesis will focus on the dendritic architecture that offers unique properties which will be described in the following section.

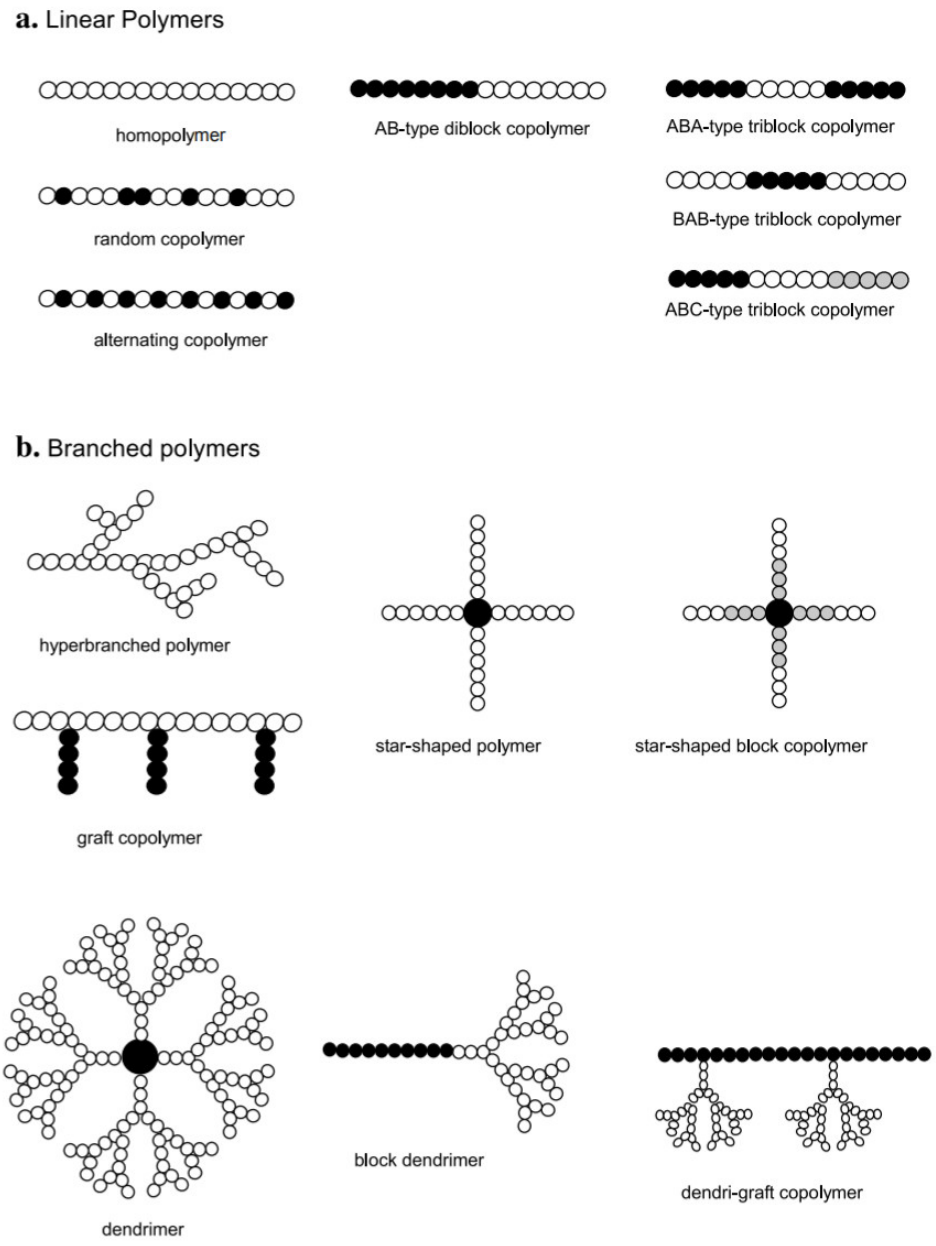

Figure 1.2. Depiction of different polymer architectures and their different connectivity. Reproduced with permission.[1] Copyright (2006) Springer Science + Business Media, Inc.

1.2 Dendrimer structure

Dendrimers are a polymer architecture which are at the extreme of branching as well as dispersity control. Both factors are key to the unique properties of the dendritic architecture. The dendritic architecture has three key features: a central core or focal point, the “backbone” or interior of the dendron that is composed of branching units making up each successive generation, and the periphery, as seen in (Figure 1.3).

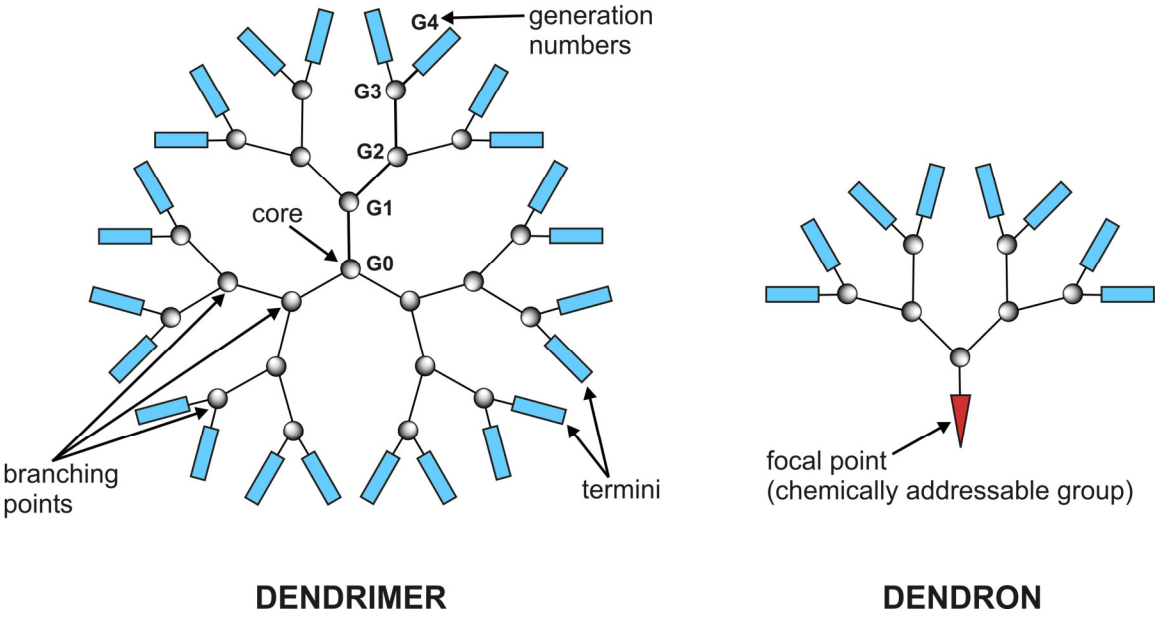

Figure 1.3. Diagram of dendrimer structures, illustrating the core, generations, and peripheral groups

The backbone of the dendrimer contains the monomer repeat units, which branch out from the central core. Each successive layer of these monomers is referred to as a “generation”. Dendrimers are often referred to based on their generation number as this is a major factor in the overall size of the dendrimer. For dendrimers with two branches per monomer, the molecular weight of a dendrimer doubles at each generation. This results in the properties

of the dendrimer being dominated by the functional groups at the periphery, since they are most accessible to the surrounding environment and constitute nearly half the overall mass of a dendrimer. Because the properties of dendrimers are dominated by these three structural features, dendrimers are often referred to with descriptors based on these three parameters. For example, a third generation dendron with a benzyl ester as the core and alcohols at the periphery would be described as "BnO-G3-(OH)", and this nomenclature will be used extensively throughout this thesis. The core of dendrimers can contain additional reactive functionality, in which these specific molecules would be termed "dendrons".

1.3 History of dendrimer development

While linear and branched polymers have been synthesized since the early 20th century, it was not until 1978 that Vögtle and co-workers developed the first synthesis of "cascade molecules", which would prove to be the first report of a dendrimer synthesis.[2] Their synthesis began with an amine core, with dendrimer growth consisting of Michael-type additions of acrylonitrile to the amine, followed by the reduction of the resulting nitrile with sodium borohydride using a cobalt catalyst, which results in a doubling of the number of amine groups per generation. This methodology suffered from poor yields and an inability to reach high molecular weights (these "cascade" molecules were not reported to be in excess of 1000 Da). Subsequently, Tomalia and co-workers at Dow Chemical developed "Starburst" polymers, and in their seminal paper coined the term "dendrimer".[3] Their work entailed the preparation of what are now commonly known as poly

amidoamine (PAMAM) dendrimers, which were prepared in a similar divergent manner as the Vögtle cascade dendrimers, though the Michael acceptor had been changed from acrylonitrile to ethyl acrylate. The resulting ethyl ester periphery dendrons can be trans-amidated using an excess of diamine such as ethylenediamine. Using this methodology, PAMAM dendrimers of high molecular weight can be prepared, though side reactions such as intramolecular cyclization and dendrimer-dendrimer coupling introduce some dispersity to the resulting polymers. The success of this method has resulted in PAMAM dendrimers being extremely popular for a wide variety of research activities, as well as the commercial availability of many generations and derivatives. Following Tomalia's work, Newkome and co-workers prepared what they referred to as "arborols" using an approach where a triol was activated by tosylation, and then extended by the addition of triethyl methanetricarboxylate and base. The resulting esters were then reduced using $LiAlH_4$ to give alcohols at the periphery, or the growth can be continued by amidation with tris(hydroxymethyl)aminomethane to give a final dendrimer with 27 hydroxyl groups at the periphery.[4]

The most recent major dendrimer architecture is that based on 2,2-bis(hydroxymethyl)propionic acid (bis-MPA). Initially developed by Ihre, Hult, and Soderlind[5] in 1995 and later improved by Fréchet and co-workers[6–8], these dendrimers are typically prepared using an acetal protecting group on the diol (such as benzylidene or acetonide), and grown using either a convergent[5,7] or divergent[9] methodology. These dendrimers are of particular interest for biological applications, as they exhibit low toxicity[10], are biodegradable[11,12], water soluble[13] and can be functionalized using a

variety of methods. For these reasons, this thesis has focused entirely on dendrimers based on this architecture.

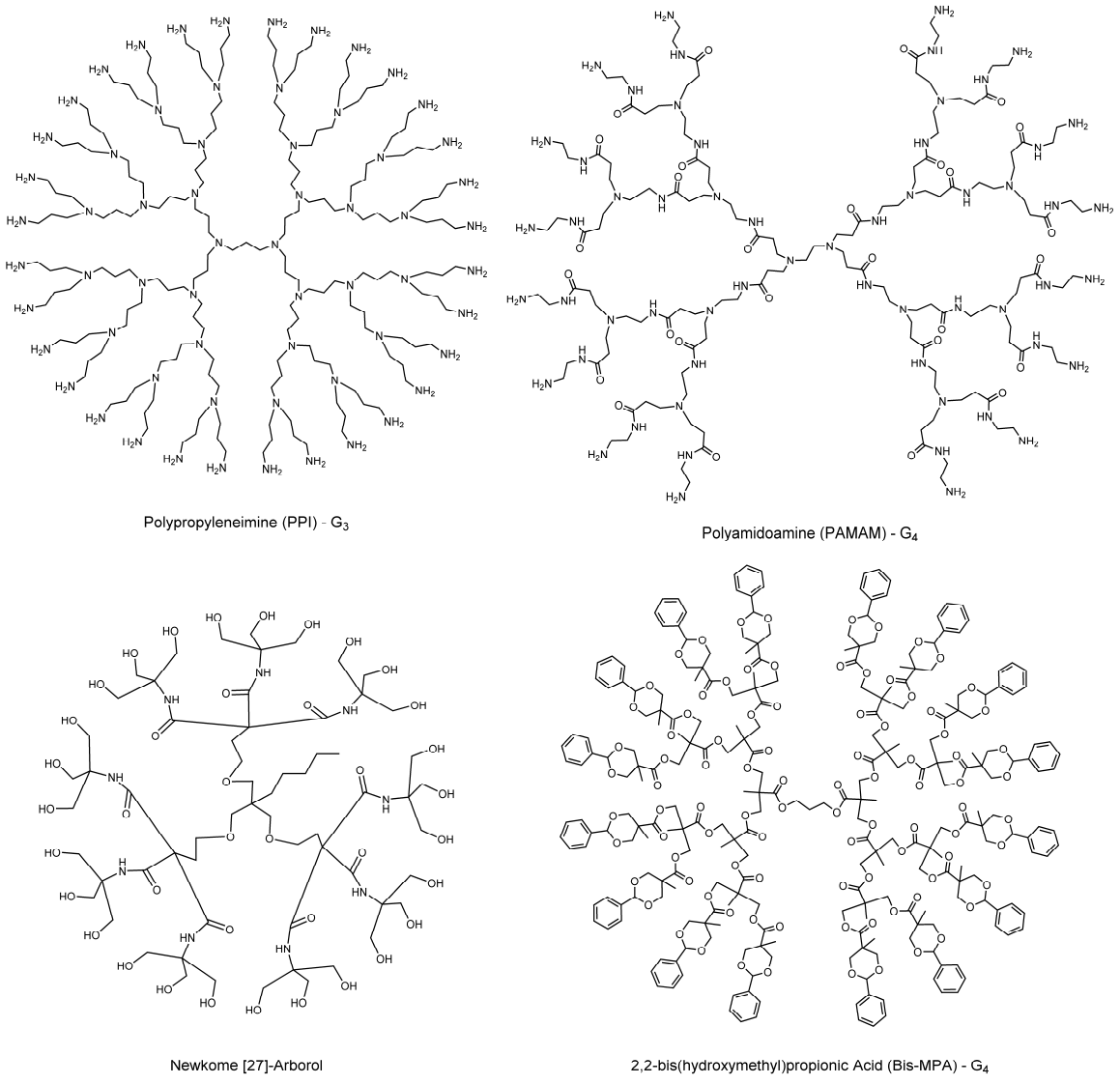

Figure 1.4. Common Dendrimer Structures

1.4 Dendrimer Synthesis

There are two general methods that are employed for the preparation of dendrimers: divergent and convergent. The divergent methodology was the first to be developed, as exemplified in the work of Vögtle, Tomalia, and Newkome discussed in the previous section and illustrated in the top portion of Figure 1.5.

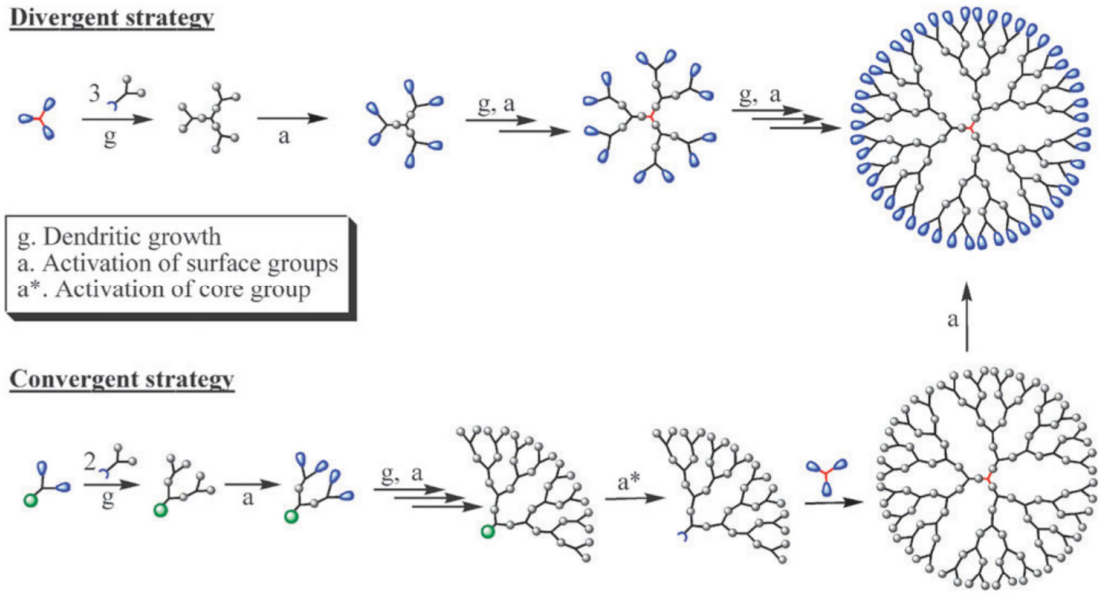

Figure 1.5. Schematic of Divergent vs. Convergent Dendrimer Synthesis. Reproduced with permission.[14] Copyright Royal Society of Chemistry (2009)

The divergent methodology starts at the core and branches out, with each successive generation being added via the addition of small molecule monomers at the periphery. This approach has the benefit of increasing the total mass of dendrimer considerably at each generation and requiring only an excess of the (comparatively) inexpensive small molecule monomer. To prevent uncontrolled polymerization of the monomers, the branching groups on the monomer must be shielded from reaction during the growth step. This is typically

accomplished by using protecting groups, or through using a scheme which uses orthogonal reactivity for each generation. One key drawback of divergent syntheses is that they require addition reactions that proceed to very high conversion, as partially functionalized material is often inseparable from fully converted dendron, particularly at high generations. Even a reaction that goes to 99% conversion is unacceptable for divergent synthesis at high generations where there are on average more than 100 peripheral functional groups.

The convergent approach developed by Hawker and Fréchet in 1990[15] is an elegant method to circumvent the need to reach very high conversions. In the convergent methodology, dendrimers are grown from the periphery towards the core. The outer dendrons are reacted at their core with a suitable monomer to couple two or more macromonomers together, and this process is repeated to prepare high generation dendrimers. Since only a small number of groups (typically two) are being attached to a core monomer in each step, any incompletely converted material is chemically very distinct from the fully functionalized material, and as such can be purified using standard organic chemistry techniques. However, this methodology suffers from poor yields at moderate to high generations owing to the steric crowding and increasing site-isolation of the core, as well as a decrease in dendrimer mass at each step. These factors have led to most dendrimers produced today to be produced using a divergent approach, as is the case in this thesis.

1.5 Dendrimer Properties

While most polymers are prepared by either chain growth or step growth polymerizations which result in a range of molecular weights due to the statistical nature of the addition of monomers, dendrimers are typically prepared by stepwise methodologies that were previously reserved for use on small molecules in synthetic organic chemistry. As a result of this, dendrimers can be produced as perfect, uniform molecular weight polymers (Figure 1.6).

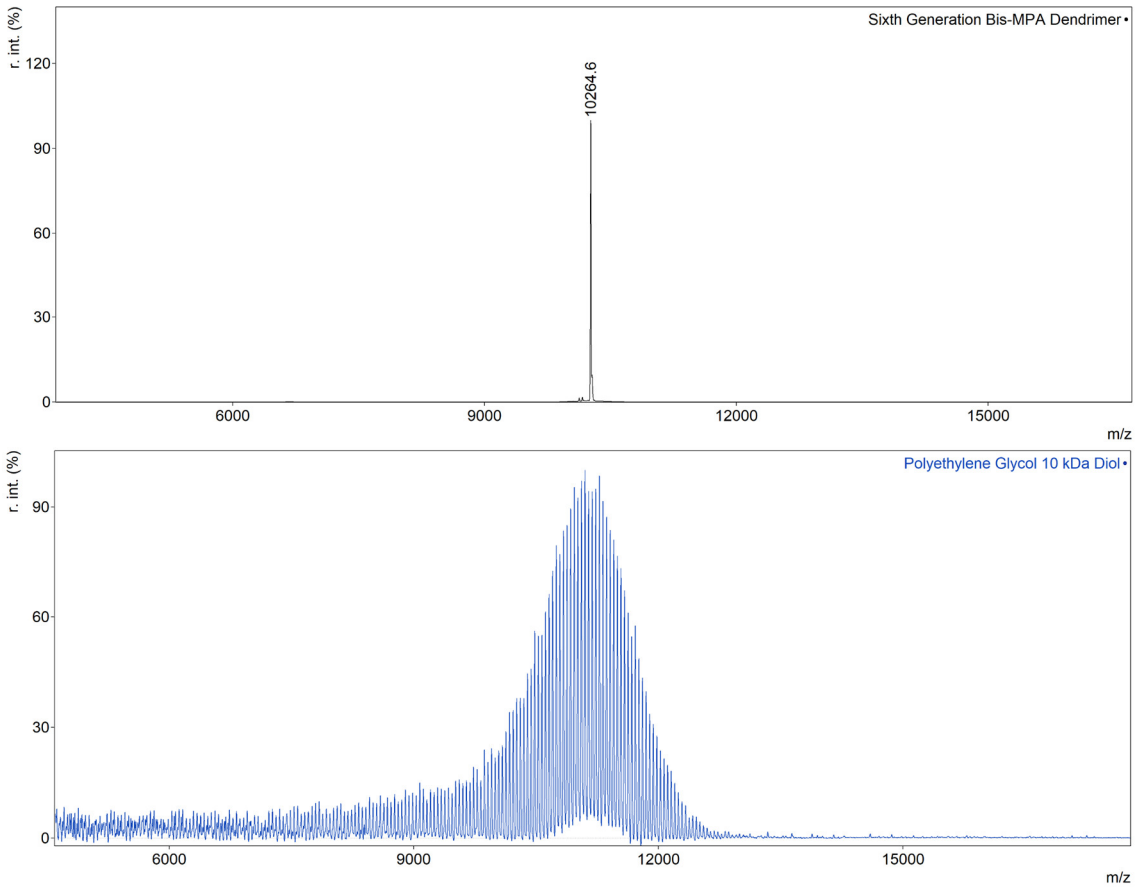

Figure 1.6. Molecular weight distribution of low-dispersity poly(ethylene glycol) vs. a dendrimer of similar nominal molecular weight.

This precise control over molecular weight allows for the synthesis of polymers in which every molecule has identical properties, which is believed to be important in the development of polymers for biological applications.[16,17] For many years, dendrimers were the only synthetic polymers with precisely defined molecular weights, though recently uniform molecular weight oligomers have been prepared by Hawker and co-workers via a post-polymerization purification approach.[18,19] Higher molecular weight linear polymers with a uniform molecular weight have also been prepared by iterative exponential growth methodologies using end groups with either protected or orthogonal reactivity[20–22], in a manner which is conceptually similar to convergent dendrimer synthesis, which has enabled access to linear polymers up to approximately 40 kDa.[23]

Due to their extremely branched architecture, dendrimers and other hyperbranched polymers exhibit physical and chemical properties that differ substantially from their corresponding linear counterparts. Fréchet and co-workers have extensively investigated the effect of polymer architecture on intrinsic viscosity,[24] solvodynamic diameter,[25] glass transition temperature,[26] among other properties. Hawker and co-workers have also elegantly prepared poly(aryl ether) dendritic and linear polymers of identical chemical composition[25,27] in order to more precisely investigate the effect of the globular morphology of dendrimers. As anticipated, they found that the dendritic polymers had a lower hydrodynamic diameter for the same molecular weight, as well as much lower crystallinity. The difference between the linear and dendritic polymer architectures was further increased with increasing generation, which is evidence that these changes are due to the globular nature of the dendrons, particularly as they cross their "dendrimer

transition" from disordered small molecules to globular morphologies. Discontinuities in dendrimer properties as a function of generation have been observed by a variety of methods in many dendrimer architectures, which supports the hypothesis that there is a conformational change at a critical generation.[28–30] The effect of the dendritic architecture has significant implications for their utility in biomedical applications, particularly in renal filtration rates. Rippe and Venturoli demonstrated that globular proteins have a substantially smaller equivalent small pore radius when compared to branched and linear polysaccharides such as ficoll and dextran, which they attributed to the more compact geometry as well as the inability of the already compact proteins to be further compressed under flow.[31] Gillies and Fréchet observed significantly increased circulation times for branched PEGylated bow-tie dendrimers vs. linear PEG counterparts of similar nominal molecular weight.[32] These results are explained by the relative rates of glomerular filtration in the kidney, compact globular polymers cannot adopt elongated conformations which would allow for their rapid filtration, resulting in great increases in circulation time. Indeed, highly branched PEGylated dendrimers with a molecular weight of ~20 kDa exhibit extended circulation, even though linear PEG counterparts require molecular weights in excess of 50 kDa.

1.6 Click Chemistry for Dendrimers

In a seminal paper in 2001, Sharpless and co-workers laid out the requirements of reactions they coined "click reactions".[33] To be considered "click", a reaction should satisfy the following criteria: they should be modular, wide in scope, give high yields, and generate

benign byproducts that can be purified non-chromatographically (or no byproducts at all). A number of click reactions are in common use, with the most prominent seen in Figure 1.7

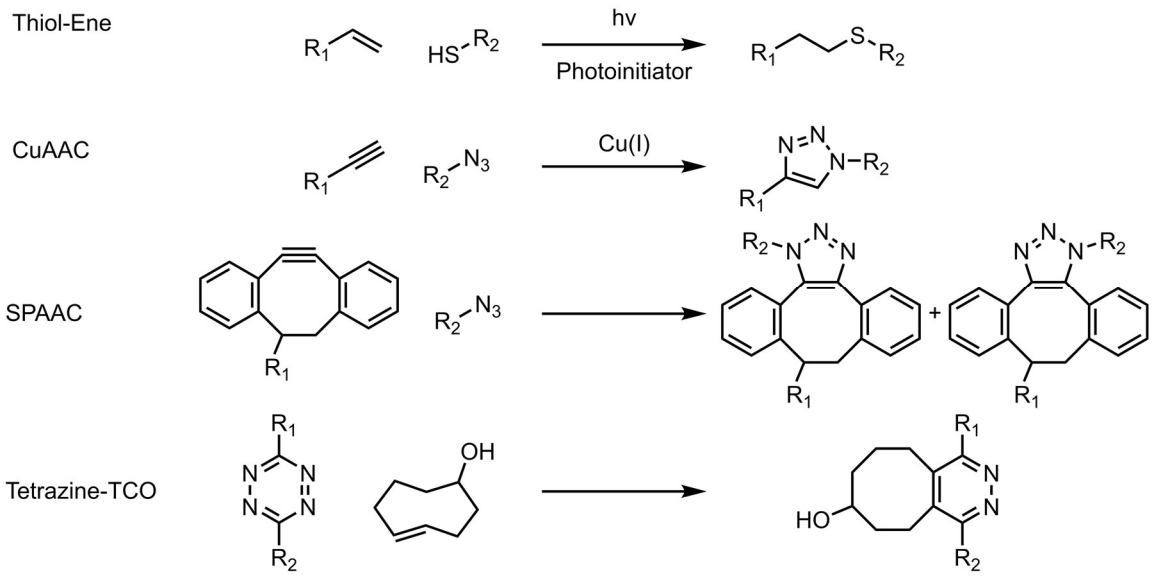

Figure 1.7. Examples of commonly used click reactions

These reactions have seen extensive use in a variety of fields, and polymer chemistry is no exception. Using a small arsenal of functional groups for click chemistry, a tremendous variety of polymers and distinct polymer architectures can be prepared, particularly in cases such as graft polymers where traditional methodologies for preparation are challenging and must be developed for each polymer.

Click chemistry is an attractive strategy for the functionalization of dendrimers, as quantitative functionalization of dendrimers is a classic challenge in dendrimer chemistry. The first examples of dendrimers prepared from click chemistry came not long after the original report of the Cu(I) catalyzed 1,3-dipolar cycloaddition.[34] The authors were able

to prepare dendrimers with a molecular weight of over 6 kDa using this approach, and it paved the way for other dendrimer syntheses which use this chemistry.[35,36] The modularity of click chemistry also allows for the preparation of libraries of related dendrimers, which was previously very challenging due to the need to optimize specific chemistry for each dendrimer architecture.[37] Orthogonal click reactions have been used to rapidly construct dendrimers, as Malkoch and co-workers performed with CuAAC and thiol-ene chemistry, in which the authors were able to prepare sixth generation dendrimers in under 24 hours, overcoming the inherent slow pace of preparation that is a constant challenge for the preparation of dendrimers.[38] Click chemistry has also been important in the peripheral functionalization of existing dendrimer architectures,[39,40] particularly those based on bis-MPA, since their hydroxyl peripheries are less reactive than the amines on PPI or PAMAM dendrimers.

1.7 Dendrimers for biological applications

Because of the unique properties of dendrimers discussed in the preceding sections, dendrimers have been extensively investigated in biological applications.[16,41,42] There are several criteria required of dendritic architectures to be valuable for biological applications: they must be water soluble, have low toxicity, be non-immunogenic, be able to penetrate to their target site, and have a long circulation time.[43] By far the most commonly used dendrimer architecture investigated for biological use is PAMAM, as these have been commercially available for many years (since 1992). PAMAM dendrimers have been used in the preparation of imaging agents[44–46] , as delivery agents for siRNA,[47–51] DNA,[52,53]

as well as being used for their own intrinsic therapeutic effect.[54] However, PAMAM dendrimers exhibit significant cytotoxicity[47,55–59], which is believed to be due to the high positive charge of their periphery at physiologic pH.[55,60] This can be ameliorated to some degree by functionalization of the terminal amines with the desired group and then capping the residual groups with acetyl or PEG groups, but this typically does not fully resolve the toxicity issue. PAMAM dendrimers also suffer from poor degradability *in vivo*,[61] which may lead to issues with bioaccumulation and elimination from the body.[62]

As alternatives to PAMAM, several other dendrimer alternatives have been used in biological applications, such as PPI[63,64] and poly(lysine).[65,66] The most recent dendrimer architectures to be used for biological applications are those based on 2,2-bis(hydroxymethyl)propionic acid (bis-MPA). These were originally developed by Ihre and coworkers[5,7,9] and have been extensively studied for biological applications, particularly by Fréchet and Szoka. Bis-MPA dendrimers and dendrons can be prepared by either a divergent or convergent methodology to high generations (at least G8[67]) and are attractive for biological use for a number of reasons. These dendrimers are water soluble,[10,68] biodegradable,[69] and exhibit low toxicity *in vivo*.[10] As such, bis-MPA dendrimers have been used for a variety of applications, such as drug carriers,[70] and as imaging agents.[67] Bis-MPA dendrimers, particularly when conjugated with polyethylene glycol chains at their periphery, can have sizes that are above the renal clearance threshold of ~ 5 nm,[71] which results in dramatically increased circulation time in blood. [32] This last point is critical for bis-MPA dendrimers used for passive tumor targeting.

1.8 Passive tumour targeting via the EPR effect

The passive accumulation of macromolecules in tumours was originally discovered by Kobayashi and Maeda, and this phenomenon is now referred to as the Enhanced Permeability and Retention (EPR) effect.[72] While the EPR effect allows for a modest accumulation of macromolecule at the tumour site (ca. 5% injected dose per gram),[73] this can be sufficient to deliver significant therapeutic benefit. Gillies and co-workers used the EPR targeting scheme with PEGylated bow-tie bis-MPA dendrimers conjugated with doxorubicin, which was able to dramatically reduce mortality in a cancer mouse model.[70] In some cases, this 5% ID/g enhanced accumulation is substantially greater than through other routes of administration. [74]

The origin of the EPR effect is from the high vascular permeability of some tumor blood vessels.[75] Macromolecules can diffuse between endothelial cells of these tumour blood vessels and accumulate in the tumor, since the lymphatic drainage of these tumours is poor and incapable of clearing macromolecules efficiently. The combination of diffusion into the tumours and inability of these materials to drain results in accumulation in the tumor tissue.

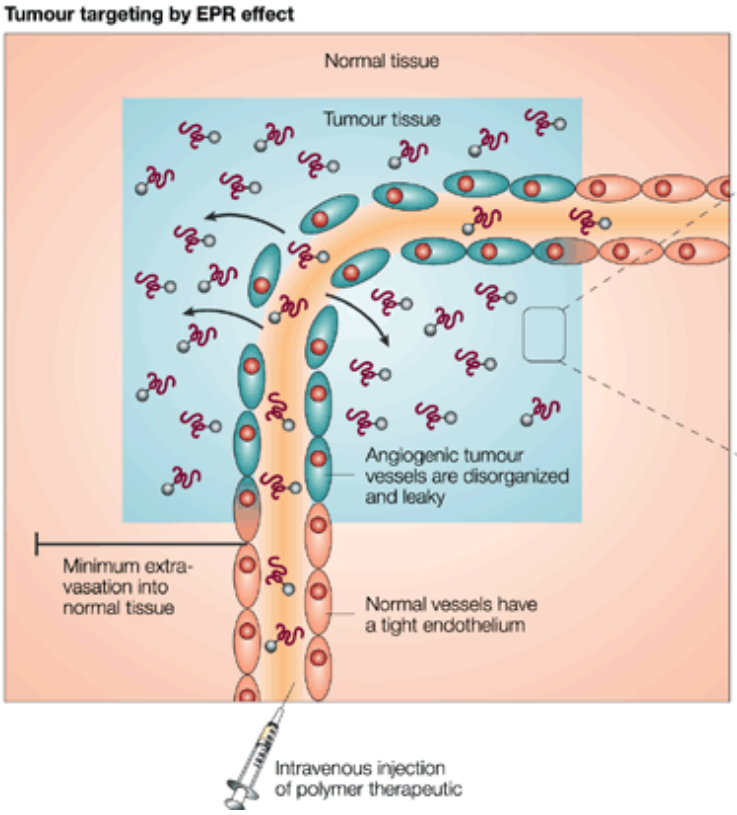

Figure 1.8. Illustration of the physiological basis for the EPR effect. Reproduced with permission.[75] Reproduced with permission. Copyright Springer Nature Publishing (2003)

In order to prepare dendrimers, or truly any macromolecule that can target via the EPR effect, several key criteria must be met. The molecule (or particle) must have a near zero zeta potential, have a hydrodynamic diameter above the renal clearance threshold of ~5 nm, be water soluble and have low protein binding. These criteria are in essence the same as those required for an extended circulation time, and indeed this is the root cause for their necessity for EPR effect targeting. Typically, it takes at least 4-6 hours to see significant accumulation at a tumor site via EPR accumulation.[73] Particles with substantial surface charge (i.e. zeta potential far from 0 mV, either positive or negative) typically results in

accumulation in either the kidney or liver, while neutrally charged particles remain in the blood pool as seen in Figure 1.9.

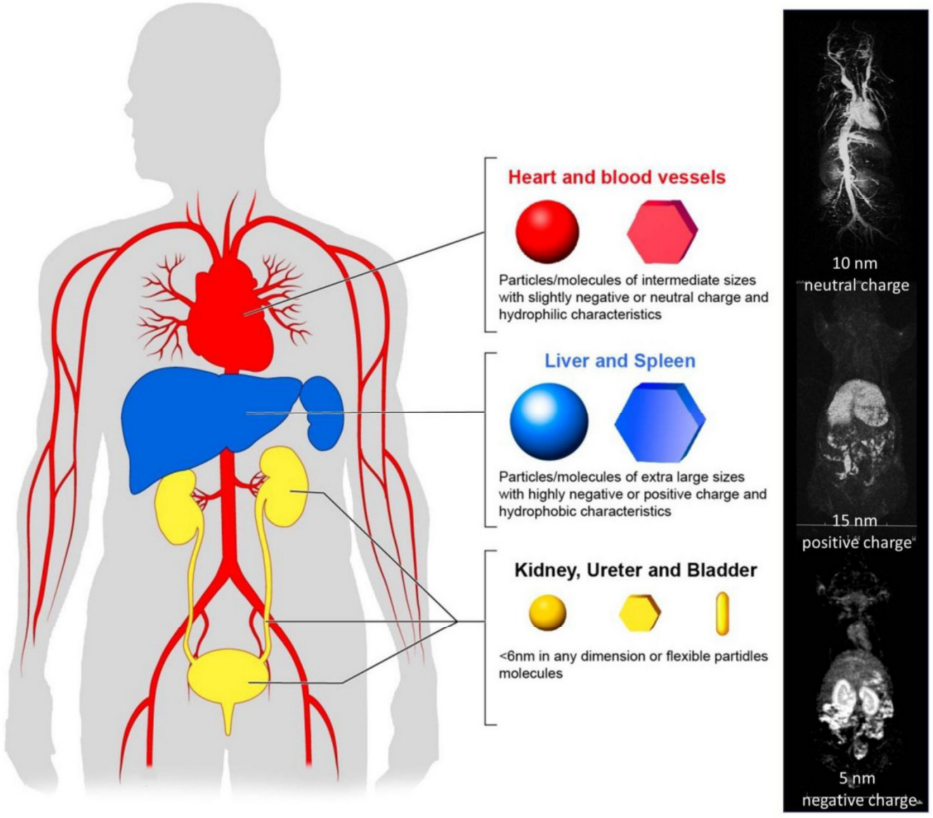

Fig 2. Pharmacokinetics of nano-sized agents. Nano-sized agents, which are favorable for operating EPR effects, should stay in the blood pool for long time.

Figure 1.9. Particle size and charge required for long blood circulation. Kobayashi et al, *Theranostics*, 2014, 81-89

Molecular shape also has dramatic effects on EPR effect targeting, particularly as it relates to circulation time. Linear polymers are more readily cleared by the kidneys due to their ability to wind through the glomerular pores, however highly branched molecules such as dendrimers are unable to squeeze through these pores and remain in the blood. [76] This effectively reduces the polymer molecular weight required from 50 kDa to as low as 15 kDa.

There are several main methods used to prepare polymers with extended circulation time. By far the most common method is PEGylation, the process of functionalizing molecules with a polyethylene glycol chain. PEGylation has been extensively used to extend the circulation time of biological molecules since its initial development by Abuchowski and co-workers,[77,78] and can enable blood clearance half-lives of over 4 days.[79] The use of moderate and high molecular weight PEGylation has been important to prepare dendrimers with extended ciruclation times as well, as it is extremely challenging to prepare dendrimers larger than the renal clearance threshold. However, recently PEGylated biological drugs have been found to elicit an immune response with antibodies specific to PEG,[80–82] and so new polymers are being developed that can solve this issue. The most common class of alternative polymers are zwitterions, most notably poly(carboxybetaine). Jiang and coworkers have demonstrated that the grafting of poly(carboxybetaine) to enzymes results in no dimished enzymatic activity, and the resulting conjugates elicit much less of an immune response than do comparable PEG-based conjugates.[83]

1.9 Dendrimers for imaging

Molecular imaging agents have two main criteria that must be met in order to allow for imaging: they must accumulate at the desired imaging site, and they must have a method for reporting their location. In general, common dendrimer architectures are not intrinsically useful as imaging agents as they offer no means to report their location. Dendrimers must be functionalized with a reporter, and the choice of reporter is what

determines the imaging modality that the dendrimer can be used with. There are several methods by which modern medical imaging operates, but the most commonly explored with dendritic imaging agents are fluorescence, CT, MRI, and nuclear imaging. In fluorescence imaging, the dendrimer is typically functionalized with a fluorophore that emits in the near IR[84] and is also functionalized with either targeting ligands or PEG chains to allow for EPR effect accumulation. This allows for imaging with excellent resolution, but poor penetration depth (< 1 cm)[85], and is of limited practical benefit for translation to human imaging. Dendrimers have seen considerably more use in the preparation of imaging agents based on MRI reporting. The first examples of dendrimers as MRI imaging agents are from PAMAM[86,87] dendrimers that were conjugated with diethylenetriaminepentaacetic acid (DTPA) chelates at their periphery. Subsequently, Gd(III) can be chelated to the periphery of the dendron, which is then detectable via MRI.[46] As MRI is a relatively low sensitivity imaging modality, dendrimers are particularly useful to serve as signal amplifiers by coupling numerous reporters such as Gd(III) atoms onto a single macromolecule.

1.10 Radiolabeled Dendrimers

The first examples of biodistribution studies with radiolabeled dendrimers are those of PAMAM dendrimers that were radioiodinated with ^{125}I. [57,88] ^{125}I labeled unfunctionalized PAMAM dendrimers from generation 1 to 5 were found to cause significant hemolysis in mice, and all generations had less than 1% of the injected dose remaining in the blood after 1 hour, with considerable uptake in the liver and kidneys. Similar shortcomings were noted with biotin functionalized PAMAM dendrimers, though it was found that low generation

PAMAM dendrimers were cleared efficiently in the urine within 1 hour, whereas high generation (5-7) dendrimers were largely present in the kidneys at the same time point. Biodistribution studies using radioiodinated low molecular weight bis-MPA dendrimers with either a hydroxyl periphery or triethylene glycol periphery have also been performed by Fréchet and Szoka. [10] While both the unfunctionalized and TEGylated bis-MPA dendron exhibited negligible toxicity, both were eliminated renally within 4 hours. This was ascribed by the authors to be due to the relatively low molecular weight of the dendrimers (3.8 kDa and 13 kDa, respectively). In order to overcome this rapid renal excretion, strategies were developed to increase the molecular weight and hence the size of the dendrimers being investigated. Following on their previous study, Gillies and Fréchet prepared bow-tie dendrimers of generation 1-3 that were conjugated with PEG chains with molecular weights of 5 kDa, 10 kDa, or 20 kDa, resulting in conjugates with a molecular weight from 20 kDa to 120 kDa.[89] Dendrimer-PEG conjugates based on this architecture were later radiolabeled with ^{125}I and all compounds were found to have dramatically increased blood half-lives when compared to the initial non-PEGylated compounds.[32] There was a clear effect of both generation and PEG length on blood clearance half-life, with higher molecular weight PEG and higher dendrimer generation both increasing the blood half-life to a range of 1.5-50 h. These results indicated that PEGylated dendrimers are large enough to avoid renal filtration, and this could potentially allow for their use as drug delivery vehicles or for imaging agents. More recently, dendrimers have been investigated as a means to increase the efficacy of *in vivo* pre-targeted nuclear imaging. Zelgis and co-workers have prepared second generation

PAMAM dendrons bearing 4 *trans*-cyclooctene units (TCO) each, and conjugated these to antibodies for pre-targeted imaging of tumours.[90,91] The use of dendrimers allowed for an increase of TCO units from ~3 per antibody to ~8, which resulted in nearly twice the accumulation at the target site (8.9% ± 1.9% ID/g vs. 4.1% ± 1.3%). This increased targeting efficacy was ascribed to the higher concentration of TCO units in the body, resulting in a faster rate of reaction with the subsequently injected ^{89}Zr labeled tetrazine.

1.11 Isotopes for Dendrimer Imaging

While ^{125}I is a convenient isotope for "cut and count" biodistribution studies, its long half-life (60 days) is inappropriate for imaging applications due to the very high radiation dose that would occur for any material which was not excreted from the body. As a result, a variety of other isotopes are typically used for imaging depending on the desired imaging modality. There are two main nuclear imaging modalities currently in use that give three-dimensional data: Single Photon Emission Computed Tomography (SPECT) and Positron Emission Tomography (PET). SPECT imaging requires an isotope that emits gamma rays of suitable energy to penetrate through the body, while PET requires isotopes that decay and release a positron, which further undergoes annihilation with an electron, releasing two anti-parallel gamma rays. Common SPECT imaging isotopes include ^{99m}Tc, ^{123}I, ^{111}In, and ^{67}Ga, though ^{99m}Tc is by far the most commonly used, accounting for more than half of all nuclear medicine procedures. ^{99m}Tc is an excellent isotope for imaging as it has a convenient half-life of 6 hours, which allows for time to prepare radiolabeled compounds without exposing the patient to an excessive radiation dose burden due the relatively rapid

decay. Combined with the convenient gamma energy (140 keV) that allows for excellent penetration of body tissues makes ^{99m}Tc a very attractive isotope for imaging. ^{99m}Tc is available from commercial ^{99}Mo/^{99m}Tc generators, which allow labs to easily produce ^{99m}Tc with high specific activity without the need for access to a cyclotron facility.

By far the most commonly used isotope for Positron Emission Tomography (PET) imaging is ^{18}F, though other isotopes such as ^{11}C ,^{64}Cu, and ^{89}Zr are also used experimentally. In the case of both ^{18}F and ^{11}C, their short half-lives of 108 minutes and 20 minutes, respectively, effectively preclude their use for imaging over extended time periods required for EPR effect imaging. ^{64}Cu is a positron emitting isotope with an unusually long half-life of 12.7 hours, and as such is useful for imaging macromolecules with extended circulation times such as PEGylated dendrimers. Limited examples exist in the literature for ^{64}Cu labeled dendrimers, however recently ^{64}Cu labeled dendrimers bearing targeting ligands have been used to image atherosclerotic plaque.[92]

1.12 PEGylated Biomacromolecules

The use of biological macromolecules for therapy has attracted considerable attention from the scientific community.[93,94] Perhaps the most important example of this is the work of Banting and Best,[95,96] who determined that treatment of diabetics with insulin was highly effective. While the replacement of proteins in patients who are deficient is often an effective treatment, in many cases the pharmacokinetics of these compounds are inconvenient. One such example is Filgrastim, a human granulocyte colony stimulating factor which is used to treat low blood neutrophils. The original recombinant protein has a

blood half-life of approximately 3-4 hours, which requires very frequent dosing to maintain its effect. Upon PEGylation, PEGfilgrastim has a half-life of up to 40 hours, which results in a dosage schedule on the order of weekly or biweekly injections, rather than daily.[97,98] Some desirable biotherapeutics however do not come from human sources at all, such as asparaginase and uricase, which can be used to treat leukemia and gout, respectively. These proteins need to be shielded from the immune system, as they are both sourced from bacteria and can cause severe allergic reactions. Polymers conjugated to these proteins can afford dramatically reduced immunogenicity, which enabled their use as clinical therapeutics. A simulation of PEG-uricase is shown in Figure 1.10, illustrating the size of the polymer coating.

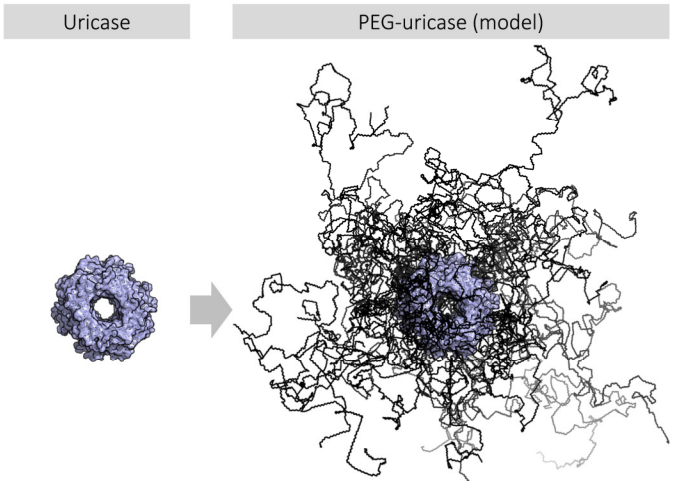

Figure 1.10. Model of PEGylated uricase

The first and by far the most commonly employed polymer for conjugation with biomacromolecules is polyethylene glycol or PEG. All polymer-macromolecule conjugate therapies currently approved by the FDA use PEG as the conjugating polymer. PEG is effective for this application for the same reasons it is effective for EPR effect imaging: it

has low protein binding, is readily water soluble, and can be large enough to avoid renal filtration. That PEG can be used to increase circulation time of biomolecules was first determined by Abuchowski and co-workers, who noted that the blood elimination half-life of bovine liver catalase could be extended from ~5 hours to over 60 hours by conjugation with 5 kDa monomthyl ether terminated PEG (mPEG).[77] This extended circulation time has proven beneficial for a wide array of therapeutics, particularly those derived from endogenous human proteins. The other critical role played by PEG is in hiding the conjugate from the immune system. The method by which this occurs has been commonly thought to be due to the formation of a coordinated shell of water molecules around the PEG chains, which prevent antibodies from binding efficiently.[99] However, more recent evidence has indicated that the formation of a protein corona around the PEG is essential, as this corona consists of proteins which discourage the immune response from attacking the nanoparticle.[100]

A tremendous amount of effort has been expended since the original work by Abuchowski on determining optimal PEGylation strategies. A number of key variables have been addressed, since factors such as degree of substitution, location of substitution, length of PEG chain, morphology of PEG chain, linker chemistry, PEG dispersity, and terminal functionalization of the chain can all have a major impact on the pharmacokinetics and ultimately on the efficacy of a given therapy.[101] In general, increasing the degree of PEGylation by using higher molecular weight PEG or increasing graft density increases blood clearance half-life and reduces first-pass immunogenicity. However, this occurs at the expense of activity, with some PEGylated proteins reducing their activity by more than

90% after PEGylation.[94] This reduction in activity is thought to occur through several primary mechanisms. The first and perhaps most expected is that the PEG shell around the biomolecule can trap moderately hydrophobic compounds, as they partition from the aqueous environment of the blood into the comparatively lipophilic PEG layer.[102]These compounds would then need to diffuse out of this PEG layer and into an aqueous environment in order to reach the active site (or binding site) of the biomolecule, which is slow. The other dominant mechanism of PEG induced reduction in activity is non-specific PEG binding to the active site (or binding site) of the biomolecule. Since PEG is ambipolar, it can bind to the typically hydrophobic active sites (or binding sites) and prevent the uptake of the intended substrate. Depending on the length of PEG and the proximity of PEG grafts to the active site, this can cause significant binding of the PEG, which causes a reduction in the activity of the protein.

1.13 Zwitterionic Polymers for Bioconjugation

Zwitterionic polymers, typically based on poly(carboxybetaine) (pCB) and poly(sulfobetaine) (pSB) have been the subject of considerable research in recent years. Prior to interest in their use for conjugation to biomolecules, pCB and pSB have been used to prepare ultra-low fouling membranes[103] and surface coatings[104] that can prevent the accumulation of biomolecules.[105–107] pCB and pSB are extremely low fouling in large part due to a layer of strongly coordinated water molecules around the highly charged polymer.[105] Indeed, pCB and pSB both satisfy the requirements mentioned in Section 1.8 for polymers that may be useful for EPR imaging: they are highly water soluble, exhibit low toxicity, and have very low protein binding. While these polymers have not seen

extensive investigation for EPR effect targeting[108] in the same manner as PEGylated polymers have in the past, there has recently been considerable work in their application as replacements for PEG in protein shielding. In a seminal paper,[83] Jiang and co-workers conjugated α-chymotrypsin with three different polymers, including a 5 kDa Mn PEG monomethyl ether, a 5 kDa pCB, and a pCB having an equivalent hydrodynamic volume as 5 kDa PEG monomethyl ether (as determined by aqueous SEC), all with three different grafting densities. When the Michaelis constants (K_m) were evaluated for these conjugates, it was found that increasing graft density of PEG reduced substrate affinity, whereas pCB with equivalent molecular weight to PEG had an effectively constant affinity at all graft densities. In the case of the pCB with R_h equal to 5 kDa PEG, increased affinity towards the substrate was observed. In further experiments with non-conjugated PEG or pCB in solution, the authors found that un-bound PEG resulted in a linear decrease in binding affinity of the substrate with increasing PEG concentration. Performing the same experiment with ammonium acetate increased the binding affinity of the substrate to α-chymotrypsin. pCB has also been conjugated to proteins with clinically used PEGylated derivatives such as interferon α-2a (PEGasys). [109] In similar fashion as with α-chymotrypsin, it was found that the activity of interferon-pCB conjugates was 3-4 times greater than the corresponding PEGylated materials, and this was largely ascribed to the reduction in non-specific binding between hydrophobic portions of the interferon receptor and PEG. Since the successful introduction of pCB as an alternative to PEGylation, numerous other studies have found that the resulting conjugates retained more activity and are much less immunogenic in comparison to PEG.[110–112]

1.14 Other PEGylation alternatives

Polymers based on a variety of structures have also been investigated for their use in polymer protein conjugates for use in pharmaceuticals, with some of the most common recent examples detailed in Figure 1.11.[113] Controlled radical polymerization (CRP) methods such as ATRP[114] and RAFT[115] have allowed access to acrylate and methacrylate polymers with narrow dispersities, which are thought to be necessary for biomedical applications due to the impact of polymer size on biodistribution and clearance. Unlike PEGylation, CRP can be used to *graft from* (i.e. polymerize on the surface of the protein), allowing for increased graft density and the formation of polymer brushes rather than "mushrooms".[116] This is believed to be important for reduced immune recognition of the protein[117] and is challenging to access via the *graft to* approach. Poly(*N*-(2-hydroxypropyl) methacrylamide (HPMA) and random copolymers containing this monomer have been used for a variety of drug delivery applications, and it has generally been found to be biocompatible.[118,119] HPMA has been less explored for conjugation to proteins, though there have been some examples of proteins modified with this polymer.[120,121] Polyvinyl pyrrolidone (PVP) conjugated to uricase has been compared to PEG of similar molecular weight, with PVP exhibiting a greater circulation time in murine models but less of a "stealth" effect than PEG.[122,123] This may be due to sequential injections PVP-conjugated proteins, which have been found to cause increased immune response after multiple injections, a phenomenon that is seen in PEG as well as other polymers. Functional polymers made by CRP incorporating pendant groups such as

saccharides[124–126] or oligoethylene glycol chains[127,128] have also been investigated for both protein stability and shielding as well.

While acrylate/methacrylate polymers are receiving increasing attention, there are several other polymer architectures that are currently being investigated. Polyoxazolines (POZ) such as poly(2-ethyl-2-oxazoline) and poly(2-methyl-2-oxazoline) have been found to have extended circulation time,[129] and low protein binding[129], which makes them attractive alternatives to PEG. Veronese and coworkers demonstrated that grafting between twenty and ninety 20 kDa PEOZ units to granulocyte colony stimulating factor (G-CSF, Neulasta) preserved the biological activity of the protein.[130] Both linear[131] and hyperbranched[132] polyglycerol have also been investigated extensively, particularly as modern ring opening polymerization procedures have allowed for the synthesis of low dispersity polymers.

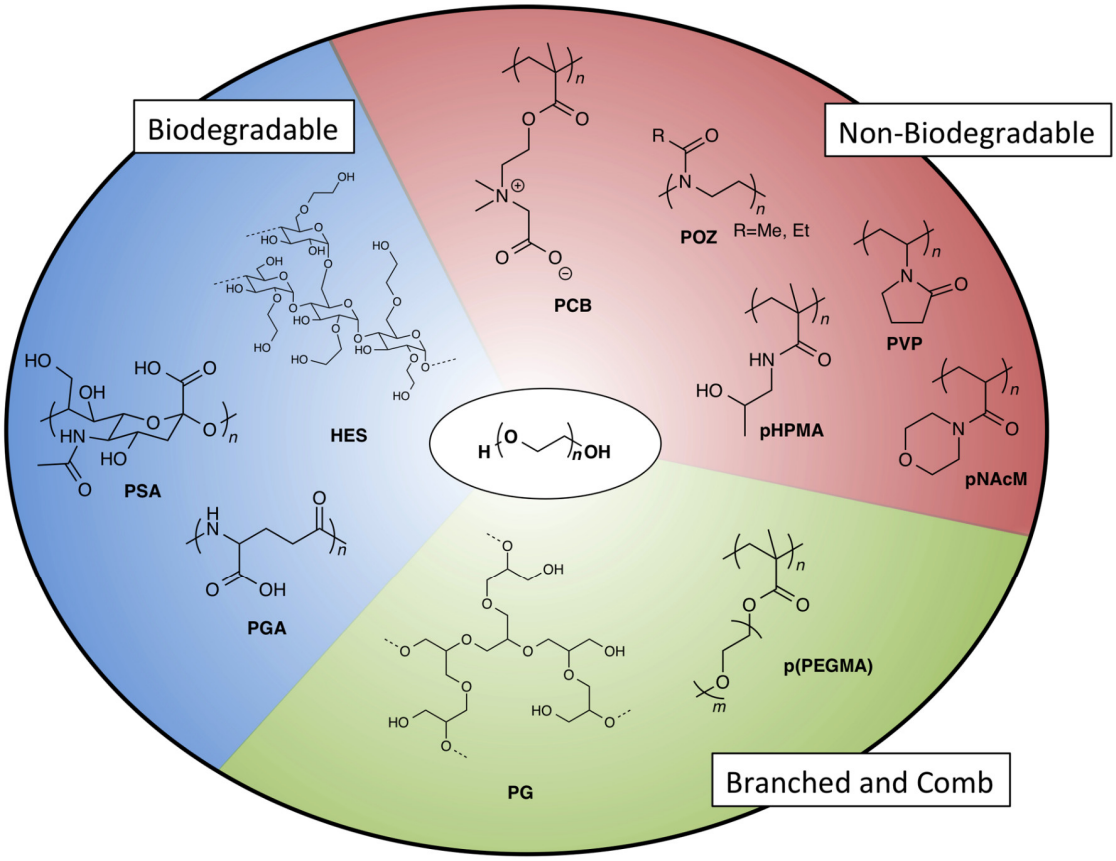

Figure 1.11. Examples of Currently investigated PEG alternative polymers. Reproduced with permission.[113] Copyright American Chemical Society (2014)

1.15 Molecular Sieving

A term coined by Gauthier and co-workers,[133] molecular sieving in the context of protein-polymer conjugates refers to the rational design and synthesis of polymer coatings that allow for unhindered reactivity against small molecules, but which prevent reaction against large molecules. In this pioneering work, α-chymotrypsin was used as a model enzyme and poly(oligoethylene glycol methacrylate) (POEGMA) was synthesized on the surface of the protein via a graft-from polymerization approach using ATRP. POEGMA was chosen due

to the variety of conformations comb polymers can adopt in solution depending on backbone length, side chain length, and the ratio of these two lengths.[134]

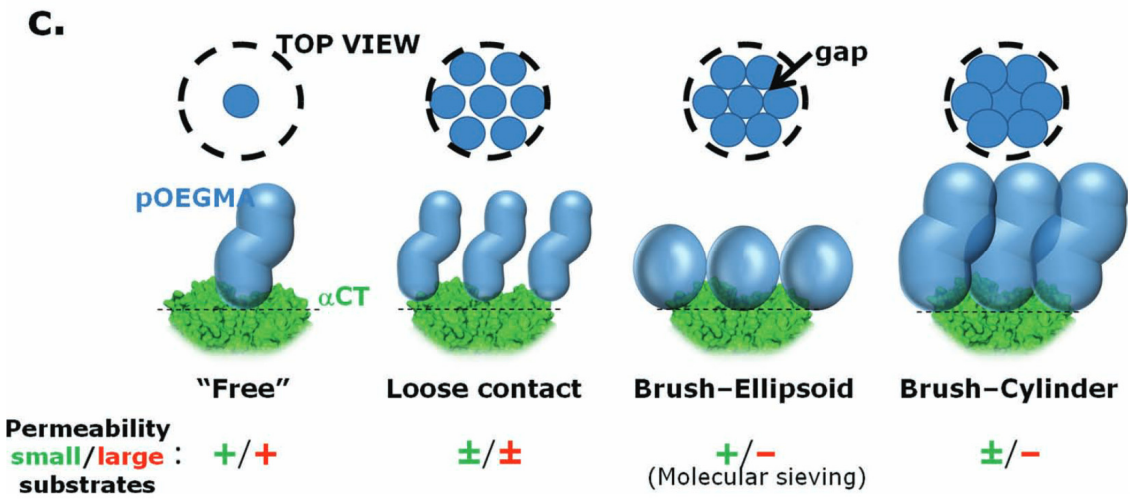

Figure 1.12. POEGMA morphology as a function of graft density and degree of polymerization. Reproduced with permission.[133] Copyright John Wiley & Sons (2013)

The authors determined several key parameters required in order for a polymer to function as a molecular sieve. As seen in Figure 1.12, a polymer that can adopt a globular or ellipsoidal shape rather than a random coil allows for small molecules to penetrate in the interstitial space between polymer grafts. Also, a high degree of surface coverage is required to ensure the whole protein is coated in polymer and that the active site is suitably shielded.

After this initial work, preliminary *in vivo* work was performed using asparaginase as a therapeutic enzyme.[135] This enzyme (and its PEGylated form) is currently used clinically for the treatment of acute lymphoblastic leukemia (ALL) due to its ability to catalyze the conversion of asparagine to aspartic acid, which is an essential nutrient require

for the continued proliferation of ALL. Using the lessons learned from their earlier work, a series of conjugates were prepared and the most promising were found to exhibit similar activity when compared to conventional PEGylated protein but were 1000-fold less immunogenic. This translated *in vivo* to much lower anti-asparaginase and anti-conjugate IgG titers, while retaining the desired reduction in asparagine concentrations. [135]

1.16 Goal of the thesis

The goal of this thesis was to prepare bis-MPA dendrons that were suitable for use in biomedical applications. In chapter 2, a series of bis-MPA dendrons with a ^{99m}Tc chelate at the core and varying lengths of PEG at the periphery were synthesized, fully characterized, and evaluated for suitability as EPR imaging agents. The most suitable dendron was then radiolabeled with ^{99m}Tc, and this was imaged in both healthy rats and xenograft tumour bearing mice, with visible accumulation of these dendrons at the tumor site. This work was one of the first examples of bis-MPA dendrimers labeled with ^{99m}Tc, and it serves as an illustration of the size and degree of PEGylation required for EPR imaging with bis-MPA dendrons. In addition, procedures for radiolabeling bis-MPA dendrons were developed, which can be useful for further imaging studies using bis-MPA dendrons. In chapter 3, a new convergent synthesis methodology for functionalized bis-MPA dendrons is presented which is based on strain-promoted alkyne-azide cycloaddition chemistry. This synthetic approach allows for the preparation of libraries of high generation dendrons using a combination of an “inner” dendron with functionality at the core such as a radioligand or fluorophore and azides at its periphery, and an “outer” dendron bearing a

strained cyclooctyne at the core and various groups at the periphery. In chapter 4, the synthesis and characterization of bis-MPA dendrons of generation 2 through 8 bearing strained cyclooctynes at the core is reported. These dendrons were used to prepare corresponding dendron-enzyme conjugates with α-chymotrypsin, and the ability of the conjugates to act as molecular sieves was evaluated. In chapter 5, the synthesis and characterization of bis-MPA dendrons with zwitterionic (sulfobetaine and carboxybetaine) peripheries are described. These were used to prepare uniform molecular weight sixth generation dendrons which were found to have suitable properties for EPR imaging as determined by DLS, SEC, and zeta-potential. Originally, these were to be used for EPR effect imaging after being labeled with $[^{99m}Tc(CO)_3]^+$, but all labeling conditions were found to hydrolyze the dendrimer.

1.17 References

[1] L. Y. Qiu, Y. H. Bae, *Pharm. Res.* **2006**, *23*, 1–30.

[2] E. Buhleier, W. Wehner, F. Vögtle, *Synth.* **1978**, *1978*, 155–158.

[3] D. a Tomalia, H. Baker, J. Dewald, M. Hall, G. Kallos, S. Martin, J. Roeck, J. Ryder, P. Smith, *Polym. J.* **1985**, *17*, 117–132.

[4] G. R. Newkome, Z. Yao, G. R. Baker, V. K. Gupta, *J. Org. Chem* **1985**, 2003–2004.

[5] H. Ihre, A. Hult, E. Söderlind, *J. Am. Chem. Soc.* **1996**, *118*, 6388–6395.

[6] H. Ihre, O. Jesús, J. M. J. Fréchet, *J. Am. Chem. Soc.* **2001**, *123*, 5908–5917.

[7] H. Ihre, A. Hult, J. M. J. Fréchet, I. Gitsov, *Macromolecules* **1998**, *31*, 4061–4068.

[8] H. R. Ihre, O. L. Padilla de Jesús, F. C. Szoka, J. M. J. Fréchet, *Bioconjug. Chem.* **2002**, *13*, 443–452.

[9] H. Ihre, O. L. Padilla De Jesús, J. M. J. Fréchet, *J. Am. Chem. Soc.* **2001**, *123*, 5908–5917.

[10] O. L. Padilla De Jesús, H. R. Ihre, L. Gagne, J. M. J. Fréchet, F. C. Szoka, *Bioconjug. Chem.* **2002**, *13*, 453–461.

[11] E. R. Gillies, E. Dy, J. M. J. Fréchet, F. C. Szoka, *Mol. Pharm.* **2005**, *2*, 129–138.

[12] B. Fadeel, M. I. Montañez, M. Malkoch, A. Nyström, A. Kunzmann, N. Feliu, M. V Walter, A. Hult, *Biomaterials* **2012**, *33*, 1970–1981.

[13] M. C. Parrott, J. F. Vaillant, A. Adronov, *Langmuir* **2006**, *22*, 5251–5255.

[14] A. Carlmark, C. Hawker, A. Hult, M. Malkoch, *Chem. Soc. Rev.* **2009**, *38*, 352–362.

[15] C. J. Hawker, J. Frechet, *J. Am. Chem. Soc.* **1990**, *112*, 7638–7647.

[16] C. C. Lee, J. A. MacKay, J. M. J. Fréchet, F. C. Szoka, *Nat. Biotechnol.* **2005**, *23*, 1517–1526.

[17] M. A. Mintzer, M. W. Grinstaff, *Chem. Soc. Rev* **2011**, *40*, 173–190.

[18] M. C. Hawker, A. J. McGrath, A. Abdilla, W. R. Gutekunst, L. A. Connal, C. J. Hawker, S.-H. Lee, A. S. Knight, A. S. Abrams, J. Lawrence, et al., *J. Am. Chem. Soc.* **2016**, *138*, 6306–6310.

[19] J. Lawrence, E. Goto, J. M. Ren, B. McDearmon, D. S. Kim, Y. Ochiai, P. G. Clark, D. Laitar, T. Higashihara, C. J. Hawker, *J. Am. Chem. Soc.* **2017**, *139*, 13735–13739.

[20] J. C. Barnes, D. J. C. Ehrlich, A. X. Gao, F. A. Leibfarth, Y. Jiang, E. Zhou, T. F. Jamison, J. A. Johnson, *Nat. Chem.* **2015**, *7*, 810–815.

[21] Y. Jiang, M. R. Golder, H. V.-T. Nguyen, Y. Wang, M. Zhong, J. C. Barnes, D. J. C. Ehrlich, J. A. Johnson, H. V-T Nguyen, Y. Wang, et al., *J. Am. Chem. Soc.* **2016**, *138*, 9369–9372.

[22] F. Amir, Z. Jia, M. J. Monteiro, *J. Am. Chem. Soc* **2016**, *138*, 16600–16603.

[23] Z. Huang, J. Zhao, Z. Wang, F. Meng, K. Ding, X. Pan, N. Zhou, X. Li, Z. Zhang, X. Zhu, *Angew. Chemie - Int. Ed.* **2017**, *56*, 13612–13617.

[24] T. H. Mourey, S. R. Turner, M. Rubinstein, J. M. J. Fréchet, C. J. Hawker, K. L. Wooley, *Macromolecules* **1992**, *25*, 2401–2406.

[25] E. M. Harth, S. Hecht, B. Helms, E. E. Malmstrom, J. M. J. Fréchet, C. J. Hawker, *J. Am. Chem. Soc.* **2002**, *124*, 3926–3938.

[26] K. L. Wooley, C. J. Hawker, J. M. Pechan, J. M. J. Fréchet, *Macromolecules* **1993**, *26*, 1514–1519.

[27] C. J. Hawker, E. E. Malmström, C. W. Frank, J. Patrick Kampf, *J. Am. Chem. Soc* **1994**, *119*, 9903–9904.

[28] C. J. Hawker, K. L. Wooley, J. M. J. Fréchet, *J. Am. Chem. Soc.* **1993**, *115*, 4375–4376.

[29] K. R. Gopidas, A. R. Leheny, G. Caminati, N. J. Turro, D. A. Tomalia, *J. Am. Chem. Soc.* **1991**, *113*, 7335–7342.

[30] M. C. Moreno-Bondi, G. Orellana, N. J. Turro, D. A. Tomalia, *Macromolecules* **1990**, *23*, 910–912.

[31] D. Venturoli, B. Rippe, *Am. J. Physiol. Physiol.* **2005**, *288*, F605–F613.

[32] E. R. Gillies, E. Dy, J. M. J. Fréchet, F. C. Szoka, *Mol. Pharm.* **2005**, *2*, 129–138.

[33] H. C. Kolb, M. G. Finn, K. B. Sharpless, *Angew. Chemie - Int. Ed.* **2001**, *40*, 2004–2021.

[34] P. Wu, A. K. Feldman, A. K. Nugent, C. J. Hawker, A. Scheel, B. Voit, J. Pyun, J. M. J. Fréchet, K. B. Sharpless, V. V. Fokin, *Angew. Chemie - Int. Ed.* **2004**, *43*, 3928–3932.

[35] D. Astruc, L. Liang, A. Rapakousiou, J. Ruiz, *Acc. Chem. Res.* **2012**, *45*, 630–640.

[36] C. Ornelas, J. Ruiz Aranzaes, E. Cloutet, S. Alves, D. Astruc, *Angew. Chemie* **2007**, *119*, 890–895.

[37] M. Malkoch, K. Schleicher, E. Drockenmuller, C. J. Hawker, T. P. Russell, P. Wu, V. V Fokin, *Macromolecules* **2005**, *38*, 3663–3678.

[38] P. Antoni, M. J. Robb, L. Campos, M. Montanez, A. Hult, E. Malmström, M. Malkoch, C. J. Hawker, *Macromolecules* **2010**, *43*, 6625–6631.

[39] S. García-Gallego, D. Hult, J. V Olsson, M. Malkoch, *Angew. Chemie - Int. Ed.* **2015**, *54*, 2416–2419.

[40] L. P. Sadowski, P. E. Edem, J. F. Valliant, A. Adronov, *Macromol. Biosci.* **2016**, 1475–1484.

[41] A. R. Menjoge, R. M. Kannan, D. a. Tomalia, *Drug Discov. Today* **2010**, *15*, 171–185.

[42] S. Svenson, D. A. Tomalia, *Adv. Drug Deliv. Rev.* **2012**, *64*, 102–115.

[43] U. Boas, P. M. H. Heegaard, *Chem. Soc. Rev.* **2004**, *33*, 43–63.

[44] Y. Zhang, Y. Sun, X. Xu, X. Zhang, H. Zhu, L. Huang, Y. Qi, Y.-M. Shen, *J. Med. Chem.* **2010**, *53*, 3262–3272.

[45] J. Criscione, L. Dobrucki, Z. Zhuang, X. Papademetris, M. Simons, A. Sinusas, T. Fahmy, *Bioconjug. Chem.* **2011**, *22*, 1784–1792.

[46] H. Kobayashi, M. W. Brechbiel, *Mol. Imaging* **2003**, *2*, 1–10.

[47] D. Luong, P. Kesharwani, R. Deshmukh, M. C. I. Mohd Amin, U. Gupta, K. Greish, A. K. Iyer, *Acta Biomater.* **2016**, *43*, 14–29.

[48] J. Zhou, J. Wu, N. Hafdi, J. P. Behr, P. Erbacher, L. Peng, *Chem. Commun.* **2006**, 2362–2364.

[49] C. L. Waite, C. M. Roth, *Bioconjug. Chem.* **2009**, *20*, 1908–1916.

[50] L. Peng, J. Iovanna, X. Liu, P. Rocchi, M. Gleave, Z. Liang, F. Qu, S. Zheng, *ChemMedChem* **2009**, *4*, 1302–1310.

[51] Y. Tang, Y. B. Li, B. Wang, R. Y. Lin, M. Van Dongen, D. M. Zurcher, X. Y. Gu,

M. M. Banaszak Holl, G. Liu, R. Qi, *Mol. Pharm.* **2012**, *9*, 1812–1821.

[52] J. S. Choi, K. Nam, J. Park, J.-B. Kim, J.-K. Lee, J. Park, *J. Control. Release* **2004**, *99*, 445–456.

[53] J. H. Lee, Y. B. Lim, J. S. Choi, Y. Lee, T. Il Kim, H. J. Kim, J. K. Yoon, K. Kim, J. S. Park, *Bioconjug. Chem.* **2003**, *14*, 1214–1221.

[54] B. C. Geiger, S. Wang, R. F. P. Jr, A. J. Grodzinsky, P. T. Hammond, *Sci. Transl. Med.* **2018**, 1–12.

[55] R. B. Kolhatkar, K. M. Kitchens, P. W. Swaan, H. Ghandehari, *Bioconjug. Chem.* **2007**, *18*, 2054–2060.

[56] J. C. Roberts, M. K. Bhalgat, R. T. Zera, *J. Biomed. Mater. Res.* **1996**, *30*, 53–65.

[57] N. Malik, R. Wiwattanapatapee, R. Klopsch, K. Lorenz, H. Frey, J. W. Weener, E. W. Meijer, W. Paulus, R. Duncan, *J. Control. Release* **2000**, *65*, 133–148.

[58] R. L. Vessella, D. S. Wilbur, P. M. Pathare, D. K. Hamlin, K. R. Buhler, *Bioconjug. Chem.* **2002**, *9*, 813–825.

[59] G. A. Brazeau, S. Attia, S. Poxon, J. A. Hughes, *Pharm. Res.* **1998**, *15*, 680–684.

[60] H. B. Agashe, T. Dutta, M. Garg, N. K. Jain, *J. Pharm. Pharmacol.* **2006**, *58*, 1491–1498.

[61] M. X. Tang, C. T. Redemann, F. C. Szoka, *Bioconjug. Chem.* **1996**, *7*, 703–714.

[62] J. Drobník, F. Rypáček, *Adv. Polym. Sci.* **1984**, 1–50.

[63] J. Hu, Y. Su, H. Zhang, T. Xu, Y. Cheng, *Biomaterials* **2011**, *32*, 9950–9959.

[64] N. a. Stasko, C. B. Johnson, M. H. Schoenfisch, T. a. Johnson, E. L. Holmuhamedov, *Biomacromolecules* **2007**, *8*, 3853–3859.

[65] M. E. Fox, S. Guillaudeu, J. M. J. Fréchet, K. Jerger, N. Macaraeg, F. C. Szoka, *Mol. Pharm.* **2009**, *6*, 1562–1572.

[66] C. J. H. Porter, R. Lessene, B. J. Boyd, G. Krippner, P. Karellas, L. M. Kaminskas, *Mol. Pharm.* **2006**, *3*, 614–627.

[67] M. C. Parrott, S. R. Benhabbour, C. Saab, J. A. Lemon, S. Parker, J. F. Valliant, A. Adronov, *J. Am. Chem. Soc* **2009**, *131*, 2906–2916.

[68] M. Parrott, E. Marchington, ‡ Valliant, A. Adronov, *J. Am. Chem. Soc.* **2005**, *127*, 12081–12089.

[69] N. Feliu, M. V. Walter, M. I. Montañez, A. Kunzmann, A. Hult, A. Nyström, M. Malkoch, B. Fadeel, *Biomaterials* **2012**, *33*, 1970–1981.

[70] C. C. Lee, E. R. Gillies, M. E. Fox, S. J. Guillaudeu, J. M. J. Fréchet, E. E. Dy, F. C. Szoka, *Proc. Natl. Acad. Sci. U. S. A.* **2006**, *103*, 16649–16654.

[71] H. Choi, W. Liu, P. Misra, E. Tanaka, J. Zimmer, B. Ipe, M. Bawendi, J. Frangioni,

Nat. Biotechnol. **2007**, *25*, 1165–1170.

[72] Y. Matsumura, H. Maeda, *Cancer Res.* **1986**, *46*, 6387–6392.

[73] C. Heneweer, J. P. Holland, V. Divilov, S. Carlin, J. S. Lewis, *J. Nucl. Med.* **2011**, *52*, 625–633.

[74] R. Duncan, *Nat. Rev. Cancer* **2006**, *6*, 688–701.

[75] R. Duncan, *Nat. Rev. Drug Discov.* **2003**, *2*, 347–360.

[76] M. E. Fox, F. C. Szoka, J. M. J. Fréchet, *Acc. Chem. Res.* **2009**, *42*, 1141–1151.

[77] A. Abuchowski, J. R. McCoy, N. C. Palczuk, T. van Es, F. F. Davis, *J. Biol. Chem.* **1977**, *252*, 3582–3586.

[78] A. Abuchowski, T. van Es, N. C. Palczuk, F. F. Davis, *J. Biol. Chem.* **1977**, *252*, 3579–3581.

[79] F. M. Veronese, A. Mero, *Biodrugs* **2008**, *22*, 315–329.

[80] Q. Yang, S. K. Lai, *Wiley Interdiscip. Rev. Nanomedicine Nanobiotechnology* **2015**, *7*, 655–677.

[81] P. Zhang, F. Sun, S. Liu, S. Jiang, *J. Control. Release* **2016**, *244*, 184–193.

[82] H. Schellekens, W. E. Hennink, V. Brinks, *Pharm. Res.* **2013**, *30*, 1729–1734.

[83] A. J. Keefe, S. Jiang, *Nat. Chem.* **2012**, *4*, 59–63.

[84] V. S. Talanov, C. A. S. Regino, H. Kobayashi, M. Bernardo, P. L. Choyke, M. W. Brechbiel, *Nano Lett.* **2006**, *6*, 1459–1463.

[85] J. V Frangioni, *Curr. Opin. Chem. Biol.* **2003**, *7*, 626–634.

[86] E. Wiener, P. C. Lauterbur, M. W. Brechbiel, R. L. Magin, D. A. Tomalia, H. Brothers, O. A. Gansow, *Magn. Reson. Med.* **1994**, *31*, 1–8.

[87] S. D. Konda, M. Aref, S. Wang, M. Brechbiel, E. C. Wiener, *Magn. Reson. Mater. Physics, Biol. Med.* **2001**, *12*, 104–113.

[88] D. S. Wilbur, P. M. Pathare, D. K. Hamlin, K. R. Buhler, R. L. Vessella, *Bioconjug. Chem.* **1998**, *9*, 813–825.

[89] E. R. Gillies, J. M. J. Fréchet, *J. Am. Chem. Soc.* **2002**, *124*, 14137–14146.

[90] B. E. Cook, R. Membreno, B. M. Zeglis, *Bioconjug. Chem.* **2018**, *29*, 2734–2740.

[91] R. Membreno, O. M. Keinänen, B. E. Cook, K. M. Tully, K. C. Fung, J. S. Lewis, B. M. Zeglis, *Mol. Pharm.* **2019**, *16*, 2259–2263.

[92] J. W. Seo, H. Baek, L. M. Mahakian, J. Kusunose, J. Hamzah, E. Ruoslahti, K. W. Ferrara, *Bioconjug. Chem.* **2014**, *25*, 231–239.

[93] A. L. Nelson, E. Dhimolea, J. M. Reichert, *Nat. Rev. Drug Discov.* **2010**, *9*, 767–774.

[94] M. A. Gauthier, H. A. Klok, *Polym. Chem.* **2010**, *1*, 1352–1373.

[95] F. Banting, C. Best, *J Lab Clin Med* **1922**, *7*, 251–266.

[96] F. Banting, C. Best, W. Campbell, A. Fletcher, *Can Med Assoc J* **1922**, *12*, 141–146.

[97] G. Molineux, *Anticancer. Drugs* **2003**, *14*, 259–264.

[98] M. D. Green, H. Koelbl, J. Baselga, A. Galid, V. Guillem, P. Gascon, S. Siena, R. I. Lalisang, H. Samonigg, M. R. Clemens, et al., *Ann. Oncol.* **2003**, *14*, 29–35.

[99] P. Del Pino, B. Pelaz, Q. Zhang, P. Maffre, G. U. Nienhaus, W. J. Parak, *Mater. Horizons* **2014**, *1*, 301–313.

[100] S. Schöttler, G. Becker, S. Winzen, T. Steinbach, K. Mohr, K. Landfester, V. Mailänder, F. R. Wurm, *Nat. Nanotechnol.* **2016**, *11*, 372–377.

[101] J. M. Harris, R. B. Chess, *Nat. Rev. Drug Discov.* **2003**, *2*, 214–221.

[102] A. J. Keefe, S. Jiang, *Nat. Chem.* **2012**, *4*, 59–63.

[103] M. Hadidi, A. L. Zydney, *J. Memb. Sci.* **2013**, *452*, 97–103.

[104] C. Gao, G. Li, H. Xue, W. Yang, F. Zhang, S. Jiang, *Biomaterials* **2010**, *31*, 1486–1492.

[105] J. B. Schlenoff, *Langmuir* **2014**, *30*, 9625–9636.

[106] S. Jiang, Z. Cao, *Adv. Mater.* **2010**, *22*, 920–932.

[107] J. Ladd, Z. Zhang, S. Chen, J. C. Hower, S. Jiang, *Biomacromolecules* **2008**, *9*, 1357–1361.

[108] W. Yang, S. Liu, T. Bai, A. J. Keefe, L. Zhang, J. R. Ella-Menye, Y. Li, S. Jiang, *Nano Today* **2014**, *9*, 10–16.

[109] Y. Han, Z. Yuan, P. Zhang, S. Jiang, *Chem. Sci.* **2018**, *9*, 8561–8566.

[110] P. Zhang, F. Sun, C. Tsao, S. Liu, P. Jain, A. Sinclair, H.-C. Hung, T. Bai, K. Wu, S. Jiang, *Proc. Natl. Acad. Sci.* **2015**, *112*, 12046–12051.

[111] S. Liu, S. Jiang, *Nano Today* **2016**, *11*, 285–291.

[112] P. Zhang, P. Jain, C. Tsao, Z. Yuan, W. Li, B. Li, K. Wu, H. C. Hung, X. Lin, S. Jiang, *Angew. Chemie - Int. Ed.* **2018**, *57*, 7743–7747.

[113] E. M. Pelegri-O'day, E.-W. Lin, H. D. Maynard, *J. Am. Chem. Soc.* **2014**, *136*, 14323–14332.

[114] J. Wang, K. Matyjaszewski, *J. Am. Chem. Soc.* **1995**, *117*, 5614–5615.

[115] J. Chiefari, F. Ercole, J. Krstina, J. Jeffery, T. P. T. Le, R. T. A. Mayadunne, G. F. Meijs, C. L. Moad, G. Moad, E. Rizzardo, et al., *Macromolecules* **1998**, *31*, 5559–5562.

[116] W. J. Brittain, S. Minko, *J. Polym. Sci. Part A Polym. Chem.* **2007**, *45*, 3505–3512.

[117] Q. Yang, S. W. Jones, C. L. Parker, W. C. Zamboni, J. E. Bear, S. K. Lai, *Mol. Pharm.* **2014**, *11*, 1250–1258.

[118] J. Kopeček, P. Kopečková, T. Minko, Z. R. Lu, *Eur. J. Pharm. Biopharm.* **2000**, *50*, 61–81.

[119] T. Lammers, K. Ulbrich, *Adv. Drug Deliv. Rev.* **2009**, *62*, 119–121.

[120] K. Ulbrich, V. Šubr, J. Strohalm, D. Plocová, M. Jelínková, B. Říhová, *J. Control. Release* **2002**, *64*, 63–79.

[121] K. Ulbrich, J. Strohalm, D. Plocova, D. Oupicky, V. Subr, J. Soucek, P. Pouckova, J. Matousek, *J. Bioact. Compat. Polym.* **2000**, *15*, 4–25.

[122] P. Caliceti, O. Schiavon, F. M. Veronese, *Bioconjug. Chem.* **1999**, *10*, 638–646.

[123] P. Caliceti, O. Schiavon, F. M. Veronese, *Bioconjug. Chem.* **2001**, *12*, 515–522.

[124] Y. Liu, J. Lee, K. M. Mansfield, J. H. Ko, S. Sallam, C. Wesdemiotis, H. D. Maynard, *Bioconjug. Chem.* **2017**, *28*, 836–845.

[125] K. M. Mansfield, H. D. Maynard, *ACS Macro Lett.* **2018**, *7*, 324–329.

[126] J. Geng, G. Mantovani, L. Tao, J. Nicolas, G. Chen, R. Wallis, D. A. Mitchell, B. R. G. Johnson, S. D. Evans, D. M. Haddleton, *J. Am. Chem. Soc.* **2007**, *129*, 15156–15163.

[127] L. Tao, G. Mantovani, F. Lecolley, D. M. Haddleton, *J. Am. Chem. Soc.* **2004**, *126*, 13220–13221.

[128] K. Bebis, M. W. Jones, D. M. Haddleton, M. I. Gibson, *Polym. Chem.* **2011**, *2*, 975–982.

[129] F. C. Gaertner, R. Luxenhofer, B. Blechert, R. Jordan, M. Essler, *J. Control. Release* **2007**, *119*, 291–300.

[130] A. Mero, Z. Fang, G. Pasut, F. M. Veronese, T. X. Viegas, *J. Control. Release* **2012**, *159*, 353–361.

[131] A. Thomas, S. S. Müller, H. Frey, *Biomacromolecules* **2014**, *15*, 1935–1954.

[132] F. Wurm, J. Klos, H. J. Räder, H. Frey, *J. Am. Chem. Soc.* **2009**, *131*, 7954–7955.

[133] M. Liu, P. Tirino, M. Radivojevic, D. J. Phillips, M. I. Gibson, J. C. Leroux, M. A. Gauthier, *Adv. Funct. Mater.* **2013**, *23*, 2007–2015.

[134] G. Cheng, Y. B. Melnichenko, G. D. Wignall, F. Hua, K. Hong, J. W. Mays, *Macromolecules* **2008**, *41*, 9831–9836.

[135] M. Liu, P. Johansen, F. Zabel, J. C. Leroux, M. A. Gauthier, *Nat. Commun.* **2014**, *5*, 1–8.

2 Synthesis, Radiolabeling, and In-Vivo Imaging of PEGylated High-Generation Polyester Dendrimers

The work detailed in this chapter was carried out in collaboration with Mr. Spencer Knight and Mrs. Nancy Janzen. Stuart McNelles and Mr. Knight synthesized and characterized the small molecule and polymer materials. Stuart McNelles performed the radiolabeling studies, and Mrs. Janzen performed the SPECT imaging studies.

Graphical Abstract:

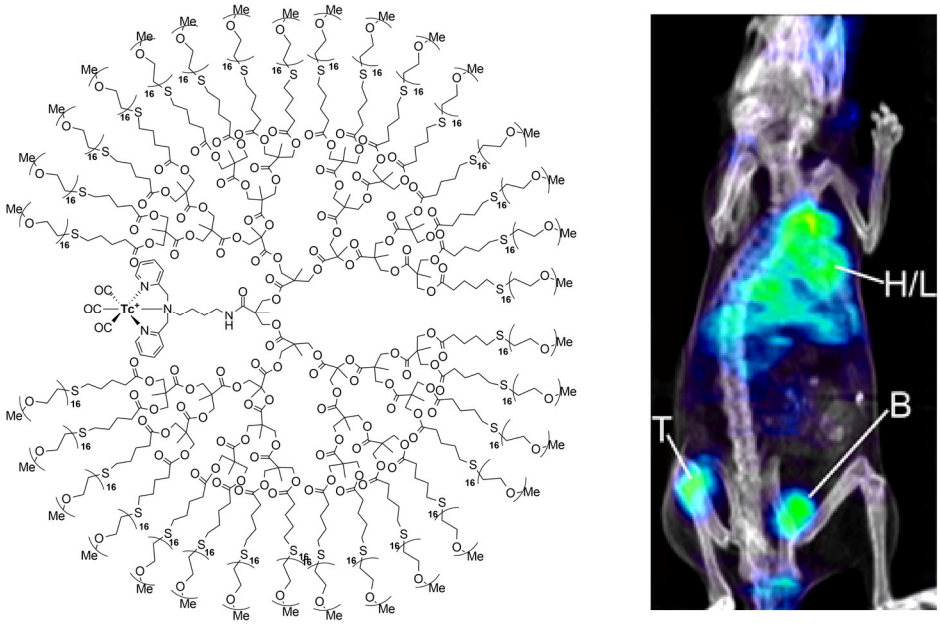

2.1 Abstract

A fifth-generation aliphatic polyester dendrimer was functionalized with vinyl groups at the periphery and a dipicolylamine Tc(I) chelate at the core. This structure was PEGylated with three different molecular weight mPEGs ($mPEG_{160}$, $mPEG_{350}$, and $mPEG_{750}$) using thiol-ene click chemistry. The size of the resulting macromolecules was evaluated using dynamic light scattering and it was found that the dendrimer functionalized with $mPEG_{750}$ was molecularly dispersed in water, exhibiting a hydrodynamic diameter of 9.2 ± 2.1 nm. This PEGylated dendrimer was subsequently radiolabeled using $[^{99m}Tc(CO)_3(H_2O)_3]^+$ and purified to high (>99%) radiochemical purity. Imaging studies were initially performed on healthy rats to allow comparison to previous Tc-labeled dendrimers, and then on xenograft murine tumor models, which collectively showed that the dendrimers circulated in the blood for an extended period of time (up to 24 hours). Furthermore, the radiolabeled dendrimer accumulated in H520 xenograft tumors, which could be visualized by single photon emission computed tomography (SPECT). The reported PEGylated aliphatic polyester dendrimers represent a new platform for developing tumor targeted molecular imaging probes and therapeutics.

2.2 Introduction

Macromolecular therapeutic agents have garnered increasing interest over the past four decades.[1–7] It has been shown repeatedly that conjugation of pharmaceuticals to water-soluble, non-toxic, biocompatible polymers results in improved drug solubility, increased blood circulation time, and decreased systemic toxicity.[8–10] In addition, the ability to

introduce multiple functionalities on a macromolecule provides potential for site-specific targeting of disease.[11–14] Of the available macromolecular architectures, dendritic macromolecules offer a number of unique advantages over their linear counterparts as scaffolds for conjugation of therapeutic agents.[15–18] The precise, step-wise synthesis of dendrimers allows unparalleled structural precision relative to other synthetic macromolecules, enabling modification of the core, interior, or periphery in a highly controlled manner.[19–21] The globular nature of high-generation dendrimers additionally permits site isolation of moieties introduced at the core or interior, with macroscopic properties dictated by the surface functionalities that are introduced.[22] This unique aspect of dendrimers opens the possibility for development of multi-functional dendritic structures capable of targeted simultaneous delivery of both therapeutic and diagnostic imaging agents, effectively resulting in a "theranostic" scaffold.[23–26]

Amongst the available dendrimer structures,[27–29] aliphatic polyester dendrimers based on the 2,2-bis(hydroxymethyl)propanoic acid (bis-MPA) branching unit are ideal scaffolds for theranostic applications.[30,31] These poly(2,2-bis(hydroxymethyl)propanoic acid) (bis-MPA) dendrimers can be readily synthesized through convergent[32,33] or divergent approaches,[34] they exhibit low in vivo toxicity, are biocompatible, and are biodegradable.[35–37] The latter two features are particularly important because macromolecules and nano-scale materials with very long circulation times must be biodegraded in order to prevent long-term accumulation. In addition, bis-MPA dendrimers are commercially available. We have already shown that Bis-MPA dendrimers of high generation can be prepared with an easily removable core protecting group that enables the

introduction of a single dipicolyl amine (DPA) ligand at the dendrimer core.[38] This allows for site-specific radiolabeling with ^{99m}Tc, the most commonly used γ-emitting radionuclide in diagnostic imaging.[39]

In our previous work, we produced a series of monodisperse, well characterized dendrimers up to the 7th generation, that contained a single ^{99m}Tc atom chelated at the core.[38] Single Photon Emission Computed Tomography (SPECT) imaging allowed real-time *in-vivo* monitoring of these Bis-MPA dendrimer structures upon injection into the bloodstream of rats. These studies showed that the circulation time of the dendrimers, regardless of generation, was extremely short, with nearly complete clearance from the blood into the bladder within fifteen minutes post injection.[38] This rapid clearance was most likely the result of their low hydrodynamic diameter, as the highest generation structure had a diameter on the order of 3-4 nm. Considering that the renal clearance threshold is 5 nm,[40] it is not surprising that these structures were rapidly filtered from the bloodstream via the kidneys. This rapid clearance was problematic as it prevents dendrimer accumulation within tumors via the enhanced permeability and retention (EPR) effect; a well-documented passive tumor targeting method that depends on long blood circulation times.[41–47] In order to lengthen dendrimer circulation time, it is necessary to increase the hydrodynamic diameter of the bis-MPA dendrimers without affecting their water-solubility and biocompatibility. To achieve this, we embarked upon their surface functionalization with poly(ethylene glycol) chains, a strategy commonly referred to as PEGylation.[48–54]

PEGylation is known to increase the circulation time of proteins, macromolecules, and nanoparticles, allowing their passive uptake in tumors through the EPR effect. Two features

of PEGylation are responsible for the increased circulation time *in-vivo*, including an increase in the hydrodynamic diameter of the PEGylated species, which impedes clearance through the kidneys,[55,56] and an increase in hydrophilicity of the structure, which reduces the ability of opsonins to bind to its surface.[50–52] PEGylation is therefore considered an effective way to control the pharmacokinetics of various nano-scale structures in therapeutic applications, and has resulted in a number of PEGylated pharmaceuticals undergoing clinical trials and FDA approval.[60,61] Here, we describe the preparation of high-generation dendrimers that have been surface-PEGylated via the thiol-ene "click" reaction and subsequently radiolabeled with ^{99m}Tc at their core. These novel dendrimers have a hydrodynamic diameter above the renal clearance threshold, and are shown to exhibit long circulation times when injected in healthy animal models. Upon injection into the bloodstream of nude mice bearing squamous cell (H520) xenograft tumors, these PEGylated bis-MPA dendrimers were found to accumulate in the tumor, allowing for visualization by SPECT imaging.

2.3 Materials and Methods

Materials

All chemicals used were sourced from Sigma Aldrich and used as supplied without further purification unless otherwise noted. 2-pyridinecarboxaldehyde was freshly distilled prior to use.

Structural Characterization

NMR spectroscopy was performed on either a Bruker AVANCE AV600 spectrometer at 600 MHz or a Bruker AVANCE AV700 at 700 MHz. $CDCl_3$ and CD_3OD were used as solvents and the residual non-deuterated solvent signals were used as internal chemical shift references for both ^1H and ^{13}C spectra. MALDI spectra were acquired using a Bruker Ultraflextreme spectrometer in positive ion mode using dithranol as matrix. Exact masses were determined using a Micromass Q-TOF Global Ultima. Analytical HPLC was performed using a Waters 1525 Binary solvent pump using a Waters 2998 Photodiode Array detector and Bio-Rad IN/US γ-detector using a Phenomenex Luna C18(2) column (4.6 mm × 150 mm). The mobile phase consisted of chromatography grade water (A) and chromatography grade acetonitrile (B). The gradient protocol consisted of a 2 minute hold at 100% solvent A, then a gradient to 50% B from 2 minutes to 7 minutes, a three minute hold at 50% B, then a gradient to 100% B from 10 minutes to 15 minutes, with a 3 minute hold at 100% B, followed by a step gradient to 100% A, which was held for 5 minutes in order to equilibrate the column for subsequent runs. All HPLC runs were performed at a flow rate of 1 mL per minute, and were monitored at a wavelength of 254 nm. Dynamic light scattering data was collected on a Malvern Zetasizer Nano ZS instrument. A solution of 1 mg per mL of PEGylated dendrimer was made in 10 mM phosphate buffered saline, and this was filtered through a 0.22 micron Teflon® syringe filter into disposable polystyrene cuvettes. This sample was then placed in the instrument and equilibrated to 37 °C for five minutes. Instrument parameters were set automatically during the beginning of the run, and samples were run in triplicate with the average hydrodynamic diameter and

zeta potential calculated from the three runs. Zeta potential measurements were taken immediately after the DLS data using the same experimental conditions using a Malvern zeta potential dip cell. $^{99m}TcO_4^-$ was eluted from a $^{99}Mo/^{99m}Tc$ generator using 4 mL of 0.9% saline in order to sufficiently concentrate the resulting $^{99m}TcO_4^-$ for chelation to the dendrimers. *Caution: ^{99m}Tc is radioactive and should only be handled in an appropriately licensed and equipped laboratory.*

Synthesis of Dipicolylamine (DPA) Ligand

Synthesis of tert-butyl (4-aminobutyl)carbamate (**6**). 1,4-diaminobutane (0.5 g, 5.7 mmol) and *t*-butyl phenyl carbonate (1.0 g, 5.7 mmol) were added to a 50 mL flame dried round bottom flask, and dissolved in 20 mL of anhydrous ethanol, which was refluxed under an argon atmosphere for 16 hours. Solvent was removed *in vacuo*, then the residual oil was diluted with 20 mL of water and acidified to pH = 3 with 2 M HCl. This was extracted with CH_2Cl_2 (3 × 10 mL), then the aqueous phase was basified by the addition of 100 mL of 2 M NaOH. This was further extracted with CH_2Cl_2 (3 × 50 mL), dried over sodium sulfate, filtered on a glass frit and dried *in vacuo* to leave a yellow oil (0.689 g, 65%). ^{1}H-NMR (700 MHz; $CDCl_3$): δ 1.43 (d, *J* = 11.1 Hz, 9H), 1.47-1.44 (m, 2H), 1.51 (dt, *J* = 14.6, 7.1 Hz, 2H), 2.70 (d, *J* = 13.7 Hz, 2H), 3.12 (d, *J* = 6.0 Hz, 2H), 4.63 (d, *J* = 145.1 Hz, 1H). ^{13}C NMR (176 MHz; CDCl3): δ 27.63, 28.56, 31.02, 40.58, 41.97, 79.16, 156.13. MS Calc'd for $C_9H_{20}N_2O_2$ $[M]^+$ = 188.1525, $[M+H]^+$ = 189.1603. Found High Resolution ES MS $[M+H]^+$ 189.1603.

Synthesis of tert-butyl (4-(bis(pyridin-2-ylmethyl)amino)butyl)carbamate (**7**). 2-Pyridinecarboxaldehyde (2.05 g, 19.2 mmol) and **6** (1.2 g, 6.4 mmol) were added to a 50 mL flame dried round bottom flask along with 20 mL of dry CH_2Cl_2. Acetic acid (0.036 mL, 0.64 mmol) was added, and the mixture was stirred for 4 hours. The reaction mixture was cooled to 0 °C, then sodium triacetoxyborohydride (4.73 g, 22.3mmol) was added, producing a bright yellow colour. After 3 hours the solution was diluted with 60 mL of CH_2Cl_2, and washed with 1 M NaOH (3 × 50 mL). The reaction mixture was then dried over magnesium sulfate, filtered through a glass frit and solvent was removed *in vacuo* to give the product as a yellow oil (1.967 g, 83%). ^{1}H-NMR (700 MHz; $CDCl_3$): δ 1.42 (s, 9H), 1.46 (q, *J* = 7.3 Hz, 2H), 1.56 (t, *J* = 7.4 Hz, 2H), 2.55 (s, 2H), 3.06-3.00 (m, 2H), 3.80 (s, 4H), 4.70 (d, *J* = 191.2 Hz, 1H), 7.13 (dd, *J* = 6.8, 5.5 Hz, 2H), 7.49 (d, *J* = 7.8 Hz, 2H), 7.64 (td, *J* = 7.6, 1.6 Hz, 2H), 8.52 (d, *J* = 4.7 Hz, 2H). ^{13}C NMR (176 MHz; CDCl3): δ 24.41, 27.90, 28.59, 40.46, 54.07, 60.58, 122.04, 123.08, 136.49, 149.14, 156.12, 159.95. MS Calc'd for $C_{21}H_{30}N_4O_2$ $[M]^+$ = 370.2369, $[M+H]^+$ = 371.2447. Found High Resolution ES MS $[M+H]^+$ = 371.2441.

Synthesis of N^1,N^1-bis(pyridin-2-ylmethyl)butane-1,4-diamine (**8**). Mono-boc protected DPA Ligand **7** (200 mg, 0.5 mmol) was dissolved in 6 mL of CH_2Cl_2. This was cooled to 0 °C, and 3 mL of trifluoroacetic acid was added dropwise and stirred for 3 hours. This was basified by the dropwise addition of 2 M NaOH, and extracted with CH_2Cl_2 (3 × 10 mL). The organic layer was then dried *in vacuo*, resulting in yellow/orange oil. (114 mg, 79%). ^{1}H-NMR (600 MHz; $CDCl_3$): δ 1.45-1.41 (m, 2H), 1.59-1.54 (m, 2H), 2.54 (s, 2H), 2.63 (t, *J* = 7.0 Hz, 2H), 3.80 (s, 4H), 7.14-7.13 (m, 2H), 7.51 (d, *J* = 7.8 Hz, 2H), 7.63 (dd,

J = 7.6, 1.8 Hz, 2H), 8.52-8.51 (m, 2H).^{13}C NMR (151 MHz; CDCl3): δ 24.64, 31.49, 42.08, 54.39, 60.62, 122.07, 123.05, 136.53, 149.14, 160.03. MS Calc'd for $C_{16}H_{22}N_4$ $[M]^+$ = 270.1844, $[M+Na]^+$ = 293.1742. Found High Resolution ES MS $[M+H]^+$ = 293.1734.

Synthesis of mPEG$_{750}$-SH

Synthesis of Allyl mPEG$_{750}$ (**9**). PEG$_{750}$ monomethyl ether (10 g, 13.3 mmol) and allyl bromide (2.42 g, 20 mmol) were added to a 300 mL round bottom flask and dissolved in 100 mL of CH_2Cl_2. To this, 20 mL of saturated aqueous potassium hydroxide was added, and the reaction was left stirring. Immediately after addition of potassium hydroxide, the solution began to turn slightly yellow. After 1 hour, the aqueous layer was removed in a separatory funnel and washed with CH_2Cl_2 (1 × 20 mL), which was added to the remaining organic phase. This was dried over sodium sulfate, filtered through a glass frit and dried *in vacuo*, leaving the product as an off white waxy solid. (10.53 g, quant.) ^{1}H NMR ($CDCl_3$, 600 MHz): δ , 3.37 (s, 3 H), 3.53-3.55 (m, 2 H), 3.59-3.61 (m, 3 H), 3.65 (q, *J* 5.8 Hz, 61 H), 4.02 (dt, *J* = 5.7, 1.4 Hz, 2 H), 5.17 (dq, *J* = 10.4, 1.5 Hz, 1 H), 5.25-5.28 (m, 1 H) 5.91 (ddt, *J* = 17.2, 10.4, 5.7 Hz, 1 H).

Synthesis of mPEG$_{750}$ thioacetate (**10**). Allyl PEG$_{750}$ monomethyl ether **9** (2.00 g, 2.53 mmol) was added to a 20 mL scintillation vial, along with 2,2-dimethoxy-2-phenylacetophenone (20 mg, 0.005 mmol). These were dissolved in 8 mL of HPLC-grade THF, and then thioacetic acid (250 mg, 3.2 mmol) was added. This was degassed with argon for 10 minutes, then irradiated with 365nm UV light for 2 hours. Solvent and excess thioacetic acid were removed *in vacuo*, leaving the product as a waxy yellow solid. (2.12

g, 97%). ^{1}H NMR ($CDCl_3$, 600 MHz): δ 1.84 (quintet, *J* = 6.7 Hz, 2 H), 2.31 (s, 3 H), 2.93 (t, *J* = 7.2 Hz, 2 H), 3.36 (s, 3 H), 3.49 (t, *J* = 6.2 Hz, 3 H), 3.53 (dd, *J* = 5.6, 3.8 Hz, 3 H), 3.56 (dd, *J* = 5.9, 3.7 Hz, 3 H) 3.62 (t, *J* = 9.1 Hz, 70 H).

Synthesis of mPEG$_{750}$-SH (**11**). PEG_{750} Monomethyl ether thioacetate **10** (2.12 g, 2.45 mmol) was added to a 50 mL round bottom flask and put under an argon atmosphere. It was subsequently dissolved in 20 mL of deoxygenated 0.25 M NaOH, producing a yellow solution which rapidly turned orange, and stirred for 12 hours. This was subsequently acidified with 1 M sodium bisulfate (10 mL), causing the solution to turn from orange to yellow. This was extracted with CH_2Cl_2 (3 × 15 mL), dried over sodium sulfate, filtered through a glass frit and dried *in vacuo* to give the desired product as a waxy yellow solid.(1.98 g, 99%). ^{1}H NMR ($CDCl_3$, 600 MHz): δ 1.37 (t, *J* = 8.0 Hz, 1 H), 1.87 (quintet, *J* = 6.6 Hz, 2 H), 2.61 (q, *J* = 7.5 Hz, 2 H), 3.37 (s, 3 H), 3.54 (dd, *J* = 5.7, 4.0 Hz, 3 H), 3.58 (dd, *J* = 6.5, 4.2 Hz, 2 H), 3.61-3.63 (m, 63 H) 3.71-3.75 (m, 1 H).

Synthesis of Dendrimers

Synthesis of Pentenoic Acid Anhydride (**2**)**.** Pentenoic acid (6.45 g, 64.6 mmol) and dicyclohexylcarbodiimide (6.82 g, 33.1 mmol) were added to a flame dried 500 mL round bottom flask along with 300 mL of CH_2Cl_2. This was left to stir overnight under an argon atmosphere, and the resulting mixture was filtered on a sintered glass frit to remove the solids. The filtrate was concentrated *in vacuo* to yield a viscous yellow oil. (5.75 g, 98%).^{1}H NMR (CDCl3, 600 MHz): δ 2.42 (dt, 4H, J= 7.2, 6.6), 2.56 (t, 4H, J= 7.5), 5.07 (m, 4H), 5.81 (m, 2H).

Synthesis of pTSe-G5-(PTA)$_{32}$ (**3**). pTSe-G5-(OH)$_{32}$, (1.8 g, 0.5 mmol), pentenoic acid anhydride (5.5 g, 30.3 mmol), and 4-dimethylaminopyridine (370 mg, 3.0 mmol) were added to a flame dried 50 mL round bottom flask, along with 12 mL of CH_2Cl_2 and 4 mL of pyridine. This was stirred overnight, and the reaction mixture was washed with 1 M $NaHSO_4$ (4 × 10 mL), 10% Na_2CO_3 (3 × 10 mL), and brine (1 × 10 mL). This was then dried over sodium sulfate, filtered through a sintered glass frit and solvent was removed by rotary evaporation *in vacuo*. The resulting mixture was purified by silica gel chromatography using an eluent consisting of 10% ethyl acetate, 40% hexanes and 50% CH_2Cl_2, which was increased to 20% ethyl acetate, 30% hexanes 50% CH_2Cl_2 after excess pentenoic anhydride had eluted. The fractions containing product were dried under reduced pressure and were collected as a viscous yellow oil. (3.01 g, 97%). ^{1}H NMR (700 MHz; MeOD): δ 1.36-1.26 (m, 93H), 2.34 (q, J = 7.0 Hz, 64H), 2.44 (t, J = 7.3 Hz, 64H), 2.48 (s, 3H), 3.62-3.61 (m, 2H), 4.35-4.20 (m, 124H), 4.52-4.51 (m, 2H), 4.98 (dd, J = 10.3, 1.3 Hz, 32H), 5.05 (dd, J = 17.2, 1.5 Hz, 32H), 5.86-5.80 (m, 32H), 7.49 (d, J = 8.2 Hz, 2H), 7.85 (d, J = 8.2 Hz, 2H). ^{13}C NMR (176 MHz; MeOD): δ 18.18, 18.34, 18.41, 29.92, 34.29, 47.75, 48.06, 66.48, 66.63, 67.11, 67.25, 67.67, 116.19, 129.37, 131.37, 138.03, 173.09, 173.15, 173.56, 173.87. MS Calc'd for $C_{324}H_{452}O_{128}S$ $[M]^+$ =6422.8581, $[M+Na]^+$ = 6445.8479. Found MALDI-TOF MS $[M+Na]^+$ = 6449.09.

Synthesis of COOH-G5-(PTA)$_{32}$ (**4**). pTSe-G5-(PTA)$_{32}$ (1 g, 0.15 mmol) and 1,8-diazabicycloundec-7-ene (0.25 mL, 1.5 mmol) were added to a flame dried 100 mL round bottom flask along with 50 mL of CH_2Cl_2 and stirred for 2 hours. This was washed with 1 M $NaHSO_4$ (2 × 20 mL), and solvent was removed by rotary evaporation *in vacuo*. Product

was isolated via silica gel chromatography in 1:1 EtOAc:Hexanes, resulting in a clear colourless oil. (900 mg, 93%). ^{1}H NMR (700 MHz; MeOD): δ 1.38-1.28 (m, 100H), 2.36 (q, *J* = 7.0 Hz, 64H), 2.46 (t, *J* = 7.3 Hz, 64H), 4.38-4.23 (m, 124H), 5.01 (dd, *J* = 10.3, 1.5 Hz, 32H), 5.09-5.07 (m, 32H), 5.85 (ddt, *J* = 17.0, 10.4, 6.5 Hz, 32H). ^{13}C NMR (176 MHz; MeOD): δ 18.33, 18.41, 29.92, 34.30, 47.92, 48.14, 66.48, 66.62, 67.08, 67.24, 67.92, 116.18, 138.03, 173.07, 173.16, 173.56, 173.88. MS Calc'd for $C_{315}H_{442}O_{126}$ $[M]^+$ =6240.8179, $[M+H]^+$ = 6241.8251. Found MALDI-TOF MS $[M+Na]^+$ = 6246.

Synthesis of NHS-G5-(PTA)$_{32}$. Synthesis of COOH-G5-(PTA)$_{32}$, (300 mg, 0.05 mmol), N-hydroxysuccinimide (22 mg, 0.2 mmol), 1-Ethyl-3-(3-dimethylaminopropyl)carbodiimide hydrochloride (30 mg, 0.2 mmol) were added to a 10 mL flame-dried round bottom flask, to which 2 mL of dry CH_2Cl_2 was added. This was stirred overnight and the resulting mixture was purified by column chromatography with 3:2 EtOAc:Hex. This was then dried *in vacuo* resulting in a clear, colourless oil. (302 mg, 99%). The product was used immediately after purification to ensure that the NHS ester did not hydrolyze. ^{1}H NMR (600MHz, $CDCl_3$): δ 1.35-1.21 (m, 93H), 2.38-2.32 (m, 64H), 2.46-2.39 (m, 64H), 2.86 (s, 4H), 4.39-4.15 (m, 124H), 5.09-4.97 (m, 64H), 5.80 (tdd, J = 6.3, 10.4, 16.9 Hz, 32H).

Synthesis of DPA-G5-(PTA)$_{32}$ (**5**). NHS-G5-(PTA)$_{32}$ (300 mg, 0.05 mmol), DPA ligand **8** (30 mg, 0.1 mmol), and triethylamine (0.07 mL, 0.25 mmol) were added to a 10 mL flame dried round bottom flask, and dissolved in 5 mL of dry CH_2Cl_2. This was stirred at room temperature for 3 days, then purified via column chromatography on silica gel with 5% methanol in CH_2Cl_2. The product fractions were collected and dried *in vacuo*, resulting in a slightly yellow oil. (298 mg, 97%). ^{1}H NMR (MeOD, 700 MHz): δ 1.26-1.35 (m, 93 H),

1.50-1.55 (m, 2 H), 1.59-1.64 (m, 2 H), 2.34 (q, *J* = 6.8 Hz, 64 H), 2.43 (t, *J* = 7.3 Hz, 64 H), 2.58 (t, *J* = 7.0 Hz, 2 H), 3.17-3.19 (m, 2 H), 3.80 (s, 4 H), 4.20-4.33 (m, 124 H), 4.98 (d, *J* = 10.2 Hz, 32 H), 5.05 (d, *J* = 17.2 Hz, 32 H), 5.82 (dd, *J* = 17.0, 10.4 Hz, 32 H), 7.28 (t, *J* = 6.2 Hz, 2 H), 7.63 (d, *J* = 7.7 Hz, 2 H), 7.79 (t, *J* = 7.6 Hz, 2 H) 8.44 (d, *J* = 4.5 Hz, 2 H). ^{13}C NMR (176 MHz; MeOD): δ 18.42, 25.54, 28.50, 29.92, 34.30, 40.78, 47.74, 48.03, 48.05, 55.40, 61.05, 66.46, 66.61, 67.02, 67.17, 68.56, 116.19, 123.79, 124.81, 138.02, 138.61, 149.58, 173.07, 173.14, 173.55, 173.85. MS Calc'd for $C_{330}H_{460}N_4O_{125}$ $[M]^+$ =6478.9761, $[M+NH_4]^+$ = 6497.0099. Found MALDI-TOF MS $[M+NH_4]^+$ = 6494.47.

Synthesis of DPA-G5-PEG$_{750}$ (**12**). DPA-G5-(PTA)$_{32}$ (100 mg, 0.015 mmol) and mPEG$_{750}$-SH **11** (1.21g, 1.49 mmol) were added to a 20 mL scintillation vial, along with 2,2-dimethoxy-2-phenylacetophenone (7 mg, 0.025 mmol). To this, 8 mL of HPLC grade THF was added and the reaction mixture was stirred until all components dissolved. This was sparged with argon with sonication for 15 minutes, then irradiated with UV at 365nm for 24 hours. After 24 hours, an additional 7 mg aliquot of 2,2-dimethoxy-2-phenylacetophenone was added, and the reaction was irradiated for a further 72 hours. Solvent was removed by rotary evaporation, and the resulting viscous orange oil was redissolved in ethanol. This was added dropwise to 500 mL of diethyl ether at 0 °C then left to warm to room temperature. The product phase separated as a viscous oil on the bottom of the flask. The residual ether was decanted and the procedure was repeated to give the final product. (201 mg, 40%). ^{1}H NMR ($CDCl_3$, 700 MHz): δ 1.28-1.34 (m, 105 H), 1.63 (s, 56 H), 1.72 (s, 50 H), 1.83 (s, 53 H), 2.39 (s, 67 H), 2.58 (d, *J* = 32.6 Hz, 95

H), 3.36 (s, 47 H), 3.54-3.64 (m, 1 H), 4.24-4.33 (m, 124 H), 5.01-5.10 (m, 15 H) 5.85 (s, 7 H). MALDI-TOF MS produced a broad mass distribution centered around m/z = 18,800 Da (PDI = 1.01) due to the polydispersity of PEG chains.

Radiolabeling Procedures

Synthesis of $^{99m}Tc(CO)_3(H_2O)_3$. To a 5mL Biotage microwave vial were added sodium potassium tartrate (22 mg, 0.078 mmol), sodium borate decahydrate (20 mg, 0.052 mmol), sodium carbonate (15 mg, 0.14 mmol) and potassium boranocarbonate (10 mg, 0.075 mmol), then the vial was sealed with a septum and purged with nitrogen gas for 15 minutes. Approximately 2960 MBq (80 mCi) of sodium pertechnetate (Na $^{99m}TcO_4$) in 4 mL of 0.9% saline was added to the vial. This was heated in a microwave reactor to 110 °C for 4 minutes. This was cooled to room temperature, then the pH adjusted to 6.5 by the dropwise addition of 1 M HCl.

Synthesis of ^{99m}TcDPA-G5-PEG750. To a 2 mL Biotage microwave vial was added 2 mg of BisPy-G5-PEG_{750} dissolved in 0.1 mL of water and 925 MBq (25 mCi) of $[^{99m}Tc(CO)_3(H_2O)_3]^+$ in 0.9% saline (1 mL) was added. The vial was sealed with a septum and purged for 10 minutes with nitrogen gas, then heated in a microwave reactor for 15 minutes at 120 °C. The reaction was cooled to room temperature, and 5 mg of histidine dissolved in 0.30 mL of 0.9% saline was added via syringe. The reaction mixture was heated to 150 °C in a microwave reactor for five minutes, and upon cooling the entire reaction mixture was passed through three GE HiTrap desalting columns in series to isolate the high molecular weight products. The final mixture was dried on a centrifugal

evaporator and re-dissolved in 0.5 mL of deionized water. The desired product was isolated by HPLC to yield the radiochemically pure labeled dendrimer. The collected HPLC eluate was dried using a centrifugal V10 evaporator (Biotage), and re-dissolved in sterile 0.9% saline to a concentration of 185 MBq per mL (5 mCi per mL).

Biological & Imaging Procedures

Cell lines

NCI-H520 (H520) cells derived from human lung squamous cell carcinoma were purchased from ATCC (HTB-182) and maintained in DMEM with supplemented with 10% FBS, and 1% Penicillin Streptomycin.

Animal Studies

All animal studies were approved by the Animal Research Ethics Board at McMaster University. Mice, female CD1 nu/nu ordered from Charles River Laboratories, were maintained under clean conditions in an established animal facility with 12 hour light/dark cycles and given food and water *ad libitum*. Rats, male Copenhagen ordered from Charles River Laboratories, were maintained under Specific Pathogen Free (SPF) conditions in an established animal facility with 12 hour light/dark cycles and given food and water *ad libitum*.

Tumor Inoculation

Female 4-5 week old CD1 nu/nu mice were injected with 2.0×10^6 H520 cells in Matrigel:DPBS (1:1) subcutaneously into the right flank. Imaging studies were conducted two weeks following tumour inoculation.

Imaging Study

X-ray images were acquired using a conebeam X-SPECT scanner (Gamma Medica, Northridge, USA) with a source voltage of 75 kVp and a current of 165 μA at the McMaster Centre for Preclinical and Translational Imaging. Projection data was acquired with 1024 projection angles (1184×1120 pixels, 0.100 mm pixels) and reconstructed using a Feldkamp cone beam backprojection algorithm in COBRA (Exxim Software, Pleasanton, CA, USA) into 512×512×512 arrays (0.155 mm isotropic voxels). A water-filled tube was included within each scan in order to convert the voxel values to Hounsfield units (HU). SPECT images were acquired on an X-SPECT system (Gamma Medica, Northridge, USA), using dual sodium iodide crystals in combination with low-energy, high-resolution, parallel-hole collimators. A total of 64 projections over 360° were acquired with an energy window of 159 ± 10% keV and then reconstructed using an OS-EM iterative reconstruction method (2 iterations/8 subsets) into 82×82×82 arrays (1.463 mm isotropic voxels) using in-house software. CT images were compressed to a 256^3 matrix (0.31 mm isotropic voxels). Fusion was achieved by a rigid-body (linear) transformation of the SPECT image, during which, it is interpolated and resampled to the same matrix dimensions and voxel size as the compressed CT image. Rats were injected with approximately 25 MBq in 0.9% NaCl via the tail vein. Dynamic images were collected from time of injection until 0.5 h post-injection with images being acquired every 15 seconds. Whole body SPECT/CT images were acquired at 4 h (10 sec projections) and 22 h (30 sec projections) post-injection. Mice were injected with approximately 9 MBq in 0.9% NaCl via the tail vein.

Whole body SPECT/CT images were acquired at 2 h (20 sec projections) and 6 h (40 sec projections) post-injection. Imaging analysis was completed using AMIDE software.

2.4 Results and Discussion

Synthesis of the 5th generation bis-MPA dendron (**1**) with hydroxyl groups at the periphery and a protected acid group at the core was accomplished following our previously reported protocol.[38] To PEGylate the periphery of this dendron, we chose to investigate the thiol-ene click reaction due to its orthogonal nature to the functional groups present in the dendron backbone, as well as its previous use in functionalizing high generation dendrimers.[62–64] We therefore modified the periphery of dendron **1** with vinyl groups via reaction with pentenoic acid anhydride (PTA, **2**) in a manner directly analogous to the dendrimer growth steps (Scheme 2.1). This procedure resulted in quantitative conversion of the 32 peripheral hydroxyl groups in 95% isolated yield (see Supporting Information for complete details and characterization).

After functionalizing the periphery with alkenes, the para-toluenesulfonylethanol (pTSe) core was removed by treating the dendron with an excess of DBU in dichloromethane, which allowed quantitative conversion to the carboxylic acid (Scheme 2.1). The resultant carboxylic acid was then activated by forming the *N*-hydroxysuccinimidyl ester, followed by efficient amidation with an aminobutyldipicolylamine ligand used for chelating $[^{99m}Tc(CO)_3]^+$ which was synthesized according to a previously reported procedure.[38] Each of these structures was characterized by NMR (Figure 2.1), as well as MALDI-TOF mass spectrometry (Figure 2.2), which shows the conversion from the protected TSe-G5-

$(PTA)_{32}$ (**3**) to the deprotected acid at the core (**4**), and finally to the ligand-functionalized structure (**5**).

Once the alkene-functionalized dendrimers were synthesized, thiol terminated poly(ethylene glycol) (PEG-SH) was required for peripheral PEGylation. Three molecular weights of PEG-SH were synthesized, including triethylene glycol, PEG_{350}, and PEG_{750}. This was accomplished by first alkylating the PEG-OH monomethyl ether with allyl bromide under phase transfer conditions (Scheme 2.2). The resulting MeO-PEG-(alkene) was then treated with a slight excess of thioacetic acid using 2,2-dimethoxy-2-phenylacetophenone (DMPA) photoinitiator and irradiated with 354 nm light to produce thioacetate terminated PEG. Hydrolysis with 0.2 M KOH liberated the desired PEG-SH in 90% overall yield.

Scheme 2.1. Synthesis of the 5th generation dendrimer bearing vinyl groups at the periphery and the DPA ligand at the core.

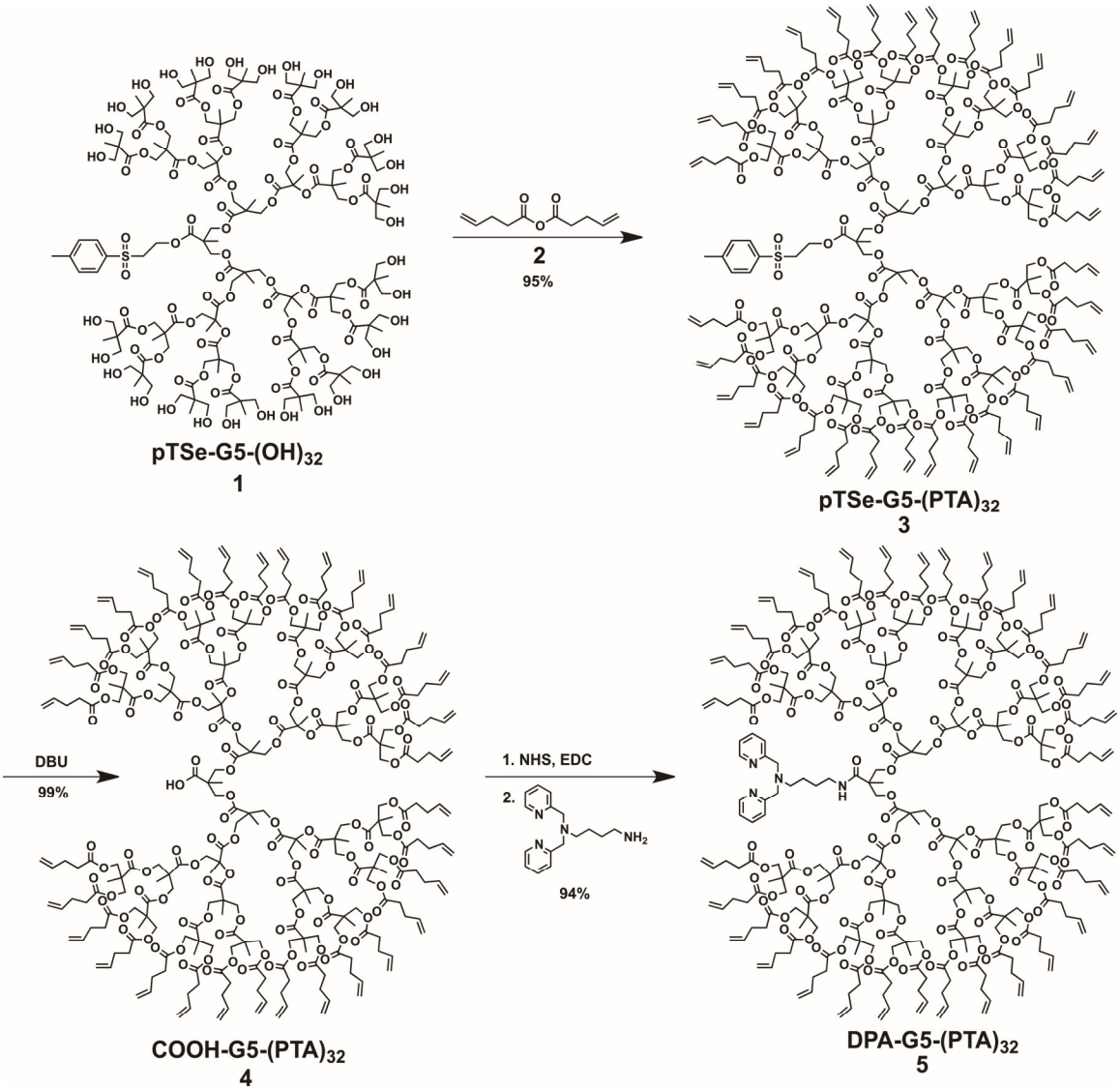

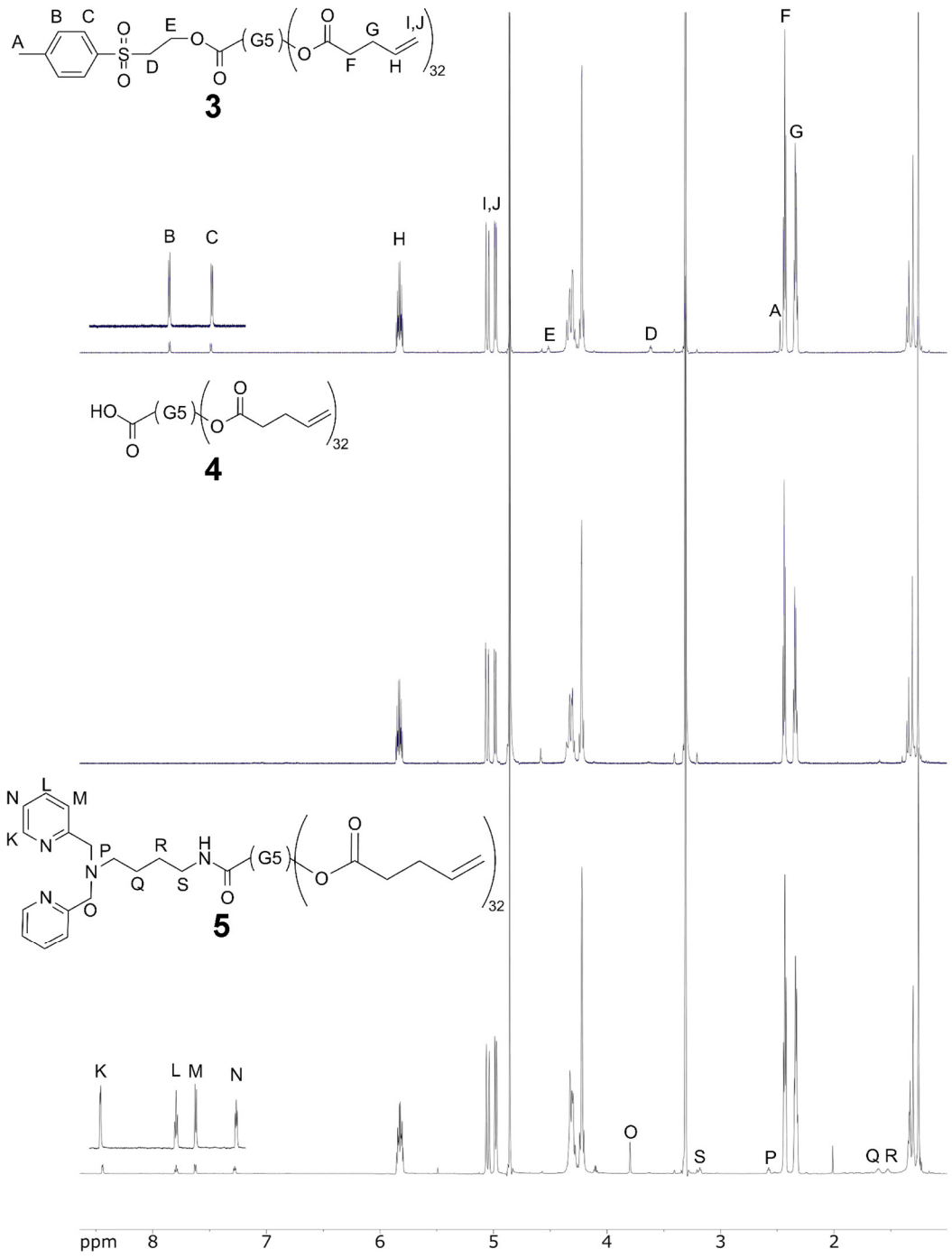

Figure 2.1.[1]H NMR (700 MHz) spectra of TSe-G5-PTA$_{32}$ (3, top), COOH-G5-PTA$_{32}$ (4, middle), and DPA-G5-PTA$_{32}$ (5, bottom), all in CD_3OD. Insets show magnified view of aromatic signals for 3 and 5.

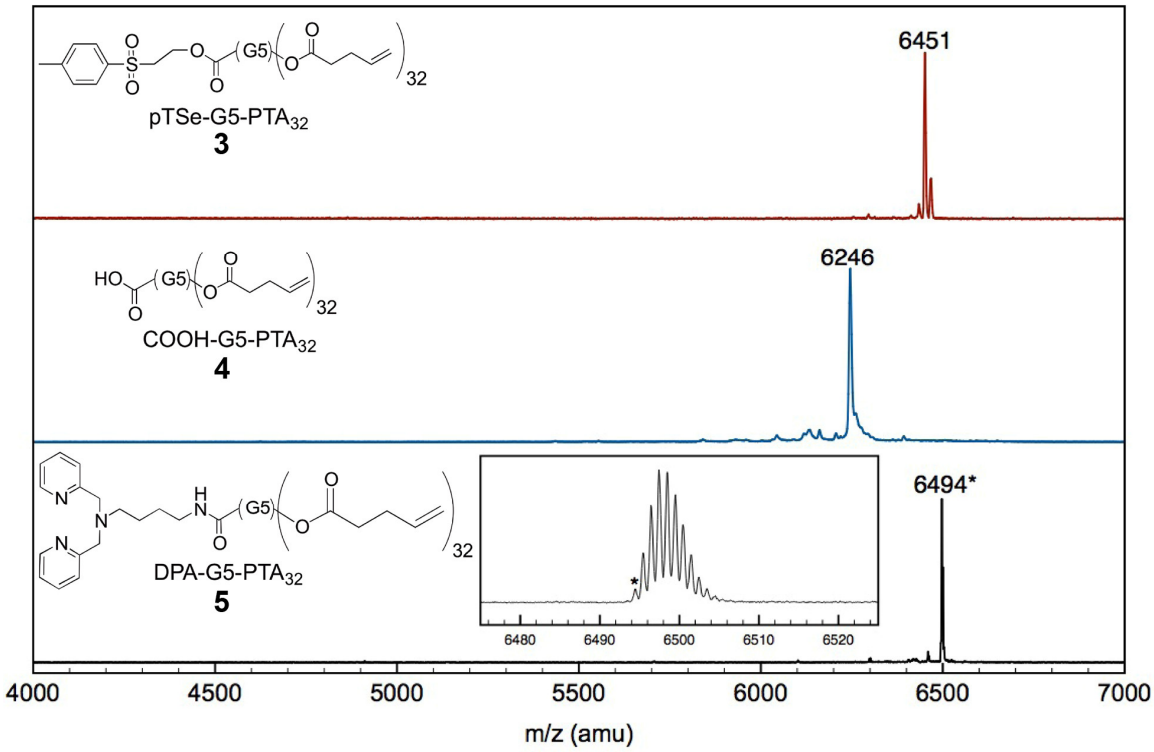

Figure 2.2. MALDI-TOF spectra of TSe-G5-PTA_{32} (top), COOH-G5-PTA_{32} (middle), and DPA-G5-PTA_{32} (bottom).

Scheme 2.2. Preparation of PEG_{750}-SH.

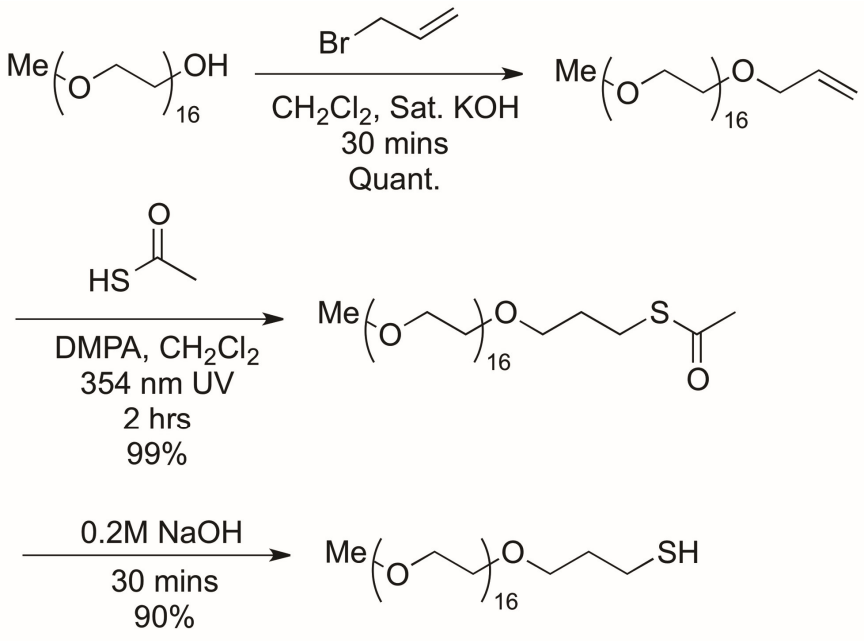

Thiol-ene click reactions on DPA-G5-$(PTA)_{32}$ were first attempted with the thiol derivative of triethylene glycol (TEG-SH). It was found that with the short TEG-SH, the thiol-ene reaction resulted in complete functionalization of the dendrimer in 16 hours, as confirmed by ^{1}H NMR spectroscopy via disappearance of the alkene protons. Complete functionalization with the longer PEG_{350}-SH required a higher concentration of PEG_{350}-SH (0.25 M vs. 0.1 M with TEG-SH), and a longer reaction time of 48 hours, again confirmed by ^{1}H NMR spectroscopy. However, when performing the thiol-ene reaction with PEG_{750}-SH, complete functionalization could not be achieved. Based on the integration of the residual alkene protons in the ^{1}H NMR, it was determined that a maximum of 24 of the 32 peripheral alkene groups were converted. Attempts to drive the reaction to higher conversion by increasing the amount of PEG_{750}-SH, photoinitiatior, or reaction time, were unsuccessful. We attribute the inability to fully functionalize the

periphery with PEG_{750}-SH to the extreme steric bulk around the residual alkene sites once most of the periphery is covered with PEG_{750}-SH. Interestingly, MALDI-TOF MS analysis of the product (Figure 2.3) indicated an M_n of 18 800 (PDI = 1.01), which corresponds to only 16 PEG_{750}-SH chains at the dendrimer periphery. This underestimation likely results from a bias toward lower molecular weight structures, which are easier to ionize and ablate into the gas phase during the MALDI-TOF measurement.

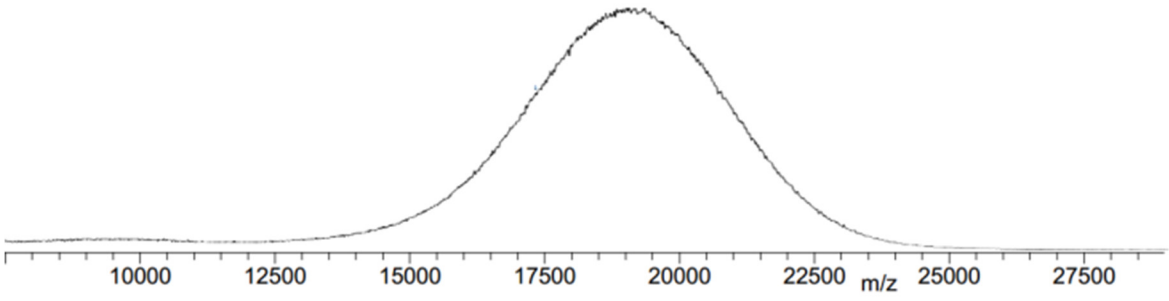

Figure 2.3. MALDI-TOF mass spectrum of DPA-G5-(PEG_{750}).

Dynamic light scattering (DLS) was used to characterize the hydrodynamic diameter of each of the PEGylated dendrimers. For both the DPA-G5-(TEG) and DPA-G5-(PEG_{350}), DLS showed that the dendrimers were not completely soluble in water, as they were found to aggregate to particle sizes of ~200 nm (data not shown). However, the DPA-G5-(PEG_{750}) was found to be readily soluble, giving a hydrodynamic diameter of 9.2 ± 2.1 nm (Figure 2.4). This is significantly larger than the renal clearance threshold, so we expected this structure to exhibit a long circulation time in vivo, despite incomplete functionalization of its periphery. Additionally, the zeta potential was measured and found to be +3.11 mV, which is very close to electrically neutral and is thus not expected to

strongly interact with charged groups in various tissues and organs (specifically, the liver and kidneys).

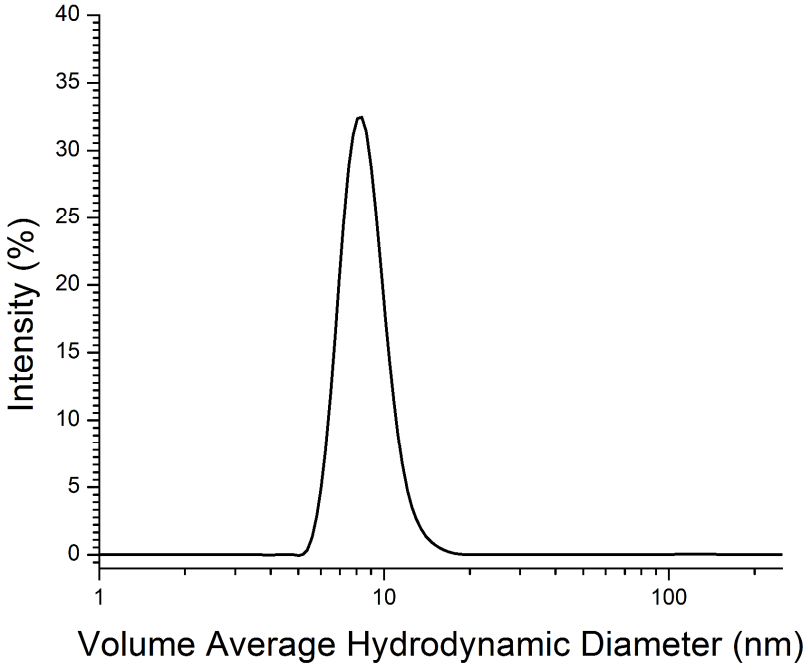

Figure 2.4. Volume average dynamic light scattering data for DPA-G5-(PEG_{750}).

Radiolabeling of DPA-G5-(PEG_{750}) with ^{99m}Tc was accomplished using the technetium tricarbonyl tris aqua $[^{99m}Tc(CO)_3(H_2O)_3]^+$ species, generated by the reduction of sodium pertechnetate ($Na^{99m}TcO_4$) using a modified procedure based on the work of Alberto and co-workers.[65–67] Addition of $[^{99m}Tc(CO)_3(H_2O)_3]^+$ to an aqueous solution of DPA-G5-(PEG_{750}) in a microwave vial was followed by purging the headspace of the vial with nitrogen for 10 min, and microwave heating to 120 °C for 15 min to yield $[^{99m}$TcDPA-G5-$(PEG_{750})]^+$ (Scheme 2.3). Since both the polyester backbone of the dendrimer and the PEG chains can weakly coordinate $[^{99m}Tc(CO)_3]^+$, the reaction mixture was subsequently challenged with 5 mg of histidine in deionized water and heated using microwave

irradiation to 150 °C for five min. The resulting mixture was passed through three SEC HiTrap desalting cartridges (GE Healthcare), which completely removed ^{99m}Tc not bound to the chelate. This was verified by a second histidine challenge on the purified material, which showed no radiolabeled histidine by HPLC. The proportion of loosely-bound ^{99m}Tc was approximately 40%, based on the activity remaining in the collected fractions after size exclusion chromatography.

Scheme 2.3. Radiolabeling of DPA-G5-(PEG_{750})

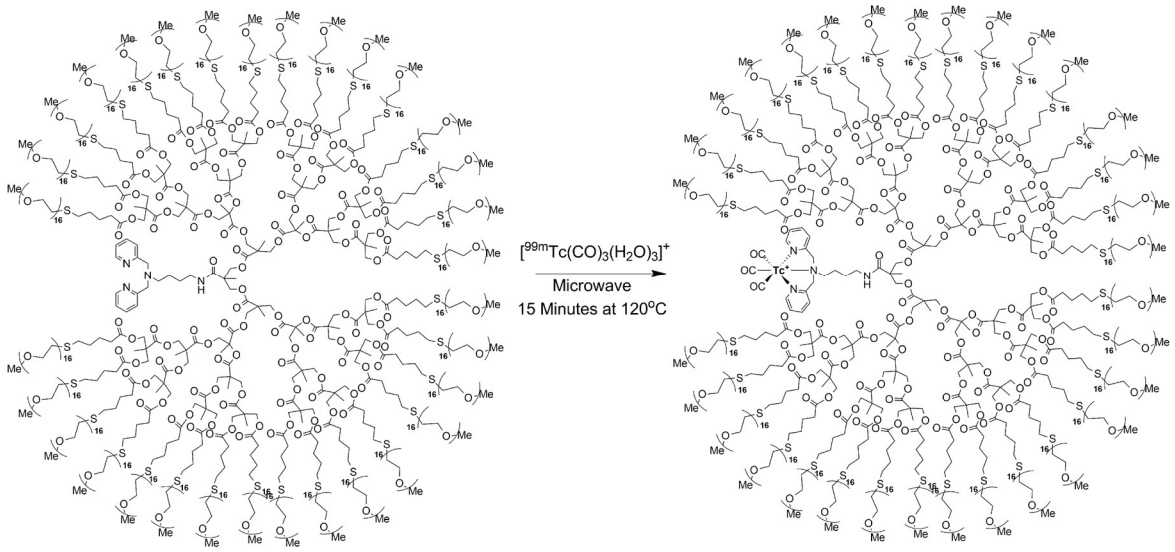

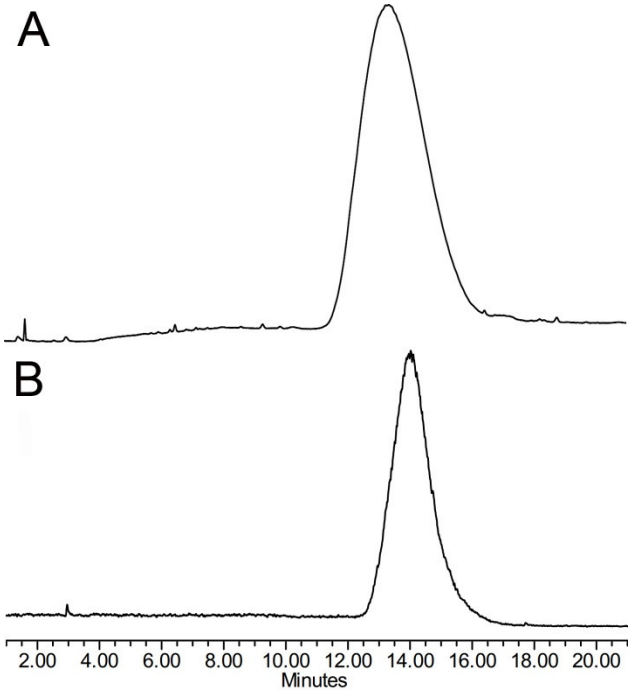

Figure 2.5. HPLC chromatograms of DPA-G5-(PEG_{750}) (A, UV detection) and [^{99m}TcDPA-G5-(PEG_{750})]$^{+}$ (B, gamma detection).

HPLC characterization of the purified, radiolabeled dendrimer, [^{99m}TcDPA-G5-(PEG_{750})]$^{+}$, indicated that there was no measurable change in the retention time of the radiolabeled dendrimer compared to the free ligand, which is expected due to the peripheral $mPEG_{750}$ chains that dominate the polarity and properties of these structures (Figure 2.5). The slight narrowing in the peak, as well as its slightly shifted retention time, is likely due to the significantly greater amount of material required to detect the unlabeled dendrimer with the UV detector compared to that needed to visualize the product in the gamma trace. After purification, [TcDPA-G5-PEG_{750}]$^{+}$ was produced in 14% ± 2% radiochemical yield in >99% radiochemical purity. Although the final yield of product was low, the synthesis

can be routinely carried out starting with 925 MBq (25 mCi) of $Na^{99m}TcO_4$ eluted from the generator, which produces sufficient quantities of labeled compound for SPECT imaging studies.

Imaging Studies. SPECT imaging was performed using a Gamma Medica X-SPECT system where the labeled dendrimer (25 MBq, 700 μCi) in 0.9% saline was injected into the tail vein of two anesthetized male Copenhagen rats. Copenhagen rats were chosen in order to allow for a direct comparison of circulation time with our previous studies using bis-MPA dendrimers with hydroxyl groups at their periphery.[38] The biodistribution was monitored by a dual head detector system with high-resolution parallel beam collimators, having a reconstruction field of view of 125 × 125 × 125 mm, with 3-4 mm spatial resolution. Individual images were collected every 15 s for the first thirty minutes of the dynamic scan. At thirty minutes, two hours, and 22 hours, SPECT scans were acquired with 10-second projections at the 2-hour time point, and 30-second projections at the 22-hour time point. Figure 6 shows individual images from the dynamic scan, each produced from 30-second acquisitions (see Supporting Information for the corresponding time-lapse video). From these images, it is clearly visible that the majority of the injected activity remains in the blood pool, the heart, and the lungs, with a small amount of activity being excreted into the kidneys. At the two-hour time point, activity is predominantly seen in the heart and lungs again, with very little activity remaining in the bladder. At 22 hours, activity is seen throughout the abdomen, and very little remains in the heart and lungs. This seems to indicate clearance of the dendrimer from the blood to the lymphatic system as well as

the liver and spleen, which have previously been identified as a method of nanoparticle elimination. [12,29]

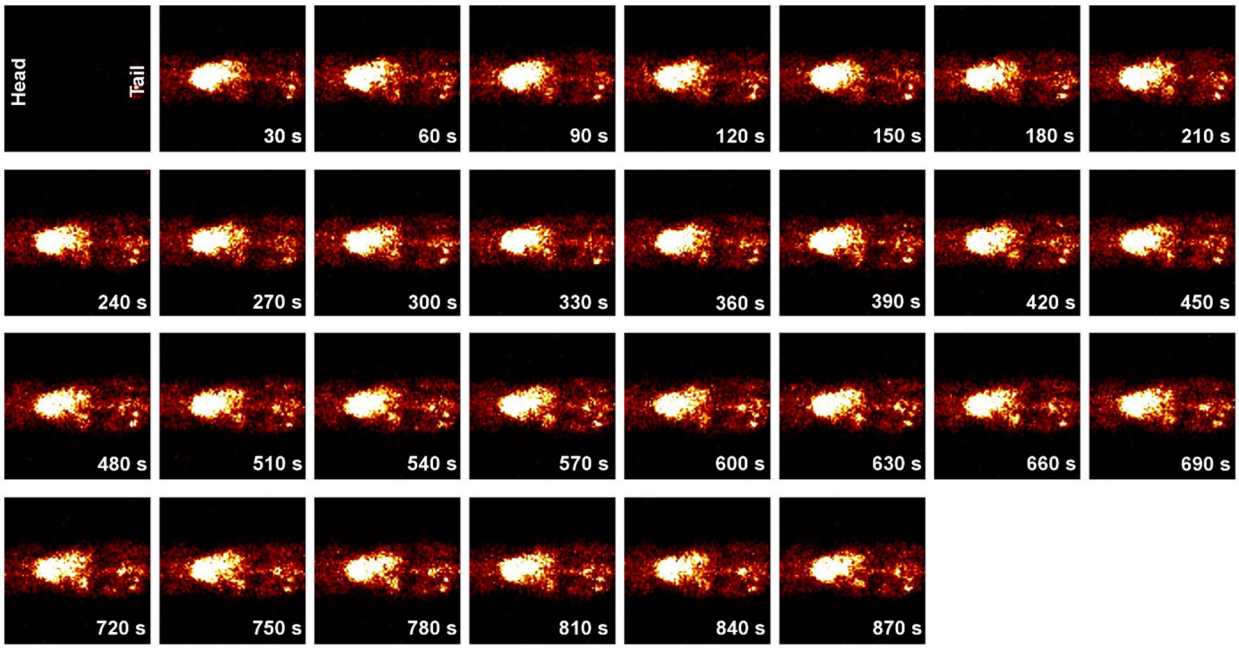

Figure 2.6. 2-D Scintigraphic images from the dynamic scanning study of [^{99m}TcDPA-G5-PEG$_{750}$]$^{+}$ in rats. Each of the images shown covers 30 seconds beginning in the top left during the course of the first 15 min after injection.

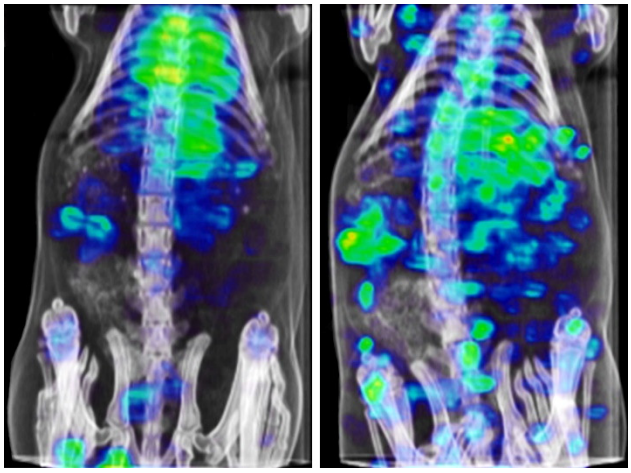

Figure 2.7. Scintigraphic-CT images of [^{99m}TcDPA-G5-(PEG$_{750}$)]$^{+}$at 2 hours post injection (left) and 21.5 hours post injection (right).

Having confirmed that the circulation time of the PEGylated dendrimers increased dramatically over that of unPEGylated dendrimers, and was sufficiently long to allow tumor uptake via the EPR effect, preliminary tumor imaging studies were undertaken. Three CD1 nude mice, bearing two week old subcutaneous squamous cell (H520) tumors on their right flank, were injected, via the tail vein, with approximately 7.5-10.4 MBq (200-280 μCi) of [^{99m}TcDPA-G5-(PEG$_{750}$)]$^{+}$, and SPECT images were acquired at two and six hours post injection. After two hours, most of the injected dose remained in circulation, with little uptake of the [TcDPA-G5-(PEG$_{750}$)]$^{+}$ observed in the tumors. However, at the six-hour time point, uptake in the tumors was clearly visible in two of the three mice (Figure 2.8). This provides compelling evidence that the radiolabeled, PEGylated, long-circulating dendrimers are able to accumulate in tumors, most likely via the EPR effect. It should be noted that, upon excision of the tumors after imaging, we found that the one mouse that did not show tumor uptake during SPECT imaging had a tumor that was

approximately half the volume of the other two. This small tumor was likely poorly vascularized in comparison to the larger tumors, and so accumulation of the dendrimer within that tumor was impaired. While additional validation studies are needed in a larger cohort of animals, this work opens the possibility for using the PEGylated dendrimer reported here as a theranostic scaffold for delivering chemotherapeutic agents to tumors via the EPR effect, while simultaneously imaging the delivery process by SPECT-CT.

Figure 2.8. Scintigraphic-CT image of H520 tumor model six hours post injection of $[^{99m}TcDPA\text{-}G5\text{-}(PEG_{750})]^{+}$ (9.2 MBq). H – heart, L – lungs, B – bladder, T – tumor.

2.5 Conclusion

In this work, high generation bis-MPA dendrimers were synthesized with a dipicolyl amine chelate at the core, and alkene functionalities at the periphery. These alkene-terminated dendrimers were PEGylated via thiol-ene "click" coupling using PEG_{750}-SH, resulting in PEGylated high-generation dendrimers with a near-zero zeta potential and a

hydrodynamic diameter of ~7 nm, slightly above the renal clearance threshold. These structures could be radiolabeled with $^{99m}Tc(CO)_3$ to produce dendritic SPECT imaging agents. Injection of these agents into healthy Copenhagen rats and imaging via SPECT indicated that they circulated in the blood for up to 24 hours, making them acceptable for tumor delivery via EPR. When imaging mouse models inoculated with H520 tumor cells, dendrimer accumulation within the tumor was clearly evident 6 hours post injection. This work demonstrates that PEGylation of the fifth-generation bis-MPA dendrimer scaffold with PEG_{750} chains produces structures that are large and hydrophilic enough to exhibit extended blood circulation times and avoid rapid renal clearance, opening the possibility for accumulation within tumors through the EPR effect.

2.6 References

(1) Ringsdorf, H. Structure and Properties of Pharmacologically Active Polymers. *J. Polym. Sci. Polym. Symp.* **1975**, *51* (1), 135–153.

(2) Kopeček, J. Soluble Biomedical Polymers. *Polim. Med.* **1977**, *7* (3), 191–221.

(3) Bader, H.; Ringsdorf, H.; Schmidt, B. Water-Soluble Polymers in Medicine. *Angew. Makromol. Chemie* **1984**, *123/124*, 457–485.

(4) Kopeček, J.; Kopečková, P.; Minko, T.; Lu, Z. R. HPMA Copolymer-Anticancer Drug Conjugates: Design, Activity, and Mechanism of Action. *Eur. J. Pharm. Biopharm.* **2000**, *50*, 61–81.

(5) Duncan, R. The Dawning Era of Polymer Therapeutics. *Nat. Rev. Drug Discov.* **2003**, *2* (5), 347–360.

(6) Twaites, B.; de las Heras Alarcón, C.; Alexander, C. Synthetic Polymers as Drugs and Therapeutics. *J. Mater. Chem.* **2005**, *15*, 441.

(7) Pasut, G.; Veronese, F. M. Polymer-Drug Conjugation, Recent Achievements and General Strategies. *Prog. Polym. Sci.* **2007**, *32*, 933–961.

(8) Park, J. H.; Lee, S.; Kim, J. H.; Park, K.; Kim, K.; Kwon, I. C. Polymeric Nanomedicine for Cancer Therapy. *Prog. Polym. Sci.* **2008**, *33*, 113–137.

(9) Kopeček, J.; Kopečková, P.; Minko, T.; Lu, Z. R.; Peterson, C. M. Water Soluble Polymers in Tumor Targeted Delivery. *J. Control. Release* **2001**, *74*, 147–158.

(10) Jensen, K. D.; Nori, A.; Tijerina, M.; Kopečková, P.; Kopeček, J. Cytoplasmic Delivery and Nuclear Targeting of Synthetic Macromolecules. *J. Control. Release* **2003**, *87*, 89–105.

(11) Duncan, R. Polymer Conjugates for Tumour Targeting and Intracytoplasmic Delivery. The EPR Effect as a Common Gateway? *Pharm. Sci. Technol. Today* **1999**, *2* (11), 441–449.

(12) Byrne, J. D.; Betancourt, T.; Brannon-Peppas, L. Active Targeting Schemes for Nanoparticle Systems in Cancer Therapeutics. *Adv. Drug Deliv. Rev.* **2008**, *60* (15), 1615–1626.

(13) Vlerken, L. E. Van; Amiji, M. M. Multi-Functional Polymeric Nanoparticles for Tumour-Targeted. *Expert Opin. Drug Deliv.* **2006**, *3* (2), 205–216.

(14) Allen, T. M. Ligand-Targeted Therapeutics in Anticancer Therapy. *Nat. Rev. Cancer* **2002**, *2* (10), 750–763.

(15) Fréchet, J. M. J. Functional Polymers and Dendrimers : Reactivity , Molecular Architecture , and Interfacial Energy Author (s): Jean M . J . Fréchet Source : Science , New Series , Vol . 263 , No . 5154 (Mar . 25 , 1994), Pp . 1710-1715 Published by : American Associat. *Science* **1994**, *263* (5154), 1710–1715.

(16) Lee, C. C.; MacKay, J. A.; Fréchet, J. M. J.; Szoka, F. C. Designing Dendrimers for Biological Applications. *Nat. Biotechnol.* **2005**, *23* (12), 1517–1526.

(17) Fox, M. E.; Szoka, F. C.; Fréchet, J. M. J. Soluble Polymer Carriers for the Treatment of Cancer: The Importance of Molecular Architecture. *Acc. Chem. Res.* **2009**, *42* (8), 1141–1151.

(18) Nanjwade, B. K.; Bechra, H. M.; Derkar, G. K.; Manvi, F. V.; Nanjwade, V. K. Dendrimers: Emerging Polymers for Drug-Delivery Systems. *Eur. J. Pharm. Sci.* **2009**, *38* (3), 185–196.

(19) Harth, E. M.; Hecht, S.; Helms, B.; Malmstrom, E. E.; Fréchet, J. M. J.; Hawker, C. J. The Effect of Macromolecular Architecture in Nanomaterials: A Comparison of Site Isolation in Porphyrin Core Dendrimers and Their Isomeric Linear Analogues. *J. Am. Chem. Soc.* **2002**, *124* (9), 3926–3938.

(20) Dykes, G. M. Dendrimers: A Review of Their Appeal and Applications. *J. Chem. Technol. Biotechnol.* **2001**, *76* (9), 903–918.

(21) Bosman, a W.; Janssen, H. M.; Meijer, E. W. About Dendrimers: Structure, Physical Properties, and Applications. *Chem. Rev.* **1999**, *99* (7), 1665–1688.

(22) Hecht, S.; Fréchet, J. M. J. Dendritic Encapsulation of Function: Applying Nature's Site Isolation Principle from Biomimetics to Materials Science. *Angew. Chemie - Int. Ed.* **2001**, *40*, 74–91.

(23) Ornelas, C.; Pennell, R.; Liebes, L. F.; Weck, M. Construction of a Well-Defined Multifunctional Dendrimer for Theranostics. *Org. Lett.* **2011**, *13* (5), 976–979.

(24) Lo, S. T.; Kumar, A.; Hsieh, J. T.; Sun, X. Dendrimer Nanoscaffolds for Potential Theranostics of Prostate Cancer with a Focus on Radiochemistry. *Mol. Pharm.* **2013**, *10*, 793–812.

(25) Muthu, M. S.; Leong, D. T.; Mei, L.; Feng, S. S. Nanotheranostics - Application and Further Development of Nanomedicine Strategies for Advanced Theranostics. *Theranostics* **2014**, *4* (6), 660–677.

(26) Janib, S. M.; Moses, A. S.; MacKay, J. A. Imaging and Drug Delivery Using Theranostic Nanoparticles. *Adv. Drug Deliv. Rev.* **2010**, *62* (11), 1052–1063.

(27) Ma, X.; Zhou, Z.; Jin, E.; Sun, Q.; Zhang, B.; Tang, J.; Shen, Y. Facile Synthesis of Polyester Dendrimers as Drug Delivery Carriers. *Macromolecules* **2013**, *46* (1), 37–42.

(28) Kaminskas, L.; Boyd, J.; Karellas, P.; Krippner, G.; Lessene, R.; Kelly, B.; Porter, C. The Impact of Molecular Weight and PEG Chain Length on the Systemic Pharmacokinetics of PEGylated Poly L-Lysine Dendrimers. *Mol. Pharm.* **2008**, 1–15.

(29) Gillies, E. R.; Dy, E.; Fréchet, J. M. J.; Szoka, F. C. Biological Evaluation of Polyester Dendrimer: Poly(Ethylene Oxide) "Bow-Tie" Hybrids with Tunable Molecular Weight and Architecture. *Mol. Pharm.* **2005**, *2* (2), 129–138.

(30) Carlmark, A.; Malmström, E.; Malkoch, M. Dendritic Architectures Based on Bis-MPA: Functional Polymeric Scaffolds for Application-Driven Research. *Chem. Soc. Rev.* **2013**, *42*, 5858–5879.

(31) García-Gallego, S.; Nyström, A. M.; Malkoch, M. Chemistry of Multifunctional Polymers Based on Bis-MPA and Their Cutting-Edge Applications. *Prog. Polym. Sci.* **2015**, *48*, 85–110.

(32) Ihre, H.; Hult, A.; Söderlind, E. Synthesis, Characterization, and 1H NMR Self-Diffusion Studies of Dendritic Aliphatic Polyesters Based on 2,2-Bis(Hydroxymethyl)Propionic Acid and 1,1,1-Tris(Hydroxyphenyl)Ethane. *J. Am. Chem. Soc.* **1996**, *118* (27), 6388–6395.

(33) Ihre, H.; Hult, A.; Fréchet, J. M. J.; Gitsov, I. Double-Stage Convergent Approach for the Synthesis of Functionalized Dendritic Aliphatic Polyesters Based on 2,2-Bis(Hydroxymethyl)Propionic Acid. *Macromolecules* **1998**, *31* (13), 4061–4068.

(34) Ihre, H.; Jesús, O.; Fréchet, J. M. J. Fast and Convenient Divergent Synthesis of Aliphatic Ester Dendrimers by Anhydride Coupling. *J. Am. Chem. Soc.* **2001**, *123* (25), 5908–5917.

(35) Ihre, H. R.; Padilla de Jesús, O. L.; Szoka, F. C.; Fréchet, J. M. J. Polyester Dendritic Systems for Drug Delivery Applications: Design, Synthesis, and Characterization. *Bioconjug. Chem.* **2002**, *13* (Figure 1), 443–452.

(36) Padilla De Jesús, O. L.; Ihre, H. R.; Gagne, L.; Fréchet, J. M. J.; Szoka, F. C.

Polyester Dendritic Systems for Drug Delivery Applications: In Vitro and in Vivo Evaluation. *Bioconjug. Chem.* **2002**, *13*, 453–461.

(37) Feliu, N.; Walter, M. V.; Montañez, M. I.; Kunzmann, A.; Hult, A.; Nyström, A.; Malkoch, M.; Fadeel, B. Stability and Biocompatibility of a Library of Polyester Dendrimers in Comparison to Polyamidoamine Dendrimers. *Biomaterials* **2012**, *33* (7), 1970–1981.

(38) Parrott, M. C.; Benhabbour, S. R.; Saab, C.; Lemon, J. A.; Parker, S.; Valliant, J. F.; Adronov, A. Synthesis, Radiolabeling, and Bio-Imaging of High-Generation Polyester Dendrimers. *J. Am. Chem. Soc* **2009**, *131* (21), 2906–2916.

(39) Bartholomä, M. D.; Louie, A. S.; Valliant, J. F.; Zubieta, J. Technetium and Gallium Derived Radiopharmaceuticals: Comparing and Contrasting the Chemistry of Two Important Radiometals for the Molecular Imaging Era. *Chem. Rev.* **2010**, *110* (I), 2903–2920.

(40) Deen, W.; Bohrer, M.; Brenner, B. Macromolecule Transport across Glomerular Capillaries: Application of Pore Theory. *Kidney Int.* **1979**, *16* (3), 353–365.

(41) Matsumura, Y.; Maeda, H. A New Concept for Macromolecular Therapeutics in Cnacer Chemotherapy: Mechanism of Tumoritropic Accumulatio of Proteins and the Antitumor Agents Smancs. *Cancer Res.* **1986**, *46*, 6387–6392.

(42) Maeda, H. The Tumor Blood Vessel as an Ideal Target for Macromolecular Anticancer Agents. *J. Control. Release* **1992**, *19* (1–3), 315–324.

(43) Maeda, H.; Greish, K.; Fang, J. The EPR Effect and Polymeric Drugs: A Paradigm Shift for Cancer Chemotherapy in the 21st Century. *Adv. Polym. Sci.* **2006**, *193* (1), 103–121.

(44) Fang, J.; Nakamura, H.; Maeda, H. The EPR Effect: Unique Features of Tumor Blood Vessels for Drug Delivery, Factors Involved, and Limitations and Augmentation of the Effect. *Adv. Drug Deliv. Rev.* **2011**, *63* (3), 136–151.

(45) Prabhakar, U.; Maeda, H.; K. Jain, R.; Sevick-Muraca, E. M.; Zamboni, W.; Farokhzad, O. C.; Barry, S. T.; Gabizon, A.; Grodzinski, P.; Blakey, D. C. Challenges and Key Considerations of the Enhanced Permeability and Retention Effect for Nanomedicine Drug Delivery in Oncology. *Cancer Res.* **2013**, *73* (8), 2412–2417.

(46) Maeda, Y.; Kimura, S. I.; Kanda, M.; Hirashima, Y.; Hasegawa, T.; Wakahara, T.; Lian, Y.; Nakahodo, T.; Tsuchiya, T.; Akasaka, T.; et al. Large-Scale Separation of Metallic and Semiconducting Single-Walled Carbon Nanotubes. *J. Am. Chem. Soc.* **2005**, *127*, 10287–10290.

(47) Iyer, A. K.; Khaled, G.; Fang, J.; Maeda, H. Exploiting the Enhanced Permeability and Retention Effect for Tumor Targeting. *Drug Discov. Today* **2006**, *11* (17–18), 812–818.

(48) Ikeda, Y.; Nagasaki, Y. PEGylation Technology in Nanomedicine. *Adv. Polym. Sci.* **2012**, *247* (May 2012), 115–140.

(49) Li, W.; Zhan, P.; De Clercq, E.; Lou, H.; Liu, X. Current Drug Research on PEGylation with Small Molecular Agents. *Prog. Polym. Sci.* **2013**, *38* (3–4), 421–444.

(50) Harris, J. M.; Chess, R. B. Effect of Pegylation on Pharmaceuticals. *Nat. Rev. Drug Discov.* **2003**, *2* (3), 214–221.

(51) Lee, C. C.; Gillies, E. R.; Fox, M. E.; Guillaudeu, S. J.; Fréchet, J. M. J.; Dy, E. E.; Szoka, F. C. A Single Dose of Doxorubicin-Functionalized Bow-Tie Dendrimer Cures Mice Bearing C-26 Colon Carcinomas. *Proc. Natl. Acad. Sci. U. S. A.* **2006**, *103* (45), 16649–16654.

(52) Guillaudeu, S. J.; Fox, M. E.; Haidar, Y. M.; Dy, E. E.; Szoka, F. C.; Fréchet, J. M. J. PEGylated Dendrimers with Core Functionality for Biological Applications. *Bioconjug. Chem.* **2008**, *19*, 461–469.

(53) Majoros, I. J.; Williams, C. R.; Baker, J. R. Current Dendrimer Applications in Cancer Diagnosis and Therapy. *Curr. Top. Med. Chem.* **2008**, *8* (14), 1165–1179.

(54) Gajbhiye, V.; Vijayaraj Kumar, P.; Kumar Tekade, R.; Jain, N. K. Pharmaceutical and Biomedical Potential of PEGylated Dendrimers. *Curr. Pharm. Des.* **2007**, *13* (4), 415–429.

(55) Veronese, F. M.; Pasut, G. PEGylation, Successful Approach to Drug Delivery. *Drug Discov. Today* **2005**, *10* (21), 1451–1458.

(56) Wolinsky, J.; Grinstaff, M. Therapeutic and Diagnostic Applications of Dendrimers for Cancer Treatment☆. *Adv. Drug Deliv. Rev.* **2008**, *60* (9), 1037–1055.

(57) Caron, W. P.; Song, G.; Kumar, P.; Rawal, S.; Zamboni, W. C. Interpatient Pharmacokinetic and Pharmacodynamic Variability of Carrier-Mediated Anticancer Agents. *Clin. Pharmacol. Ther.* **2012**, *91* (5), 802–812.

(58) Nagayama, S.; Ogawara, K.; Fukuoka, Y.; Higaki, K.; Kimura, T. Time-Dependent Changes in Opsonin Amount Associated on Nanoparticles Alter Their Hepatic Uptake Characteristics. *Int. J. Pharm.* **2007**, *342* (1–2), 215–221.

(59) Petros, R. A.; DeSimone, J. M. Strategies in the Design of Nanoparticles for Therapeutic Applications. *Nat. Rev. Drug Discov.* **2010**, *9* (July), 615–627.

(60) Otsuka, H.; Nagasaki, Y.; Kataoka, K. PEGylated Nanoparticles for Biological and Pharmaceutical Applications. *Adv. Drug Deliv. Rev.* **2012**, *64* (SUPPL.), 246–255.

(61) Pang, X.; Du, H. L.; Zhang, H. Q.; Zhai, Y. J.; Zhai, G. X. Polymer-Drug Conjugates: Present State of Play and Future Perspectives. *Drug Discov. Today* **2013**, *18* (23–24), 1316–1322.

(62) Killops, K. L.; Campos, L. M.; Hawker, C. J. Robust, Efficient, and Orthogonal

Synthesis of Dendrimers via Thiol-Ene “Click” Chemistry. *J. Am. Chem. Soc.* **2008**, *130*, 5062–5064.

(63) Antoni, P.; Robb, M.; Campos, L.; Montanez, M.; Hult, A.; Malmström, E.; Malkoch, M.; Hawker, C. Pushing the Limits for Thiol−Ene and CuAAC Reactions: Synthesis of a 6th Generation Dendrimer in a Single Day. *Macromolecules* **2010**, *43* (16), 6625–6631.

(64) Walter, M. V.; Malkoch, M. Simplifying the Synthesis of Dendrimers: Accelerated Approaches. *Chem. Soc. Rev.* **2012**, *41* (13), 4593–4609.

(65) Alberto, R.; Schibli, R.; Egli, A.; Schubiger, A. P.; Abram, U.; Kaden, T. A. A Novel Organometallic Aqua Complex of Technetium for the Labeling of Biomolecules: Synthesis of [99mTc(OH2)3(CO)3]+ from [99mTcO4]- in Aqueous Solution and Its Reaction with a Bifunctional Ligand [8]. *J. Am. Chem. Soc.* **1998**, *120* (13), 7987–7988.

(66) Alberto, R.; Schibli, R.; Schubiger, A. P.; Abram, U.; Pietzsch, H. J.; Johannsen, B. First Application of Fac-[(99m)Tc(OH2)3(CO)3]+ in Bioorganometallic Chemistry: Design, Structure, and in Vitro Affinity of a 5-HT(1A) Receptor Ligand Labeled with (99m)Tc. *J. Am. Chem. Soc.* **1999**, *121* (4), 6076–6077.

(67) Alberto, R.; Ortner, K.; Wheatley, N.; Schibli, R.; Schubiger, A. P. Synthesis and Properties of Boranocarbonate: A Convenient in Situ CO Source for the Aqueous Preparation of [99mTc(OH2)3(CO)3]+. *J. Am. Chem. Soc.* **2001**, *123* (12), 3135–3136.

3 Rapid Synthesis of High Generation Polyester Dendrimers via Strain Promoted Alkyne-Azide Cycloaddition

Stuart A. McNelles and Alex Adronov*

This chapter has been reproduced with permission from S. A. McNelles, A. Adronov, *Macromolecules* **2017**, *50*, 7993–8001.

Graphical Abstract:

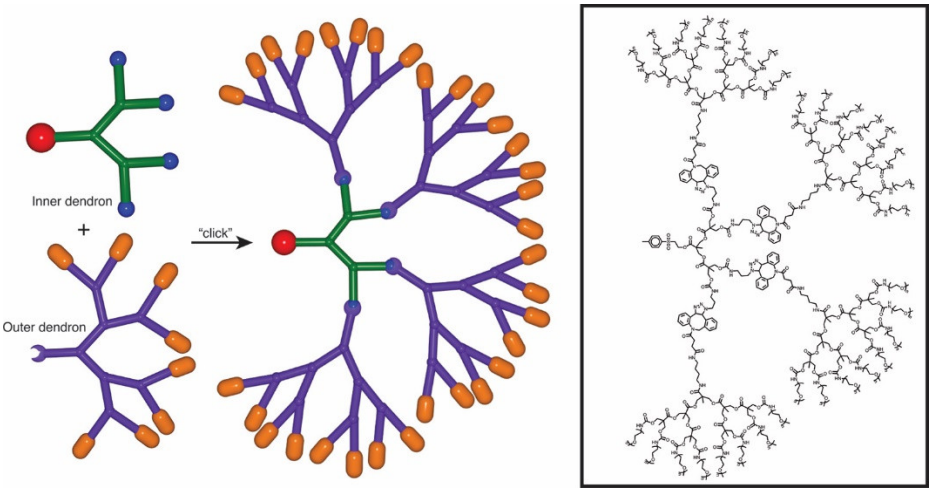

3.1 Abstract

Preparation of structurally perfect high-generation dendrimer libraries with different peripheral groups is challenging as divergent synthesis introduces peripheral defects and convergent synthesis leads to low yields. Here, we prepare a third generation polyester dendron, based on the bisMPA monomer structure, having eight peripheral azide functionalities, as an "inner" dendron. We also prepare a series of low-generation "outer" dendrons (G2 and G3) with various peripheral groups, including aromatic, aliphatic, and polar structures, each having a single dibenzoazacyclooctyne (DIBAC) at the core. Efficient strain-promoted azide-alkyne cycloaddition (SPAAC) enables quantitative coupling between the outer and inner dendrons, producing high-generation (G5 and G6) dendrimers in a single coupling step. Characterization by NMR spectroscopy and mass spectrometry shows that the coupling products are structurally perfect. Using this strategy, we prepared a small dendrimer library that includes the first high-generation monodisperse peripherally PEGylated dendrimers, as well as a structure bearing bulky protected amino acids at its periphery. This general strategy allows for rapid, efficient, and quantitative preparation of high-generation dendrimers with a variety of peripheral and core functional groups, starting from small, easily prepared fragments.

3.2 Introduction

The rapid, efficient preparation of high-generation dendrimers[1] is important to the development of macromolecular therapeutics,[2–8] diagnostic agents,[9–13] catalysts,[14–18] and encapsulants.[19–21] Dendrimers are a particularly attractive platform for macromolecular therapeutics owing to their precisely defined molecular structure, which can be tuned at the core, interior, and periphery.[22–24] However, the synthesis of *monodisperse* high-generation dendrimers, which are critical to many biomedical applications, remains a major challenge.[25] Divergent dendrimer synthesis methods commonly suffer from incomplete conversion or side reactions at the dendrimer periphery,[26] while convergent methods often suffer from poor yields or slow reaction times when high-generation dendrimers are needed. In addition, libraries of dendrimers with different peripheral groups are challenging to prepare convergently, as synthetic optimization must be carried out to accommodate differences in polarity, solubility, sterics, and other factors, for each type of peripheral group.

While several dendrimer structures have been investigated for therapeutic use,[6,8,27,28] dendritic architectures based on bis-MPA dendrons offer significant advantages such as low toxicity and biodegradability.[29,30] Previous methods for the preparation of bis-MPA dendrons have relied upon both divergent[25,31] and convergent[32,33] methodologies. While many bis-MPA dendron structures have been evaluated,[34–38] their preparation can often be laborious and require optimization for each desired structure, with these difficulties being exaggerated at high generations. Low-generation bis-MPA dendrimers

(G1-G3), on the other hand, are relatively easy to prepare and functionalize at the periphery in a quantitative manner. Thus, one solution to the difficulty in preparing perfect, monodisperse high-generation dendrimers is to prepare low-generation dendritic precursors, and couple them together using highly efficient linkage chemistry.

Click chemistry has seen explosive interest since its initial codification by Sharpless in 2001.[39] A variety of reactions are currently referred to as "click", such as thiol-ene[40], tetrazine-*trans*-cyclooctene[41], Cu(I) catalyzed 1,3-dipolar cycloaddition[42], and strain-promoted alkyne-azide cycloaddition (SPAAC).[43] In particular, SPAAC reactions are rapid and use synthetically accessible reagents, with azides being common functional handles within chemical precursors for a variety of applications. A number of SPAAC cyclooctynes are also commercially available, and their preparation on moderate scale has been reported.[44] The SPAAC reaction requires no copper catalyst, which is particularly attractive for biomedical applications due to the cytotoxicity of copper. Despite the mild reaction conditions, SPAAC is nevertheless efficient at coupling highly sterically strained systems, as demonstrated in the preparation of graft copolymers,[45] making it a potentially viable approach to the synthesis of structurally perfect high-generation dendrimers. Previously, examples of dendrimers (or dendrons) that have been functionalized by Cu(I) click reactions[46–50] and thermal Huisgen cycloadditions[51] have been reported, but the use of SPAAC in dendrimer synthesis has been somewhat limited.[52–54] Boons and co-workers have recently described a multi-stage click scheme in which SPAAC was used to assemble the two halves of Janus type dendrimers.[55] However, to our knowledge, the use of SPAAC

to convergently assemble high-generation dendrimer structures has not been reported in the literature.

Here, we demonstrate the utility of SPAAC for coupling low-generation dendrons together in the rapid preparation of high-generation dendrimers. This approach involves the use of a low-generation inner dendron, having any desired core functionality and an azide terminated periphery, reacting with multiple outer dendrons that bear a reactive cyclooctyne at their core, as schematically illustrated in Figure 1. Using this strategy, a library of high-generation dendrimers can be easily prepared, with individual structures tailored to different applications.

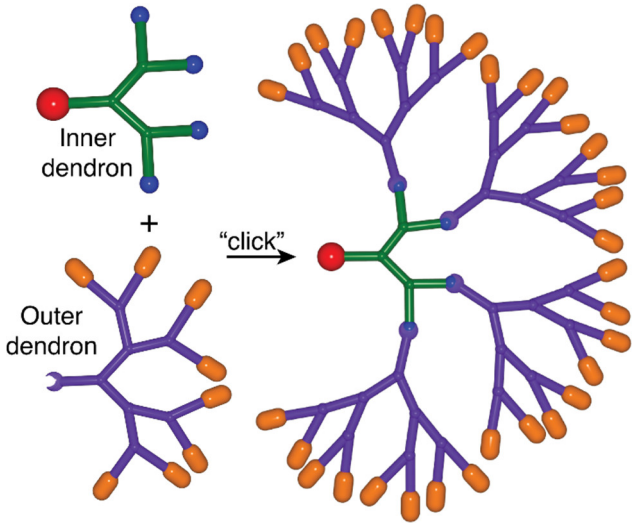

Figure 3.1. Schematic illustration of "click" coupling between appropriately functionalized "inner" and "outer" dendrons to produce a high-generation dendrimer.

3.3 Results and Discussion

Synthesis of bis-MPA dendrons bearing peripheral hydroxyl groups was carried out according to previously reported protocols.[10] This produced G1, G2, and G3 dendrons bearing 2, 4, and 8 hydroxyl groups at their periphery, respectively, and a *p*-toluenesulfonyl ethanol (pTSe) protecting group at their core. The peripheral groups were activated with *p*-nitrophenyl chloroformate according to literature procedures, as shown in Scheme 1 for the G3 dendron.[36] Each of the activated dendrons was then treated with 3-azidopropylamine to furnish dendrons bearing azides at their periphery (Scheme 3.1). This methodology resulted in complete functionalization of the dendron periphery, as determined by electrospray ionization mass spectrometry (ESI-MS, see supporting information). With three generations of azide-functionalized "internal" dendrons available, the "outer" dendrons, bearing different functional groups at their periphery and a cyclooctyne at their core, were required to complete the dendrimer synthesis.

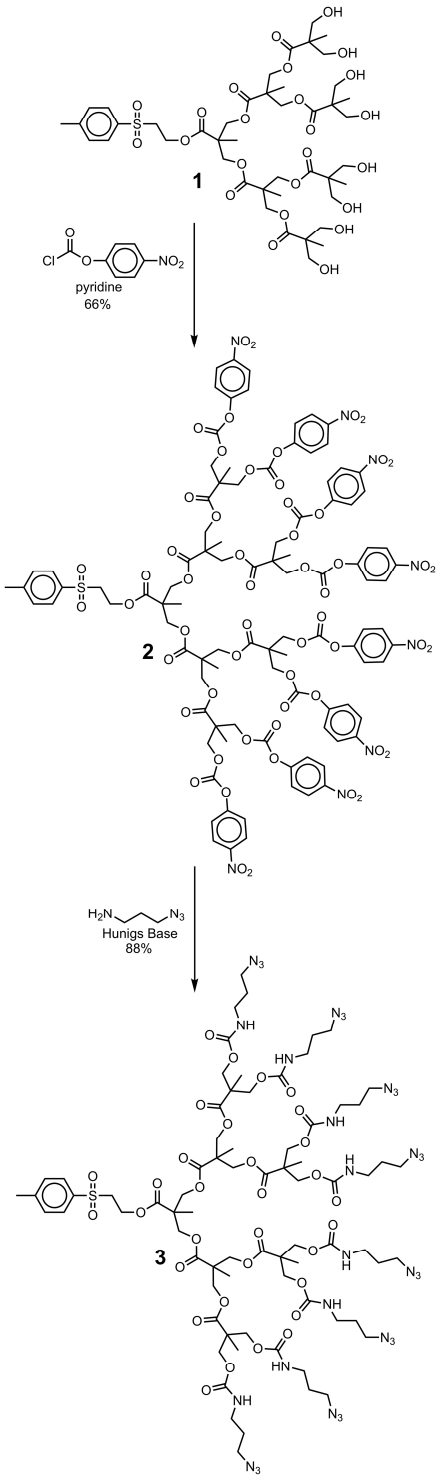

Scheme 3.1. Synthesis of the third-generation azide-terminated dendron.

As stated above, SPAAC chemistry between azides and cyclooctynes is extremely efficient, allowing facile coupling of sterically strained reaction partners. We chose to investigate dibenzoazacyclooctyne (DIBAC) as the reaction partner at the core of the outer dendrons, as it reacts very rapidly with azides, has demonstrated long-term stability at -20°C, and can be synthesized on moderate scale, requiring minimal chromatographic purification.[44] Initially, attempts were made to prepare a DIBAC derivative with an amine terminated spacer, which could then be coupled directly to the carboxylic acid group at the core of a bis-MPA dendron. However, though several such derivatives were prepared, they were found to rapidly decompose upon storage. We observed that only DIBAC derivatives that are solid at room temperature exhibited long-term stability, while those that form oils decomposed within a few hours, even when stored at low temperature. This prompted the preparation of DIBAC-NHS (**5**), which is a solid and exhibits long-term stability when stored in the freezer as a dry powder. This DIBAC derivative was synthesized via reaction of the corresponding DIBAC-acid **4** (prepared by literature methods[44]) with *N*-hydroxysuccinimide (Scheme 2). The DIBAC-NHS could then be coupled with any dendron bearing an amine at the core to produce a structure capable of SPAAC chemistry with any azide-bearing reaction partner, such as the inner dendron with azides at its periphery.

The outer dendrons were prepared from both second- and third-generation benzylidene protected bis-MPA dendrons by initial core deprotection of the pTSe group using 1,8-diazobicyclo[5.4.0]undec-7-ene (DBU), followed by activation of the carboxylic acid using *N*-hydroxysuccinimide/*N*-(3-dimethylaminopropyl)-*N*'-ethylcarbodiimide

hydrochloride (NHS/EDC·HCl). The resulting activated acid was then reacted with mono-Cbz protected 1,4-butanediamine, with subsequent global deprotection via palladium catalyzed hydrogenolysis of both the Cbz groups and benzylidenes (Scheme 3.2). Reaction of the resulting amino functionalized dendron with DIBAC-NHS gave a dendron with the desired strained cyclooctyne at the core. Subsequent functionalization of the dendron periphery was initially attempted using the same p-nitrophenyl chloroformate-mediated protocol to activate the peripheral hydroxyls that was used for the inner dendron (Scheme 1). However, treatment of the DIBAC-core dendron with *p*-nitrophenyl chloroformate resulted in rapid decomposition of the DIBAC group. To address this, the peripheral hydroxyls were instead treated with 1,1'-carbonyldiimidazole (CDI) to yield the acyl imidazole activated dendron (**10**), which was the substrate for subsequent derivatization. CDI has been used to great effect by Malkoch to activate carboxylic acids for subsequent addition to bis-MPA dendrimers via fluoride promoted esterification.[25] In our hands, the acyl imidazole activated **10** reacted very cleanly with primary amines, allowing the preparation of various outer dendrons.

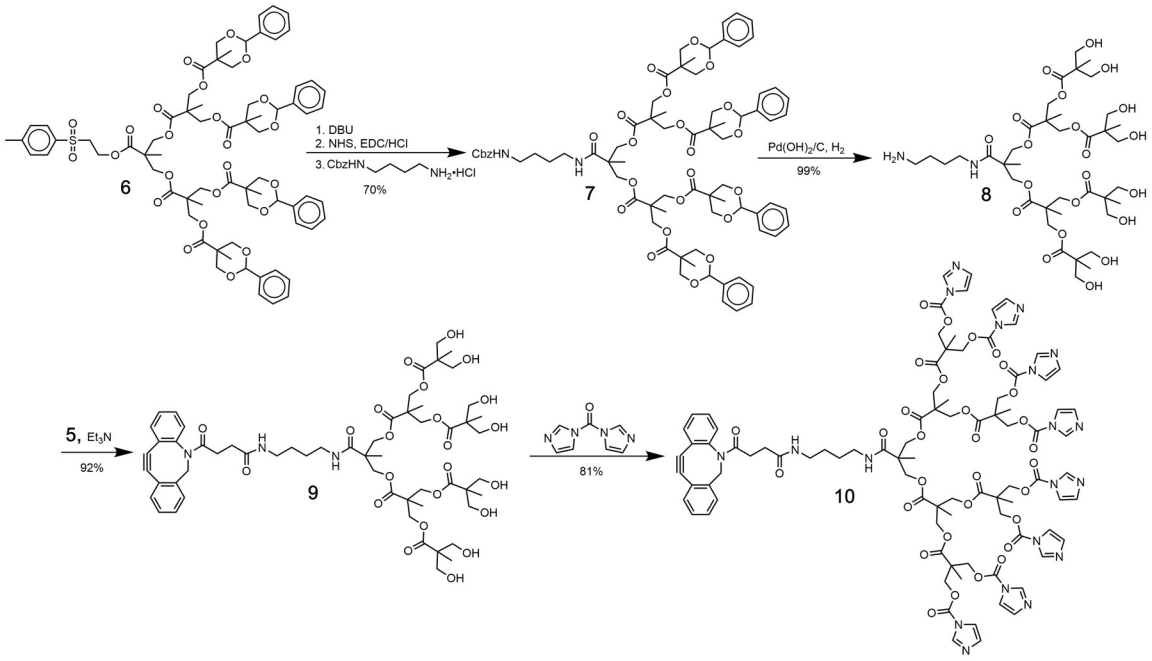

Scheme 3.2. Synthesis of DIBAC-G3-(imid)$_8$.

As a proof-of-concept, a small library of outer dendrons was prepared by reaction of the activated **10** with hydrophobic groups such as benzyl amine and dodecylamine (dendrons **11** and **12**, respectively), as well as sterically demanding polar groups such as N$^{\alpha}$-Boc-Lys(H)-OtBu (dendron **13**). In all cases, peripheral functionalization was complete within 4 hours, liberating products in yields greater than 80% (Scheme 3.3). Full characterization of these three dendrons is provided in the supporting information.

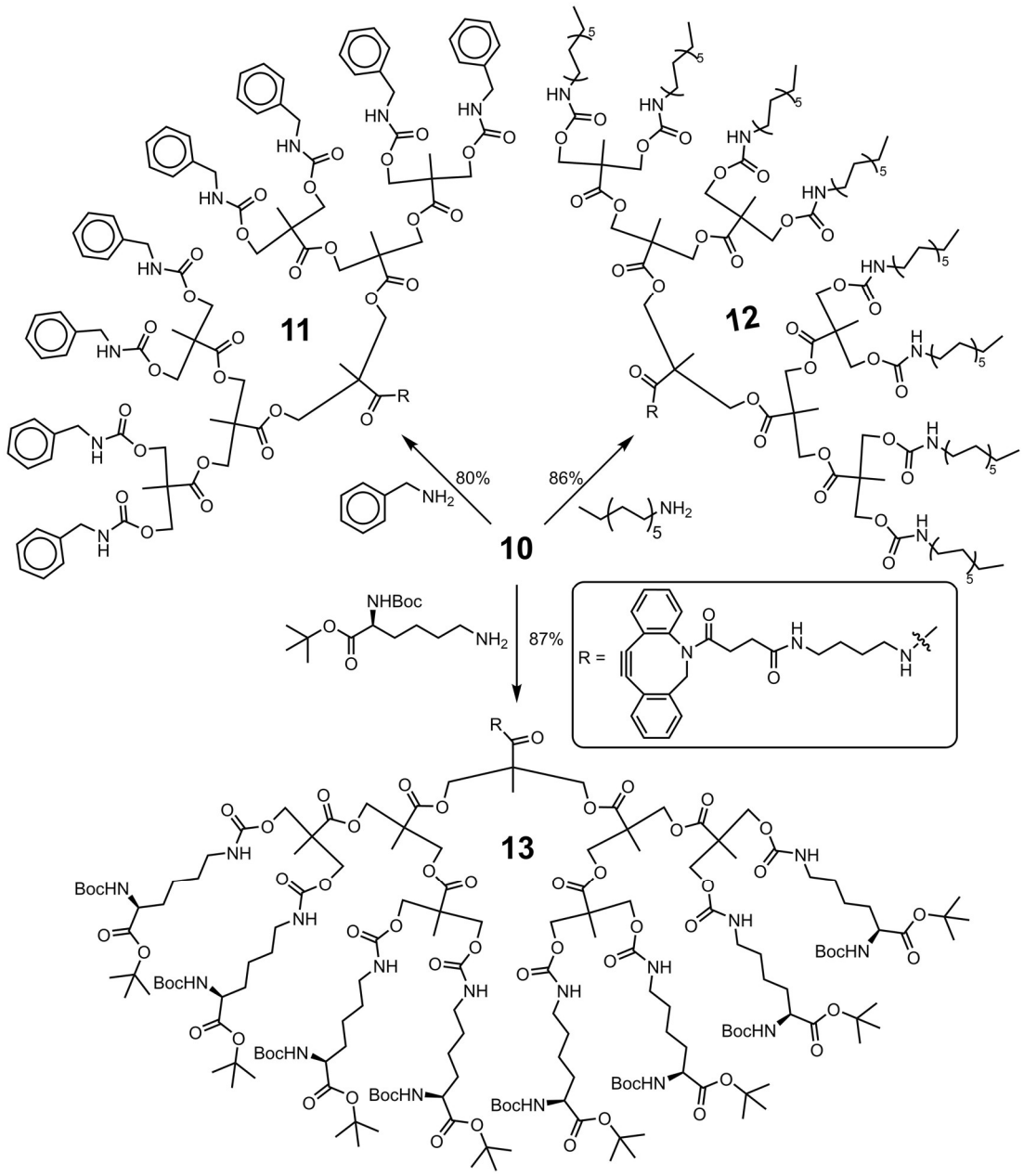

Scheme 3.3. Derivitization of DIBAC-G3-(imid)$_8$ dendron.

Having completed the synthesis of the inner dendrons (G1-G3) and the three outer dendrons (G3), SPAAC coupling between these structures was carried out to produce high-

generation dendrimers (G4-G6). It was found that the click reaction proceeded extremely rapidly for all generations of the inner dendron. In fact, stirring the components in a reaction vessel was not necessary to achieve quantitative conversion. Instead, the components were added to a vial in a minimum amount of solvent and, instead of stirring, the solvent was simply evaporated on a rotary evaporator until a viscous oil remained. The oil was sampled within 5 minutes, and mass spectral analysis indicated that the reaction had gone to completion, producing the 6th generation dendrimers (**15**, **16**, and **17a**) quantitatively (structures of the products are given in Figure 2). To our knowledge, this level of reaction efficiency in the synthesis of high-generation dendrimers is unprecedented. Although chromatographic purification was required in order to remove the 5-10 mol% excess outer dendron that was used to ensure complete conversion, the separation was easily achieved for the benzyl- and alkyl-terminated dendrimers (MALDI-TOF mass spectral data for the G4-G6 benzyl- and alkyl-terminated structures is provided in Figure 3). For the N$^{\alpha}$-Boc-Lys(H)-OtBu structure (**17a**), this separation proved challenging because it forms broad bands on silica gel, making it impossible to resolve the high-generation product from the excess outer dendron. To circumvent this purification problem, a G4 inner dendron was prepared, using the same protocols described above, and coupled with the G2 outer dendron to produce the G6 product **17b**. The reaction proceeded identically to the case with the G3 analogs, and chromatographic separation of the excess G2 from the desired G6 product was easily accomplished (see Supporting Information for details). Thus, this methodology allows for the preparation of structurally perfect high-

generation dendrimers, even with sterically demanding terminal groups such as the multiple tert butyl groups encountered in protected amino acids, without difficulty.

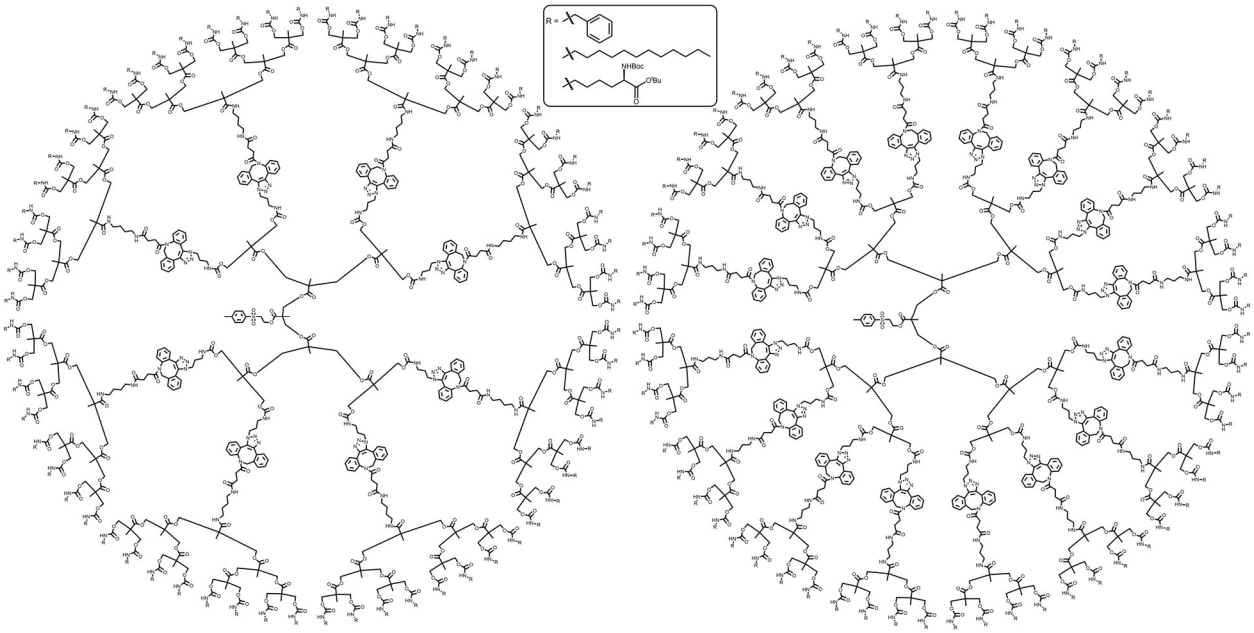

Figure 3.2. Chemical structures of benzyl-, dodecyl-, and N^{α}-Boc-Lys(H)-OtBu-terminated dendrimers (**15**, **16**, and **17a/b**, respectively).

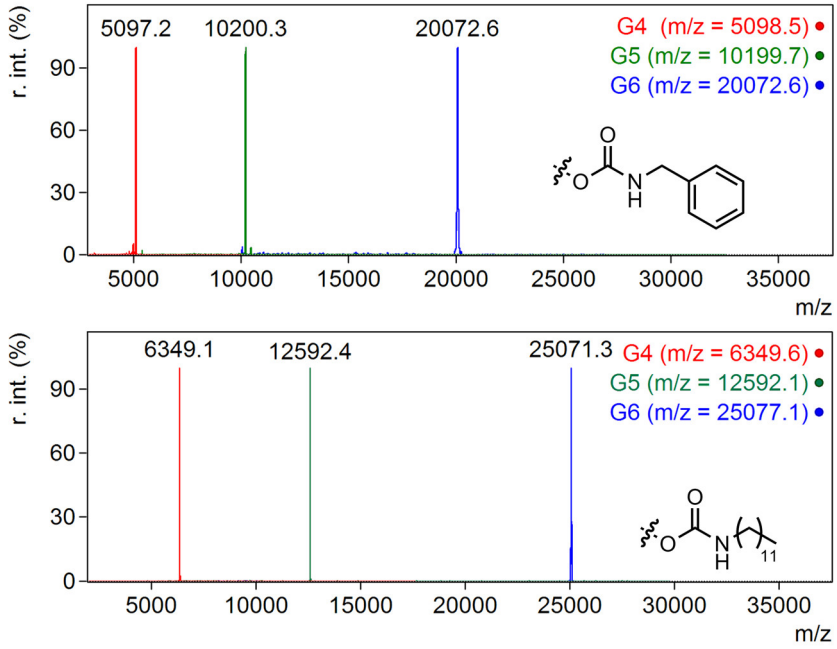

Figure 3.3. MALDI Mass spectra of pTSe-Gx-Benzyl (**15**, top) and pTSe-Gx-Dodecyl (**16**, bottom) dendrimers, where x = 4, 5, or 6. Calculated mass values for each structure are provided in the legend.

Previously, we prepared high-generation PEGylated dendrimers using thiol-ene chemistry to install the terminal PEG chains. However, complete conversion of the dendrimer periphery was not possible due to the extreme steric crowding introduced by the PEG chains, leading to a product that was not structurally perfect.[12] Thus, as the final member of our dendrimer library, we undertook the preparation of a structurally perfect high-generation PEGylated dendrimer using the SPAAC methodology. To do this, we used a commercially available monodisperse polyethylene glycol monoamine (MeO-PEG_{15}-NH_2) precursor so as to eliminate any dispersity associated with the PEG chains. Reaction of MeO-PEG_{15}-NH_2 with the third generation activated dendron **10** proceeded smoothly to produce the PEGylated outer dendron **14** (Scheme 5). Subsequent reaction of **14** with the

second-generation inner dendron proceeded identically to what is described above, and produced the fully PEGylated G5 dendrimer structure (**18**). MALDI-TOF mass spectral data for this PEGylated G5 structure is provided in Figure 4, showing the presence of the fifth-generation structure. It should be noted that PEGylated dendrimers are difficult to observe by mass spectrometry, and this measurement required high laser power in the MALDI instrument, which resulted in some structural fragmentation. While structurally perfect low generation dendrimers have been prepared previously,[53] to our knowledge, this is the first truly monodisperse high-generation PEGylated dendron ever reported, and its precisely defined structure is advantageous in medicinal applications, such as in diagnostic imaging and molecular therapeutics, where there is a need for excellent control of the biodistribution and clearance rate, as well as control over the structure for regulatory purposes.[56–59]

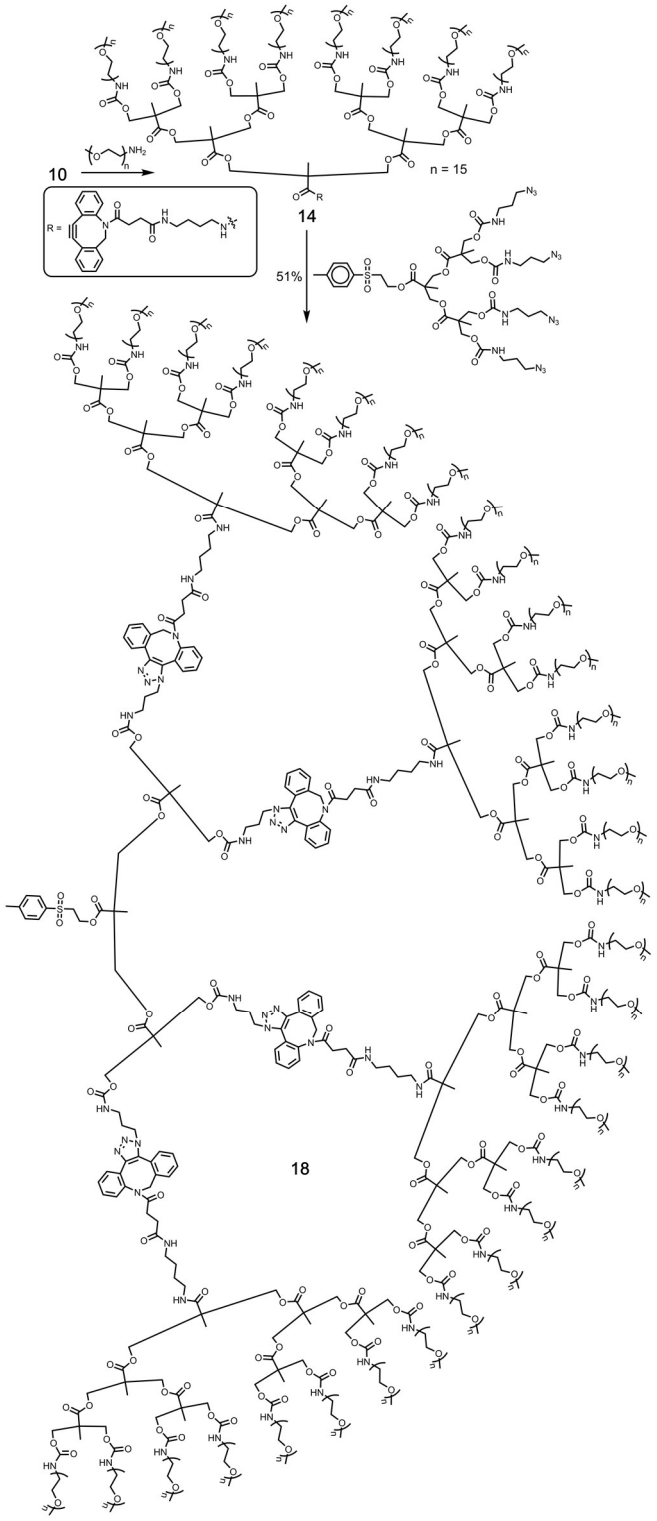

Scheme 3.4. Preparation of a monodisperse PEGylated G5 dendrimer (**18**).

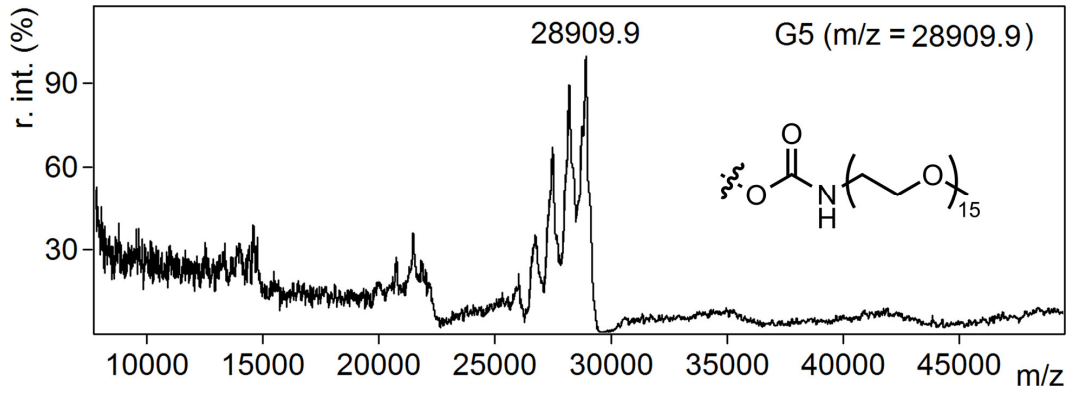

Figure 3.4. MALDI-TOF mass spectrum of pTSe-G5-$(PEG_{15})_{32}$ (calculated mass value provided in the legend).

The convergent click methodology also allows for the rapid preparation of different "inner" dendrons by functionalization of the core carboxylic acid with amine containing functional groups. To demonstrate the compatibility of various core groups in the SPAAC reaction to form high generation dendrons, two additional structures were appended by EDC-HOBt coupling, which included pyrene and dipicolylamine (DPA), depicted in Figure 5. These core structures were chosen so as to introduce a fluorophore and a transition metal ligand (DPA is ideal for chelation of the radiometal ^{99m}Tc, used in diagnostic imaging).[60] The resulting inner dendrons were then reacted with compound **9** to provide sixth generation hydroxylated dendrons with varied core functionality in the same short reaction times as described above. In this case, purification of the hydroxyl periphery dendrons could not be accomplished by silica gel chromatography due to extensive streaking of the products. However, excess outer dendron could be removed by purification using Sephadex LH-20 in methanol, which easily separates the low molecular weight components. MALDI-TOF mass spectral data for the set of three G6 dendrimers is

provided in Figure 5. Interestingly, site-isolation of the core functionality in the sixth-generation dendrimers was readily observed in the structure bearing pyrene at the core. For the third-generation precursor, the fluorescence spectrum (in methanol) exhibited both the pyrene monomer emission (360-420 nm), and a small amount of pyrene excimer emission (centered at 480 nm) arising from the interaction of an excited-state pyrene unit with a nearby ground-state pyrene (Figure 3.5). However, the fluorescence spectrum of the clicked sixth-generation dendrimer exhibited no pyrene excimer emission, indicating complete site-isolation of this core functionality, preventing its interaction with pyrene cores on neighboring dendrimers (Figure 3.5).

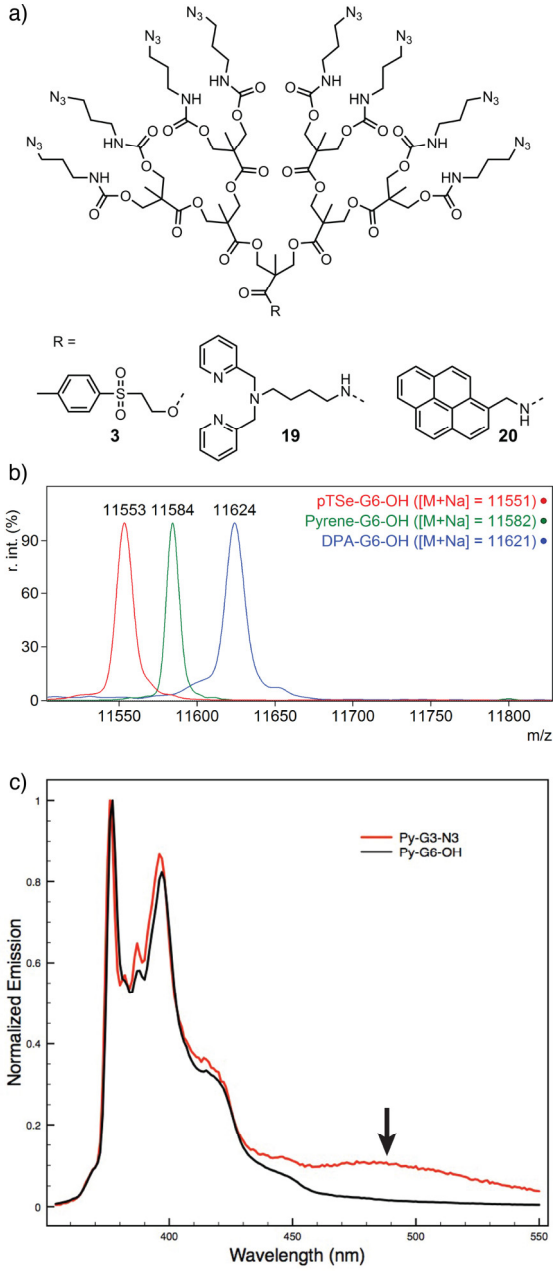

Figure 3.5. (a) Structures of the various "inner" dendron investigated; (b) MALDI-TOF mass spectral data for core functionalized sixth generation dendrons (calculated mass values provided in the legend); (c) Fluorescence spectra of the pyrene-labeled G3 dendron and the corresponding G6 dendrimer structure after click coupling. Arrow points out the excimer emission in the G3 dendron, which disappears in the G6 dendrimer.

3.4 Conclusion

We have developed a convergent dendrimer synthesis approach that can be used to rapidly prepare a library of high-generation dendrons with a variety of core and peripheral functionalities. This approach results in a common intermediate from which all "outer" dendrons can be prepared from primary amines, which are endogenous functional groups in a variety of biomolecules of interest. The approach allows for the rapid parallel synthesis of both fluorescently labeled and potentially radiolabeled compounds using identical reaction conditions, only requiring a minor change in inner dendron. Perhaps more importantly, the SPAAC reaction was found to be exceedingly rapid when performed neat, thus allowing the preparation of high generation dendrons in less than five minutes under extremely mild conditions. This methodology will be useful for further studies involving the preparation of high generation monodisperse dendrimers for diagnostic imaging and therapeutic applications.

3.5 Experimental

Monodisperse $mPEG_{15}$-NH_2 was purchased from Quanta Biodesign. Amino acids and Boc anhydride were purchased from Chem-Impex. Dry solvents were obtained from a solvent system packed with *in situ* activated 3Å molecular sieves, with the exception of THF which was dried with *in situ* activated alumina beads. Amine bases (trimethylamine, DBU, pyridine, diisopropylethylamine) were distilled over KOH and stored under nitrogen to remove N-Oxides. All other chemicals were sourced from Sigma-Aldrich and used without further purification. ^{1}H NMR spectroscopy was performed on a Bruker Avance AV600 or

AV700 spectrometer equipped with a cryoprobe, at 600 MHz and 700 MHz, respectively. ^{13}C NMR spectroscopy was performed on a Bruker Avance AV700 at 176 MHz. Residual non-deuterated solvent signals were used as internal chemical shift references for both ^{1}H and ^{13}C spectra. All chemical shifts are reported in ppm. MALDI spectra were collected on a Bruker UltraFlextreme spectrometer in positive ion mode using dithranol as matrix. Electrospray MS was performed using a Micromass Quattro triple quadrupole instrument in positive mode. Exact masses were collected on either a Micromass Q-TOF Global Ultima or a Bruker Maxis II Q-TOF. Analytical HPLC was performed on a Waters 2695 instrument with a Waters 2996 photodiode array detector at a flow rate of 0.76 mL/min for 3 mm ID columns, and 1.5 mL/min for 4.6 mm ID columns. Chromatograms were primarily collected on a Phenomenex Kinetex column (3 mm x 100 mm, 2.6 μm particle size), though in select cases when different selectivity was required a Phenomenex Luna Phenyl Hexyl column (4.6 mm x 150 mm, 3 um particle) or a Phenomenex Gemini (4.6 mm x 150 mm, 3 um particles) were used instead. HPLC of macromolecules (in this case, MW > ~3000 Da) was carried out using a Phenomenex Jupiter column (4.6 mm x 250 mm, 5 μm particles) at a flow rate of 1 mL/min. The general analytical gradient for the Kinetex column was as follows: Solvent A was 5% HPLC grade acetonitrile in HPLC grade water, solvent B 100% HPLC grade acetonitrile. The gradient consisted of an isocratic hold at 100% A for 1 minute, ramping to 100% by 6 minutes, an isocratic hold at 100% B for 2 minutes, then immediately returning to 100% A for 2 minutes to equilibrate between runs. Scaled to column volumes, these conditions were also used for the Phenyl Hexyl and Gemini columns. All HPLC runs were monitored using a UV detector from a range of 190

to 600 nm, and chromatograms are presented using wavelengths which are indicated on the chromatograms. Preparative size exclusion chromatography was performed using GE HiTrap desalting cartridges packed with fine Sephadex G-25 media, and were operated using a Waters 2695 separations module equipped with a Waters 2996 PDA detector, with collection of the eluate performed according to instructions from the manufacturer. Flash chromatography was performed using an AnaLogix Intelliflash 280 automated flash chromatography system, equipped with a variable wavelength (200-320 nm) UV detector. Empty Biotage SNAP columns packed with Silicycle R60 20-45 um silica gel were used as chromatography media. UV-Vis-NIR absorption spectra were recorded on a Cary 5000 spectrometer in dual beam mode, using matching 10 mm quartz cuvettes. Fluorescence spectra were measured on a Jobin-Yvon SPEX Fluorolog 3.22 equipped with a 450 W Xe arc lamp, digital photon counting photomultiplier, and an InGaAs detector, also using a 10 mm quartz cuvette. Slit widths for both excitation and emission were set to 2 nm band-pass, and correction factor files were applied to account for instrument variations.

3.6 Experimental Procedures

General Procedure for Dendron Click Reactions

15 mg Scale. The inner azide dendron was dissolved in 0.5 mL of dichloromethane in a 20 mL scintillation vial. Separately, a slight excess (1.05 eq per azide) of the outer alkyne-cored dendron was dissolved in 0.5 mL of dichloromethane. This was then transferred to the azide dendron solution, and the combined reaction mixture was crudely dried on a rotary evaporator until the reaction mixture was a viscous oil. This was left for 5 min, and

was then sampled for analysis by mass spectrometry (MALDI or ESI-MS) as well as FTIR to determine the complete conversion of the azide. Products were purified by silica gel chromatography or size exclusion chromatography, then characterized by ^{1}H NMR and mass spectrometry.

Synthesis of 3-azidopropyl amine

Prepared from 3-chloropropylamine hydrochloride with sodium azide according to literature procedures.[61]

^{1}H NMR (600 MHz; $CDCl_3$): δ 3.36 (t, J = 6.7, 2H), 2.79 (t, J = 6.8, 2H), 1.72 (quintet, J = 6.8, 2H)

Synthesis of DPA ligand

Prepared according to literature procedures.[12]

^{1}H NMR (600 MHz; $CDCl_3$): δ 8.52 (d, J = 4.7, 2H), 7.64 (td, J = 7.6, 1.4, 2H), 7.52 (d, J = 7.8, 2H), 7.14 (t, J = 6.1, 2H), 3.80 (s, 4H), 2.62 (t, J = 7.0, 2H), 2.55 (t, J = 7.3, 2H), 1.57 (dt, J = 14.9, 7.5, 2H), 1.41 (quintet, J = 7.4, 2H)

Synthesis of BocLys(H)-OtBu

Prepared from Cbz-N^{ε}-Lysine according to literature procedures.[62]

^{1}H NMR (700 MHz; DMSO-*d*6): δ 7.08-6.73 (m, 1H), 3.76-3.64 (m, 1H), 1.57-1.52 (m, 2H), 1.38 (d, J = 40.9, 19H), 1.30 (dt, J = 7.4, 4.0, 6H)

Synthesis of DIBAC-COOH (4)

Prepared according to modified literature procedures.[44]

Synthesis of DIBAC-NHS (5)

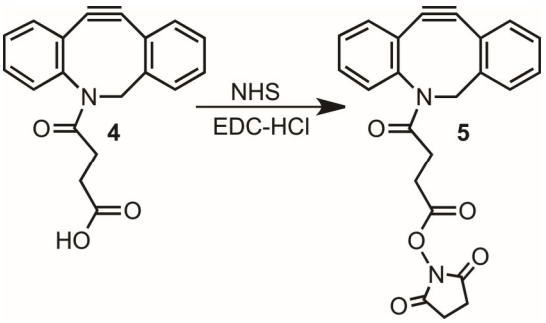

DIBAC-COOH (**4**, 0.500 g, 1.638 mmol) was added to 25 mL of dichloromethane, along with *N*-hydroxysuccinimide (282 mg, 2.456 mmol). To this, *N*-(3-dimedthylaminopropyl)-*N*'-ethylcarbodiimide hydrochloride (471 mg, 2.456 mmol) was added, which resulted in the rapid dissolution of the previously insoluble *N*-hydroxysuccinimide. After stirring for 1 hour, the crude reaction mixture was loaded on a 25 gram Biotage Snap column equilibrated with 40% ethyl acetate in hexanes, and the product was purified by flash chromatography using a gradient from 40% to 100% ethyl acetate in hexanes over 15 column volumes, with collection at 254 nm. The fractions containing product were combined, and solvent was removed *in vacuo*. The resulting oil was dissolved in 1 mL of dichloromethane, then precipitated into 50 mL of stirring pentane to give the product as a white powder. (599 mg, 91%).

^{1}H NMR (600 MHz; $CDCl_3$): δ 7.69 (d, J = 7.6, 1H), 7.42-7.36 (m, 5H), 7.31 (t, J = 7.5, 1H), 7.25 (d, J = 7.2 Hz, 1H), 5.18 (d, J = 13.9, 1H), 3.69 (d, J = 13.9, 1H), 2.97 (dt, J = 17.0, 8.2, 1H), 2.63 (dt, J = 17.7, 6.6, 1H), 2.07 (dt, J = 16.8, 6.6, 1H)

Synthesis of Alcohol periphery Bis-MPA dendrons

Bis-MPA dendrons of generation 1 through 3 were prepared according to literature procedures.[10]

Synthesis of pTSe-G1-(NO_2Ph)$_2$

pTSe-G1-$(OH)_2$ (0.75 g, 2.371 mmol) was dissolved in 2 mL of pyridine, then diluted to 15 mL with dichloromethane. The reaction mixture was cooled to 0 °C in an ice bath, and after 10 min of cooling, *p*-nitrophenyl chloroformate (1.911g, 9.483 mmol) dissolved in 5 mL of dichloromethane was quickly added, resulting in immediate formation of a fine white precipitate that persisted throughout the reaction. The reaction mixture was removed from the ice bath and allowed to stir for 16 h. After stirring overnight, the reaction mixture was diluted with 20 mL of dichloromethane, then extracted with 3 × 25 mL of 1 M $NaHSO_4$, and 1 × 40 mL of brine, dried with $MgSO_4$, filtered, and solvent was removed by rotary evaporation. The crude material was then purified by silica gel chromatography using a step gradient consisting of 4 column volumes of 100% dichloromethane, followed by 4 column volumes of 5% ethyl acetate in dichloromethane, and finally 4 column volumes of 10% ethyl acetate in dichloromethane. The fractions containing product were combined, and solvent was removed *in vacuo*. This was dried on the vac line overnight to give the product as a white foam. (1.423g, 93%).

^{1}H NMR (700 MHz; C_6D_6): δ 7.65-7.63 (m, 6H), 6.80-6.77 (m, 4H), 6.75 (d, J = 7.9, 2H), 4.53 (d, J = 11.0, 2H), 4.43 (d, J = 11.0, 2H), 4.13 (t, J = 5.5, 2H), 2.76 (t, J = 5.5, 2H), 1.86 (s, 3H), 1.13 (s, 3H)

^{13}C NMR (176 MHz; C_6D_6): δ 1.43, 17.29, 21.17, 46.69, 54.59, 58.46, 69.60, 121.69, 125.24, 128.33, 128.35, 130.05, 137.16, 144.82, 145.78, 152.53, 155.22, 171.48

MS Calcd for $[M+NH_4]^+$ = 664.1448. Found ESI-MS $[M+NH_4]^+$ = 664.1445

Synthesis of pTSe-G2-(NO_2Ph)$_4$

pTSe-G2-(OH)$_4$ (1.300 g, 2.37 mmol) was dissolved in 2 mL of pyridine, then diluted to 15 mL with dichloromethane. The reaction mixture was cooled to 0 °C in an ice bath, and after 10 min of cooling, *p*-nitrophenyl chloroformate (3.821g, 18.957 mmol) dissolved in 8 mL of dichloromethane was quickly added, resulting in immediate formation of a fine white precipitate that persisted throughout the reaction. The reaction mixture was removed from the ice bath and allowed to stir for 16 h. After stirring overnight, the reaction mixture was diluted with 20 mL of dichloromethane, then extracted with 3 × 25 mL of 1 M $NaHSO_4$, and 1 × 40 mL of brine, dried with $MgSO_4$, filtered, and solvent was removed by rotary evaporation *in vacuo*. The crude material was then purified by silica gel chromatography using a step gradient consisting of 4 column volumes of 100% dichloromethane, followed by 4 column volumes of 5% ethyl acetate in dichloromethane, and finally 4 column volumes of 10% ethyl acetate in dichloromethane. The fractions containing product were combined, and solvent was removed *in vacuo*. This was dried on the vac line overnight to give the product as a white foam. (2.385 g, 83%).

^{1}H NMR (600 MHz; $CDCl_3$): δ 8.25-8.23 (m, 8H), 7.76 (d, J = 8.2, 2H), 7.38-7.36 (m, 8H), 7.34 (d, J = 8.2, 2H), 4.53-4.49 (m, 6H), 4.45 (dd, J = 11.0, 2.2, 4H), 4.39-4.35 (m, 4H), 3.39 (t, J = 5.8, 2H), 2.43 (s, 3H), 1.38 (s, 6H), 1.31 (s, 3H)

^{13}C NMR (176 MHz; C_6D_6): δ 171.5, 155.2, 152.5, 145.8, 144.8, 137.2, 130.0, 128.35, 128.33, 125.2, 121.7, 69.6, 58.5, 54.6, 46.7, 21.2, 17.3, 1.4

MS Calcd for $[M+NH_4]^+$ = 1226.2520. Found ESI-MS $[M+NH_4]^+$ = 1226.2511

Synthesis of pTSe-G3-(NO_2Ph)$_8$ (2)

pTSe-G3-(OH)$_8$ (0.75 g, 0.740 mmol) was dissolved in 2 mL of pyridine, then diluted to 15 mL with dichloromethane. The reaction mixture was cooled to 0 °C in an ice bath, and after 10 min of cooling, *p*-nitrophenyl chloroformate (2.388 g, 11.845 mmol) dissolved in 5 mL of dichloromethane was quickly added, resulting in immediate formation of a fine white precipitate that persisted throughout the reaction. The reaction mixture was removed from the ice bath and allowed to stir for 16 h. After stirring overnight, the reaction mixture was diluted with 20 mL of dichloromethane, then extracted with 3 × 25 mL of 1 M $NaHSO_4$, and 1 × 40 mL of brine, dried with $MgSO_4$, filtered, and solvent was removed by rotary evaporation *in vacuo*. The crude material was then purified by silica gel chromatography using a step gradient consisting of 4 column volumes of 100% dichloromethane, followed by 4 column volumes of 5% ethyl acetate in dichloromethane, and finally 4 column volumes of 10% ethyl acetate in dichloromethane. The fractions containing product were combined, and solvent was removed *in vacuo*. This was dried on the vac line overnight to give the product as a white foam (1.140 g, 65%).

^{1}H NMR (700 MHz; $CDCl_3$): δ 8.24-8.22 (m, 16H), 7.73 (d, J = 8.1, 2H), 7.35 (m, 18H), 4.51-4.21 (m, 30H), 3.35 (t, J = 5.6, 2H), 2.42 (s, 3H), 1.36 (s, 12H), 1.31 (s, 6H), 1.24 (s, 3H)

^{13}C NMR (176 MHz; $CDCl_3$): δ 171.75, 171.61, 171.2, 155.3, 152.2, 145.73, 145.60, 136.4, 130.3, 128.0, 69.3, 66.3, 65.6, 58.3, 54.8, 46.85, 46.78, 21.8, 17.79, 17.76, 17.4

MS Calcd for $[M+Na]^+$ = 2355.4216. Found ESI-MS $[M+Na]^+$ = 2355.4232

Synthesis of pTSe-G1-$(N_3)_2$

pTSe-G1-$(NO_2Ph)_2$ (1.072 g, 1.658 mmol) was dissolved in 10 mL of dichloromethane. To this 3-azidopropylamine (0.664 g, 6.632 mmol) was added, immediately colouring the reaction mixture an intense yellow colour. Diisopropylethylamine (1.444 mL, 8.290 mmol) was added, then the reaction was stirred for 2 h. After 2 h, the reaction was determined to be fully converted by HPLC. The reaction mixture was diluted with 20 mL of dichloromethane, then washed with 3 × 25 mL of 1 M $NaHSO_4$, 3 × 25 mL of 10% Na_2CO_3, and 1 × 40 mL of brine, dried with $MgSO_4$, filtered and solvent was removed by rotary evaporation *in vacuo*. The crude material was then purified by silica gel chromatography using 40% acetone in hexanes, with peaks being detected at 225 nm. The fractions containing product were combined and solvent was removed *in vacuo*, then dried under vacuum overnight to give the product as a clear, colourless oil. (0.904 g, 96%)

^{1}H NMR (700 MHz; CD_2Cl_2): δ 7.78 (d, J = 8.2, 2H), 7.40 (d, J = 8.3, 2H), 5.06 (s, 2H), 4.39 (t, J = 5.8, 2H), 4.08–4.04 (m, 4H), 3.42 (t, J = 5.9, 2H), 3.33 (t, J = 6.6, 4H), 3.20 (q, J = 6.2, 4H), 2.44 (s, 3H), 1.73 (quintet, J = 6.5, 4H), 1.09 (s, 3H)

^{13}C NMR (176 MHz; DMSO-*d*6): δ 173.0, 156.2, 145.8, 136.6, 130.3, 66.1, 58.4, 55.4, 49.4, 47.2, 38.7, 29.4, 21.7, 17.3

MS Calcd for $[M+H]^+$ = 569.2142. Found ESI-MS $[M+H]^+$ = 569.2131

Synthesis of pTSe-G2-$(N_3)_4$

pTSe-G2-$(NO_2Ph)_4$ (2.350 g, 1.944 mmol) was dissolved in 15 mL of dichloromethane then 3-azidopropylamine (1.168 g, 11.662 mmol) was added immediately colouring the reaction mixture an intense yellow colour. Diisopropylethylamine (1.444 mL, 8.290 mmol) was added, then the reaction was stirred for 1 hour. After 1 hour, the reaction was determined to be fully converted by HPLC. The reaction mixture was diluted with 20 mL of dichloromethane, then washed with 3 × 25 mL of 1 M $NaHSO_4$, 3 × 25 mL of 10% Na_2CO_3, and 1 × 40 mL of brine, dried with $MgSO_4$, filtered and solvent was removed by rotary evaporation *in vacuo*. The crude material was then purified using a gradient from 0 to 100% acetone in hexanes over 15 column volumes, with fractions collected by monitoring at 225 nm. The fractions containing product were combined and solvent was removed by rotary evaporation. This was subsequently dried under vacuum overnight to give the product as a clear, colourless oil. (1.965 g, 96%)

^{1}H NMR (700 MHz; $CDCl_3$): δ 7.80 (d, J = 8.2, 2H), 7.39 (d, J = 8.0, 2H), 5.55–5.38 (m, 4H), 4.77 (s), 4.50 (t, J = 5.5, 2H), 4.29–4.09 (m, 12H), 3.45 (t, J = 5.8, 2H), 3.36 (t, J = 6.6, 8H), 3.24 (q, J = 6.4, 8H), 2.46 (s, 3H), 1.78 (quintet, J = 6.6, 8H), 1.23 (t, J = 19.3, 9H)

^{13}C NMR (176 MHz; $CDCl_3$): δ 173.2, 172.2, 156.1, 145.5, 136.2, 130.3, 128.2, 66.2, 65.0, 58.3, 55.0, 49.1, 47.3, 46.5, 38.6, 29.2, 21.8, 17.80, 17.67

MS Calcd for $[M+NH_4]^+$ = 1070.4437. Found ESI-MS $[M+NH_4]^+$ = 1070.4436

Synthesis of pTSe-G3-$(N_3)_8$ (3)

pTSe-G3-$(NO_2Ph)_8$ (0.500 g, 0.214 mmol) was dissolved in 5 mL of dichloromethane then 3-azidopropylamine (0.343 g, 3.425 mmol) was added immediately colouring the reaction mixture an intense yellow colour. Diisopropylethylamine (0.298 mL, 1.712 mmol) was added, then the reaction was stirred for 2 h. After 2 h, the reaction was determined to be fully converted by HPLC. The reaction mixture was diluted with 20 mL of dichloromethane, then washed with 3 × 25 mL of 1 M $NaHSO_4$, 3 × 25 mL of 10% Na_2CO_3, and 1 × 40 mL of brine, dried with $MgSO_4$, filtered and solvent was removed by rotary evaporation *in vacuo*. The crude material was then purified using a gradient from 0 to 100% acetone in hexanes over 15 column volumes, with fractions collected by monitoring at 225 nm. The fractions containing product were combined and solvent was removed by rotary evaporation. This was subsequently dried under vacuum overnight to give the product as a clear, colourless oil. (0.383 g, 88%)

^{1}H NMR (700 MHz; CD_2Cl_2): δ 7.79 (d, J = 8.0, 2H), 7.42 (d, J = 8.0, 2H), 5.43 (m, 7H), 4.95 (s, 1H), 4.46 (t, J = 5.8, 2H), 4.31–4.09 (m, 29H), 3.47 (t, J = 5.7, 2H), 3.35 (t, J = 6.26, 16H), 3.20 (q, J = 5.97, 16H), 2.45 (s, 3H), 1.75 (t, J = 6.4, 16H), 1.26–1.18 (m, 22H)

^{13}C NMR (176 MHz; CD_2Cl_2): δ 173.4, 172.34, 172.24, 156.3, 145.9, 136.6, 128.3, 70.9, 66.3, 65.2, 58.8, 55.1, 49.4, 47.5, 46.9, 38.7, 29.4, 21.8, 18.0, 17.66, 17.47

MS Calcd for $[M+NH_4]^+$ = 2038.8497. Found ESI-MS $[M+NH_4]^+$ = 2038.8418

Synthesis of pTSe-G4-$(N_3)_{16}$

pTSe-G4-OH (0.100 g, 0.052 mmol) was dissolved in 1 mL of pyridine, then 4 mL of dichloromethane was added. This was cooled to 0 °C in an ice bath. Separately, nitrophenyl chloroformate (0.249 g, 1.237 mmol) was dissolved in 1 mL of dichloromethane and then added rapidly to the stirring solution of dendrimer, which was left to react overnight. 3-azidopropylamine (0.206 g, 2.061 mmol) was added along with triethylamine (0.359 mL, 2.576 mmol), and this was stirred for 2 h. The reaction mixture was diluted with 20 mL of dichloromethane, then washed with 3 × 25 mL of 1 M $NaHSO_4$, 3 × 25 mL of 10% Na_2CO_3, and 1 × 40 mL of brine, dried with $MgSO_4$, filtered and solvent was removed by rotary evaporation *in vacuo*. The crude material was then purified using a gradient from 0 to 100% acetone in hexanes over 15 column volumes, with fractions collected by monitoring at 225 nm. The fractions containing product were combined and solvent was removed by rotary evaporation. This was subsequently dried under vacuum overnight to give the product as a clear, colourless oil. (0.131 g, 64%)

^{1}H NMR (700 MHz; $CDCl_3$): δ 7.80 (d, J = 8.2, 2H), 7.41 (d, J = 8.4, 2H), 5.65–5.48 (m, 16H), 4.49 (t, J = 5.8, 2H), 4.34–4.09 (m, 62H), 3.48 (t, J = 5.4, 2H), 3.37 (q, J = 6.0, 32H), 3.24 (q, J = 6.3, 32H), 2.47 (s, 3H), 1.78 (quintet, J = 6.6, 36H), 1.28–1.19 (m, 46H)

^{13}C NMR (176 MHz; $CDCl_3$): δ 173.15, 172.98, 172.1, 171.82, 171.72, 170.4, 156.2, 145.6, 136.4, 130.4, 128.1, 66.5, 66.0, 65.8, 65.2, 64.9, 58.5, 54.8, 49.6, 47.3, 46.80, 46.69, 39.2, 37.4, 29.40, 29.35, 29.0, 23.5, 21.8, 18.0, 17.65, 17.56, 17.3

MS Calcd for $[M+H+K]^{2+}$ = 1998.7989. Found ESI-MS $[M+H+K]^{2+}$ = 1998.7969

Outer Dendrons

Synthesis of NHS-G2-$(O_2Bn)_2$

COOH-G2-$(O_2Bn)_2$ (2.171 g, 3.999 mmol) was dissolved in 20 mL of dichloromethane, along with *N*-hydroxysuccinimide (1.381 g, 11.998 mmol). *N*-(3-dimethylaminopropyl)-*N*'ethylcarbodiimide hydrochloride (2.301g, 11.998 mmol) was added, and the reaction mixture was stirred for 4 h at room temperature, when TLC analysis indicated complete conversion of the starting material. Solvent was removed by rotary evaporation, and the reaction mixture was purified by silica gel chromatography using a gradient from 40% to 100% ethyl acetate in hexanes over 10 column volumes with fractions collected at 254 nm. The fractions containing product were combined and solvent was removed by rotary evaporation. The resulting oil was dissolved in 15 mL of dichloromethane and precipitated into 250 mL of rapidly stirring ice cold hexanes. The solids were collected by vacuum filtration on a Buchner funnel and were washed with pentanes, dried on the filter for 10 min, then dried overnight *in vacuo* to give the product as a white powder. (2.328 g, 90%)

^{1}H NMR (700 MHz; $CDCl_3$): δ 7.41 (d, J = 5.9, 4H), 7.31 (d, J = 6.5, 6H), 5.43 (s, 2H), 4.65 (d, J = 11.1, 4H), 4.61 (d, J = 11.1, 2H), 4.39 (d, J = 11.1, 2H), 3.62 (t, J = 10.0, 4H), 2.74 (s, 4H), 1.44 (s, 3H), 0.99 (s, 6H)

^{13}C NMR (176 MHz; $CDCl_3$): δ 173.3, 168.6, 138.0, 129.0, 128.3, 126.3, 101.9, 73.69, 73.57, 65.0, 47.0, 42.8, 25.7, 17.77, 17.63

MS Calcd for $[M+Na]^+$ = 662.2208. Found ESI-MS $[M+Na]^+$ = 662.2209

Synthesis of Cbz-G2-(O_2Bn)$_2$

NHS-G2-(O_2Bn)$_2$ (1.000 g, 1.563 mmol) was dissolved in 5 mL of dichloromethane, then *N*-Cbz-1,4-diaminobutane hydrochloride (0.470 g, 1.954 mmol) was added, followed by triethylamine (0.327 mL, 2.345 mmol). After 4 h, the reaction was deemed complete by TLC, and the reaction mixture was diluted with 20 mL of dichloromethane, washed with 3 × 25 mL of 1 M $NaHSO_4$ and 1 × 40 mL of brine, dried with $MgSO_4$, filtered and solvent was removed by rotary evaporation *in vacuo*. The crude material was then purified using a gradient from 10 to 100% acetone in hexanes over 15 column volumes, with fractions collected by monitoring at 205 nm. The fractions containing product were combined and solvent was removed by rotary evaporation. This was subsequently dried under vacuum overnight to give a white powder. (0.984 g, 86%)

^{1}H NMR (700 MHz; $CDCl_3$): δ 7.41 (d, J = 6.1, 4H), 7.37 (d, J = 3.7, 4H), 7.31 (d, J = 6.7, 7H), 6.41 (s, 1H), 5.43 (s, 2H), 5.10 (s, 2H), 4.97 (s, 1H), 4.59 (t, J = 9.0, 4H), 4.41 (d, J = 11.2, 2H), 4.31 (d, J = 11.2, 2H), 3.62 (d, J = 11.5, 4H), 2.99 (q, J = 6.0, 2H), 2.87 (q, J = 5.9, 2H), 1.20 (d, J = 22.6, 7H), 0.98 (s, 6H)

^{13}C NMR (176 MHz; $CDCl_3$): δ 173.4, 172.3, 156.3, 137.6, 136.7, 129.0, 128.5, 128.17, 128.08, 126.1, 101.8, 73.59, 73.51, 66.5, 46.5, 42.7, 40.5, 38.9, 26.8, 26.4, 17.7

MS Calcd for $[M+Na]^+$ = 769.3312. Found ESI-MS $[M+Na]^+$ = 769.3310

Synthesis of H_2N-G2-(OH)$_4$

Cbz-G2-(O_2Bn)$_2$ (0.700 g, 0.960 mmol) was dissolved in 5 mL of dichloromethane, then diluted with 5 mL of methanol. To this, Palladium hydroxide on carbon (105 mg of 20 wt%

$Pd(OH)_2$) was added, and the reaction mixture was placed under a hydrogen atmosphere via balloon. After 2 h, the balloon was replaced with a fresh hydrogen balloon, and at 4 h the reaction was found to be complete by ESI-MS. The reaction mixture was filtered through a plug of celite, then solvent was removed by rotary evaporation. The residue was then dried *in vacuo* overnight to give the product as a white foam. (0.411 g, 99%)

^{1}H NMR (700 MHz; CD_3OD): δ 4.27 (q, J = 15.7, 4H), 3.69 (d, J = 10.9, 4H), 3.60 (d, J = 10.9, 4H), 3.25 (t, J = 6.7, 2H), 2.95 (t, J = 7.5, 2H), 1.67 (quintet, J = 7.5, 2H), 1.60 (quintet, J = 7.1, 2H), 1.29 (s, 3H), 1.15 (s, 6H)

^{13}C NMR (176 MHz; CD_3OD): δ 176.0, 175.5, 67.2, 51.9, 49.8, 47.5, 40.4, 39.7, 27.4, 25.9, 18.3

MS Calcd for $[M+H]^+$ = 437.2494. Found ESI-MS $[M+H]^+$ = 437.2488

Synthesis of DIBAC-G2-$(OH)_4$

H_2N-G2-$(OH)_4$ (0.456 g, 1.044 mmol) was dissolved in 2.5 mL of methanol. To this, DIBAC-NHS (0.400 g, 0.994 mmol) dissolved in 2.5 mL of dichloromethane was added, along with triethylamine (0.174 mL, 1.243 mmol). The reaction mixture was stirred for 45 min, at which time HPLC analysis indicated no residual DIBAC-NHS. Solvent was removed by rotary evaporation, and the reaction mixture was diluted in 3 mL of 1:1 DMSO:Water and purified by reversed phase flash chromatography using a gradient of 15 % to 100% acetonitrile in water over 15 column volumes, with collection at 254 nm. The fractions containing product combined and concentrated by rotary evaporation, then

diluted with 30 mL of water and lyophilized to give the product as a fluffy white solid. (664 mg, 92%).

^{1}H NMR (700 MHz; CD_3OD): δ 7.64 (d, J = 7.5, 1H), 7.60–7.58 (m, 1H), 7.47–7.44 (m, 3H), 7.36 (td, J = 7.5, 1.4, 1H), 7.32 (td, J = 7.5, 1.0, 1H), 7.24 (dd, J = 7.5, 1.2, 1H), 5.12 (d, J = 14.1, 1H), 4.27–4.23 (m, 4H), 3.68 (dd, J = 12.5, 7.9, 5H), 3.59 (d, J = 10.9, 4H), 3.17 (t, J = 6.9, 2H), 3.09–3.02 (m, 2H), 2.69 (dt, J = 16.5, 7.5, 1H), 2.32 (dt, J = 15.2, 7.5, 1H), 2.15 (dt, J = 15.2, 6.8, 1H), 1.97 (dt, J = 16.6, 6.8, 1H), 1.46–1.39 (m, 4H), 1.26 (s, 3H), 1.14 (s, 6H)

^{13}C NMR (176 MHz; CD_3OD): δ 175.9, 175.1, 174.4, 174.0, 152.6, 149.4, 133.4, 130.6, 130.0, 129.6, 129.1, 128.8, 128.1, 126.4, 124.4, 123.7, 115.6, 108.8, 67.2, 65.9, 56.7, 51.8, 47.5, 40.3, 40.0, 31.9, 31.3, 27.69, 27.65, 18.3, 17.3

MS Calcd for $[M+Na]^+$ = 746.3265. Found ESI-MS $[M+Na]^+$ = 746.3258

Synthesis of DIBAC-G2-(Imid)$_4$

DIBAC-G2-(OH)$_4$ (0.200 g, 0.276 mmol) was dissolved in 1 mL of acetonitrile with gentle heating. To this, 1,1'-carbonyldiimidazole (0.224 g, 1.382 mmol) was added, and the reaction was stirred for 30 min. The reaction mixture was then precipitated into rapidly stirring toluene, then collected on a Hirsch funnel and washed with small amounts of toluene, then diethyl ether, then pentane. The solids were collected from the filter, then dried *in vacuo* to give the product as an off-white powder. (202 mg, 66%)

^{1}H NMR (600 MHz; DMSO-*d*6): δ 8.25 (s, 4H), 7.81 (t, J = 5.4, 1H), 7.67–7.61 (m, 3H), 7.57 (s, 4H), 7.50–7.43 (m, 3H), 7.38–7.28 (m, 3H), 7.05 (t, J = 0.6, 4H), 5.02 (d, J = 14.1,

1H), 4.62–4.47 (m, 8H), 4.20 (q, J = 13.4, 4H), 3.60 (d, J = 14.0, 1H), 2.92–2.87 (m, 4H), 2.55 (dd, J = 16.2, 8.0, 1H), 2.21 (dt, J = 15.4, 7.7, 1H), 1.97 (ddd, J = 15.0, 8.4, 6.2, 1H), 1.75 (ddd, J = 16.4, 7.9, 5.9, 1H), 1.34–1.20 (m, 10H), 1.16–1.06 (m, 3H)

^{13}C NMR (176 MHz; DMSO-*d*6): δ 171.23, 171.06, 170.8, 151.6, 148.4, 147.8, 137.3, 134.9, 132.4, 130.3, 129.6, 128.9, 128.08, 127.95, 127.6, 126.7, 125.1, 122.5, 121.4, 121.0, 117.5, 114.2, 108.1, 67.97, 67.93, 66.3, 54.9, 46.0, 45.4, 38.4, 38.1, 30.4, 29.7, 26.46, 26.33, 17.2

MS Calcd for $[M+H]^+$ = 1100.4108. Found ESI-MS $[M+H]^+$ = 1100.4079

Synthesis of NHS-G3-$(O_2Bn)_4$

COOH-G3-$(O_2Bn)_4$ (1.441 g, 1.216 mmol), prepared by literature methods,[10] was dissolved in 20 mL of dichloromethane, along with *N*-hydroxysuccinimide (0.421 g, 3.653 mmol). *N*-(3-dimethylaminopropyl)-*N*'ethylcarbodiimide hydrochloride (0.700 g, 3.653 mmol) was added, and the reaction mixture was stirred for 4 h at room temperature, when TLC analysis indicated complete conversion of the starting material. Solvent was removed by rotary evaporation, and the reaction mixture was purified by silica gel chromatography using a gradient from 40% to 100% ethyl acetate in hexanes over 10 column volumes with fractions collected by monitoring at 254 nm. The fractions containing product were combined and solvent was removed by rotary evaporation. The resulting oil was dissolved in 15 mL of dichloromethane and precipitated into 250 mL of rapidly stirring ice cold hexanes. The solids were collected by vacuum filtration on a Buchner funnel and were

washed with pentanes, dried on the filter for 10 min, then dried overnight *in vacuo* to give the product as a white powder. (1.472 g, 94%)

^{1}H NMR (700 MHz; $CDCl_3$): δ 7.40 (d, J = 7.0, 8H), 7.31 (q, J = 7.1, 12H), 5.40 (s, 4H), 4.57 (t, J = 9.2, 8H), 4.42–4.38 (m, 8H), 4.16 (d, J = 11.2, 2H), 4.01 (d, J = 11.2, 2H), 3.58 (dd, J = 11.4, 3.7, 8H), 2.64 (m, 4H), 1.27 (s, 7H), 1.17 (s, 3H), 0.94 (d, J = 5.2, 12H)

^{13}C NMR (176 MHz; $CDCl_3$): δ 173.3, 171.9, 168.5, 138.0, 129.0, 126.34, 126.26, 101.8, 73.60, 73.57, 65.7, 65.41, 65.38, 47.1, 46.4, 42.7, 25.6, 17.8, 17.55, 17.42

MS Calcd for $[M+NH_4]^+$ = 1297.5179. Found ESI-MS $[M+NH_4]^+$ = 1297.5201

Synthesis of Cbz-G3-$(O_2Bn)_4$ (7)

NHS-G3-$(O_2Bn)_4$ (1.001 g, 0.781 mmol) was dissolved in 15 mL of dichloromethane. To this, *N*-Cbz-1,4-diaminobutane hydrochloride (0.303 g, 1.172 mmol) was added, followed by triethylamine (0.541 mL, 3.124 mmol). After 4 h, the reaction was deemed complete by HPLC, and the reaction mixture was diluted with 20 mL of dichloromethane, washed with 3 × 25 mL of 1 M $NaHSO_4$ and 1 × 40 mL of brine, dried with $MgSO_4$, filtered, and solvent was removed by rotary evaporation *in vacuo*. The crude material was then purified using a gradient from 10 to 100% acetone in hexanes over 15 column volumes, with fractions collected by monitoring at 205 nm. The fractions containing product were combined and solvent was removed by rotary evaporation. This was subsequently dried under vacuum overnight to give a white powder. (0.755 g, 70%).

^{1}H NMR (700 MHz; $CDCl_3$): δ 7.40–7.27 (m, 25H), 5.77 (t, J = 5.7, 1H), 5.42 (t, J = 6.1, 1H), 5.40 (s, 4H), 5.09 (m, 2H), 4.58–4.55 (m, 8H), 4.33 (m, 8H), 4.04 (d, J = 11.1, 2H),

3.94 (d, J = 11.1, 2H), 3.57 (dd, J = 17.3, 11.8, 8H), 3.08 (q, J = 6.0, 2H), 2.87 (q, J = 6.5, 2H), 1.29 (s, 4H), 1.21 (s, 6H), 0.93 (t, J = 9.2, 15H)

^{13}C NMR (176 MHz; $CDCl_3$): δ 173.5, 172.0, 171.5, 156.7, 137.9, 137.0, 129.0, 128.6, 128.28, 128.10, 126.24, 126.18, 101.78, 101.70, 73.69, 73.63, 73.59, 73.52, 66.9, 66.6, 65.50, 65.39, 47.0, 46.3, 42.8, 40.6, 39.3, 32.0, 27.3, 27.0, 22.8, 17.8, 17.5, 14.3

MS Calcd for $[M+H]^+$ = 1387.6007. Found ESI-MS $[M+H]^+$ = 1387.5988

Synthesis of H_2N-G3-$(OH)_8$ (8)

Cbz-G3-$(O_2Bn)_4$ (1.400 g, 1.009 mmol) was dissolved in 25 mL of dichloromethane, then diluted to 50 mL with methanol. Pd(OH)2/C (280 mg) was added, and the reaction was placed under a hydrogen atmosphere by evacuation and backfilling with a hydrogen balloon and left to stir vigorously for 4.5 h. The reaction mixture was filtered through a celite plug in a glass fritted funnel, and the solvent was removed via rotary evaporation. The residue was dried overnight *in vacuo*, giving the product as a white foam. (0.906 g, 99%).

^{1}H NMR (700 MHz; CD_3OD): δ 4.30–4.22 (m, 12H), 3.68 (dd, J = 10.9, 4.0, 8H), 3.59 (d, J = 10.9, 8H), 3.24 (t, J = 7.1, 2H), 3.00 (t, J = 7.4, 2H), 1.68 (dt, J = 14.9, 7.4, 2H), 1.62 (dt, J = 14.5, 7.1, 2H), 1.30 (d, J = 3.8, 9H), 1.15 (d, J = 0.8, 12H)

^{13}C NMR (176 MHz; CD_3OD): δ 176.0, 174.7, 173.7, 68.2, 66.4, 65.9, 51.9, 47.95, 47.76, 40.4, 40.1, 27.5, 26.0, 18.24, 18.12, 17.3

MS Calcd for $[M+H]^+$ = 901.4387. Found ESI-MS $[M+H]^+$ = 901.4348

Synthesis of DIBAC-G3-(OH)$_8$ (9)

H_2N-G3-(OH)$_8$ (0.822 g, 0.913 mmol) was dissolved in 10 mL of methanol. To this, DIBAC-NHS (**5**, 0.350 g, 0.870 mmol) dissolved in 5 mL of dichloromethane was added, followed by diisopropylethylamine (0.182 mL, 1.044 mmol). After 45 min, solvent was removed by rotary evaporation and the crude residue was diluted with 2 mL of 1:1 DMSO:water and purified by reverse phase flash chromatography using a gradient of 15% to 100% acetonitrile in water over 15 column volumes. The fractions containing product were combined and solvent was removed by rotary evaporation. The resulting residue was dissolved in 40 mL of water and lyophilized overnight to give the product as a fluffy white solid. (0.955 g, 92%)

^{1}H NMR (700 MHz; CD_3OD): δ 7.65 (d, J = 7.5, 1H), 7.61–7.60 (m, 1H), 7.48–7.45 (m, 3H), 7.37 (td, J = 7.5, 1.4, 1H), 7.33 (td, J = 7.5, 0.9, 1H), 7.25 (dd, J = 7.5, 1.2, 1H), 5.13 (d, J = 14.1, 1H), 4.30–4.22 (m, 12H), 3.71 (d, J = 14.1, 1H), 3.67 (dt, J = 10.8, 1.4, 8H), 3.58 (d, J = 10.9, 8H), 3.18 (t, J = 7.1, 2H), 3.11–3.04 (m, 2H), 2.70 (dt, J = 16.4, 7.7, 1H), 2.34 (dt, J = 15.2, 7.5, 1H), 2.17 (dt, J = 15.3, 6.9, 1H), 1.98 (dt, J = 16.6, 6.8, 1H), 1.48 (pentet, J = 7.3, 2H), 1.40 (quintet, J = 7.4, 2H), 1.28 (s, 9H), 1.14 (s, 11H)

^{13}C NMR (176 MHz; CD_3OD): δ 175.9, 174.41, 174.37, 174.1, 173.8, 152.7, 149.5, 133.5, 130.6, 130.0, 129.7, 129.2, 128.9, 128.1, 126.5, 124.4, 123.7, 115.6, 108.8, 68.1, 66.3, 65.9, 56.7, 51.9, 49.0, 40.5, 40.0, 32.0, 31.4, 27.79, 27.72, 18.25, 18.16, 17.3

MS Calcd for $[M+Na]^+$ = 1210.5159. Found ESI-MS $[M+Na]^+$ = 1210.5183

Synthesis of DIBAC-G3-(Imid)$_8$ (10)

1,1'-carbonyldiimidazole (1.638 g, 10.01 mmol) was dissolved in 15 mL of acetonitrile, then a solution of DIBAC-G3-(OH)$_8$ (0.300 g, 0.252 mmol) in 2 mL of acetonitrile was added. After 3 h, visible solids had formed and the reaction was deemed complete by HPLC. The reaction mixture was cooled to 0 °C in an ice bath to ensure complete precipitation, and the resulting solids were collected by vacuum filtration on a Hirsch funnel and washed with ether and pentane, then dried *in vacuo* to give the product as an off-white solid. (0.395 g, 81%).

^{1}H NMR (600 MHz; DMSO-*d*6): δ 8.24 (s, 8H), 7.73 (t, J = 5.3, 1H), 7.67–7.60 (m, 2H), 7.55 (s, 8H), 7.49–7.42 (m, 3H), 7.37–7.27 (m, 3H), 7.03 (s, 8H), 5.01 (d, J = 14.1, 1H), 4.59–4.54 (m, 16H), 4.21 (s, 8H), 4.06 (d, J = 10.7, 2H), 4.01 (d, J = 10.9, 2H), 3.60 (d, J = 14.0, 1H), 2.96 (q, J = 5.9, 2H), 2.89 (q, J = 6.0, 2H), 2.24–2.18 (m, 1H), 1.99–1.94 (m, 1H), 1.76 (ddd, J = 16.3, 8.0, 5.9, 1H), 1.32–1.24 (m, 16H), 1.10 (d, J = 9.8, 9H)

^{13}C NMR (176 MHz; DMSO-*d*6): δ 171.3, 171.12, 171.08, 170.88, 170.77, 151.6, 148.4, 144.7, 138.8, 137.3, 135.1, 132.4, 130.6, 129.6, 128.9, 128.06, 127.94, 127.6, 126.8, 125.1, 122.5, 121.4, 119.5, 114.2, 108.1, 67.9, 66.6, 65.4, 54.9, 46.11, 46.03, 45.4, 38.5, 38.1, 30.4, 29.7, 26.45, 26.38, 17.0, 16.7

MS Calcd for $[M+2Na]^{2+}$ = 1461.5267. Found ESI-MS $[M+2Na]^{2+}$ = 1461.5244

Synthesis of DIBAC-G3-(Benzyl)$_8$ (11)

DIBAC-G3-(Imid)$_8$ (0.050 g, 0.026 mmol) was dissolved in 1 mL of dichloromethane, to which benzylamine (0.045 mL, 0.412 mmol) and diisopropylethylamine (0.090 mL, 0.515

mmol) were added. This was stirred for 4 h until HPLC indicated complete conversion. The reaction mixture was diluted with 20 mL of dichloromethane, then extracted with 3 × 25 mL of 1 M $NaHSO_4$, and 1 × 40 mL of brine, dried with $MgSO_4$, filtered and solvent was removed by rotary evaporation. The resulting oil was purified by silica gel chromatography using a gradient of 10% to 100% acetone in hexanes over 15 column volumes, with fractions collected by monitoring at 205 nm. The fractions containing product were combined and solvent was removed by rotary evaporation. The resulting oil was dried overnight *in vacuo* to give the product as a white foam. (35 mg, 60%).

^{1}H NMR (700 MHz; CD_3OD): δ 7.61–7.19 (m, 48H), 5.08 (d, J = 14.1, 1H), 4.16 (m, 44H), 3.65 (d, J = 14.1, 1H), 3.119 (s, 2H), 3.003 (s, 2H), 2.65 (dt, J = 16.2, 7.8, 1H), 2.29 (dd, J = 14.9, 7.4, 1H), 2.08 (dt, J = 14.0, 6.5, 1H), 1.91 (dt, J = 16.51, 6.86, 1H), 1.405 (s, 2H), 1.331 (s, 2H), 1.15 (m, 20H)

^{13}C NMR (176 MHz; CD_3OD): δ 174.3, 174.09, 173.99, 173.4, 158.4, 157.85, 157.78, 157.74, 152.7, 149.5, 140.7, 140.4, 133.5, 130.6, 129.97, 129.83, 129.2, 128.87, 128.79, 128.09, 127.90, 127.75, 126.5, 124.4, 123.7, 115.6, 108.8, 68.2, 67.1, 66.67, 66.61, 48.4, 47.9, 47.5, 46.1, 45.5, 40.5, 40.0, 32.0, 31.4, 27.84, 27.72, 18.19, 18.01

MS Calcd for $[M+2Na]^{2+}$ = 1148.9633. Found ESI-MS $[M+2Na]^{2+}$ = 1148.9645

Synthesis of DIBAC-G3-(Alkyl)$_8$ (12)

DIBAC-G3-(Imid)$_8$ (0.050 g, 0.026 mmol) was dissolved in 1 mL of tetrahydrofuran. To this, dodecylamine (0.076 g, 0.412 mmol) was added, along with diisopropylethylamine (0.090 mL, 0.515 mmol). The reaction mixture was stirred for 4 h, until full conversion

was determined by TLC. The reaction mixture was diluted with 20 mL of dichloromethane, then extracted with 3 × 25 mL of 1 M $NaHSO_4$, and 1 × 40 mL of brine, dried with $MgSO_4$, filtered and solvent was removed by rotary evaporation. The resulting oil was purified by silica gel chromatography using a gradient of 10% to 55% acetone in hexanes over 15 column volumes, with fractions being collected at 215 nm. The fractions containing product were combined, and solvent was removed by rotary evaporation. The resulting oil was dried overnight *in vacuo* to give the product as a glassy solid. (64 mg, 86%).

^{1}H NMR (700 MHz; $CDCl_3$): δ 7.64 (d, J = 7.4, 1H), 7.51 (s, 1H), 7.40–7.37 (m, 3H), 7.33 (t, J = 7.4, 1H), 7.30 (t, J = 7.4, 1H), 7.25 (d, J = 7.2, 1H), 6.95 (m, 1H), 6.26 (m, 1H), 5.47–5.32 (m, 7H), 5.13 (d, J = 13.9, 1H), 4.27–4.10 (m, 28H), 3.67 (d, J = 13.9, 1H), 3.21–3.10 (m, 20H), 2.78 (dt, J = 16.3, 7.8, 1H), 2.41 (dt, J = 14.5, 7.0, 1H), 2.22–2.17 (m, 1H), 1.96–1.91 (m, 1H), 1.66 (s, 6H), 1.47 (d, J = 0.2, 20H), 1.30–1.25 (m, 155H), 1.16 (s, 11H), 0.87 (t, J = 7.1, 24H)

Synthesis of DIBAC-G3-(BocLys(H)OtBu)$_8$ (13)

DIBAC-G3-(Imid)$_8$ (0.100 g, 0.052 mmol) was dissolved in 1 mL of dichloromethane, to which N^{α}-BocLys(H)OtBu (0.218 g, 0.721 mmol) and diisopropylethylamine (0.162 mL, 0.927 mmol) were added. This was stirred for 5 h until HPLC indicated complete conversion. The reaction mixture was diluted with 20 mL of dichloromethane, then extracted with 3 × 25 mL of 1 M $NaHSO_4$, and 1 × 40 mL of brine, dried with $MgSO_4$, filtered and solvent was removed by rotary evaporation. The resulting oil was purified by silica gel chromatography using a gradient of 10% to 100% acetone in hexanes over 15

column volumes, with fractions collected by monitoring at 225 nm. The fractions containing product were combined and solvent was removed by rotary evaporation. The resulting oil was dried overnight *in vacuo* to give the product as a white foam (172 mg, 87%)

^{1}H NMR (700 MHz; $CDCl_3$): δ 7.69 (dd, J = 38.3, 7.7, 1H), 7.49–7.47 (m, 1H), 7.41–7.39 (m, 1H), 7.37 (dd, J = 8.1, 0.6, 1H), 7.31 (td, J = 7.5, 0.9, 1H), 7.20 (td, J = 7.5, 1.0, 1H), 7.11 (ddd, J = 8.4, 6.5, 1.0, 1H), 5.46 (t, J = 161.8, 14H), 4.35–4.07 (m, 38H), 3.25–3.22 (m, 4H), 3.13–3.09 (m, 18H), 2.67–2.66 (m, 2H), 2.49–2.48 (m, 2H), 1.76–1.73 (m, 14H), 1.64–1.60 (m, 19H), 1.54–1.49 (m, 31H), 1.47 (s, 167H), 1.41–1.33 (m, 22H), 1.28–1.17 (m, 33H)

^{13}C NMR (176 MHz; $CDCl_3$): δ 173.21, 173.17, 173.0, 172.54, 172.44, 172.11, 171.97, 171.90, 156.24, 156.13, 156.05, 155.66, 155.49, 151.5, 148.2, 137.2, 132.6, 132.4, 130.92, 130.88, 130.73, 129.8, 129.5, 129.2, 128.81, 128.75, 128.33, 128.23, 127.9, 127.2, 125.6, 123.3, 122.5, 114.8, 108.0, 81.9, 79.7, 65.9, 60.5, 60.2, 55.69, 55.58, 55.2, 54.1, 47.33, 47.31, 46.7, 40.9, 32.6, 29.83, 29.78, 29.62, 28.5, 28.2, 22.7, 21.2, 17.97, 17.90, 17.6, 14.3

MS Calcd for $[M+3Na]^{3+}$ = 1294.0312. Found ESI-MS $[M+3Na]^{3+}$ = 1294.0331

Synthesis of DIBAC-G2-(BocLysO^{t}Bu)$_4$

DIBAC-G2-(Imid)$_4$ (0.070 g, 0.064 mmol) was dissolved in 1 mL of dichloromethane, then BocLys(H)-O^{t}Bu (0.154 g, 0.509 mmol) and triethylamine (0.089 mL, 0.636 mmol) were added. This was stirred at room temperature for 4 h until HPLC indicated complete conversion. Solvent was removed via rotary evaporation, and the resulting oil was

dissolved in 1 mL of DMSO and purified by reversed phase flash chromatography using a gradient of 50% to 100% acetonitrile in water over 15 column volumes, with fraction monitoring at 254 nm. The fractions containing product were combined and solvent was removed by rotary evaporation, and the resulting oil was dried overnight *in vacuo* to give the product as a white foam (77 mg, 60%).

^{1}H NMR (700 MHz; CD_3OD): δ 7.65 (d, J = 7.4, 1H), 7.61–7.59 (m, 1H), 7.48–7.45 (m, 3H), 7.36 (td, J = 7.5, 1.0, 1H), 7.33 (td, J = 7.5, 1.2, 1H), 7.25 (dd, J = 7.5, 1.3, 1H), 5.14 (d, J = 14.1, 1H), 4.25 (s, 4H), 4.18–4.13 (m, 8H), 3.94–3.85 (m, 4H), 3.71 (d, J = 14.1, 1H), 3.19 (t, J = 7.0, 2H), 3.07 (q, J = 5.9, 10H), 2.70 (dtd, J = 16.6, 7.5, 2.0, 1H), 2.34 (dt, J = 15.1, 7.5, 1H), 2.16 (dt, J = 14.8, 7.2, 1H), 1.98 (ddd, J = 16.5, 7.2, 6.5, 1H), 1.76–1.71 (m, 4H), 1.61 (dtd, J = 14.0, 9.3, 4.8, 4H), 1.53–1.44 (m, 95H), 1.25 (dd, J = 35.8, 21.2, 9H)

^{13}C NMR (176 MHz; CD_3OD): δ 174.5, 174.33, 174.15, 173.99, 173.95, 173.79, 158.3, 158.1, 152.7, 149.5, 133.5, 130.6, 130.0, 129.6, 129.2, 128.9, 128.1, 126.5, 124.4, 123.7, 115.6, 108.8, 82.5, 80.4, 67.7, 66.9, 57.0, 56.7, 48.4, 47.6, 42.3, 41.6, 40.4, 40.0, 32.4, 32.0, 31.4, 30.82, 30.80, 30.75, 30.4, 28.7, 27.8, 24.2, 18.36, 18.18, 17.99

MS Calcd for $[M+H]^+$ = 2047.1433. Found ESI-MS $[M+H]^+$ = 2037.1393

Synthesis of DIBAC-G2-(PEG$_{15}$)$_4$

DIBAC-G2-(Imid)$_4$ (0.025 g, 0.023 mmol) was dissolved in 0.5 mL of dichloromethane, and to this MeO-PEG$_{15}$-NH$_2$ (0.079 g, 0.114 mmol) and triethylamine (0.016 mL, 0.114 mmol) were added and the reaction mixture was stirred at room temperature overnight.

After overnight stirring, solvent was removed by rotary evaporation, and the resulting oil was dissolved in 1 mL of deionized water and was purified by size exclusion chromatography using 5 × 5 mL GE Healthcare HiTrap columns using deionized water as eluent. The fractions containing product were combined and were lyophilized overnight to give the product as a waxy white solid. (0.068 g, 83%).

^{1}H NMR (700 MHz; CD_3OD): δ 7.66 (d, J = 7.4, 1H), 7.62 (m, 1H), 7.49–7.46 (m, 3H), 7.38 (td, J = 7.5, 1.2, 1H), 7.34 (t, J = 7.4, 1H), 7.27 (d, J = 7.4, 1H), 7.16 (d, J = 66.8, 1H), 5.14 (d, J = 14.1, 1H), 4.24–4.17 (m, 12H), 3.63 (s, 212H), 3.54–3.52 (m, 16H), 3.36 (s, 12H), 3.26 (t, J = 5.3, 8H), 3.19 (t, J = 7.1, 2H), 3.08 (t, J = 6.9, 2H), 2.73–2.69 (m, 1H), 2.35 (ddd, J = 16.2, 8.6, 4.3, 1H), 2.16 (dt, J = 14.7, 7.2, 1H), 1.97 (dt, J = 16.5, 6.8, 1H), 1.50–1.47 (m, 2H), 1.43–1.40 (m, 2H), 1.22 (m, 9H)

^{13}C NMR (176 MHz; CD_3OD): δ 174.43, 174.33, 174.00, 173.96, 158.3, 152.8, 149.5, 133.5, 130.7, 130.1, 129.7, 129.2, 128.9, 128.2, 126.5, 124.4, 123.7, 115.6, 108.9, 73.0, 67.8, 67.0, 59.1, 56.7, 42.5, 41.8, 40.4, 40.0, 32.0, 31.4, 27.8, 18.31, 18.16, 18.04

MS Calcd for $[M+5Na]^{5+}$ = 741.5883. Found ESI-MS $[M+5Na]^{5+}$ = 738.5854

Synthesis of DIBAC-G3-$(PEG_{15})_8$ (14)

DIBAC-G3-$(Imid)_8$ (20 mg, 10 μmol) was dissolved in 0.5 mL of dichloromethane. To this, NH_2-PEG_{15}-OMe (86 mg, 124 μmol) and diisopropylethylamine (32 μL, 185 μmol) were added and the reaction mixture was stirred overnight at room temperature. The following day, solvent was removed by rotary evaporation and the reaction mixture was dissolved in 1 mL of deionized water. The crude reaction mixture was then purified by size

exclusion chromatography using 3 × 5 mL GE-HiTrap desalting columns in series, collecting the high molecular weight components as per the manufacturer's instructions. The high molecular weight fraction was lyophilized overnight to give the product as a white solid (67 mg, 93%)

^{1}H NMR (700 MHz; $CDCl_3$): δ 7.65 (d, J = 7.4, 1H), 7.53–7.52 (m, 1H), 7.41–7.29 (m, 5H), 7.24 (d, J = 7.4, 1H), 7.10 (t, J = 36.3, 1H), 6.88 (m, 1H), 6.37 (m, 1H), 5.57 (d, J = 194.3, 8H), 5.13 (d, J = 13.9, 1H), 4.18 (d, J = 94.5, 28H), 3.65 (d, J = 6.5, 1H), 3.54 (t, J = 4.7, 18H), 3.52 (t, J = 5.0, 16H), 3.37 (s, 24H), 3.31–3.20 (m, 18H), 3.09 (td, J = 14.2, 7.1, 2H), 2.77 (ddd, J = 16.9, 7.9, 6.8, 1H), 2.42–2.37 (m, 1H), 2.17 (dt, J = 15.1, 6.3, 1H), 1.93 (dt, J = 16.8, 6.2, 1H), 1.45–1.44 (m, 2H), 1.39–1.36 (m, 2H), 1.22 (m, 21H)

^{13}C NMR (176 MHz; $CDCl_3$): δ 172.8, 172.49, 172.38, 172.1, 156.2, 151.6, 149.21, 149.12, 148.5, 148.3, 135.6, 132.4, 129.6, 128.9, 128.3, 127.2, 126.6, 125.6, 123.3, 122.5, 114.8, 108.1, 72.1, 70.4, 70.0, 67.3, 65.9, 65.27, 65.13, 59.2, 55.7, 47.1, 46.88, 46.73, 46.5, 41.6, 40.9, 40.4, 39.7, 31.2, 30.4, 26.98, 26.84, 17.9, 17.6

MS Calcd for $[M+7Na]^{7+}$ = 1012.5383. Found ESI-MS $[M+7Na]^{7+}$ = 1012.5425

Click Reactions

Synthesis of pTSe-G4-(benzyl)$_{16}$

pTSe-G1-$(N_3)_2$ (1 mg, 1.7 μmol) was dissolved in 0.5 mL of dichloromethane. To this, a solution of DIBAC-G3-$(Benzyl)_8$ (10 mg, 4.4 μmol) was added and solvent was removed by rotary evaporation, leaving a viscous oil. After 5 min, MALDI-MS indicated that the reaction was complete, and the oil was purified by precipitation into methanol, then

filtration. The collected solids were dried overnight *in vacuo* to give the product as a white powder. (6 mg, 67%)

^{1}H NMR (700 MHz; $CDCl_3$): δ 7.74 (d, J = 2.5, 2H), 7.63–6.99 (m, 117H), 6.88–5.44 (m, 25H), 4.48–3.96 (m, 115H), 3.40–2.74 (m, 14H), 2.41 (s, 3H), 2.28–1.62 (m, 16H), 1.33–0.99 (m, 66H)

^{13}C NMR (176 MHz; $CDCl_3$): δ 173.1, 172.80, 172.68, 172.24, 172.13, 171.89, 171.82, 171.1, 156.44, 156.24, 155.9, 145.4, 143.0, 141.1, 140.2, 138.6, 136.2, 135.7, 134.6, 133.5, 132.6, 132.0, 131.6, 131.3, 131.1, 130.3, 129.81, 129.70, 129.57, 129.2, 128.32, 128.14, 128.02, 127.5, 127.2, 124.0, 67.1, 66.3, 65.28, 65.13, 58.1, 55.0, 53.0, 51.6, 47.32, 47.14, 47.04, 46.7, 46.3, 46.0, 45.7, 45.1, 39.7, 39.18, 39.00, 38.5, 37.5, 31.02, 30.87, 30.5, 29.99, 29.83, 29.68, 29.3, 27.0, 26.67, 26.61, 21.8, 17.9, 17.6, 17.2

MALDI: m/z calc: 5075.5, exp: 5098.9 ($[M+Na]^+$)

Synthesis of pTSe-G5-(benzyl)$_{32}$

pTSe-G2-$(N_3)_4$ (1 mg, 0.95 μmol) was dissolved in 0.5 mL of dichloromethane. To this, a solution of DIBAC-G3-$(Benzyl)_8$ (10.7 mg, 4.7 μmol) was added and solvent was removed by rotary evaporation, leaving a viscous oil. After 5 min, MALDI-MS indicated that the reaction was complete, and the oil was purified by precipitation into methanol, then filtration. The collected solids were dried overnight *in vacuo* to give the product as a white powder. (6 mg, 63%)

^{1}H NMR (700 MHz; $CDCl_3$): δ 7.75 (dd, J = 5.5, 1.8, 2H), 7.59–7.11 (m, 205H), 7.05–5.43 (m, 47H), 4.47–4.08 (m, 204H), 3.45–2.77 (m, 26H), 2.39 (s, 3H), 2.20–2.13 (m, 13H), 1.99–1.89 (m, 6H), 1.62–1.60 (m, 4H), 1.32–1.01 (m, 112H)

^{13}C NMR (176 MHz; $CDCl_3$): δ 173.1, 172.6, 172.1, 171.9, 171.2, 156.3, 156.0, 145.5, 145.0, 143.0, 141.2, 140.2, 138.7, 136.3, 135.7, 134.6, 133.5, 132.7, 132.0, 131.7, 131.4, 131.0, 130.3, 129.83, 129.69, 129.58, 129.2, 128.1, 127.2, 126.7, 124.2, 67.1, 66.2, 65.28, 65.16, 58.4, 55.5, 54.9, 53.0, 51.7, 47.3, 46.7, 46.42, 46.30, 46.0, 45.7, 45.1, 39.7, 39.17, 39.02, 38.6, 37.8, 30.9, 30.7, 30.2, 29.7, 27.0, 26.70, 26.62, 17.9, 17.6

MALDI: m/z calc: 10066.8, exp: 10091.0 ($[M+Na]^+$)

Synthesis of pTSe-G6-(benzyl)$_{64}$ (15)

pTSe-G3-$(N_3)_8$ (1 mg, 0.49 μmol) was dissolved in 0.5 mL of dichloromethane. To this, a solution of DIBAC-G3-$(Benzyl)_8$ (11.1 mg, 4.7 μmol) was added and solvent was removed by rotary evaporation, leaving a viscous oil. After 5 min, MALDI-MS indicated that the reaction was complete, and the oil was purified by precipitation into methanol, then filtration. The collected solids were dried overnight *in vacuo* to give the product as a white powder. (7 mg, 71%)

^{1}H NMR (700 MHz; $CDCl_3$): δ 7.74–7.73 (m, 2H), 7.55–6.91 (m, 1H), 6.58–5.43 (m, 87H), 4.44–4.07 (m, 1H), 3.48–2.80 (m, 52H), 2.35 (s, 3H), 2.31–2.10 (m, 27H), 1.96–1.88 (m, 11H), 1.60–1.54 (m, 8H), 1.29–1.02 (m, 243H)

^{13}C NMR (176 MHz; $CDCl_3$): δ 173.1, 172.6, 172.1, 171.9, 156.3, 155.9, 145.0, 143.0, 141.3, 140.2, 135.7, 134.6, 133.6, 132.6, 132.0, 131.6, 131.4, 131.0, 130.3, 129.99, 129.83,

129.67, 129.54, 129.3, 128.28, 128.11, 127.2, 126.7, 124.2, 116.5, 67.0, 66.2, 65.26, 65.15, 52.9, 51.7, 47.3, 46.9, 46.7, 46.41, 46.28, 46.0, 45.7, 39.7, 39.16, 39.05, 38.85, 38.68, 38.1, 37.9, 30.9, 30.3, 29.84, 29.71, 27.1, 26.75, 26.67, 21.8, 17.9, 17.6

MALDI: m/z calc: 20049.8, exp: 20072.9 ($[M+Na]^+$)

Synthesis of pTSe-G4-(alkyl)$_{16}$

pTSe-G1-$(N_3)_2$ (1 mg, 1.7 μmol) was dissolved in 0.5 mL of dichloromethane. To this, a solution of DIBAC-G3-$(Alkyl)_8$ (13 mg, 4.4 μmol) was added and solvent was removed by rotary evaporation, leaving a viscous oil. After 5 min, MALDI-MS indicated that the reaction was complete, and the oil was purified by flash chromatography using 10 column volumes of 40% acetone in hexanes, then 10 column volumes of 80% acetone in hexanes, with fraction collection monitored at 215 nm. The fractions containing product were combined and solvent was removed by rotary evaporation. The resulting oil was dried overnight *in vacuo* to give the product as a glassy solid. (8 mg, 73%).

^{1}H NMR (700 MHz; $CDCl_3$): δ 7.79–7.28 (m, 14H), 7.16–6.96 (m, 5H), 6.61–5.33 (m, 19H), 4.55–3.96 (m, 65H), 3.44–3.43 (m, 2H), 3.22–3.10 (m, 41H), 2.69–2.66 (m, 1H), 2.48–2.39 (m, 3H), 2.34–1.92 (m, 8H), 1.47 (d, J = 0.3, 38H), 1.26 (d, J = 15.3, 1H), 1.17 (s, 22H), 0.87 (t, J = 7.1, 48H)

^{13}C NMR (176 MHz; $CDCl_3$): δ 173.2, 172.88, 172.73, 172.2, 171.9, 156.2, 131.4, 130.3, 129.9, 129.6, 128.7, 128.2, 127.8, 67.1, 66.0, 65.15, 65.08, 55.1, 51.7, 47.3, 46.7, 46.4, 42.0, 41.3, 39.7, 39.26, 39.06, 37.5, 32.1, 30.1, 29.8, 29.5, 27.0, 22.8, 18.0, 17.6, 14.3

MALDI: m/z calc: 6326.6, exp: 6350.7 ($[M+Na]^+$)

Synthesis of pTSe-G5-(alkyl)$_{32}$

pTSe-G2-$(N_3)_4$ (1 mg, 0.95 μmol) was dissolved in 0.5 mL of dichloromethane. To this, a solution of DIBAC-G3-$(Alkyl)_8$ (13.7 mg, 4.7 μmol) was added and solvent was removed by rotary evaporation, leaving a viscous oil. After 5 min, MALDI-MS indicated that the reaction was complete, and the oil was purified by flash chromatography using 10 column volumes of 40% acetone in hexanes, then 10 column volumes of 80% acetone in hexanes, with fraction collection monitored at 215 nm. The fractions containing product were combined and solvent was removed by rotary evaporation. The resulting oil was dried overnight *in vacuo* to give the product as a glassy solid. (8 mg, 72%).

^{1}H NMR (700 MHz; $CDCl_3$): δ 7.79–7.78 (m, 2H), 7.64–7.36 (m, 26H), 7.23–7.14 (m, 5H), 6.61–4.98 (m, 42H), 4.52–4.08 (m, 139H), 3.50–2.87 (m, 93H), 2.43 (t, J = 3.5, 3H), 2.40–1.99 (m, 25H), 1.67 (s, 7H), 1.47 (s, 85H), 1.27–1.16 (m, 1H), 0.87 (t, J = 7.2, 96H)

^{13}C NMR (176 MHz; $CDCl_3$): δ 173.1, 172.81, 172.63, 172.2, 171.91, 171.82, 156.2, 145.4, 145.1, 143.1, 141.3, 140.3, 136.3, 135.7, 134.7, 133.6, 132.7, 132.0, 131.8, 131.4, 131.0, 130.4, 130.00, 129.85, 129.79, 129.61, 129.51, 129.3, 128.83, 128.65, 128.4, 128.18, 128.00, 127.78, 127.59, 127.47, 127.35, 124.3, 67.0, 66.0, 65.52, 65.48, 65.0, 60.5, 58.5, 54.9, 53.1, 51.8, 47.3, 46.7, 46.4, 46.0, 41.9, 39.7, 39.23, 39.08, 38.7, 37.8, 32.1, 30.24, 30.05, 29.5, 26.99, 26.83, 22.8, 18.0, 17.6, 14.3

MALDI: m/z calc: 12569.1, exp: 12592.4 ($[M+Na]^+$)

Synthesis of pTSe-G6-(alkyl)$_{64}$ (16)

pTSe-G3-(N_3)$_8$ (1 mg, 0.49 μmol) was dissolved in 0.5 mL of dichloromethane. To this, a solution of DIBAC-G3-(Alkyl)$_8$ (14.2 mg, 4.9 μmol) was added and solvent was removed by rotary evaporation, leaving a viscous oil. After 5 min, MALDI-MS indicated that the reaction was complete, and the oil was purified by flash chromatography using 10 column volumes of 40% acetone in hexanes, then 10 column volumes of 80% acetone in hexanes, with fraction collection monitored at 215 nm. The fractions containing product were combined and solvent was removed by rotary evaporation. The resulting oil was dried overnight *in vacuo* to give the product as a glassy solid. (8 mg, 71%).

^{1}H NMR (700 MHz; $CDCl_3$): δ 7.77 (d, J = 5.9, 2H), 7.61–7.29 (m, 48H), 7.21–6.97 (m, 26H), 6.66–5.06 (m, 78H), 4.48–4.10 (m, 1H), 3.50–3.00 (m, 184H), 2.41–1.95 (m, 49H), 1.65–1.56 (m, 15H), 1.45 (d, J = 28.9, 148H), 1.16 (s, 1H), 0.87 (t, J = 6.9, 192H)

^{13}C NMR (176 MHz; $CDCl_3$): δ 173.1, 172.79, 172.60, 172.2, 171.9, 171.2, 158.3, 156.2, 145.1, 143.1, 141.4, 140.2, 135.7, 134.7, 133.6, 132.7, 132.0, 131.8, 131.4, 131.0, 130.3, 130.1, 129.8, 129.5, 128.8, 128.4, 128.2, 127.95, 127.80, 127.65, 127.55, 127.3, 125.7, 124.5, 66.9, 66.0, 65.1, 53.1, 51.8, 47.3, 46.7, 46.4, 46.0, 41.9, 41.3, 40.9, 39.7, 39.2, 38.7, 38.0, 32.1, 30.4, 30.1, 29.5, 27.0, 22.8, 18.0, 17.6, 14.3

MALDI: m/z calc: 25054.1, exp: 25073 ($[M+Na]^+$)

Synthesis of pTSe-G4-(BocLysOtBu)$_{16}$

pTSe-G2-(N_3)$_4$ (2 mg, 1.9 μmol) was dissolved in 0.5 mL of dichloromethane. To this, a solution of DIBAC-G2-(BocLysO^{t}Bu)$_4$ (16.2 mg, 8 μmol) in 0.5 mL of dichloromethane

was added, and solvent was removed by rotary evaporation, leaving a viscous oil. After 5 minutes, ESI-MS indicated that the reaction was complete, and the oil was purified by flash chromatography using 10 column volumes of 50% acetone in hexanes, followed by 4 column volumes of 80% acetone in hexanes, with fraction collection monitored at 215 nm. The fractions containing product were combined and solvent was removed by rotary evaporation. The resulting oil was dried overnight *in vacuo* to give the product as a white foam. (15 mg, 86%).

^{1}H NMR (700 MHz; CD_3OD): δ 7.83–7.81 (m, 2H), 7.63–7.17 (m, 33H), 6.92–6.75 (m, 4H), 6.33–6.33 (m, 1H), 6.08–5.92 (m, 3H), 5.65–5.64 (m, 1H), 4.57–4.16 (m, 70H), 3.94–3.85 (m, 15H), 3.65 (ddd, J = 1.1, 0.9, 0.8, 2H), 3.41–3.35 (m, 2H), 3.20 (s, 8H), 3.08–2.90 (m, 42H), 2.63 (s, 16H), 2.43–2.27 (m, 14H), 2.09–1.91 (m, 8H), 1.73–1.71 (m, 19H), 1.63–1.61 (m, 18H), 1.28–1.26 (m, 68H), 1.20 (s, 20H)

^{13}C NMR (176 MHz; CD_3OD): δ 211.4, 174.48, 174.40, 174.14, 174.05, 173.95, 173.77, 172.8, 158.3, 158.1, 157.5, 146.6, 146.0, 144.9, 144.1, 143.7, 142.6, 141.6, 137.9, 136.8, 136.0, 135.1, 134.7, 133.47, 133.38, 132.9, 132.67, 132.57, 132.3, 131.3, 131.1, 130.85, 130.71, 130.48, 130.41, 130.01, 129.88, 129.6, 129.3, 128.8, 128.4, 125.3, 82.5, 81.2, 80.4, 78.2, 70.6, 67.79, 67.77, 67.60, 67.15, 67.12, 66.9, 59.8, 57.0, 56.0, 55.8, 53.8, 52.6, 48.4, 47.8, 47.55, 47.43, 42.3, 41.6, 40.4, 40.08, 40.03, 39.5, 38.8, 32.4, 32.1, 30.8, 30.4, 28.7, 27.87, 27.84, 24.2, 21.9, 18.4, 18.0, 14.4, 11.8

MS Calcd for $[M+6H]^{6+}$ = 1534.80. Found ESI-MS $[M+6H]^{6+}$ = 1534.75

Synthesis of pTSe-G5-(BocLysOtBu)$_{32}$

pTSe-G3-$(N_3)_8$ (2 mg, 1 μmol) was dissolved in 0.5 mL of dichloromethane. To this, a solution of DIBAC-G2-(BocLysO^{t}Bu)$_4$ (17 mg, 8.4 μmol) in 0.5 mL of dichloromethane was added, and solvent was removed by rotary evaporation, leaving a viscous oil. After 5 min, ESI-MS indicated that the reaction was complete, and the oil was purified by flash chromatography using 10 column volumes of 50% acetone in hexanes, followed by 4 column volumes of 80% acetone in hexanes, with fraction collection monitored at 215 nm. The fractions containing product were combined and solvent was removed by rotary evaporation. The resulting oil was dried overnight *in vacuo* to give the product as a white foam. (15 mg, 83%).

^{1}H NMR (700 MHz; $CDCl_3$): δ 7.76 (d, J = 0.3, 2H), 7.61–7.28 (m, 44H), 7.21–7.04 (m, 26H), 6.84–5.21 (m, 88H), 4.51–3.89 (m, 179H), 3.39–3.32 (m, 8H), 3.13 (d, J = 59.7, 99H), 2.62 (d, J = 3.2, 6H), 2.40 (s, 3H), 2.40 (s, 4H), 2.35–2.21 (m, 24H), 1.89 (s, 18H), 1.74 (s, 33H), 1.60 (t, J = 6.4, 41H), 1.53–1.32 (m, 1H), 1.26–1.17 (m, 117H)

^{13}C NMR (176 MHz; $CDCl_3$): δ 173.33, 173.13, 172.99, 172.6, 172.12, 171.95, 156.3, 155.9, 155.7, 148.10, 148.06, 143.0, 141.4, 140.3, 136.3, 135.8, 134.7, 132.7, 131.7, 131.4, 131.0, 130.4, 130.1, 129.84, 129.72, 129.58, 129.51, 129.34, 128.8, 128.2, 127.9, 127.5, 124.3, 114.0, 81.8, 79.6, 66.0, 54.09, 53.93, 51.7, 47.4, 46.4, 46.1, 40.9, 40.69, 40.58, 39.6, 39.2, 32.5, 31.1, 29.58, 29.41, 28.5, 28.2, 27.2, 26.92, 26.82, 26.76, 22.7, 18.4, 17.9, 17.5

MS Calcd for $[M+8H]^{8+}$ = 2291.13. Found ESI-MS $[M+8H]^{8+}$ = 2291.14

Synthesis of pTSe-G6-(BocLysO^{t}Bu)$_{64}$ (17b)

pTSe-G4-$(N_3)_{16}$ (2 mg, 0.5 μmol) was dissolved in 0.5 mL of dichloromethane. To this, a solution of DIBAC-G2-(BocLysO^{t}Bu)$_4$ (17 mg, 8.4 μmol) in 0.5 mL of dichloromethane was added, and solvent was removed by rotary evaporation, leaving a viscous oil. After 5 min, ESI-MS indicated that the reaction was complete, and the oil was purified by flash chromatography using 10 column volumes of 50% acetone in hexanes, followed by 4 column volumes of 80% acetone in hexanes, with fraction collection monitored at 215 nm. The fractions containing product were combined and solvent was removed by rotary evaporation. The resulting oil was dried overnight *in vacuo* to give the product as a white foam. (15 mg, 81%).

^{1}H NMR (700 MHz; CDCl3): δ 7.52–7.39 (m, 77H), 7.12–7.05 (m, 55H), 6.81 (d, J = 7.0, 12H), 6.00 (d, J = 68.4, 9H), 5.59–5.55 (m, 40H), 5.24–5.24 (m, 46H), 4.39–4.05 (m, 1H), 3.89 (s, 9H), 3.18–3.11 (m, 167H), 1.75–1.71 (m, 87H), 1.62–1.59 (m, 89H), 1.49 (t, J = 8.0, 124H), 1.44 (d, J = 15.8, 1H), 1.39–1.34 (m, 175H), 1.26–1.16 (m, 1H)

^{13}C NMR (176 MHz; CDCl3): δ 172.0, 156.1, 155.5, 81.7, 79.5, 65.9, 53.85, 53.75, 40.8, 39.5, 32.4, 31.7, 31.0, 29.7, 29.47, 29.28, 28.4, 28.0, 22.5, 17.4

Synthesis of pTSe-G5-(PEG$_{15}$)$_{32}$ (18)

pTSe-G2-$(N_3)_4$ (1 mg, 0.49 μmol) was dissolved in 0.5 mL of dichloromethane. To this, a solution of DIBAC-G3-$(PEG_{15})_8$ (15.1 mg, 4.2 μmol) in 0.5 mL of dichloromethane was added, and the solvent was removed by rotary evaporation, leaving a viscous oil. After 5 min, there was no residual azide detectable by FTIR, and the reaction mixture was

dissolved in 100 μL of deionized water and purified by size exclusion through a column of Sephacryl-S100 in water. The high molecular weight fraction was collected, and solvent was removed by lyophilisation to give the product as a white powder. (8 mg, 52%)

^{1}H NMR (700 MHz; CDCl3): δ 7.59 (m, 24H), 7.05 (m, 8H), 6.03–5.33 (m, 32H), 4.49–4.12 (m, 128H), 3.64 (s, 1644H), 3.37 (s, 96H), 3.32 (s, 64H), 2.28 (m, 24H), 1.52 (m, 31H), 1.21 (m, 121H), 0.84 (m, 29H)

MALDI: m/z calc: 28777.0, exp: 28909.9 ($[M+Cs]^+$). Note: CsF was added to the matrix for this experiment.

Core Functionalization Reactions

Synthesis of COOH-G3-$(N_3)_8$

pTSe-G3-$(N_3)_8$ (100 mg, 49 μmol) was dissolved in 1 mL of dichloromethane. DBU (44 μL, 297 μmol) was added and the reaction mixture was stirred for 30 min. Diethylene triamine (32 μL, 297 μmol) was then added and left to react for an additional 30 min, at which time the reaction mixture was dried using rotary evaporation to remove the dichloromethane. The entire reaction mixture was then diluted in 1 mL of DMSO, and was acidified with 50 uL of acetic acid and loaded on a 10 gram C18 silica gel flash column. The compound was eluted using a gradient of 5% to 100% acetonitrile in water, with 0.1% TFA in both phases. Fractions containing product were combined, then dried using rotary evaporation The resulting oil was taken up in 20 mL of dichloromethane and transferred to a separatory funnel where it was extracted with 1 × 30 mL brine to remove residual water. The organic phase was then dried with $MgSO_4$, filtered, and solvent was removed by rotary

evaporation and subsequent drying *in vacuo*. The product was a clear, colourless oil. (90 mg, 99%)

^{1}H NMR (700 MHz; $CDCl_3$): δ 5.65–5.11 (m, 8H), 4.39–4.12 (m, 28H), 3.38 (t, J = 6.6, 16H), 3.26 (q, J = 5.9, 16H), 1.79 (pentet, J = 6.5, 16H), 1.34–1.20 (m, 22H)

^{13}C NMR (176 MHz; $CDCl_3$): δ 173.5, 173.14, 173.09, 172.8, 172.1, 156.4, 66.8, 66.0, 65.0, 64.8, 49.1, 47.3, 46.8, 46.3, 39.3, 38.6, 29.1, 18.2, 17.70, 17.57

MS Calcd for $[M+Na]^+$ = 1861.7645. Found ESI-MS $[M+Na]^+$ = 1861.7635

Synthesis of DPA-G3-$(N_3)_8$ (19)

COOH-G3-$(N_3)_8$ (44 mg, 24 μmol) was dissolved in 1 mL of dichloromethane. To this, *N*-(3-dimethylaminopropyl)-*N*′-ethylcarbodiimide hydrochloride (14 mg, 72 μmol) and HOBt-hydrate (16 mg, 120 μmol) were added and the reaction mixture was stirred for 30 min. After 30 min, the reaction mixture was filtered through a polypropylene syringe filter to remove residual HOBt. To this filtered reaction material, N^1,N^1-bis(pyridin-2-ylmethyl)butane-1,4-diamine (13 mg, 46 μmol) and triethylamine (10 μL, 70 μmol) were added and the reaction was stirred overnight. The following day, solvent was removed by rotary evaporation, and the entire reaction mixture was then diluted in 1 mL of DMSO, then acidified with 50 μL of acetic acid and loaded on a 10 gram C_{18} silica gel flash column. The compound was eluted using a gradient of 5% to 100% acetonitrile in water, with 0.1% TFA in both phases. Fractions containing product were combined, then dried using rotary evaporation. The resulting oil was taken up in 20 mL of dichloromethane and transferred to a separatory funnel where it was extracted with 3 × 30 mL 1 M KOH then 1 × 40 mL

brine to basify the sample. The organic phase was then dried with $MgSO_4$, filtered, and solvent was removed by rotary evaporation and subsequent drying *in vacuo*. The product was a slightly yellow oil. (38 mg, 79%)

^{1}H NMR (700 MHz; $CDCl_3$): δ 8.50 (d, J = 4.0, 2H), 7.66 (t, J = 7.3, 2H), 7.48 (d, J = 7.6, 2H), 7.17 (t, J = 5.5, 2H), 6.88 (s, 1H), 5.75–5.19 (m, 8H), 4.32–4.08 (m, 28H), 3.79 (s, 4H), 3.36 (t, J = 6.6, 16H), 3.23 (q, J = 6.3, 17H), 2.54 (s, 2H), 1.77 (quintet, J = 6.6, 16H), 1.52 (d, J = 63.0, 4H), 1.27–1.17 (m, 22H)

^{13}C NMR (176 MHz; $CDCl_3$): δ 173.18, 173.01, 172.97, 172.2, 171.8, 159.6, 149.0, 136.7, 123.4, 122.3, 67.1, 66.1, 65.12, 65.02, 60.2, 53.5, 49.0, 47.3, 46.7, 46.4, 39.6, 39.2, 38.5, 29.8, 29.4, 29.2, 27.1, 23.7, 18.0, 17.6

MS Calcd for $[M+2H]^{2+}$ = 1057.4728. Found ESI-MS $[M+2H]^{2+}$ = 1057.4738

Synthesis of Pyrene-G3-$(N_3)_8$ (20)

COOH-G3-$(N_3)_8$ (44 mg, 24 μmol) was dissolved in 1 mL of dichloromethane. To this, *N*-(3-dimethylaminopropyl)-*N*′-ethylcarbodiimide hydrochloride (14 mg, 72 μmol) and HOBt-hydrate (16 mg, 120 μmol) were added and the reaction mixture was stirred for 30 min. After 30 min, the reaction mixture was filtered through a polypropylene syringe filter to remove residual HOBt. To this filtered reaction material, pyrene methylamine-hydrochloride (12 mg, 45 μmol) was added, along with triethylamine (13 μL, 92 μmol) and this was stirred overnight to allow for complete amidation. The resulting reaction mixture was diluted with 15 mL of dichloromethane, then washed with 3 × 15 mL of 1 M H_3PO_4, 3 × 15 mL of 10% Na_2CO_3, 1 × 30 mL of brine, and dried with $MgSO_4$, filtered

through a Hirsch funnel and evaporated to dryness by rotary evaporation. The crude material was purified by silica gel chromatography using a 10-gram silica cartridge using a gradient from 20% to 100% ethyl acetate in hexanes over 20 column volumes, with fraction collection monitored at 270 nm. The fractions containing product were combined, solvent was removed by rotary evaporation and then dried *in vacuo* to give the product as a slightly yellow oil. (37 mg, 75%)

^{1}H NMR (600 MHz; $CDCl_3$): δ 8.27 (d, J = 9.3, 1H), 8.21 (t, J = 7.05, 2H), 8.17 (d, J = 9.3, 1H), 8.12 (d, J = 7.7, 1H), 8.09–8.02 (m, 3H), 7.96 (d, J = 7.0, 1H), 5.61–5.19 (m, 9H), 4.31 (t, J = 12.3, 4H), 4.15–3.99 (m, 23H), 3.30 (dd, J = 12.5, 5.7, 15H), 3.19 (dt, J = 13.8, 7.4, 16H), 1.88 (dt, J = 1.7, 1.1, 1H), 1.75–1.61 (m, 16H), 1.33 (s, 3H), 1.24 (s, 1H), 1.08 (s, 17H)

^{13}C NMR (176 MHz; $CDCl_3$): δ 173.13, 173.08, 172.94, 172.90, 172.87, 172.1, 171.7, 156.12, 155.97, 155.7, 131.28, 131.15, 130.8, 129.0, 128.4, 127.8, 127.4, 127.19, 127.13, 126.4, 125.72, 125.59, 125.1, 124.83, 124.72, 122.8, 67.2, 66.0, 65.06, 64.90, 49.0, 47.26, 47.21, 46.65, 46.58, 42.3, 38.5, 29.1, 18.1, 17.6

MS Calcd for $[M+Na]^+$ = 2074.8587. Found ESI-MS $[M+Na]^+$ = 2074.8557

Synthesis of pTSe-G6-$(OH)_{64}$

pTSe-G3-$(N_3)_8$ (5 mg, 2.47 μmol) was dissolved in 1 mL of methanol. To this, DIBAC-G3-$(OH)_8$ (25 mg, 20 μmol) was added and the combined reaction mixture was concentrated by rotary evaporation at 40 °C for 5 min. The reaction mixture was then dissolved in 300 μL of methanol and purified by size exclusion chromatography using

Sephadex LH-20 in methanol. The fractions containing high molecular weight components were dried by rotary evaporation, then were dried *in vacuo* overnight to give the product as a clear, colourless oil. (23 mg, 82%)

^{1H} NMR (700 MHz; CD_3OD): δ 7.79 (s, 2H), 7.63–7.15 (m, 66H), 6.05–5.63 (m, 8H), 4.56–4.17 (m, 147H), 3.67 (d, J = 10.9, 63H), 3.59 (d, J = 10.9, 63H), 3.14 (m, 38H), 2.91 (s, 5H), 2.39–1.97 (m, 42H), 1.66 (s, 7H), 1.46 (d, J = 37.1, 31H), 1.27 (s, 82H), 1.14 (s, 108H)

^{13}C NMR (176 MHz; CD_3OD): δ 176.2, 175.9, 174.31, 174.24, 174.0, 173.8, 173.4, 172.9, 158.20, 158.08, 146.0, 144.1, 143.7, 142.6, 141.6, 136.8, 136.1, 135.1, 134.7, 134.1, 133.5, 133.13, 132.94, 132.6, 132.4, 131.4, 131.1, 130.89, 130.75, 130.5, 130.02, 129.93, 129.69, 129.52, 129.35, 129.16, 129.02, 128.84, 128.3, 128.0, 125.3, 68.2, 66.9, 66.4, 53.8, 52.6, 51.9, 47.9, 47.7, 40.6, 40.1, 39.5, 38.8, 31.71, 31.61, 31.3, 30.8, 27.9, 18.3, 17.4

MALDI: m/z calc: 11528, exp: 11553 ($[M+Na]^+$)

Synthesis of Pyrene-G6-$(OH)_{64}$

Pyrene-G3-$(N_3)_8$ (5 mg, 2.38 μmol) was dissolved in 1 mL of methanol. To this, DIBAC-G3-$(OH)_8$ (25 mg, 20 μmol) was added and the combined reaction mixture was concentrated by rotary evaporation at 40 °C for 5 min. The reaction mixture was then dissolved in 300 μL of methanol and purified by size exclusion chromatography using Sephadex LH-20 in methanol. The fractions containing high molecular weight components were dried by rotary evaporation, then were dried *in vacuo* overnight to give the product as a clear, yellow oil. (23 mg, 82%)

^{1}H NMR (700 MHz; CD_3OD): δ 8.36 (s, 1H), 8.15 (s, 4H), 8.03 (s, 4H), 7.57–7.06 (m, 64H), 5.85 (t, J = 144.7, 8H), 5.19 (s, 2H), 4.48–4.16 (m, 145H), 3.67 (d, J = 10.8, 64H), 3.58 (d, J = 10.8, 64H), 3.17 (s, 16H), 3.06 (d, J = 49.4, 21H), 2.87 (s, 5H), 2.27–1.89 (m, 39H), 1.64 (s, 7H), 1.44 (m, 34H), 1.27 (s, 72H), 1.14 (s, 123H)

^{13}C NMR (176 MHz; CD_3OD): δ 175.9, 174.31, 174.22, 174.0, 173.79, 173.62, 173.50, 172.9, 158.22, 158.08, 146.0, 144.0, 142.5, 141.6, 136.8, 136.0, 135.1, 133.53, 133.47, 133.39, 132.9, 132.55, 132.50, 132.33, 131.1, 130.80, 130.72, 130.46, 130.36, 130.00, 129.91, 129.49, 129.31, 129.1, 128.77, 128.66, 128.58, 128.54, 128.45, 128.33, 128.23, 126.6, 126.1, 125.2, 68.1, 66.99, 66.89, 66.4, 53.8, 52.5, 51.9, 49.8, 47.95, 47.81, 47.72, 47.4, 40.6, 40.1, 39.5, 38.8, 31.70, 31.59, 31.3, 30.8, 27.9, 18.32, 18.25, 17.4

MALDI: m/z calc: 11559, exp: 11584 ($[M+Na]^+$)

Synthesis of DPA-G6-$(OH)_{64}$

DPA-G3-$(N_3)_8$ (5 mg, 2.38 μmol) was dissolved in 1 mL of methanol. To this, DIBAC-G3-$(OH)_8$ (25 mg, 20 μmol) was added and the combined reaction mixture was concentrated by rotary evaporation at 40 °C for 5 min. The reaction mixture was then dissolved in 300 μL of methanol and purified by size exclusion chromatography using Sephadex LH-20 in methanol. The fractions containing high molecular weight components were dried by rotary evaporation, then were dried *in vacuo* overnight to give the product as a clear, colourless oil. (22 mg, 79%)

^{1}H NMR (700 MHz; CD_3OD): δ 8.40 (s, 2H), 7.73 (s, 2H), 7.62–7.15 (m, 70H), 6.05–5.65 (m, 8H), 5.04 (d, J = 71.9, 2H), 4.55–4.16 (m, 149H), 3.75 (s, 4H), 3.67 (d, J = 10.8, 64H),

3.59 (d, J = 10.9, 63H), 3.18 (m, 19H), 3.09 (m, J = 5.9, 22H), 2.91 (m, 6H), 2.51 (m, 2H), 2.35–1.98 (m, 40H), 1.66 (m, 7H), 1.46 (d, J = 37.3, 37H), 1.27 (s, 83H), 1.14 (s, 109H)

^{13}C NMR (176 MHz; CD_3OD): δ 176.10, 175.94, 174.50, 174.31, 174.23, 174.04, 173.8, 173.4, 172.9, 160.7, 158.22, 158.08, 149.5, 146.0, 145.0, 144.1, 143.7, 142.6, 141.6, 138.7, 136.8, 136.1, 135.1, 133.58, 133.47, 132.9, 132.6, 132.4, 131.1, 130.87, 130.75, 130.5, 130.03, 129.93, 129.52, 129.37, 129.17, 129.13, 128.8, 128.46, 128.34, 128.32, 128.0, 125.3, 124.8, 123.8, 68.2, 67.00, 66.84, 66.4, 61.1, 53.8, 52.6, 51.9, 47.95, 47.85, 47.72, 40.8, 40.6, 40.10, 40.06, 39.5, 39.2, 38.86, 38.78, 31.72, 31.61, 31.51, 31.45, 31.32, 30.90, 30.82, 30.1, 29.5, 28.4, 27.9, 25.6, 18.3, 17.90, 17.87

MALDI: m/z calc: 11598, exp: 11624 ($[M+Na]^+$)

3.7 References

(1) Newkome, G. R.; Moorefield, C. N.; Vogtle, F. *Dendrimers and Dendrons. Concepts, Syntheses, Applications*; Wiley-VCH: Weinheim, 2001.

(2) Kojima, C. Preclinical Studies of Dendrimer Prodrugs. *Expert Opin. Drug Metab. Toxicol.* **2015**, *11* (8), 1303–1315.

(3) Mintzer, M. A.; Grinstaff, M. W. Biomedical Applications of Dendrimers: A Tutorial. *Chem. Soc. Rev.* **2011**, *40* (1), 173–190.

(4) Noriega-Luna, B.; Godínez, L. A.; Rodríguez, F. J.; Rodríguez, A.; Zaldívar-Lelo De Larrea, G.; Sosa-Ferreyra, C. F.; Mercado-Curiel, R. F.; Manríquez, J.; Bustos, E. Applications of Dendrimers in Drug Delivery Agents, Diagnosis, Therapy, and Detection. *J. Nanomater.* **2014**, *2014*.

(5) Wijagkanalan, W.; Kawakami, S.; Hashida, M. Designing Dendrimers for Drug Delivery and Imaging: Pharmacokinetic Considerations. *Pharm. Res.* **2011**, *28* (7), 1500–1519.

(6) Cheng, Y.; Zhao, L.; Li, Y.; Xu, T. Design of Biocompatible Dendrimers for Cancer Diagnosis and Therapy: Current Status and Future Perspectives. *Chem. Soc. Rev.* **2011**, *40*, 2673–2703.

(7) Lee, C. C.; MacKay, J. A.; Fréchet, J. M. J.; Szoka, F. C. Designing Dendrimers for Biological Applications. *Nat. Biotechnol.* **2005**, *23* (12), 1517–1526.

(8) Wu, L. P.; Ficker, M.; Christensen, J. B.; Trohopoulos, P. N.; Moghimi, S. M. Dendrimers in Medicine: Therapeutic Concepts and Pharmaceutical Challenges. *Bioconjug. Chem.* **2015**, *26* (7), 1198–1211.

(9) Wolinsky, J.; Grinstaff, M. Therapeutic and Diagnostic Applications of Dendrimers for Cancer Treatment☆. *Adv. Drug Deliv. Rev.* **2008**, *60* (9), 1037–1055.

(10) Parrott, M. C.; Benhabbour, S. R.; Saab, C.; Lemon, J. A.; Parker, S.; Valliant, J. F.; Adronov, A. Synthesis, Radiolabeling, and Bio-Imaging of High-Generation Polyester Dendrimers. *J. Am. Chem. Soc* **2009**, *131* (21), 2906–2916.

(11) Sadowski, L. P.; Edem, P. E.; Valliant, J. F.; Adronov, A. Synthesis of Polyester Dendritic Scaffolds for Biomedical Applications. *Macromol. Biosci.* **2016**, 1475–1484.

(12) McNelles, S. A.; Knight, S. D.; Janzen, N.; Valliant, J. F.; Adronov, A. Synthesis, Radiolabeling, and In Vivo Imaging of PEGylated High-Generation Polyester Dendrimers. *Biomacromolecules* **2015**, *16*, 3033–3041.

(13) You, S.; Jung, H. Y.; Lee, C.; Choe, Y. H.; Heo, J. Y.; Gang, G. T.; Byun, S. K.; Kim, W. K.; Lee, C. H.; Kim, D. E.; et al. High-Performance Dendritic Contrast Agents for X-Ray Computed Tomography Imaging Using Potent Tetraiodobenzene Derivatives. *J. Control. Release* **2016**, *226*, 258–267.

(14) Deraedt, C.; Astruc, D. Supramolecular Nanoreactors for Catalysis. *Coord. Chem. Rev.* **2016**, *324*, 106–122.

(15) Caminade, A.-M. Inorganic Dendrimers: Recent Advances for Catalysis, Nanomaterials, and Nanomedicine. *Chem. Soc. Rev.* **2016**, *45*, 5174–5186.

(16) He, Y. M.; Feng, Y.; Fan, Q. H. Asymmetric Hydrogenation in the Core of Dendrimers. *Acc. Chem. Res.* **2014**, *47* (10), 2894–2906.

(17) Wang, D.; Astruc, D. Dendritic Catalysis-Basic Concepts and Recent Trends. *Coord. Chem. Rev.* **2013**, *257* (15–16), 2317–2334.

(18) Hecht, S.; Fréchet, J. M. J. Light-Driven Catalysis within Dendrimers : Designing Amphiphilic Singlet Oxygen Sensitizers. *J. Am. Chem. Soc* **2001**, *123*, 6959–6960.

(19) Caminade, A. M.; Ouali, A.; Laurent, R.; Turrin, C. O.; Majoral, J. P. The Dendritic Effect Illustrated with Phosphorus Dendrimers. *Chem. Soc. Rev.* **2015**, *44*, 3890–3899.

(20) Kaminskas, L. M.; McLeod, V. M.; Porter, C. J. H.; Boyd, B. J. Association of Chemotherapeutic Drugs with Dendrimer Nanocarriers: An Assessment of the Merits of Covalent Conjugation Compared to Noncovalent Encapsulation. *Mol. Pharm.* **2012**, *9* (3), 355–373.

(21) Helms, B.; Fréchet, J. M. J. The Dendrimer Effect in Homogeneous Catalysis. *Adv. Synth. Catal.* **2006**, *348* (10–11), 1125–1148.

(22) Walter, M. V.; Malkoch, M. Simplifying the Synthesis of Dendrimers: Accelerated Approaches. *Chem. Soc. Rev.* **2012**, *41* (13), 4593–4609.

(23) Antoni, P.; Hed, Y.; Nordberg, A.; Nyström, D.; Von Holst, H.; Hult, A.; Malkoch, M. Bifunctional Dendrimers: From Robust Synthesis and Accelerated One-Pot Postfunctionalization Strategy to Potential Applications. *Angew. Chemie - Int. Ed.* **2009**, *48* (12), 2126–2130.

(24) Wu, P.; Malkoch, M.; Hunt, J. N.; Vestberg, R.; Kaltgrad, E.; Finn, M. G.; Fokin, V. V; Sharpless, K. B.; Hawker, C. J. Multivalent, Bifunctional Dendrimers Prepared by Click Chemistry. *Chem. Commun.* **2005**, 5775.

(25) García-Gallego, S.; Hult, D.; Olsson, J. V.; Malkoch, M. Fluoride-Promoted Esterification with Imidazolide-Activated Compounds: A Modular and Sustainable Approach to Dendrimers. *Angew. Chemie - Int. Ed.* **2015**, *54*, 2416–2419.

(26) Hummelen, J. C.; Dongen, J. L. J. Van; Meijer, E. W. Electronspray Mass Spectroscopy of Poly(Propylene Imine) Dendrimers - The Issue of Dendritic Purity or Polydispersity. *Chem. - A Eur. J.* **1997**, *3* (9), 1489–1493.

(27) Lo, S. T.; Kumar, A.; Hsieh, J. T.; Sun, X. Dendrimer Nanoscaffolds for Potential Theranostics of Prostate Cancer with a Focus on Radiochemistry. *Mol. Pharm.* **2013**, *10*, 793–812.

(28) Wolinsky, J. B.; Grinstaff, M. W. Therapeutic and Diagnostic Applications of Dendrimers for Cancer Treatment. *Adv. Drug Deliv. Rev.* **2008**, *60* (9), 1037–1055.

(29) García-Gallego, S.; Nyström, A. M.; Malkoch, M. Chemistry of Multifunctional Polymers Based on Bis-MPA and Their Cutting-Edge Applications. *Prog. Polym. Sci.* **2015**, *48*, 85–110.

(30) Carlmark, A.; Malmström, E.; Malkoch, M. Dendritic Architectures Based on Bis-MPA: Functional Polymeric Scaffolds for Application-Driven Research. *Chem. Soc. Rev.* **2013**, *42*, 5858–5879.

(31) Ihre, H.; Padilla De Jesús, O. L.; Fréchet, J. M. J. Fast and Convenient Divergent Synthesis of Aliphatic Ester Dendrimers by Anhydride Coupling. *J. Am. Chem. Soc.* **2001**, *123* (8), 5908–5917.

(32) Ihre, H.; Hult, A.; Fréchet, J. M. J.; Gitsov, I. Double-Stage Convergent Approach for the Synthesis of Functionalized Dendritic Aliphatic Polyesters Based on 2,2-Bis(Hydroxymethyl)Propionic Acid. *Macromolecules* **1998**, *31* (13), 4061–4068.

(33) Grayson, S. M.; Fréchet, J. M. J. Convergent Dendrons and Dendrimers: From Synthesis to Applications. *Chem. Rev.* **2001**, *101* (12), 3819–3867.

(34) Fox, M. E.; Guillaudeu, S.; Fréchet, J. M. J.; Jerger, K.; Macaraeg, N.; Szoka, F. C. Synthesis and In Vivo Antitumor Efficacy of PEGylated Poly(L- Lysine) Dendrimer-Camptothecin Conjugates. *Mol. Pharm.* **2009**, *6* (5), 1562–1572.

(35) Almutairi, A.; Rossin, R.; Shokeen, M.; Hagooly, A.; Ananth, A.; Capoccia, B.;

Guillaudeu, S.; Abendschein, D.; Anderson, C. J.; Welch, M. J.; et al. Biodegradable Dendritic Positron-Emitting Nanoprobes for the Noninvasive Imaging of Angiogenesis. **2009**, *106* (3), 685–690.

(36) Gillies, E. R.; Dy, E.; Fréchet, J. M. J.; Szoka, F. C. Biological Evaluation of Polyester Dendrimer: Poly(Ethylene Oxide) "Bow-Tie" Hybrids with Tunable Molecular Weight and Architecture. *Mol. Pharm.* **2005**, *2* (2), 129–138.

(37) Lee, C. C.; Gillies, E. R.; Fox, M. E.; Guillaudeu, S. J.; Fréchet, J. M. J.; Dy, E. E.; Szoka, F. C. A Single Dose of Doxorubicin-Functionalized Bow-Tie Dendrimer Cures Mice Bearing C-26 Colon Carcinomas. *Proc. Natl. Acad. Sci. U. S. A.* **2006**, *103* (45), 16649–16654.

(38) Ihre, H. R.; Padilla de Jesús, O. L.; Szoka, F. C.; Fréchet, J. M. J. Polyester Dendritic Systems for Drug Delivery Applications: Design, Synthesis, and Characterization. *Bioconjug. Chem.* **2002**, *13* (Figure 1), 443–452.

(39) Kolb, H. C.; Finn, M. G.; Sharpless, K. B. Click Chemistry: Diverse Chemical Function from a Few Good Reactions. *Angew. Chemie - Int. Ed.* **2001**, *40*, 2004–2021.

(40) Hoyle, C. E.; Bowman, C. N. Thiol-Ene Click Chemistry. *Angew. Chemie - Int. Ed.* **2010**, *49*, 1540–1573.

(41) Blackman, M. L.; Royzen, M.; Fox, J. M. Tetrazine Ligation: Fast Bioconjugation Based on Inverse-Electron-Demand Diels-Alder Reactivity. *J. Am. Chem. Soc.* **2008**, *130*, 13518–13519.

(42) Rostovtsev, V. V.; Green, L. G.; Fokin, V. V.; Sharpless, K. B. A Stepwise Huisgen Cycloaddition Process: Copper(I)-Catalyzed Regioselective "Ligation" of Azides and Terminal Alkynes. *Angew. Chemie - Int. Ed.* **2002**, *41* (14), 2596–2599.

(43) Agard, N. J.; Prescher, J. a.; Bertozzi, C. R.; Nicholas J. Agard; Jennifer A. Prescher, and; Bertozzi*, C. R. A Strain-Promoted [3 + 2] Azide-Alkyne Cycloaddition for Covalent Modification of Biomolecules in Living Systems. *J. Am. Chem. Soc.* **2004**, *126*, 15046–15047.

(44) Chadwick, R. C.; Van Gyzen, S.; Liogier, S.; Adronov, A. Scalable Synthesis of Strained Cyclooctyne Derivatives. *Synth.* **2014**, *46* (05), 669–677.

(45) Kardelis, V.; Chadwick, R. C.; Adronov, A. Click Functionalization of a Dibenzocyclooctyne-Containing Conjugated Polyimine. *Angew. Chemie - Int. Ed.* **2016**, *55*, 945–949.

(46) Arnusch, C. J.; Branderhorst, H.; Kruijff, B. De; Liskamp, R. M. J.; Breukink, E.; Pieters, R. J. Enhanced Membrane Pore Formation by Multimeric / Oligomeric Antimicrobial. *Society* **2007**, 13437–13442.

(47) Wu, P.; Feldman, A. K.; Nugent, A. K.; Hawker, C. J.; Scheel, A.; Voit, B.; Pyun, J.; Fréchet, J. M. J.; Sharpless, K. B.; Fokin, V. V. Efficiency and Fidelity in a Click-

Chemistry Route to Triazole Dendrimers by the Copper(I)-Catalyzed Ligation of Azides and Alkynes. *Angew. Chemie - Int. Ed.* **2004**, *43*, 3928–3932.

(48) Antoni, P.; Robb, M.; Campos, L.; Montanez, M.; Hult, A.; Malmström, E.; Malkoch, M.; Hawker, C. Pushing the Limits for Thiol−Ene and CuAAC Reactions: Synthesis of a 6th Generation Dendrimer in a Single Day. *Macromolecules* **2010**, *43* (16), 6625–6631.

(49) Lundberg, P.; Hawker, C. J.; Hult, A.; Malkoch, M. Click Assisted One-Pot Multi-Step Reactions in Polymer Science: Accelerated Synthetic Protocols. *Macromol. Rapid Commun.* **2008**, *29*, 998–1015.

(50) Carlmark, A.; Hawker, C.; Hult, A.; Malkoch, M. New Methodologies in the Construction of Dendritic Materials. *Chem. Soc. Rev.* **2009**, *38* (2), 352–362.

(51) Gonzaga, F.; Sadowski, L. P.; Rambarran, T.; Grande, J.; Adronov, A.; Brook, M. a. Highly Efficient Divergent Synthesis of Dendrimers via Metal-Free "Click" Chemistry. *J. Polym. Sci. Part A Polym. Chem.* **2013**, *51* (6), 1272–1277.

(52) Huang, B.; Kukowska-Latallo, J. F.; Tang, S.; Zong, H.; Johnson, K. B.; Desai, A.; Gordon, C. L.; Leroueil, P. R.; Baker, J. R. The Facile Synthesis of Multifunctional PAMAM Dendrimer Conjugates through Copper-Free Click Chemistry. *Bioorganic Med. Chem. Lett.* **2012**, *22* (9), 3152–3156.

(53) Ornelas, C.; Broichhagen, J.; Weck, M. Strain-Promoted Alkyne Azide Cycloaddition for the Functionalization of Poly(Amide)-Based Dendrons and Dendrimers. *J. Am. Chem. Soc.* **2010**, *132* (24), 3923–3931.

(54) Huang, B.; Desai, A.; Zong, H.; Tang, S.; Leroueil, P.; Baker, J. R. Copper-Free Click Conjugation of Methotrexate to a PAMAM Dendrimer Platform. *Tetrahedron Lett.* **2011**, *52* (13), 1411–1414.

(55) Ledin, P. a.; Friscourt, F.; Guo, J.; Boons, G. J. Convergent Assembly and Surface Modification of Multifunctional Dendrimers by Three Consecutive Click Reactions. *Chem. - A Eur. J.* **2011**, *17*, 839–846.

(56) Choi, H.; Liu, W.; Misra, P.; Tanaka, E.; Zimmer, J.; Ipe, B.; Bawendi, M.; Frangioni, J. Renal Clearance of Quantum Dots. *Nat. Biotechnol.* **2007**, *25* (10), 1165–1170.

(57) Alexis, F.; Pridgen, E.; Molnar, L. K.; Farokhzad, O. C. Factors Affecting the Clearance and Biodistribution of Polymeric Nanoparticles. *Mol. Pharm.* **2008**, *5* (4), 505–515.

(58) Rijcken, C. J.; Snel, C. J.; Schiffelers, R. M.; Nostrum, C. F. Van; Ã, W. E. H. Hydrolysable Core-Crosslinked Thermosensitive Polymeric Micelles : Synthesis , Characterisation and in Vivo Studies. *Biomaterials* **2007**, *28* (36), 5581–5593.

(59) Pelegri-O'day, E. M.; Lin, E.-W.; Maynard, H. D. Therapeutic Protein-Polymer Conjugates: Advancing beyond Pegylation. *J. Am. Chem. Soc.* **2014**, *136* (41),

14323–14332.

(60) Banerjee, S. R.; Levadala, M. K.; Lazarova, N.; Wei, L.; Valliant, J. F.; Stephenson, K. A.; Babich, J. W.; Maresca, K. P.; Zubieta, J.; Street, S. Bifunctional Single Amino Acid Chelates for Labeling of Biomolecules with the {Tc(CO)3}+ and {Re(CO)3}+ Cores. Crystal and Molecular Structures of [ReBr(CO)3(H2NCH2C5H4N)], [Re(CO)3{(C5H4NCH2)2NH}]Br, [Re(CO)3{(C5H4NCH2)2NCH2CO2H}]Br, [Re(CO)3{X(Y)NCH2CO2. *Inorg. Chem.* **2002**, *41* (24), 6417–6425.

(61) Agut, W.; Agnaou, R.; Lecommandoux, S.; Taton, D. Synthesis of Block Copolypeptides by Click Chemistry. *Macromol. Rapid Commun.* **2008**, *29*, 1147–1155.

(62) Shetty, D.; Jeong, J. M.; Ju, C. H.; Kim, Y. J.; Lee, J.-Y.; Lee, Y.-S.; Lee, D. S.; Chung, J.-K.; Lee, M. C. Synthesis and Evaluation of Macrocyclic Amino Acid Derivatives for Tumor Imaging by Gallium-68 Positron Emission Tomography. *Bioorg. Med. Chem.* **2010**, *18* (21), 7338–7347.

4 Globular Polymer Grafts Require a Critical Size for Efficient Sieving of Enzyme Substrates

Stuart A. McNelles, Victoria M. Marando, and Alex Adronov*

This chapter has been reproduced with permission from S. McNelles, V. Marando, A. Adronov, *Angew. Chemie Int. Ed.* **2019**, *58*, 8448-8453.

The work detailed in this chapter was carried out in collaboration with Ms. Victoria Marando. Stuart McNelles and Victoria Marando synthesized, purified, and characterized the dendrimers and dendrimer-enzyme conjugates. Stuart McNelles and Victoria Marando also both ran assays for determining protein activity. Stuart McNelles and Alex Adronov wrote the manuscript.

Graphical Abstract:

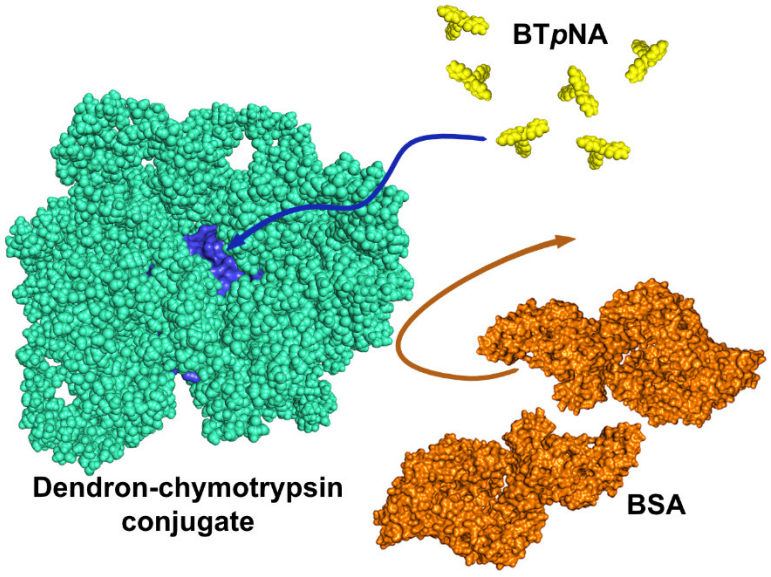

4.1 Abstract

A series of bis(2,2-hydroxymethylpropionic acid) dendrons of generation 2 through 8 having a strained cyclooctyne at the core and hydroxyl groups at the periphery were prepared by a divergent methodology and used to functionalize azide-decorated α-chymotrypsin. The conjugates were characterized by size exclusion chromatography (SEC). The ability of the appended dendrons to selectively block enzyme activity (via a molecular sieving effect) was investigated using a small molecule substrate (benzoyl-L-tyrosine *p*-nitroanilide), as well as two proteins of different size (casein and bovine serum albumin). Additionally, the ability of dendrons to block complexation with a chymotrypsin antagonist, α-antichymotrypsin, was investigated, and it was found that the dendron coating effectively prevented inhibition by this antagonist. We found that there is a critical generation required to achieve efficient sieving with bis-MPA dendrons, which illustrates the importance of macromolecular architecture and size in the shielding of proteins.

4.2 Introduction

The increasing utility of protein-based therapeutic agents has spawned efforts to improve their efficacy and *in-vivo* stability, while reducing their immunogenicity.[1–8] One potential approach to achieving these goals involves decoration of the protein surface with polymeric structures, which has been shown to improve protein pharmacokinetics and reduce immunogenicity.[9–11] Arguably, the most prevalent polymer used for protein conjugation is poly(ethylene glycol) (PEG),[12–14] which has been introduced on the surface of many proteins using a broad range of recently-developed coupling strategies.[15–19] Indeed, PEGylation has been shown to improve bioavailability, circulation time, and stability of a

wide array of proteins.[12] In addition, this approach has been found to suppress the immune response, as the PEG shell can prevent recognition by antibodies.[20–22] As a result of the success of PEGylation, numerous other polymer-protein conjugates have been investigated, involving polymers such as poly(amino acid)s,[23,24] poly(vinyl pyrrolidone),[9] poly(acrylate)s,[25,26] poly(acrylamide)s,[27,28] poly(sarcosine),[29] and poly(glycerol)s.[30–32] However, in the case of enzymes, attachment of linear polymers to the protein surface can dramatically reduce specific activity of the polymer-enzyme conjugate,[33] as flexible polymers can block access to the enzyme's active site.[34] Thus, to advance the therapeutic utility of polymer-enzyme conjugates, particularly in the case of enzymes acting on small molecule substrates, it is important to identify structures that can prevent interactions of enzymes with macromolecules such as antibodies, without adversely affecting native reactivity. This concept has recently been dubbed "molecular sieving".[35]

One polymer that has been found to function as a molecular sieve is poly[oligo(ethylene glycol) methacrylate] (POEGMA). Efforts by Gauthier and co-workers have elegantly demonstrated that conjugates of POEGMA with α-chymotrypsin and L-asparaginase exhibit the sieving effect.[35,36] In their work, they highlighted several key points required for effective molecular sieving with protein-POEGMA conjugates.[35] Specifically, the polymer should adopt a globular morphology and the coating of the polymer should be dense around the surface of the protein. Although POEGMA has been shown effective,[35,36] both criteria can arguably be most ideally satisfied by dendrimers, which adopt dense globular morphologies of uniform size and, if attached to multiple sites on a

protein surface, should result in high surface coverage. Furthermore, the precise structural definition of dendrimers provides a key advantage over disperse polymers in therapeutic applications,[37,38] as this eliminates the possibility of adverse side-effects from non-ideal structural homologs. We therefore chose to investigate dendrimer-enzyme conjugates to determine if a molecular sieving effect could be achieved.

Of all the available dendrimer architectures, we elected to use polyester dendrimers based on the bis-(2,2-hydroxymethyl)propionic acid (bis-MPA), as these can be prepared to a high generation using a variety of methods,[39–42] they exhibit low toxicity,[43] are water soluble,[38] and are biodegradable.[44] However, few examples of high-generation dendrimer conjugates with proteins have been reported, as this requires highly efficient grafting chemistry to achieve quantitative functionalization.[45] Herein, we describe the synthesis of bis-MPA dendrons having functional handles at their core for the preparation of dendron-protein conjugates with α-chymotrypsin (α-CT) via Strain-Promoted Azide-Alkyne Cycloaddition (SPAAC) chemistry. We then investigate the relative activity of these conjugates toward a model small molecule (benzoyl-L-tyrosine *p*-nitroanilide, BT*p*NA) as a function of surface dendron generation. Finally, we demonstrate the differential ability of the dendritic coating to suppress activity of α-CT toward different macromolecular substrates, including casein and bovine serum albumin (BSA).

4.3 Results & Discussion

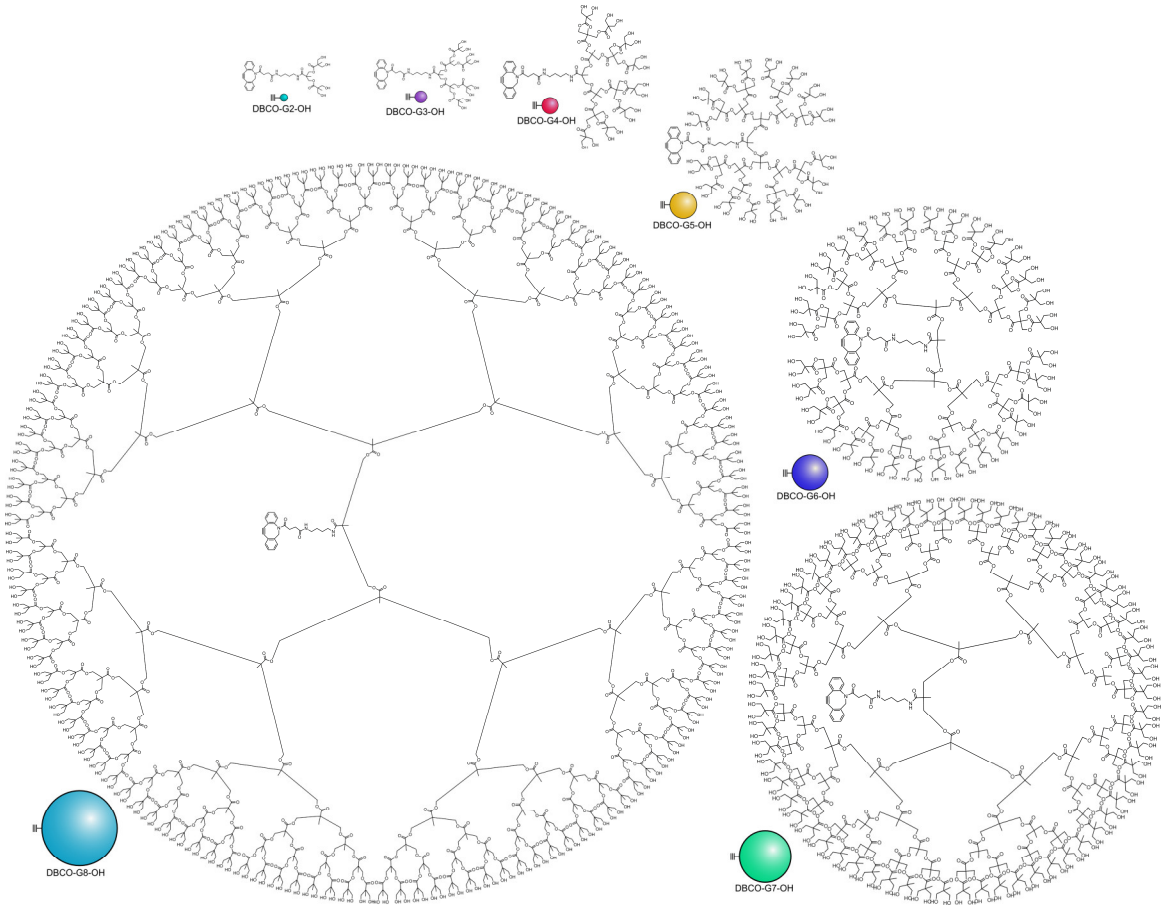

Figure 4.1. Structures of G2-G8 DBCO-core dendrons having hydroxyl groups at the periphery.

In order to prepare the dendron-protein conjugates, we chose to employ the SPAAC reaction,[46] as it is rapid, requires no catalyst, and produces no byproducts. Specifically, dibenzoazacyclooctyne (DBCO) was chosen as the strained alkyne because it exhibits rapid reaction kinetics and is relatively stable, especially when stored at -20 °C.[47] Since α-CT requires a reactive handle for SPAAC, we acylated the lysine residues non-specifically using NHS-activated azidoacetic acid (Scheme 4.1). The product α-CT-N_3 was verified to

be completely azide-functionalized by MALDI-TOF-MS and UV-Vis spectroscopy (see Supporting Information). Despite quantitative azidification of the lysines, the resulting enzyme remained water soluble.

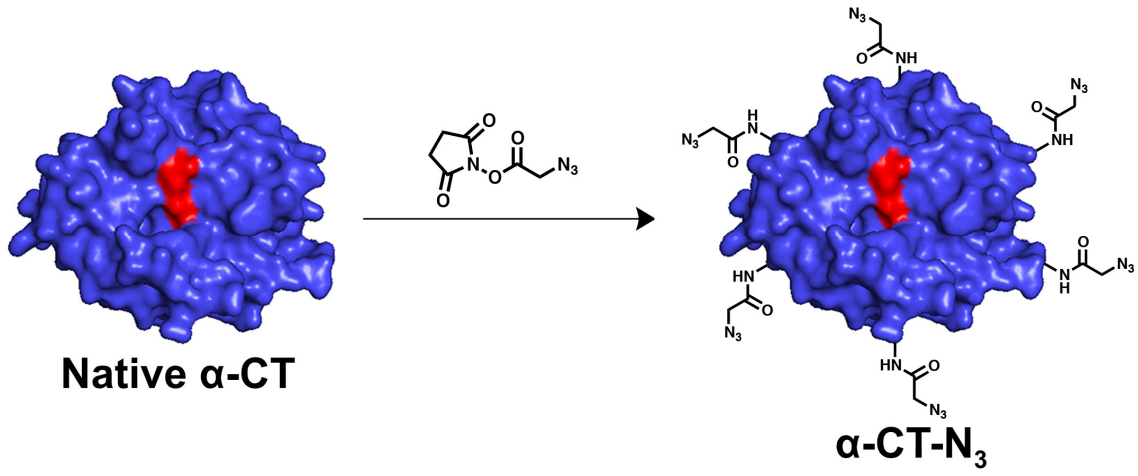

Scheme 4.1. Derivatization of native α-chymotrypsin (α-CT) with NHS-activated azidoacetic acid to install azide functionalities.

To complement the α-CT-N_3, a series of bis-MPA dendrons with hydroxyl groups at their periphery were functionalized with DBCO at the core (Figure 4.1). Dendron synthesis was completed according to modified literature procedures.[48] In brief, a series of bis-MPA dendrons with a *para*-toluenesulfonyl ethanol (*p*TSe) group at the core, generation 2 through 8, were prepared using a divergent synthesis approach,[49] which is detailed in the Supporting Information. For each generation, the core was deprotected using DBU and the resulting carboxylic acid was amidated via EDC-NHS coupling with mono-Cbz protected butanediamine hydrochloride to give dendrons with a protected amine at the core and protected hydroxyls at the periphery. This was subjected to global deprotection by hydrogenolysis over $Pd(OH)_2/C$, and the resulting amine at the dendron core was acylated

using DBCO-NHS to give dendrons with the strained cyclooctyne at the core and alcohols at the periphery. This procedure worked effectively to prepare the second to seventh generation DBCO core dendrons, however the amine at the core of the G8 dendron was not accessible to the DBCO-NHS. To prepare the G8 derivative, a divergent strategy involving the DBCO-G7-OH dendron reacting with acetonide protected bis-MPA anhydride was used (see Supporting Information). Subsequent *p*-TsOH-catalyzed deprotection of the acetonide groups to alcohols provided the DBCO-G8-OH dendron in good yield. It should be noted that this acid catalyzed deprotection can slowly decompose the DBCO moiety, so this methodology was not suitable for the divergent growth of all generations.

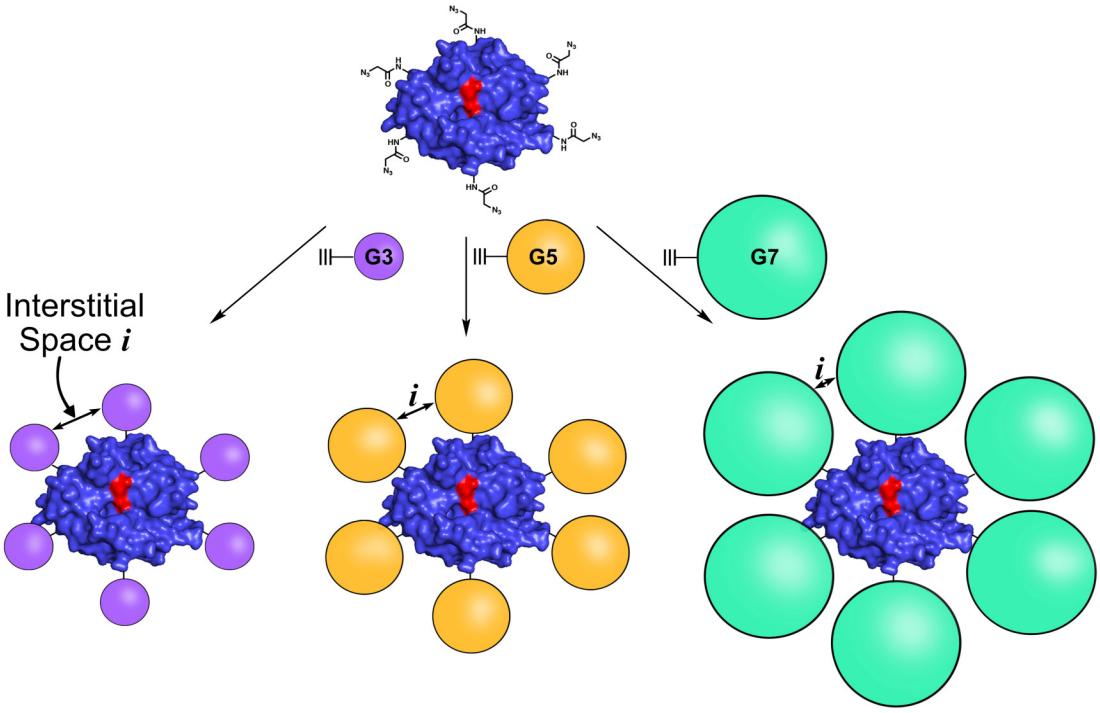

Figure 4.2. Schematic representation of the preparation of α-CT-dendron conjugates via SPAAC coupling. Increasing dendron generation decreases the interstitial space (*i*) between dendrons, forming a molecular sieve. Structures are not drawn to scale.

With the generation 2 through 8 dendrons having DBCO at the core and alcohols at the periphery in hand (structures shown in Figure 4.1), we were able to prepare the dendron-enzyme conjugates by simply mixing the α-CT-N_3 and the dendron in phosphate buffer at 4 °C overnight (Figure 4.2). Critically, since the number of azides added to the protein can be easily determined and the dendrons are monodisperse, the resulting dendron-enzyme conjugates exhibit well-defined structures. The dendron-enzyme conjugates had molecular weights of between 36 and 446 kDa (Table 1). The degree of conjugation was assessed by UV-Vis spectroscopy, FTIR spectroscopy, as well as quantitative ^{1}H NMR spectroscopy[50] (see Supporting Information). All three methods indicated that the majority of each

conjugate sample had the expected 14 of 14 possible dendrons appended. The conjugates were also analyzed by aqueous SEC, and their elution times decreased smoothly as dendron generation increased, as seen in Figure 4.3. This linear decrease in elution time with increasing generation beyond G3 clearly shows that the hydrodynamic volume of the conjugates consistently increases with the size of the dendron. Below G3, the dendrons are simply too small to impact the conjugate size (Figure 4.1), and it is likely that the linker plays a major role in modifying the retention time.

Table 4.1. DBCO-OH dendron molecular weights and α-CT-dendron conjugate molecular weights.

Generation	Dendron Molecular Weight*	Conjugate Molecular Weight (Calculated)
2	724	36,776
3	1,188	43,272
4	2,117	56,278
5	3,975	82,290
6	7,691	134,314
7	15,037	237,158
8	29,984	446,416

*Acquired from MALDI-TOF mass spectrometry.

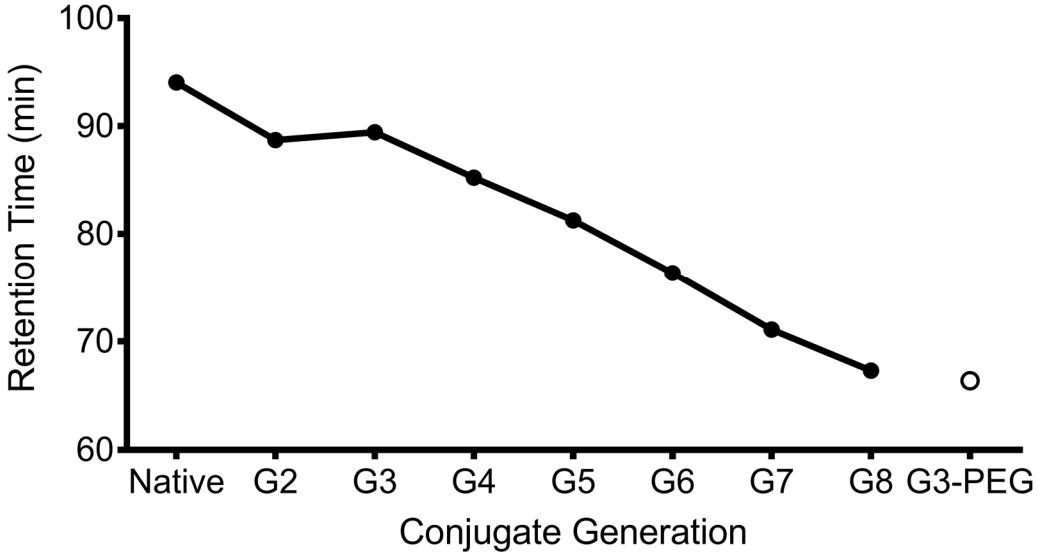

Figure 4.3. SEC elution times of native chymotrypsin and the chymotrypsin-dendron conjugates shows a linear decrease vs. generation.

Conjugate activity was then determined on three substrates: a small molecule (BT*p*NA), a small protein (milk casein, ~22 kDa), and a large protein (bovine serum albumin, ~66 kDa). The native α-CT activity was first measured against all three substrates and this rate was taken as the reference point for all conjugate activity measurements. We initially found that all conjugates had no diminished activity against BT*p*NA, and indeed there appeared to be a consistent slight increase in activity against this substrate (ca. 50%, Figure 4). This may be due to the conversion of the cationic lysine groups into neutral amide groups altering the accessibility of the active site, or from partitioning of the relatively lipophilic BT*p*NA toward the DBCO-clicked dendritic portions of the conjugate, thereby increasing the local concentration and accelerating the rate of reaction. The apparent increase in activity of conjugates relative to native α-CT in this assay has been reported previously,[35] and our observations are consistent with the published studies. As a control experiment, we also

performed this assay using native α-CT in the presence of un-conjugated seventh and eighth generation dendrons, and the activity was very similar to that of the native enzyme (Figure 4).

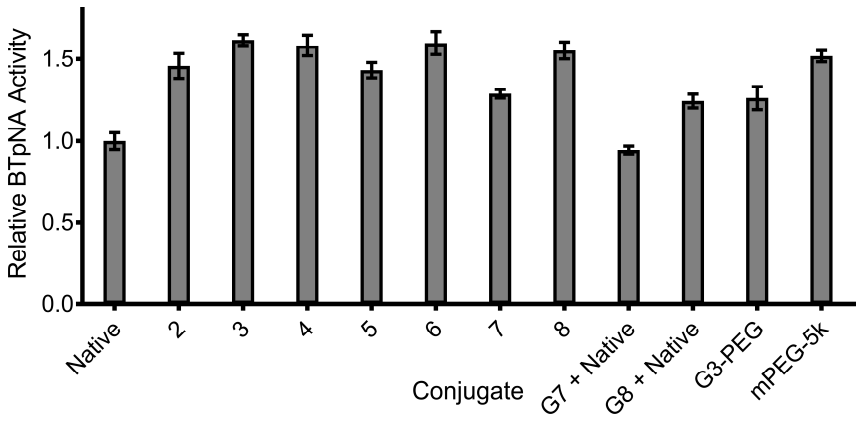

Figure 4.4. Relative activity of dendron-α-CT conjugates against BT*p*NA vs. native chymotrypsin, illustrating dendron conjugation does not diminish α-CT activity.

The activity of the conjugates against casein and BSA was then measured, with detailed methods for the assay provided in the Supporting Information. Specifically, we calculated a sieving ratio, which is the measured activity toward the small molecule (BT*p*NA) divided by the activity toward the large molecule (casein or BSA), as shown in Figure 4.5. None of the dendron-α-CT conjugates displayed reduced activity against the casein substrate, which we hypothesize is due to the intrinsically flexible and disordered nature of casein.[51] This flexibility may allow casein to adopt structures that can fit through the interstitial space (*i*) between dendrons (Figure 4.2) conjugated to the α-CT. However, when the activity of the dendron-α-CT conjugates was measured against BSA, a larger and more rigid protein, we found that there was a critical generation at which activity against BSA was dramatically reduced, as shown in Figure 4.5. The G6-α-CT exhibited a modest reduction in activity against BSA, and the G7 and G8 conjugates exhibited extremely low

activity against BSA. To determine if this was due to a non-specific interaction of the dendrons with the α-CT, this assay was once again performed using a sample of native α-CT with un-conjugated G7 or G8 dendron. This unconjugated dendron had no effect on the native α-CT activity toward BSA (Figure 4.5). It appears that efficient sieving requires a critical size of dendron and, in this case, the transition from the G6 to the G7 conjugate crosses the required size threshold. This supports the hypothesis that the primary requirement for effective sieving is the formation of a globular polymer shell spread throughout the protein surface, ensuring there is limited interstitial space between polymer globules to prevent ingress of macromolecules. Circular dichroism confirmed that the secondary structure of α-CT within the dendron-α-CT conjugates was not substantially changed from the native enzyme (Figure S104). Thus, any reduced activity against BSA is solely due to the dendron size and morphology, rather than a structural change in the enzyme upon conjugation.[52]

To assess the appropriate polymer size for conjugation, we used dynamic light scattering to measure the hydrodynamic diameter of the G6-G8 dendrons as well as the native α-CT (Table 4.2). The DBCO-G6-OH dendron is substantially smaller than the native α-CT, and is insufficient to provide effective surface coverage with only the 14 conjugated dendrons. The DBCO-G7-OH dendron is nearly the same size as the α-CT, and this structure is sufficiently large to result in extensive surface coverage when the 14 dendrons are conjugated. The DBCO-G8-OH dendron is slightly larger in diameter than α-CT, and is likely large enough to fully cover the enzyme surface. Thus, we conclude that, with high degrees of functionalization (~12-14 functionalized lysines), the grafted unit must be

approximately the same size as, or larger than the protein being shielded to achieve sieving. This is analogous to the close packing of spheres, in which a sphere of a particular diameter can have a maximum of 12 spheres of the same diameter close-packed around it in 3-dimensional space.[53] Such packing of spheres would readily allow for entry of small compounds in the interstitial spaces but would prevent the ingress of large substrates, especially ones reaching a similar size to the native enzyme. We have also modeled the conjugates using properly scaled spheres, based on the measured size data provided in Table 4.2, to represent the globular dendron structures (G6-G8). The representative spheres were placed at the positions of the lysine residues in the native α-CT, as shown in Figure S105 (Supporting Information). From these models, it appears that the size of a G6 dendron is not large enough to appreciably cover the active site of α-CT, while G7 and G8 provide much more extensive coverage. However, even with the largest dendrons, there may still be pathways available for small or flexible substrates to access the active site (Figure S105(c), "front view"). These models are consistent with our experimental observations.

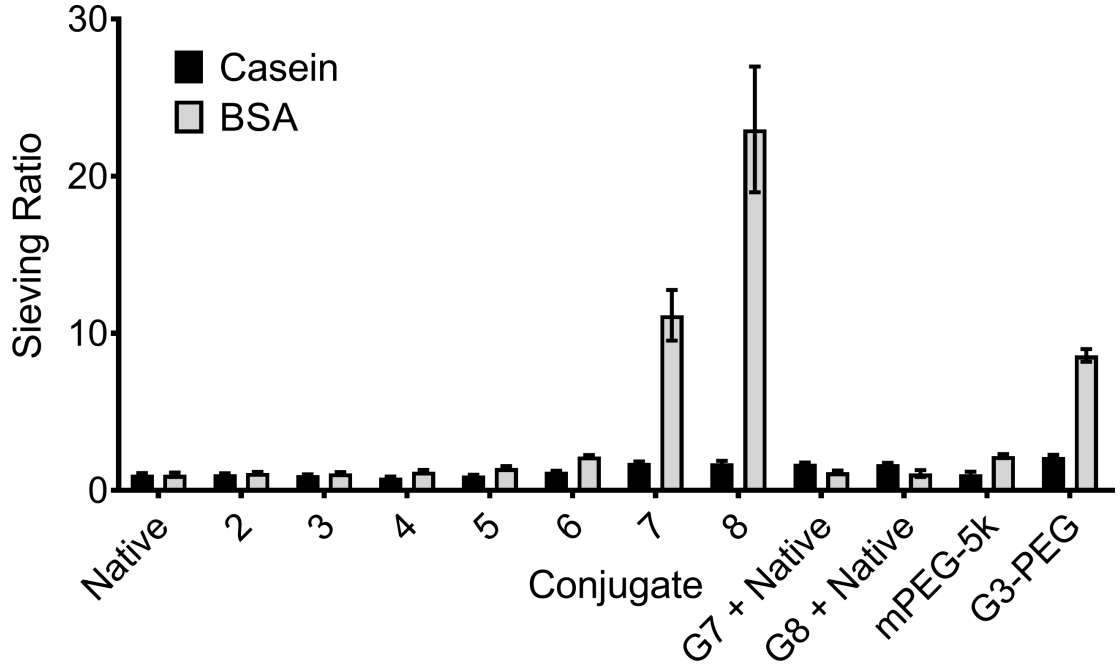

Figure 4.5. Sieving efficiency of dendron-α-CT conjugates vs. casein and BSA. Error bars indicate standard deviation.

Table 4.2. Volume average hydrodynamic diameters of DBCO dendrons and native α-CT as determined by DLS.

Dendron	Diameter (nm)
DBCO-G6-$(OH)_{64}$	3.21
DBCO-G7-$(OH)_{128}$	4.50
DBCO-G8-$(OH)_{256}$	5.96
DBCO-G3-$(PEG_{15})_8$	4.10
Native α-CT	5.21

To confirm that the size of the conjugate relative to the protein is a key parameter for effective sieving, we prepared a G3 DBCO-core dendron functionalized with monodisperse

$mPEG_{15}$ chains. This was characterized by SEC and DLS and was found to be similar in size to the G7-OH and G8-OH dendrons. We then prepared the corresponding G3-PEG-α-CT conjugate and assayed its activity against all three substrates. We found that it displayed no reduced activity against BT*p*NA or casein, but exhibited a similar reduction in activity against BSA as the G7-α-CT conjugate, resulting in a sieving ratio of 8.59. It should be noted that sieving with the G8-α-CT conjugate was more effective than with the G3-PEG-α-CT (Table S4). This can be attributed to the significantly lower internal density of the G3-PEG dendron vs. the G8-OH dendron, which can be gleaned from the fact that the two structures are similar in size but very different in molecular weight (6.9 kDa vs. 30 kDa respectively). Additionally, we grafted 5,500 Da PEG monomethyl ether chains to α-CT and compared their sieving efficiency to that of the dendronized enzyme. Interestingly, we found that this conjugate did not exhibit any significant sieving ability when exposed to either casein or BSA (sieving ratios were 1.05 and 2.11, respectively, Tables S3 and S4).

As a final test of the sieving efficacy, the BT*p*NA activity assay was performed in the presence of α-anti-CT protein, which forms a high affinity complex with the active site of chymotrypsin, thus inhibiting catalytic activity. Native chymotrypsin and each of the dendron-enzyme conjugates that displayed significant sieving against BSA were treated with 1.5 equivalents of α-anti-CT and then the activity of the conjugates against BT*p*NA was measured. The activity of the native α-CT was nearly entirely blocked, however the G7, G8, and G3-PEG conjugates remained mostly active, as seen in Figure 4.6. These results confirm that the dendron coating of α-CT strongly restricts the interaction of the α-CT with macromolecules.

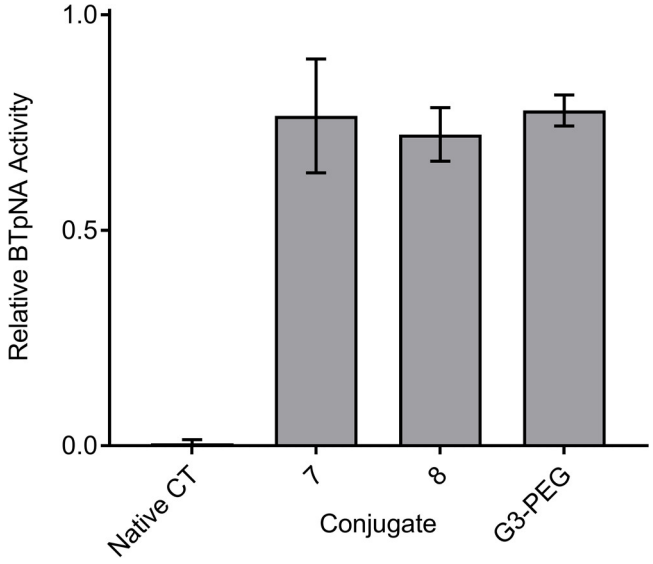

Figure 4.6. Activity of conjugates against BT*p*NA in the presence of anti-α-CT.

In conclusion, we have prepared a series of bis-MPA dendrons from generation 2 through 8 with a strained cyclooctyne (DBCO) at the core and alcohols at the periphery. We also prepared α-CT with all lysine groups functionalized with azides, and found that this conjugate remained water soluble. Dendron-α-CT conjugates were readily prepared with full conversion of all azides, and the resulting conjugates had a linear increase in volume upon increasing dendron generation. These conjugates all displayed full activity against a small molecule substrate, however the seventh and eighth generation dendron-α-CT conjugates displayed very efficient sieving against BSA. These dendrons also shield α-CT from macromolecular inhibitors such as α-anti-CT. This study illustrates that dendrons can perform molecular sieving efficiently at very high molecular weights, which we believe is due to their globular architecture. While small molecules are able to readily diffuse through the interstitial spaces between dendrons, macromolecules cannot. These results are useful

in predicting the required size of globular polymers grafted to proteins to enable effective molecular sieving.

4.4 Experimental

4.5 Experimental Procedures

4.5.1 Synthesis of Dendrimers

Synthesis of Benzylidene Protected bis-MPA Dendrimers

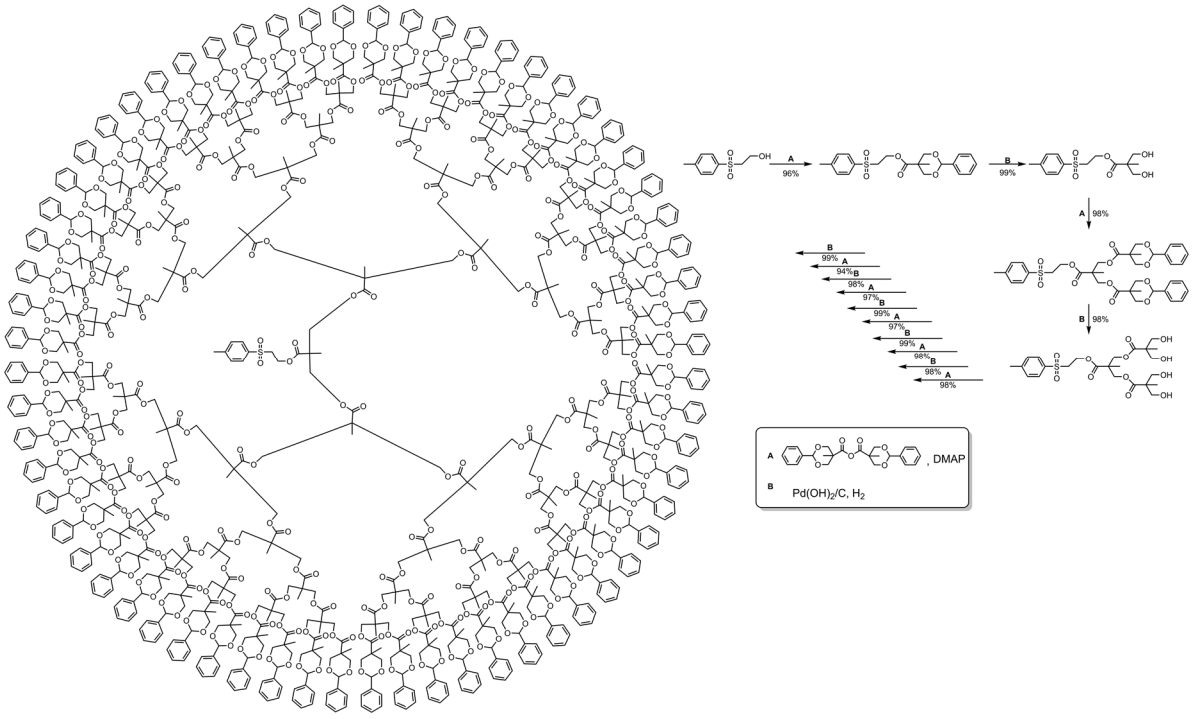

Scheme 4.2. General scheme for preparation of *para*-toluenesulfonyl (*p*TSe) core bis-MPA dendrons of generation 1 through 7.

Synthesis of DBCO core dendrimers

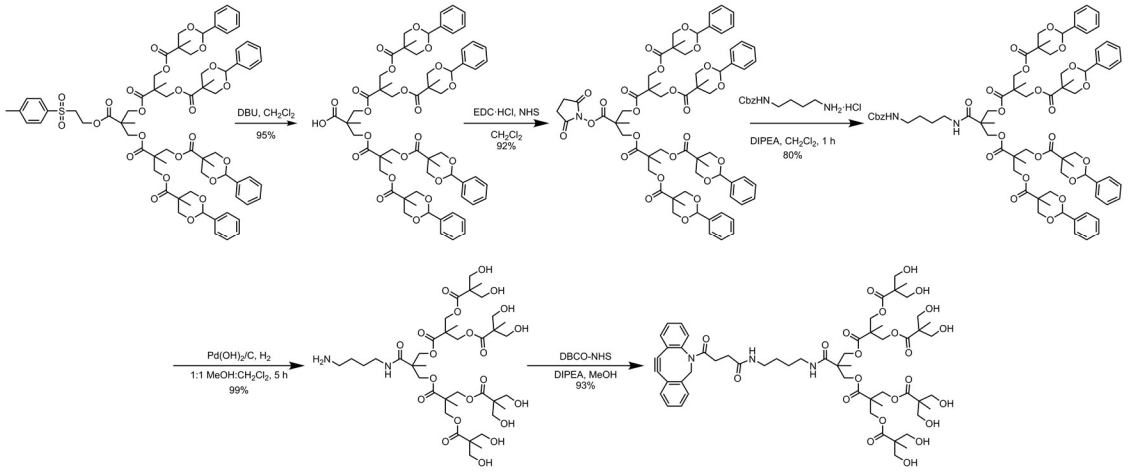

Scheme 4.3. Example synthetic scheme to convert *p*TSe-Gx-(O_2Bn) dendrons to the corresponding DBCO-alcohol periphery dendron, demonstrated using the third generation bis-MPA dendron. This process was completed for dendrimers of generation 2 through 7.

DBCO-G2-$(OH)_4$

Prepared according to literature procedures.[48] (664 mg, 92%)

^{1}H NMR (700 MHz; CD_3OD): δ 7.64 (s, 1H), 7.59 (s, 1H), 7.45 (s, 3H), 7.34 (dd, J = 25.3, 1.2, 2H), 7.25 (s, 1H), 5.12 (d, J = 14.1, 1H), 4.26 (s, 4H), 3.68 (d, J = 20.3, 5H), 3.60 (s, 4H), 3.17 (s, 2H), 3.06 (s, 2H), 2.69 (d, J = 16.6, 1H), 2.31 (d, J = 7.6, 1H), 2.15 (d, J = 15.2, 1H), 1.97 (d, J = 16.6, 1H), 1.46-1.39 (m, 4H), 1.26 (s, 3H), 1.14 (s, 6H)

DBCO-G3-$(OH)_8$

Prepared according to literature procedures.[48] (0.955 g, 92%)

^{1}H NMR (700 MHz; CD_3OD): δ 7.65 (d, J = 7.5, 1H), 7.61-7.60 (m, 1H), 7.48-7.45 (m, 3H), 7.35 (dtd, J = 25.2, 7.5, 1.2, 2H), 7.25 (dd, J = 7.5, 1.2, 1H), 5.13 (d, J = 14.1, 1H), 4.30-4.22 (m, 12H), 3.71 (d, J = 14.1, 1H), 3.68-3.57 (m, 16H), 3.19-3.17 (m, 2H), 3.07

(td, J = 6.9, 4.0, 2H), 2.72-2.67 (m, 1H), 2.34 (dt, J = 15.2, 7.5, 1H), 2.19-2.15 (m, 1H), 1.98 (dt, J = 16.6, 6.8, 1H), 1.50-1.46 (m, 2H), 1.42-1.39 (m, 2H), 1.28 (s, 9H), 1.14 (s, 12H)

DBCO-G3-$(PEG_{15})_8$

Prepared according to literature procedures.[1] (41 mg, 82%)

^{1}H NMR (600 MHz; $CDCl_3$): δ 7.64 (d, J = 7.7, 1H), 7.51 (d, J = 7.5, 1H), 7.39-7.35 (m, 3H), 7.32 (t, J = 7.4, 1H), 7.28 (t, J = 7.6, 1H), 7.23 (d, J = 7.2, 1H), 7.01-6.92 (m, 1H), 6.45-5.44 (m, 8H), 5.12 (d, J = 14.0, 1H), 4.25-4.08 (m, 28H), 3.63-3.59 (m, 1H), 3.53 (t, J = 4.7, 16H), 3.50 (s, 16H), 3.35 (s, 24H), 3.29 (d, J = 4.9, 15H), 3.17 (q, J = 5.7, 2H), 3.06 (dt, J = 13.9, 7.1, 2H), 2.75 (dt, J = 16.4, 8.0, 1H), 2.38 (dt, J = 15.7, 7.6, 1H), 2.15 (dt, J = 14.5, 6.9, 1H), 1.91 (dt, J = 16.4, 6.3, 1H), 1.43 (t, J = 6.6, 2H), 1.38-1.35 (m, 2H), 1.21 (t, J = 27.0, 21H)

COOH-G4-$(O_2Bn)_8$

*p*TSe-G4-$(O_2Bn)_8$ (800 mg, 0.302 mmol) was dissolved in 5 mL of dichloromethane. To this, 1,8-diazabicyclo[5.4.0]undec-7-ene (226 μL, 1.512 mmol) (DBU) was added, and this was left to stir for 2 hours, at which point the reaction mixture was diluted with 30 mL of dichloromethane then washed with 3 × 30 mL of 1 M H_3PO_4, 1 × 50 mL brine, dried with $MgSO_4$, filtered, then dried by rotary evaporation. The crude material was redissolved in 30 mL of ethyl acetate, and this was then precipitated three times into rapidly stirring cold hexanes to give the product as a white powder. (0.507 g, 68%)

^{1}H NMR (700 MHz; $CDCl_3$): δ 7.39 (d, J = 6.4, 16H), 7.29 (q, J = 6.8, 24H), 5.39 (s, 8H), 4.56 (d, J = 11.7, 16H), 4.38-4.33 (m, 16H), 4.14 (s, 4H), 4.08 (dd, J = 17.9, 11.2, 4H),

3.99 (t, J = 11.5, 4H), 3.57 (d, J = 11.5, 16H), 1.20 (s, 12H), 1.13 (s, 3H), 1.01 (s, 6H), 0.91 (s, 24H)

^{13}C NMR (176 MHz; $CDCl_3$): δ 173.61, 173.54, 173.49, 172.9, 172.0, 171.6, 137.9, 129.0, 128.3, 126.3, 101.85, 101.82, 73.63, 73.56, 66.7, 65.7, 65.3, 47.0, 46.7, 46.1, 42.7, 17.8, 17.4

MALDI: m/z calc: $[M+K]^+$ = 2502.94 exp: $[M+K]^+$ = 2506.3

NHS-G4-(O_2Bn)$_8$

COOH-G4-(O_2Bn)$_8$ (0.450 g, 0.18 mmol) was dissolved in 3 mL of dichloromethane, then *N*-hydroxysuccinimide (84 mg, 0.73 mmol) and *N*-(3-dimethylaminopropyl)-*N'*-ethylcarbodiimide hydrochloride (175 mg, 0.91 mmol) were added and this was left to react overnight. The reaction mixture was then diluted with 30 mL of dichloromethane, then washed with 3 × 30 mL of 1 M H_3PO_4, 3 × 30 mL of 1% sodium bicarbonate, 1 × 50 mL brine, then dried with $MgSO_4$, filtered, and solvent was removed by rotary evaporation. The crude material was then dissolved in ethyl acetate and precipitated into 250 mL of rapidly stirring cold hexanes to give the product as a white powder. (419 mg, 90%)

^{1}H NMR (700 MHz; $CDCl_3$): δ 7.40-7.38 (m, 16H), 7.29 (q, J = 7.1, 24H), 5.39 (s, 8H), 4.57-4.54 (m, 16H), 4.38-4.26 (m, 18H), 4.15-4.09 (m, 10H), 3.58-3.55 (m, 16H), 2.53 (d, J = 37.6, 4H), 1.32 (s, 3H), 1.20 (s, 12H), 1.09 (s, 6H), 0.91 (d, J = 4.3, 24H)

13C NMR (176 MHz; $CDCl_3$): δ 173.3, 172.1, 171.5, 168.9, 168.2, 138.0, 129.0, 128.3, 126.3, 101.8, 73.6, 66.3, 65.9, 65.3, 47.0, 46.8, 46.6, 42.7, 25.6, 17.84, 17.80, 17.6, 17.2

MALDI: m/z calc: $[M+Na]^+$ = 2584.7 exp: $[M+Na]^+$ = 2584.1

CBz-G4-(O_2Bn)$_8$

NHS-G4-(O_2Bn)$_8$ (0.350 g, 0.14 mmol) was dissolve in 2 mL of dichloromethane, to which benzyl (4-aminobutyl) carbamate hydrochloride (91 mg, 0.41 mmol) and triethylamine (0.152 mL, 1.09 mmol) were added and this was left to stir for 3 hours. At this point, the reaction was diluted with 20 mL of dichloromethane, washed with 3 × 30 mL of 1 M H_3PO_4, 3 ×30 mL of 10% Na_2CO_3, 1 × 50 mL of brine, then dried with $MgSO_4$, filtered, and solvent was removed by rotary evaporation. The resulting crude material was purified by flash chromatography using a 25 gram Biotage Snap column equilibrated in 30% Ethyl acetate in hexanes, with purification using a gradient from 30% to 90% ethyl acetate in hexanes over 20 column volumes. The fractions containing product were pooled and solvent was removed by rotary evaporation and the product was dried *in vacuo* to give a white foam (245 mg, 67%)

^{1}H NMR (600 MHz; $CDCl_3$): δ 7.38 (dd, J = 7.4, 1.8, 16H), 7.36-7.32 (m, 5H), 7.31-7.27 (m, 24H), 6.25 (t, J = 5.3, 1H), 5.38 (s, 8H), 5.21 (t, J = 5.8, 1H), 5.06 (s, 2H), 4.55-4.53 (m, 16H), 4.36-4.31 (m, 16H), 4.14 (d, J = 12.0, 2H), 4.08 (d, J = 11.1, 2H), 4.03 (s, 8H), 3.56 (dd, J = 11.6, 3.4, 16H), 3.11 (q, J = 6.1, 2H), 3.05 (q, J = 5.8, 2H), 1.40-1.35 (m, 4H), 1.19 (s, 12H), 1.09 (s, 3H), 1.00 (s, 6H), 0.90 (d, J = 3.2, 24H)

^{13}C NMR (176 MHz; $CDCl_3$): δ 173.4, 172.7, 172.12, 172.10, 171.65, 171.60, 171.49, 138.0, 129.0, 128.62, 128.55, 128.41, 128.27, 126.3, 101.78, 101.69, 77.34, 77.16, 73.62, 73.57, 72.2, 67.3, 66.6, 65.77, 65.72, 65.2, 46.82, 46.69, 46.4, 42.7, 40.6, 39.5, 27.3, 26.9, 17.94, 17.82, 17.68, 17.43, 17.34

MALDI: m/z calc: $[M+Na]^+$ = 2691.9 exp: $[M+Na]^+$ = 2691.4

H_2N-G4-$(OH)_{16}$

Cbz-G4-$(O_2Bn)_8$ (200 mg, 0.075 mmol) was dissolved in 5 mL of dichloromethane, then diluted with 5 mL of methanol. To this, palladium hydroxide on carbon (20 mg, 10 wt%) was added, and the reaction was purged and backfilled with hydrogen gas three times with vigorous stirring, then left to stir overnight under a hydrogen atmosphere. The reaction mixture was then filtered through a 0.2 μm polypropylene filter membrane, and solvent was removed by rotary evaporation then dried *in vacuo* to give the product as a white foam. (150 mg, quantitative)

^{1}H NMR (700 MHz; CD_3OD): δ 4.33-4.31 (m, 17H), 4.27-4.24 (m, 11H), 3.68 (dd, J = 10.9, 4.2, 16H), 3.60 (d, J = 10.8, 16H), 3.27 (t, J = 7.2, 2H), 3.01 (t, J = 7.5, 2H), 1.70 (dt, J = 15.1, 7.4, 2H), 1.64 (dt, J = 14.6, 7.2, 2H), 1.34 (s, 3H), 1.32 (s, 6H), 1.31 (s, 12H), 1.15 (s, 24H)

^{13}C NMR (176 MHz; CD_3OD): δ 175.9, 174.6, 173.8, 173.3, 68.3, 67.1, 66.2, 65.9, 51.8, 48.11, 47.98, 47.7, 40.4, 40.1, 27.7, 26.0, 18.31, 18.15, 17.4

MALDI: m/z calc: $[M+H]^+$ = 1852.8 exp: $[M+H]^+$ = 1855.4

DBCO-G4-$(OH)_{16}$

H_2N-G4-$(OH)_{16}$ (100 mg, 0.05 mmol) was dissolved in 0.5 mL of methanol. To this, a solution of DBCO-NHS (24 mg, 0.06 mmol) in 0.25 mL of dichloromethane was added, along with triethylamine (15 μL, 0.11 mmol). This was left to stir for 5 hours, at which point the solvent was removed by rotary evaporation. The crude material was dissolved in 1 mL of DMSO and diluted with 1 mL of water, and this was loaded onto a 10 gram Biotage Snap column packed with reverse phase C18 silica equilibrated in 5% acetonitrile in water.

The compound was purified using a gradient from 10% to 75% acetonitrile in water over 20 column volumes, and the fractions containing product were combined and organic solvent was removed by rotary evaporation. The resulting aqueous portion was diluted with 50 mL of water, then lyophilized for two days to give the product as a fluffy white powder. (68 mg, 58%)

^{1}H NMR (700 MHz; CD_3OD): δ 7.65 (d, J = 7.4, 1H), 7.62-7.60 (m, 1H), 7.49-7.45 (m, 3H), 7.37 (td, J = 7.4, 1.1, 1H), 7.34 (t, J = 7.3, 1H), 7.26 (d, J = 6.7, 1H), 5.14 (d, J = 14.2, 1H), 4.32-4.24 (m, 28H), 3.72-3.66 (m, 17H), 3.60 (dd, J = 13.5, 7.9, 16H), 3.21-3.19 (m, 2H), 3.08 (q, J = 6.3, 2H), 2.73-2.68 (m, 1H), 2.36-2.32 (m, 1H), 1.99 (dt, J = 16.6, 6.8, 1H), 1.49 (dt, J = 14.3, 7.1, 2H), 1.42 (dd, J = 14.3, 7.5, 2H), 1.32-1.29 (m, 18H), 1.20 (s, 3H), 1.15 (s, 24H)

^{13}C NMR (151 MHz; CD_3OD): δ 175.9, 174.8, 174.39, 174.20, 174.06, 173.77, 173.64, 173.42, 173.31, 152.6, 149.4, 133.4, 130.6, 130.0, 129.6, 129.2, 128.9, 128.1, 126.5, 124.4, 123.7, 115.6, 108.8, 68.3, 67.1, 66.7, 66.2, 65.8, 65.5, 56.7, 51.8, 40.5, 40.0, 32.0, 31.4, 27.80, 27.71, 18.32, 18.19, 18.13, 17.8, 17.4

MALDI: m/z calc: $[M+Na]^+$ = 2140.2 exp: $[M+Na]^+$ = 2142.6

COOH-G5-(O_2Bn)$_{16}$ [49]

*p*TSe-G5-(O_2Bn)$_{16}$ (3.101 g, 0.576 mmol) was dissolved in 20 mL of dichloromethane. To this, DBU (345 μL, 2.303 mmol) was added, and this was left to stir for 2 hours, at which point the reaction mixture was diluted with 50 mL of dichloromethane then washed with 3 × 30 mL of 1 M H_3PO_4, 1 × 50 mL brine, dried with $MgSO_4$, filtered, then dried by rotary

evaporation. The crude material was redissolved in 30 mL of ethyl acetate, and this was then precipitated three times into 500 mL of rapidly stirring cold hexanes to give the product as a white powder. (2.797 g, 93%)

^{1}H NMR (700 MHz; $CDCl_3$): δ 7.39 (d, J = 6.6, 32H), 7.29 (q, J = 7.4, 48H), 5.37 (s, 16H), 4.54 (d, J = 12.0, 32H), 4.37-4.31 (m, 32H), 4.25 (d, J = 11.0, 2H), 4.16-4.11 (m, 10H), 4.09-4.04 (m, 16H), 3.54 (dd, J = 11.6, 5.0, 32H), 1.21 (s, 3H), 1.19 (s, 24H), 1.12 (s, 6H), 1.02 (d, J = 1.9, 12H), 0.89 (d, J = 1.6, 48H)

^{13}C NMR (176 MHz; $CDCl_3$): δ 173.3, 172.9, 172.13, 172.10, 172.08, 172.03, 171.96, 171.48, 171.44, 171.25, 138.0, 129.0, 128.2, 126.3, 101.8, 73.56, 73.51, 66.9, 65.8, 65.5, 65.2, 47.0, 46.69, 46.61, 46.3, 31.7, 22.8, 17.8, 17.46, 17.40, 17.34

MALDI: m/z calc: $[M+Na]^+$ = 5050.3 exp: $[M+Na]^+$ = 5052.3

NHS-G5-$(O_2Bn)_{16}$

COOH-G5-$(O_2Bn)_{16}$ (2.910 g, 0.579 mmol) was dissolved in 15 mL of dichloromethane, then *N*-hydroxysuccinimide (200 mg, 1.738 mmol) and *N*-(3-dimethylaminopropyl)-*N'*-ethylcarbodiimide hydrochloride (332 mg, 1.738 mmol) were added and this was left to react overnight. The reaction mixture was then diluted with 50 mL of dichloromethane, washed with 3 × 30 mL of 1 M H_3PO_4, 3 × 30 mL of 1% sodium bicarbonate, 1 × 50 mL brine, then dried with $MgSO_4$, filtered, and solvent was removed by rotary evaporation. The crude material was then dissolved in 30 mL ethyl acetate and precipitated into 500 mL of rapidly stirring cold hexanes to give the product as a white powder (2.321 g, 78%).

^{1}H NMR (700 MHz; $CDCl_3$): δ 7.39-7.38 (m, 32H), 7.30-7.26 (m, 48H), 5.37 (s, 16H), 4.55-4.53 (m, 32H), 4.37-4.31 (m, 34H), 4.20-4.17 (m, 10H), 4.10-4.05 (m, 16H), 3.54 (dd, J = 11.1, 5.7, 32H), 2.44 (d, J = 24.4, 4H), 1.37 (s, 3H), 1.19 (d, J = 2.7, 30H), 1.03 (s, 12H), 0.89 (d, J = 4.0, 48H)

^{13}C NMR (176 MHz; $CDCl_3$): δ 173.3, 172.0, 171.48, 171.35, 169.0, 168.3, 138.0, 129.0, 128.2, 126.3, 101.7, 73.56, 73.51, 66.7, 65.8, 65.4, 65.1, 46.94, 46.75, 46.62, 42.6, 25.5, 17.8, 17.42, 17.33, 17.19

MALDI: m/z calc: $[M+Na]^+$ = 5147.4 exp: $[M+Na]^+$ = 5149.0

Cbz-G5-$(O_2Bn)_{16}$

NHS-G5-$(O_2Bn)_{16}$ (2.153 g, 0.42 mmol) was dissolved in 15 mL of dichloromethane, to which benzyl (4-aminobutyl) carbamate hydrochloride (326 mg, 1.26 mmol) and triethylamine (0.469 mL, 3.361 mmol) was added and this was left to stir for 3 hours. At this point, the reaction was diluted with 50 mL of dichloromethane, washed with 3 × 30 mL of 1 M H_3PO_4, 3 × 30 mL of 10% Na_2CO_3, 1 × 50 mL of brine, then dried with $MgSO_4$, filtered, and solvent was removed by rotary evaporation. The resulting material was redissolved in 30 mL of ethyl acetate then precipitated into 500 mL of rapidly stirring cold hexanes to give the product as a white powder. (1.988 g, 91%)

^{1}H NMR (700 MHz; $CDCl_3$): δ 7.32-7.26 (m, 53H), 7.32-7.26 (m, 55H), 6.43 (t, J = 5.3, 1H), 5.36 (s, 16H), 5.31 (t, J = 5.6, 1H), 5.04 (s, 2H), 4.54-4.52 (m, 32H), 4.34 (dtd, J = 15.3, 10.1, 5.1, 32H), 4.23 (d, J = 10.8, 2H), 4.15-4.11 (m, 8H), 4.09-4.03 (m, 18H), 3.55-

3.52 (m, 32H), 3.09 (q, J = 6.0, 2H), 3.00 (q, J = 6.4, 2H), 1.36-1.30 (m, 4H), 1.18 (s, 27H), 1.13 (s, 6H), 1.02 (s, 12H), 0.88 (d, J = 3.4, 48H)

^{13}C NMR (176 MHz; $CDCl_3$): δ 173.3, 172.0, 171.60, 171.41, 171.32, 156.6, 138.0, 137.0, 129.0, 128.6, 128.2, 126.3, 101.7, 73.57, 73.51, 67.8, 66.5, 65.8, 65.4, 65.1, 47.0, 46.64, 46.50, 42.7, 40.6, 39.6, 27.3, 26.9, 17.8, 17.49, 17.34, 17.28

MALDI: m/z calc: $[M+Na]^+$ = 5254.6 exp: $[M+Na]^+$ = 5255.8

H_2N-G5 -$(OH)_{32}$

Cbz-G5-$(O_2Bn)_8$ (200 mg, 0.075 mmol) was dissolved in 5 mL of dichloromethane, then diluted with 5 mL of methanol. To this, palladium hydroxide on carbon (20 mg, 10 wt%) was added, and the reaction was purged and backfilled with hydrogen gas three times with vigorous stirring, then left to stir overnight under a hydrogen atmosphere. The reaction mixture was then filtered through a 0.2 μm polypropylene filter membrane, and solvent was removed by rotary evaporation, then dried *in vacuo* to give the product as a white foam. (150 mg, quantitative)

^{1}H NMR (700 MHz; CD_3OD): δ 4.35-4.25 (m, 60H), 3.68 (dd, J = 10.8, 3.9, 32H), 3.61 (d, J = 10.8, 32H), 3.28 (d, J = 7.3, 2H), 3.04 (t, J = 7.5, 2H), 1.72 (dt, J = 15.0, 7.3, 2H), 1.65 (dt, J = 14.5, 7.3, 2H), 1.38 (s, 3H), 1.35 (s, 6H), 1.32 (d, J = 5.8, 36H), 1.16 (s, 48H)

^{13}C NMR (176 MHz; CD_3OD): δ 176.0, 174.5, 173.8, 173.36, 173.19, 68.6, 67.3, 67.0, 66.2, 65.9, 51.8, 48.10, 47.97, 47.80, 40.5, 40.2, 27.7, 26.1, 18.40, 18.27, 18.22, 18.16, 17.4

MALDI: m/z calc: $[M+Na]^+$ = 3710.7 exp: $[M+Na]^+$ 3713.6

DBCO-G5-$(OH)_{32}$

H_2N-G5-$(OH)_{32}$ (145 mg, 0.039 mmol) was dissolved in 0.5 mL of methanol. To this, a solution of DBCO-NHS (24 mg, 0.06 mmol) in 0.25 mL of dichloromethane was added, along with triethylamine (15 μL, 0.11 mmol). This was left to stir for 5 hours, at which point the solvent was removed by rotary evaporation. The crude material was redissolved in 1.5 mL of methanol and was purified by size exclusion chromatography through Sephadex LH-20 in methanol, with collection of the high molecular weight components. These fractions were combined and solvent was removed by rotary evaporation then diluted with 5 mL of water and lyophilized overnight to give the product as a fluffy white powder. (114 mg, 73%)

^{1}H NMR (700 MHz; CD_3OD): δ 7.73-7.02 (m, 8H), 5.15-5.10 (m, 1H), 5.04-5.03 (m, 2H), 4.32-4.25 (m, 60H), 3.69-3.60 (m, 64H), 3.21-3.21 (m, 2H), 3.08-3.08 (m, 1H), 2.71 (s, 1H), 2.35-2.33 (m, 1H), 2.17 (s, 1H), 2.00-1.96 (m, 1H), 1.57-1.42 (m, 4H), 1.32 (d, J = 38.5, 45H), 1.15 (s, 48H)

^{13}C NMR (176 MHz; CD_3OD): δ 175.9, 174.4, 174.10, 174.05, 173.8, 173.28, 173.17, 152.6, 149.4, 133.4, 130.6, 130.0, 129.7, 129.2, 128.9, 128.11, 128.11, 126.5, 124.3, 123.6, 115.6, 110.3, 108.8, 68.5, 67.2, 67.0, 66.1, 56.7, 51.8, 48.04, 47.90, 47.71, 40.6, 40.1, 32.0, 31.4, 30.2, 27.87, 27.75, 18.38, 18.20, 17.4

MALDI: m/z calc: $[M+Na]^+$ = 3998.1 exp: : $[M+Na]^+$ = 4002.1

COOH-G6-$(O_2Bn)_{32}$ [49]

*p*TSe-G6-$(O_2Bn)_{32}$ (3.001 g, 0.290 mmol) was dissolved in 20 mL of dichloromethane. To this, DBU (174 μL, 1.161 mmol) was added, and this was left to stir for 2 hours, at which

point the reaction mixture was diluted with 50 mL of dichloromethane then washed with 3 × 30 mL of 1 M H_3PO_4, 1 × 50 mL brine, dried with $MgSO_4$, filtered, then dried by rotary evaporation. The crude material was redissolved in 30 mL of ethyl acetate, and this was then precipitated three times into 500 mL of rapidly stirring cold hexanes to give the product as a white powder. (2.933 g, 99%)

^{1}H NMR (600 MHz; $CDCl_3$): δ 7.37 (d, J = 6.4, 64H), 7.26 (s, 96H), 5.33 (s, 32H), 4.51 (s, 64H), 4.32 (s, 64H), 4.18 (s, 16H), 4.08 (s, 28H), 4.04 (s, 16H), 3.50 (s, 64H), 1.26-1.24 (m, 3H), 1.16 (s, 68H), 1.00-1.00 (m, 18H), 0.96-0.93 (m, 6H), 0.85 (s, 96H)

^{13}C NMR (176 MHz; $CDCl_3$): δ 173.3, 172.6, 172.0, 171.65, 171.60, 171.44, 138.1, 129.0, 126.35, 126.27, 101.71, 101.57, 73.53, 73.49, 72.2, 65.3, 65.1, 47.0, 46.6, 42.7, 17.89, 17.84, 17.58, 17.40

MALDI: m/z calc: $[M+Na]^+$ = 10167.4 exp: : $[M+Na]^+$ = 10175.8

NHS-G6-$(O_2Bn)_{32}$

COOH-G6-$(O_2Bn)_{32}$ (2.933 g, 0.289 mmol) was dissolved in 15 mL of dichloromethane, then *N*-hydroxysuccinimide (100 mg, 0.867 mmol) and *N*-(3-dimethylaminopropyl)-*N'*-ethylcarbodiimide hydrochloride (166 mg, 0.867 mmol) were added and left to react overnight. The reaction mixture was then diluted with 50 mL of dichloromethane, washed with 3 × 30 mL of 1 M H_3PO_4, 3 × 30 mL of 1% sodium bicarbonate, 1 × 50 mL brine, then dried with $MgSO_4$, filtered, and solvent was removed by rotary evaporation. The crude material was then dissolved in ethyl acetate and precipitated into 500 mL of rapidly stirring cold hexanes to give the product as a white powder. (2.483 g, 84%)

^{1}H NMR (700 MHz; $CDCl_3$): δ 7.37-7.36 (m, 64H), 7.28-7.25 (m, 96H), 5.33 (s, 32H), 4.51-4.49 (m, 64H), 4.34-4.29 (m, 73H), 4.19 (dd, J = 11.1, 0.3, 9H), 4.12-4.09 (m, 26H), 4.05-4.03 (m, 16H), 3.50 (dd, J = 11.0, 6.2, 64H), 2.47 (s, 4H), 1.43-1.38 (m, 3H), 1.26 (s, 6H), 1.16 (s, 48H), 1.14 (s, 12H), 1.02 (s, 24H), 0.85 (s, 96H)

^{13}C NMR (176 MHz; $CDCl_3$): δ 173.3, 172.0, 171.55, 171.49, 171.32, 169.1, 168.3, 138.1, 129.0, 128.2, 126.3, 101.7, 73.54, 73.49, 67.0, 65.8, 65.32, 65.17, 65.09, 46.9, 46.65, 46.61, 42.7, 41.2, 25.6, 17.84, 17.79, 17.56, 17.42, 17.2

MALDI: m/z calc: $[M+Na]^+$ = 10272.8.4 exp: : $[M+Na]^+$ = 10264.6

Cbz-G6-$(O_2Bn)_{32}$

NHS-G6-$(O_2Bn)_{32}$ (2.463 g, 0.240 mmol) was dissolved in 15 mL of dichloromethane, to which benzyl (4-aminobutyl) carbamate hydrochloride (326 mg, 1.26 mmol) and triethylamine (0.168 mL, 1.201 mmol) was added and this was left to stir for 3 hours. At this point, the reaction was diluted with 50 mL of dichloromethane, washed with 3 × 30 mL of 1 M H_3PO_4, 3 × 30 mL of 10% Na_2CO_3, 1 × 50 mL of brine, then dried with $MgSO_4$, filtered, and solvent was removed by rotary evaporation. The resulting material was redissolved in 30 mL of ethyl acetate then precipitated into 500 mL of rapidly stirring cold hexanes to give the product as a white powder. (2.071g, 84%)

^{1}H NMR (700 MHz; $CDCl_3$): δ 7.38 (d, J = 6.8, 64H), 7.29-7.25 (m, 101H), 6.40 (t, J = 5.4, 1H), 5.40 (t, J = 5.4, 1H), 5.35 (s, 32H), 5.02 (s, 2H), 4.52 (t, J = 6.1, 64H), 4.35-4.30 (m, 66H), 4.21 (d, J = 11.3, 16H), 4.12 (t, J = 8.6, 24H), 4.05 (t, J = 8.6, 18H), 3.51 (dd, J

= 11.1, 6.3, 64H), 3.11 (s, 2H), 2.97 (q, J = 6.2, 2H), 1.62 (s, 4H), 1.24 (s, 3H), 1.21 (s, 6H), 1.17 (s, 48H), 1.15 (s, 12H), 1.03 (d, J = 3.6, 24H), 0.86 (d, J = 3.0, 96H)

^{13}C NMR (176 MHz; $CDCl_3$): δ 173.3, 172.0, 171.55, 171.36, 171.24, 156.6, 138.1, 137.0, 129.0, 128.6, 128.2, 126.3, 101.7, 73.53, 73.48, 68.4, 66.4, 65.9, 65.1, 46.94, 46.83, 46.63, 46.59, 42.7, 40.5, 39.6, 27.5, 26.8, 17.83, 17.78, 17.59, 17.42, 17.15, 17.05

MALDI: m/z calc: $[M+Na]^+$ = 10380.0 exp: : $[M+Na]^+$ = 10373.7

H_2N-G6 -$(OH)_{64}$

CBz-G6-$(O_2Bn)_{32}$ (200 mg, 0.019 mmol) was dissolved in 5 mL of dichloromethane, then diluted with 5 mL of methanol. To this, palladium hydroxide on carbon (20 mg, 10 wt%) was added, and the reaction was purged and backfilled with hydrogen gas three times with vigorous stirring, then left to stir overnight under a hydrogen atmosphere. The reaction mixture was then filtered through a 0.2 μm polypropylene filter membrane, and solvent was removed by rotary evaporation then dried *in vacuo* to give the product as a white foam. (141 mg, 99%)

^{1}H NMR (700 MHz; CD_3OD): δ 4.34 (d, J = 10.0, 124H), 3.68 (dd, J = 10.9, 4.2, 64H), 3.61 (d, J = 10.9, 64H), 3.29 (m, J = 1.6, 2H), 3.06 (t, J = 6.8, 2H), 1.74 (dt, J = 14.9, 7.5, 2H), 1.67 (dt, J = 14.6, 7.4, 2H), 1.39-1.32 (m, 93H), 1.16 (s, 96H)

^{13}CNMR (176 MHz; CD_3OD): δ 175.9, 174.4, 173.8, 173.32, 173.26, 173.18, 68.9, 67.18, 67.03, 66.93, 66.1, 65.9, 51.8, 49.9, 49.5, 48.05, 47.93, 40.6, 40.3, 27.8, 26.1, 18.49, 18.37, 18.31, 18.1, 17.5

MALDI: m/z calc: $[M+Na]^+$ = 7426.5 exp: : $[M+Na]^+$ = 7417.7

DBCO-G6-$(OH)_{64}$

H_2N-G6-$(OH)_{64}$ (120 mg, 0.016 mmol) was dissolved in 0.5 mL of methanol. To this, a solution of DBCO-NHS (10 mg, 0.024 mmol) in 0.25 mL of dichloromethane was added, along with triethylamine (7 μL, 0.049 mmol). This was left to stir for 5 hours, at which point the solvent was removed by rotary evaporation. The crude material was redissolved in 1.5 mL of methanol and was purified by size exclusion chromatography through Sephadex LH-20 in methanol, with collection of the high molecular weight components. These fractions were combined and solvent was removed by rotary evaporation, then diluted with 5 mL of water and lyophilized overnight to give the product as a fluffy white powder. (101 mg, 81%)

^{1}H NMR (700 MHz; CD_3OD): δ 7.67 (d, J = 7.4, 1H), 7.64-7.63 (m, 1H), 7.51-7.47 (m, 3H), 7.39 (td, J = 7.5, 1.0, 1H), 7.35 (t, J = 7.3, 1H), 7.27 (d, J = 6.8, 1H), 5.15 (d, J = 14.2, 1H), 4.35-4.26 (m, 124H), 3.69-3.67 (m, 65H), 3.61 (d, J = 10.9, 64H), 3.25 (s, 2H), 2.73 (dt, J = 16.1, 7.9, 2H), 2.36 (dt, J = 15.2, 7.5, 1H), 2.19 (dt, J = 14.8, 7.2, 1H), 1.99 (dt, J = 16.6, 6.8, 1H), 1.51 (t, J = 6.7, 2H), 1.44 (t, J = 7.7, 2H), 1.40-1.32 (m, 93H), 1.14 (d, J = 3.6, 96H)

^{13}CNMR (176 MHz; CD_3OD): δ 176.0, 174.4, 174.1, 173.8, 173.34, 173.24, 152.7, 149.5, 133.5, 130.7, 130.2, 129.7, 129.3, 129.0, 128.2, 126.5, 124.4, 123.7, 115.7, 111.4, 108.9, 71.6, 69.1, 67.08, 66.96, 66.2, 65.9, 56.8, 51.8, 49.8, 48.08, 47.95, 40.7, 40.2, 32.0, 31.4, 28.00, 27.91, 18.52, 18.40, 18.34, 18.1, 17.60, 17.50

MALDI: m/z calc: $[M+Na]^+$ = 7713.8 exp: : $[M+Na]^+$ = 7707.3

COOH-G7-(O_2Bn)$_{64}$ [49]

*p*TSe-G7-(O_2Bn)$_{64}$ (0.800 g, 0.039 mmol) was dissolved in 2 mL of dichloromethane. To this, DBU (29 μL, 0.194 mmol) was added, and this was left to stir for 2 hours, at which point the reaction mixture was diluted with 30 mL of dichloromethane then washed with 3 × 30 mL of 1 M H_3PO_4, 1 × 50 mL brine, dried with $MgSO_4$, filtered, then dried by rotary evaporation. The crude material was redissolved in 30 mL of ethyl acetate, and this was then precipitated three times into 500 mL of rapidly stirring cold hexanes to give the product as a white powder. (0.623 g 78%)

^{1}H NMR (700 MHz; $CDCl_3$): δ 7.35 (d, J = 6.9, 128H), 7.24 (t, J = 8.3, 192H), 5.30 (s, 64H), 4.46 (s, 128H), 4.29 (s, 128H), 4.23-4.01 (m, 124H), 3.46 (dd, J = 8.7, 5.9, 128H), 1.20 (d, J = 12.1, 21H), 1.13 (d, J = 17.0, 120H), 0.99 (d, J = 5.5, 48H), 0.81 (s, 192H)

^{13}C NMR (176 MHz; $CDCl_3$): δ 173.3, 172.0, 171.6, 138.2, 128.9, 128.2, 126.4, 101.62, 101.59, 73.4, 65.0, 46.9, 46.6, 42.6, 17.84, 17.75, 17.67, 17.4

MALDI: m/z calc: $[M+Na]^+$ = 20426.7 exp: : $[M+Na]^+$ = 20426.0

NHS-G7-(O_2Bn)$_{64}$

COOH-G7-(O_2Bn)$_{64}$ (0.540 g, 0.03 mmol) was dissolved in 3 mL of dichloromethane, then *N*-hydroxysuccinimide (100 mg, 0.867 mmol) and *N*-(3-dimethylaminopropyl)-*N'*-ethylcarbodiimide hydrochloride (166 mg, 0.867 mmol) were added and this was left to react overnight. The reaction mixture was then diluted with 30 mL of dichloromethane, washed with 3 × 30 mL of 1 M H_3PO_4, 3 × 30 mL of 1% sodium bicarbonate, 1 × 50 mL

brine, then dried with $MgSO_4$, filtered, and solvent was removed by rotary evaporation. The crude material was then dissolved in ethyl acetate and precipitated into 500 mL of rapidly stirring cold hexanes to give the product as a white powder, which was used directly without further purification. (464 mg, 85%)

^{1}H NMR (700 MHz; $CDCl_3$): δ 7.35 (d, J = 7.0, 128H), 7.23 (dt, J = 15.7, 7.5, 192H), 5.29 (s, 64H), 4.47 (d, J = 7.0, 128H), 4.29 (s, 128H), 4.23-4.01 (m, 124H), 3.45 (dd, J = 9.9, 7.3, 128H), 2.37 (s, 4H), 1.29 (s, 9H), 1.22 (s, 12H), 1.13-1.11 (m, 120H), 0.99 (d, J = 5.3, 48H), 0.81 (s, 192H)

^{13}CNMR (176 MHz; $CDCl_3$): δ 173.3, 172.0, 171.59, 171.56, 171.3, 138.2, 128.9, 128.2, 126.4, 101.6, 76.4, 73.8, 73.2, 65.0, 60.6, 46.9, 46.6, 42.6, 25.4, 17.84, 17.76, 17.67, 17.62, 17.46, 16.9

MALDI: m/z calc: $[M+Na]^+$ = 20523.8 exp: : $[M+Na]^+$ = 20527.6

CBz-G7-$(O_2Bn)_{64}$

NHS-G7-$(O_2Bn)_{64}$ (0.400 g, 0.02 mmol) was dissolved in 2 mL of dichloromethane, to which benzyl (4-aminobutyl) carbamate hydrochloride (13 mg, 0.06 mmol) and triethylamine (22 μL, 0.16 mmol) was added and this was left to stir for 3 hours. At this point, the reaction was diluted with 50 mL of dichloromethane, washed with 3 × 30 mL of 1 M H_3PO_4, 3 × 30 mL of 10% Na_2CO_3, 1 × 50 mL of brine, then dried with $MgSO_4$, filtered, and solvent was removed by rotary evaporation. The resulting material was redissolved in 30 mL of ethyl acetate then precipitated into 100 mL of rapidly stirring cold hexanes to give the product as a white powder. (310 mg, 77%)

^{1}H NMR (700 MHz; $CDCl_3$): δ 7.35 (d, J = 6.9, 128H), 7.25 (s, 197H), 5.29 (s, 64H), 4.97 (s, 2H), 4.46 (s, 128H), 4.29 (s, 128H), 4.23-4.01 (m, 124H), 3.45 (t, J = 8.0, 128H), 3.09 (s, 2H), 2.91 (s, 2H), 1.20 (s, 25H), 1.12 (d, J = 15.3, 120H), 0.99 (d, J = 6.1, 48H), 0.80 (s, 192H)

^{13}C NMR (176 MHz; $CDCl_3$): δ 173.3, 172.0, 171.60, 171.56, 171.29, 171.19, 171.12, 138.2, 128.9, 128.2, 126.4, 101.6, 73.5, 65.0, 46.9, 46.6, 42.6, 17.85, 17.76, 17.68, 17.5, 17.2

MALDI: m/z calc: $[M+Na]^+$ = 20630.9 exp: : $[M+Na]^+$ = 20618.9

H_2N-G7 -$(OH)_{128}$

CBz-G7-$(O_2Bn)_{64}$ (180 mg, 0.009 mmol) was dissolved in 2 mL of dichloromethane, then diluted with 2 mL of methanol. To this, palladium hydroxide on carbon (18 mg, 10 wt%) was added, and the reaction was purged and backfilled with hydrogen gas three times with vigorous stirring, then left to stir overnight under a hydrogen atmosphere. The reaction mixture was then filtered through a 0.2 μm polypropylene filter membrane, and solvent was removed by rotary evaporation then dried *in vacuo* to give the product as a white foam. (130 mg, quant.)

^{1}H NMR (700 MHz; CD_3OD): δ 4.35 (t, J = 11.4, 179H), 4.27 (d, J = 10.5, 73H), 3.69 (dd, J = 10.8, 4.6, 128H), 3.62 (d, J = 10.9, 128H), 3.21 (s, 2H), 3.10 (t, J = 3.7, 1H), 1.77 (s, 2H), 1.68 (s, 2H), 1.37-1.33 (m, 188H), 1.16 (s, 192H)

^{13}C NMR (176 MHz; CD_3OD): δ 176.0, 173.9, 173.40, 173.29, 66.9, 66.2, 65.9, 51.8, 48.07, 47.95, 18.63, 18.53, 18.47, 17.6

MALDI: m/z calc: $[M+Na]^+$ = 14834.9 exp: : $[M+Na]^+$ = 14832.4

DBCO-G7-$(OH)_{128}$

H_2N-G7-$(OH)_{128}$ (100 mg, 0.007 mmol) was dissolved in 0.5 mL of methanol. To this, a solution of DBCO-NHS (3 mg, 0.0077 mmol) in 0.25 mL of dichloromethane was added, along with triethylamine (2 μL, 0.021 mmol). This was left to stir for 5 hours, at which point the solvent was removed by rotary evaporation. The crude material was redissolved in 1.5 mL of methanol and was purified by size exclusion chromatography through Sephadex LH-20 in methanol, with collection of the high molecular weight components. These fractions were combined and solvent was removed by rotary evaporation, then diluted with 5 mL of water and lyophilized overnight to give the product as a fluffy white powder. (95 mg, 93%)

^{1}H NMR (700 MHz; CD_3OD): δ 8.02-7.29 (m, 8H), 5.16 (s, 1H), 4.37 (d, J = 161.0, 177H), 4.28 (s, 75H), 3.68 (s, 129H), 3.63 (s, 128H), 3.25 (s, 2H), 3.08 (s, 2H), 2.75 (s, 1H), 2.35 (s, 1H), 2.20 (s, 1H), 2.00 (s, 1H), 1.33 (s, 193H), 1.16 (s, 192H)

^{13}CNMR (176 MHz; CD_3OD): δ 174.6, 172.5, 171.98, 171.88, 65.5, 64.7, 64.5, 50.4, 46.65, 46.54, 39.3, 38.5, 29.3, 29.0, 17.22, 17.12, 17.06, 16.2

MALDI: m/z calc: $[M+Na]^+$ = 15152.3 exp: : $[M+Na]^+$ = 15152.4

DBCO-G8-$(Acet)_{128}$

Acetonide protected bis-MPA[40] (570 mg, 3.27 mmol) and EDC·HCl (312 mg, 1.634 mg) were added to a 10 mL round bottom flask and dissolved in 1 mL of dichloromethane. This was left to stir for 1 hour to form the anhydride. Separately, DBCO-G7-OH (97 mg, 0.006

mmol) was dissolved in 1 mL of pyridine and was then added to the solution of anhydride in dichloromethane, along with 4-dimethylaminopyridine (50 mg, 0.408 mmol). The reaction mixture was stirred overnight, then quenched by the addition of 0.5 mL of water with stirring for 1 hour. The reaction mixture was then diluted with 30 mL of DCM and washed with 3 × 30 mL of 1 M H_3PO_4, 3 × 30 mL of 10% Na_2CO_3, 1 × 50 mL of brine, then dried with $MgSO_4$, filtered, and solvent was removed by rotary evaporation. The crude material was then purified using a column of Sephadex LH-20 in methanol and the high molecular weight fractions were combined. Solvent was removed by rotary evaporation and dried *in vacuo* overnight to give the product as a white foam. (192 mg, 85%)

^{1}H NMR (600 MHz; $CDCl_3$): δ 4.37-4.23 (m, 1H), 4.13 (d, J = 11.2, 1H), 3.62 (d, J = 11.1, 1H), 1.40 (s, 1H), 1.34 (s, 1H), 1.29 (s, 1H), 1.16 (d, J = 16.3, 1H)

^{13}C NMR (176 MHz; $CDCl_3$): δ 173.5, 172.0, 171.7, 171.5, 98.1, 66.00, 65.95, 65.1, 64.7, 46.86, 46.70, 42.1, 25.2, 22.4, 17.92, 17.74, 17.4

MALDI: m/z calc: $[M+Na]^+$ = 35136 exp: : $[M+Na]^+$ = 33281

DBCO-G8-$(OH)_{256}$

DBCO-G8-$(acet)_{128}$ (50 mg, 1.4 μmol) was dissolved in 20 mL of MeOH. To this, *p*-toluenesulfonic acid (3 mg, 1.6 μmol) was added, and this was stirred at room temperature for 3 hours. The reaction was quenched by the addition of Et_3N (6.5 uL, 4.9 μmol) and this was left to stir for 20 minutes. Solvent was then removed by rotary evaporation, and the reaction mixture was then purified using Sephadex LH-20 in methanol. The high molecular

weight fractions were pooled and solvent was removed, and then this was re-dissolved in deionized water and lyophilized overnight to give a fluffy white powder (41 mg, 95%)

^{1}H NMR (700 MHz; CD_3OD): δ 7.70-7.32 (m, 8H), 4.36-4.27 (m, 510H), 3.69 (dd, J = 10.6, 4.1, 256H), 3.63 (d, J = 10.9, 256H), 1.36-1.34 (m, 381H), 1.17 (s, 384H)

^{13}C NMR (151 MHz; CD_3OD): δ 176.3, 176.0, 174.9, 173.9, 173.53, 173.34, 71.6, 66.78, 66.62, 66.14, 65.94, 65.6, 51.8, 49.9, 48.02, 47.92, 18.68, 18.61, 18.2, 17.69, 17.62

MALDI: m/z calc: $[M+Na]^+$ = 30008 exp: : $[M+Na]^+$ = 29709

DBCO-G3-(mPEG$_{15}$)$_8$

Prepared according to literature procedures.[48] (41 mg, 82%)

^{1}H NMR (600 MHz; $CDCl_3$): δ 7.64 (d, J = 7.7, 1H), 7.51 (d, J = 7.5, 1H), 7.39-7.35 (m, 3H), 7.32 (t, J = 7.4, 1H), 7.28 (t, J = 7.6, 1H), 7.23 (d, J = 7.2, 1H), 7.01-6.92 (m, 1H), 6.45-5.44 (m, 8H), 5.12 (d, J = 14.0, 1H), 4.25-4.08 (m, 28H), 3.63-3.59 (m, 1H), 3.53 (t, J = 4.7, 16H), 3.50 (s, 16H), 3.35 (s, 23H), 3.29 (d, J = 4.9, 15H), 3.17 (q, J = 5.7, 2H), 3.06 (dt, J = 13.9, 7.1, 2H), 2.75 (dt, J = 16.4, 8.0, 1H), 2.38 (dt, J = 15.7, 7.6, 1H), 2.15 (dt, J = 14.5, 6.9, 1H), 1.91 (dt, J = 16.4, 6.3, 1H), 1.43 (t, J = 6.6, 2H), 1.38-1.35 (m, 2H), 1.21 (t, J = 27.0, 22H)

DBCO-mPEG$_{5500}$

mPEG$_{5500}$-NH_2 (0.150 g, 0.027 mmol) was dissolved in 0.5 mL of dichloromethane. To this, DBCO-NHS (0.022 g, 0.054 mmol) and Et_3N (11 μL, 0.082 mmol) were added and the reaction mixture was stirred for 3 hours at room temperature. After 3 hours, the reaction

mixture was precipitated into 50 mL of 1:1 ether:hexanes and collected on a Hirsch funnel. The filter cake was then washed with 3 aliquots of ether, then 3 aliquots of ice-cold ethanol, then with 1 final aliquot of ether. This was then dried *in vacuo* overnight to give the product as a white powder. (118 mg, 74%)

^{1}H NMR (600 MHz; $CDCl_3$): δ 7.67 (d, J = 7.4, 1H), 7.52-7.51 (m, 1H), 7.40-7.33 (m, 3H), 7.29 (t, J = 7.7, 1H), 7.24 (d, J = 7.5, 2H), 6.18 (t, J = 4.4, 1H), 5.14 (d, J = 13.9, 1H), 3.63 (d, J = 26.6, 1H), 3.48-3.41 (m, 2H), 3.33 (q, J = 5.2, 2H), 2.81 (dt, J = 16.5, 8.0, 1H), 2.46 (dt, J = 15.4, 7.6, 1H), 2.16 (dt, J = 15.2, 6.2, 1H)

4.6 MALDI-TOF Spectra

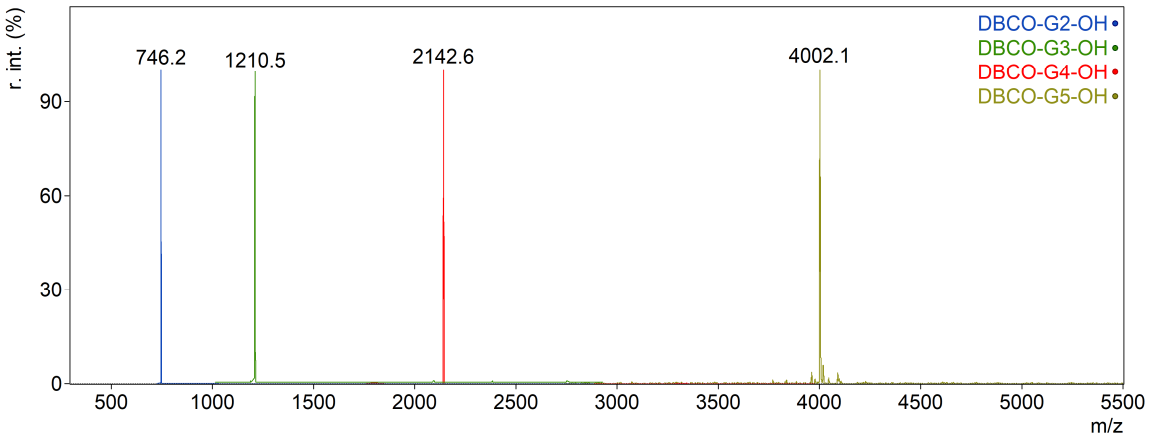

Figure 4.7. MALDI-TOF Spectra of DBCO core dendrons from G2-G5

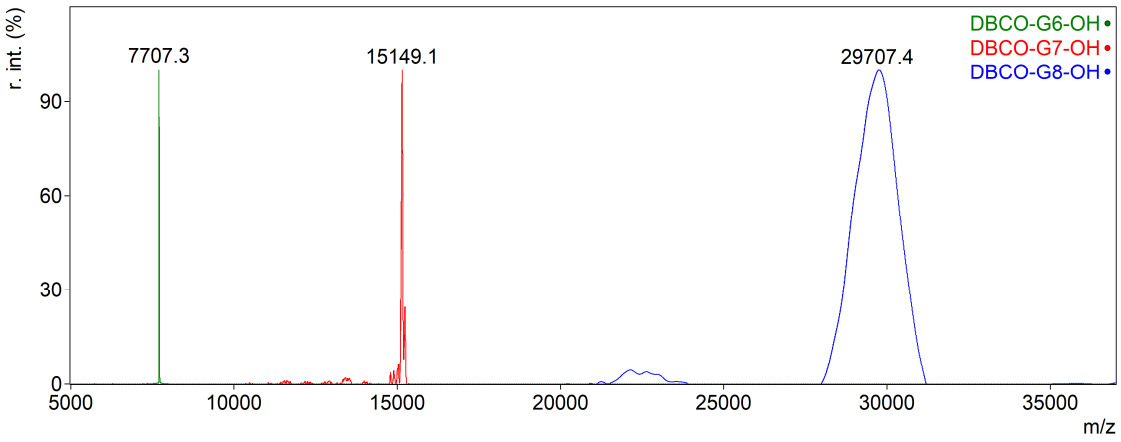

Figure 4.8. MALDI-TOF Spectra of DBCO core dendrons from G6-G8

4.7 Preparation of α-Chymotrypsin Conjugates

4.7.1 Preparation of α-Chymotrypsin azide (α-CT-N_3)

2-Azidoacetic acid (51 mg, 0.5 mmol) was dissolved in 150 µL of 0.1 M phosphate buffer (pH 8), along with *N*-hydroxysuccinimide (116 mg, 1.01 mmol). To this, *N*-(3-dimethylaminopropyl)-*N'*-ethylcarbodiimide hydrochloride (290 mg, 1.51 mmol) was added in a solution of 100 µL of additional buffer. This was stirred at room temperature for one hour, at which point it was directly added to a solution of α-chymotrypsin (90 mg) dissolved in 2.5 mL of 0.1 M phosphate buffer (pH 8). The reaction mixture was then stirred at 4 °C in a fridge for 2 hours, at which point the pH was adjusted back to ~ 8 via dropwise addition of 2 M KOH, then left to stir for an additional hour at 4 °C. At this point the reaction mixture was loaded onto a column of 3 × 5 mL GE HiTrap desalting columns in series and eluted with phosphate buffer. The high molecular weight fractions were pooled and dialyzed against deionized water for 24 hours then lyophilized, giving α-CT-N_3 as a fluffy white powder. (60 mg, 65%)

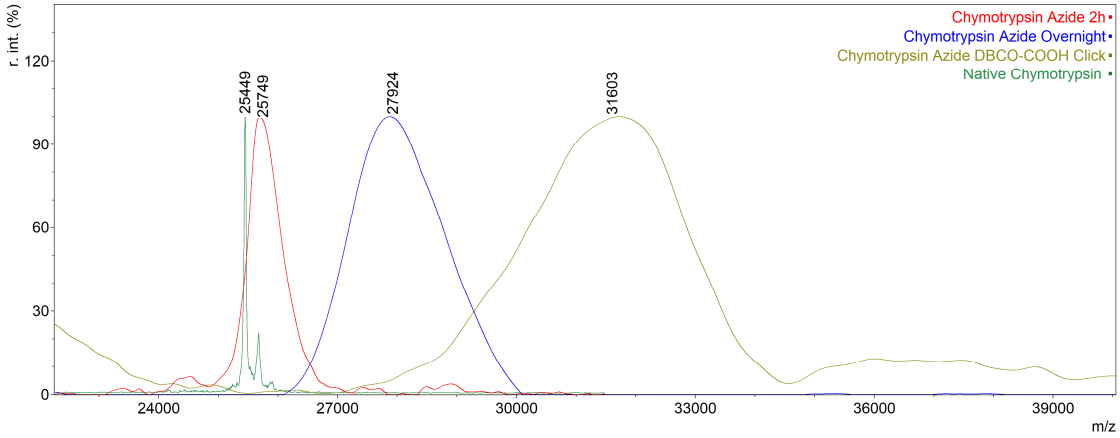

Figure 4.9. MALDI mass spectra of the functionalization of α-CT with azidoacetic acid. Upon conversion of any of the lysine residues to amides, the MALDI peak broadens substantially. To confirm the number of reactive azide groups on α-CT, DBCO-COOH was clicked on and the corresponding mass change is in line with that expected for 14 DBCO-COOH units being appended.

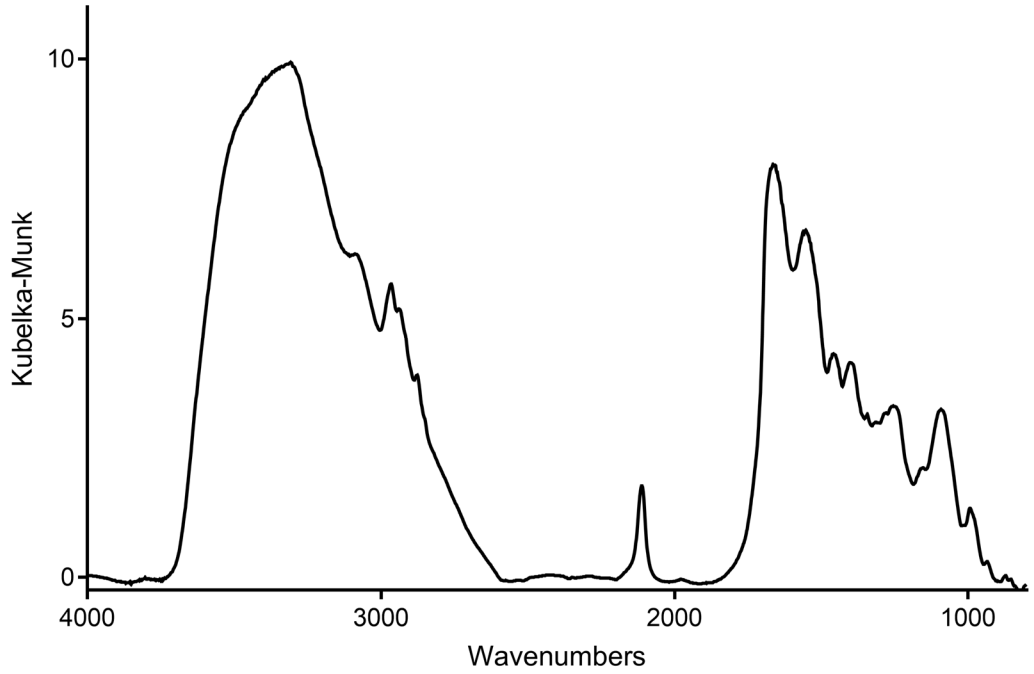

Figure 4.10. FTIR spectrum of α-CT-N_3 conjugate. A small azide absorbance is visible at ~2100 cm^{-1}.

4.7.2 Preparation of α-CT Dendrimer Conjugates

General Procedure

Approximately 2 to 5 mg of α-CT-N_3 was dissolved in 3 mL of 100 mM phosphate buffer (pH 8). To this, 3 equivalents per azide (42 eq total) of the DBCO core dendron were added, and this was stirred overnight at 4 °C. The solution was then purified by aqueous FPLC using a Superdex S200 column, with collection by UV at 230 nm. The fractions containing the conjugate were pooled and dialyzed against deionized water, then lyophilized to give the conjugates as white powders. The reactions were confirmed to be complete in this time frame by monitoring the UV absorbance at 340 nm over time. As a model reaction, the α-CT-G3 conjugate was prepared in a quartz cuvette held at 4 °C. Absorbance at 340 nm was monitored until it remained steady for 10 minutes, at which point the experiment was ended. The results are shown in Figure 4.11

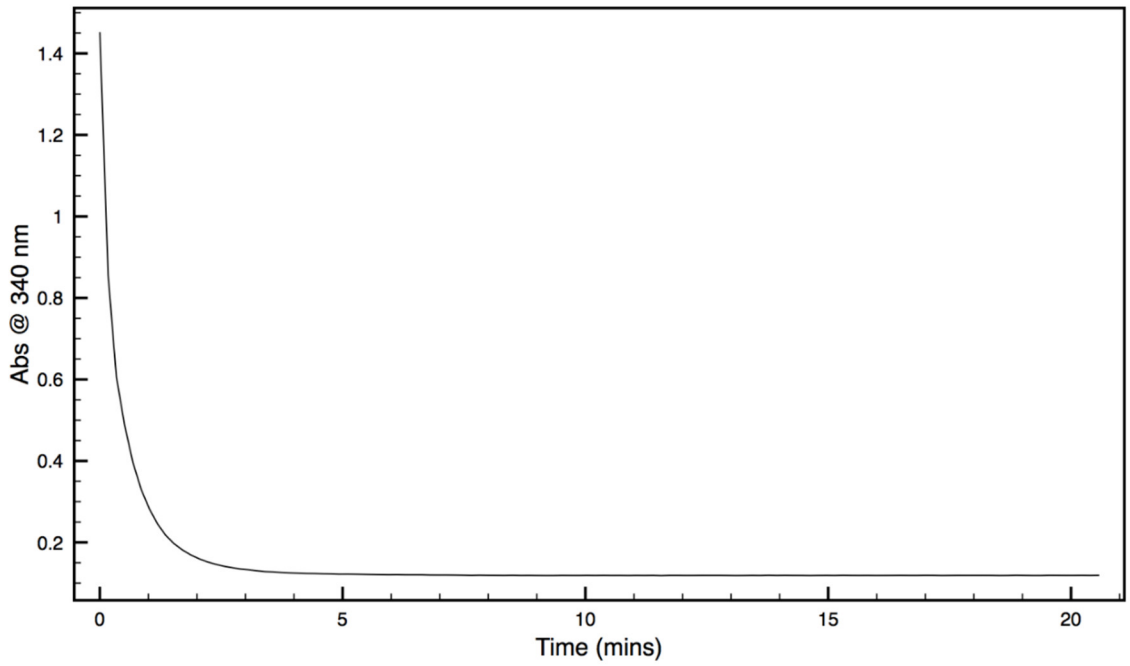

Figure 4.11. UV trace of α-CT-G3 synthesis over time, monitored at 340 nm. Reaction is completed within 10 minutes.

Since α-CT is a protease, we also performed a control experiment in which native chymotrypsin was reacted with the DBCO-core dendrons, as cleavage of this amide would result in decomposition of the DBCO moiety.[54] Figure 4.12 demonstrates that the enzyme does not cleave the DBCO from the dendron, and absorbance at 310 nm is only reduced by reaction with the α-CT-N_3.

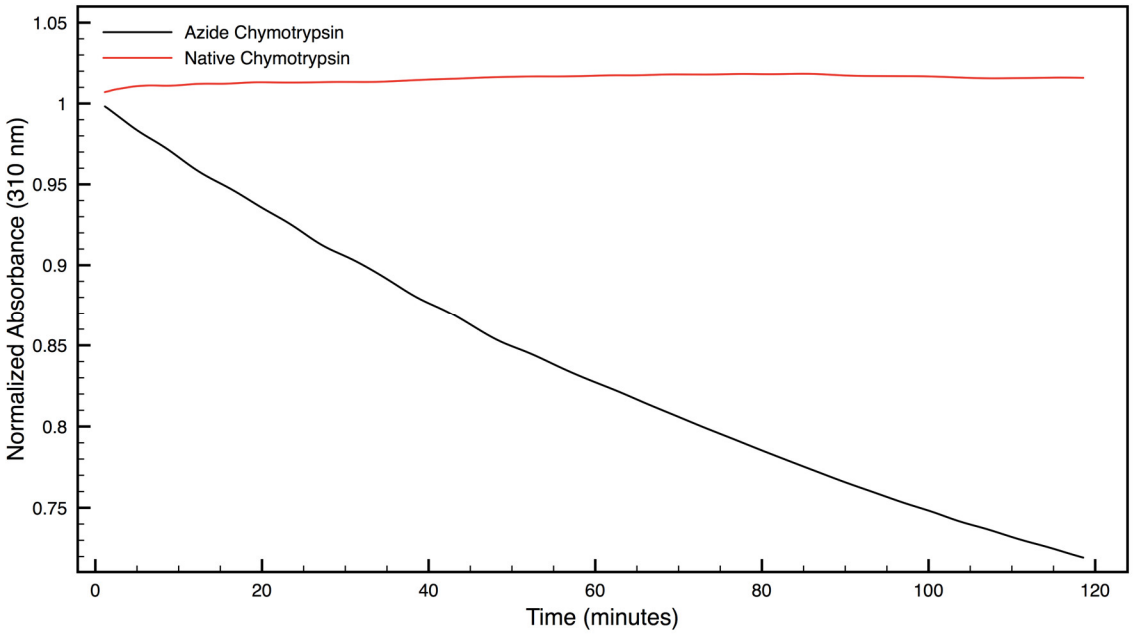

Figure 4.12. Absorbance of α-CT-N_3 vs. native chymotrypsin upon addition of DBCO-G3-$(OH)_8$ dendron. There is no reaction of native chymotrypsin with the dendron.

α-CT-G2-OH

α-CT-N_3 (5.0 mg, 0.19 μmol) was dissolved in 3 mL of 0.1 M phosphate buffer (pH 8). To this, DBCO-G2-$(OH)_4$ (6.0 mg, 8.23 μmol) was added and this was left to react overnight at 4 °C. The solution was then purified by aqueous FPLC using a Superdex S200 column, with collection by UV at 230 nm. The fractions containing the conjugate were pooled and dialyzed against deionized water, then lyophilized to give the conjugate as a white powder.

α-CT-G3-OH

α-CT-N_3 (5.0 mg, 0.19 μmol) was dissolved in 3 mL of 0.1 M phosphate buffer (pH 8). To this, DBCO-G3-$(OH)_8$ (9.8 mg, 8.23 μmol) was added and this was left to react overnight at 4 °C. The solution was then purified by aqueous FPLC using a Superdex S200 column, with collection by UV at 230 nm. The fractions containing the conjugate were pooled and dialyzed against deionized water, then lyophilized to give the conjugate as a white powder.

α-CT-G4-OH

α-CT-N_3 (5.0 mg, 0.19 μmol) was dissolved in 3 mL of 0.1 M phosphate buffer (pH 8). To this, DBCO-G4-$(OH)_{16}$ (17.4 mg, 8.23 μmol) was added and this was left to react overnight at 4 °C. The solution was then purified by aqueous FPLC using a Superdex S200 column, with collection by UV at 230 nm. The fractions containing the conjugate were pooled and dialyzed against deionized water, then lyophilized to give the conjugate as a white powder.

α-CT-G5-OH

α-CT-N_3 (5.0 mg, 0.19 μmol) was dissolved in 3 mL of 0.1 M phosphate buffer (pH 8). To this, DBCO-G5-$(OH)_{32}$ (32 mg, 8.23 μmol) was added and this was left to react overnight at 4 °C. The solution was then purified by aqueous FPLC using a Superdex S200 column, with collection by UV at 230 nm. The fractions containing the conjugate were pooled and dialyzed against deionized water, then lyophilized to give the conjugate as a white powder.

α-CT-G6-OH

α-CT-N_3 (2.0 mg, 0.075 μmol) was dissolved in 3 mL of 0.1 M phosphate buffer (pH 8). To this, DBCO-G6-$(OH)_{64}$ (24 mg, 3.29 μmol) was added and this was left to react overnight at 4 °C. The solution was then purified by aqueous FPLC using a Superdex S200

column, with collection by UV at 230 nm. The fractions containing the conjugate were pooled and dialyzed against deionized water, then lyophilized to give the conjugate as a white powder.

α-CT-G7-OH

α-CT-N_3 (2.0 mg, 0.07 μmol) was dissolved in 3 mL of 0.1 M phosphate buffer (pH 8). To this, DBCO-G7-$(OH)_{128}$ (49.8 mg, 3.29 μmol) was added and this was left to react overnight at 4 °C. The solution was then purified by aqueous FPLC using a Superdex S200 column, with collection by UV at 230 nm. The fractions containing the conjugate were pooled and dialyzed against deionized water, then lyophilized to give the conjugate as a white powder.

α-CT-G8-OH

α-CT-N_3 (1.0 mg, 0.038 μmol) was dissolved in 3 mL of 0.1 M phosphate buffer (pH 8). To this, DBCO-G8-$(OH)_{256}$ (47.4 mg, 3.29 μmol) was added and this was left to react overnight at 4 °C. The solution was then purified by aqueous FPLC using a Superdex S200 column, with collection by UV at 230 nm. The fractions containing the conjugate were pooled and dialyzed against deionized water, then lyophilized to give the conjugate as a white powder.

α-CT-G3-$(dPEG_{15})_8$

α-CT-N_3 (1.5 mg, 0.056 μmol) was dissolved in 200 uL of 0.1 M phosphate buffer (pH 8). To this, DBCO-G3-$(PEG_{15})_8$ (17.1 mg, 2.47 μmol) dissolved in 300 uL of 0.1 M phosphate buffer was added and this was left to react overnight at 4 °C. The solution was then purified by aqueous FPLC using a Superdex S200 column, with collection by UV at 230 nm. The

fractions containing the conjugate were pooled and dialyzed against deionized water, then lyophilized to give the conjugate as a white powder.

α-CT-mPEG$_{5500}$

α-CT-N_3 (5.0 mg, 0.19 μmol) was dissolved in 200 uL of 0.1 M phosphate buffer (pH 8). To this, DBCO-mPEG$_{5500}$ (42 mg, 7.92 μmol) dissolved in 300 uL of 0.1 M phosphate buffer was added and this was left to react overnight at 4 °C. The solution was then purified by dialysis using 14 kDa MWCO dialysis tubing, changing the dialysate 5 total times over 2 days. After dialysis, the absorbance at 309 nm of the solution was measured to assess the amount of residual DBCO, and none was detected. This was then lyophilized overnight to give the conjugate as a fluffy white powder.

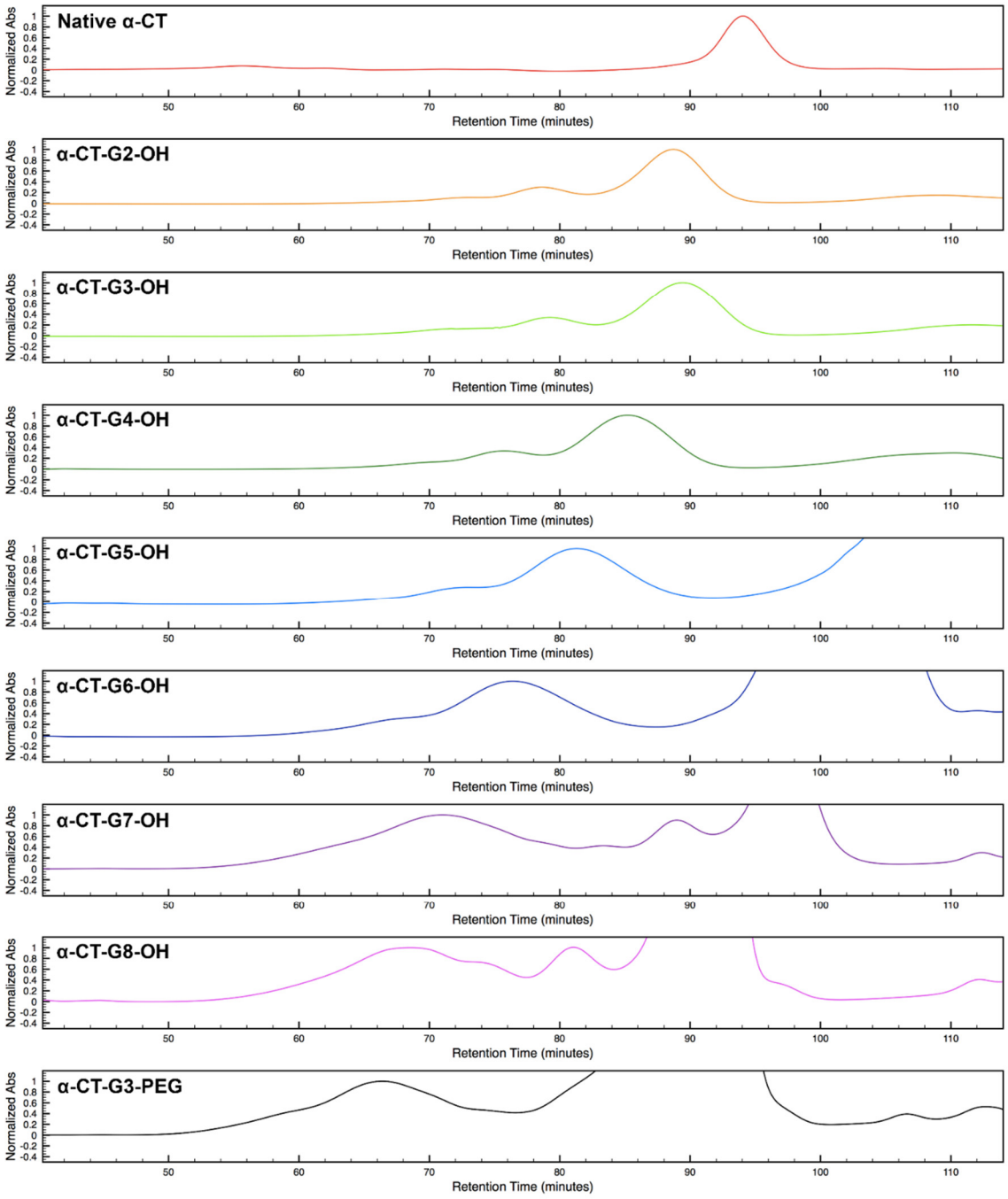

Figure 4.13. Aqueous size exclusion chromatograms of native chymotrypsin as well as the G2-G8 dendrimer-chymotrypsin conjugates and G3-PEG dendrimer conjugate. Cut off signal is due to the excess DBCO-Gx-(OH) dendron which is not collected as part of the purification.

The SEC chromatograms in Figure 4.13 are of the crude conjugation reaction mixture purification from the FPLC. We found that the conjugates generally had high non-specific binding to a range of different SEC media (Agilent Zorbax SEC columns, Agilent Aquagel-OH columns, GE Superose columns, as well as to a substantial degree the Superdex-S200 media used to purify the conjugates). Subsequent re-injection of analytical quantities of the conjugates did not elute any significant material, and as a result only the crude chromatograms are presented.

4.7.3 Sample Calculation for Degree of Functionalization via UV-Vis (α-CT-G6-OH)

The initial α-CT-N_3 concentration was determined from the literature extinction coefficient of α-CT,[55] $\varepsilon_{1\%}$ = 20.4. A stock solution of α-CT-N_3 was prepared in 500 μL of 0.1 M phosphate buffer (pH 8). A 30 μL aliquot was taken and diluted in 3 mL of buffer to give an A_{280} = 0.065251 and a concentration of 0.0306 mg/mL. Therefore, the total mass of protein present in the stock solution is 1.53 mg.

Separately, a stock solution of DBCO-G6-OH was prepared in 1 mL of 0.1 M phosphate buffer (pH 8). The concentration of this stock was determined using the literature extinction coefficient[56] ε = 12000 $M^{-1}cm^{-1}$ A 10 μL aliquot was taken and diluted in 3 mL of buffer to give an A_{309} = 0.12242 and a concentration of 1.02 x 10^{-5} M. Therefore, the total mass of dendron was 22.6 mg.

The two solutions were combined and stirred at 4°C. After 10 minutes, a 15 μL aliquot was taken from the reaction mixture and diluted in 3 mL of buffer. The absorbance was

measured to be A_{309} = 0.08485. Therefore, the total mass of unclicked DBCO-dendron is 15.68 mg.

There was a measured decrease of 6.9 mg of dendron from the reaction mixture. For full functionalization with 14 dendrons, it is expected that there would be a decrease of 6.2 mg. Therefore, it can be concluded that the resultant conjugate was fully functionalized.

Calculation for degree of functionalization via ^{1}H NMR Spectroscopy

To further confirm the degree of functionalization for the high generation dendrimer-enzyme conjugates (G6-G8), the weight fraction of dendrimer conjugated to α-CT was assessed by quantitative ^{1}H NMR spectroscopy against an internal standard, using a literature procedure. [50] In brief, a known mass of the conjugate (~ 10 mg) was weighed out into a 20 mL scintillation vial, and this was dissolved in 700 uL of D_2O. To this, precisely 10.0 μL of DMSO was added and mixed thoroughly into the solution. The ^{1}H NMR spectroscopy experiment was run with a relaxation delay of 30 s to ensure full relaxation of all the ^{1}H signals from the conjugate. The resulting dendrimer signals were integrated with the assumption of 1 molar equivalent of dendron, which allowed for the determination of the molar ratio of DMSO to dendron. Since the number of moles of dendron can now be determined, this allows for the calculation of the mass of dendron, and this can be compared to the initial mass of dendron added to the vial to determine the mass fraction.

As an example, the mass fraction of dendron in the α-CT-G6-OH conjugate was determined as follows:

Volume of DMSO = 0.010 mL
Density of DMSO = 1.10 g/mL
Mass of DMSO = 0.011 g
Molecular weight of DMSO = 78.13 g/mol
Moles of DMSO = $1.408 * 10^{-4}$ mol

Molar ratio of DMSO to dendron = $\frac{\text{DMSO Integration}}{6}$, since DMSO has 6 equivalent H's.

$= \frac{1160}{6} = 193.33$ molar equivalents of DMSO per dendron

Since the # of moles of DMSO is known, the # of moles of dendron can be calculated by dividing the moles of DMSO by the molar equivalents of DMSO per dendron

Moles of dendron = $\frac{1.408*10^{-4}\ mol}{193.33} = 7.28 * 10^{-7}$ mol of dendron

Multiplying this by the molar mass of the DBCO-G6-OH (7690 g/mol) results in the total mass of added dendron

Mass of dendron = $7.28 * 10^{-7} mol * 7690 \frac{g}{mol} = 0.0056\ g$

Since the mass of conjugate added initially is known (0.0071g),

Experimental mass fraction of dendron = $\frac{0.0056g}{0.0071g} * 100\% = 78.9\%$

The expected mass of dendron in the conjugate (assuming full 14/14 conjugations) would be the mass of 14 dendrons divided by the total conjugate mass

Conjugate molecular weight = 134314 g/mol

Dendron Molecular weight (x14) = 107660 g/mol

Nominal mass fraction of dendron = $\frac{107660 \frac{g}{mol}}{134314 \frac{g}{mol}} = 80.2\%$

Table 4.3. Theoretical vs. experimental dendron mass fractions in high-generation conjugates, as determined by quantitative ^{1}H NMR spectroscopy.

Dendrimer-Enzyme Conjugate	Mass of Conjugate Added	Theoretical Mass Fraction of Dendrimer	^{1}H NMR Experimental Dendrimer Mass Fraction
α-CT-G6-OH	7.1 mg	80.2%	78.9%
α-CT-G7-OH	9.8 mg	88.8%	89.8%
α-CT-G8-OH	8.7 mg	94.0%	90.4%

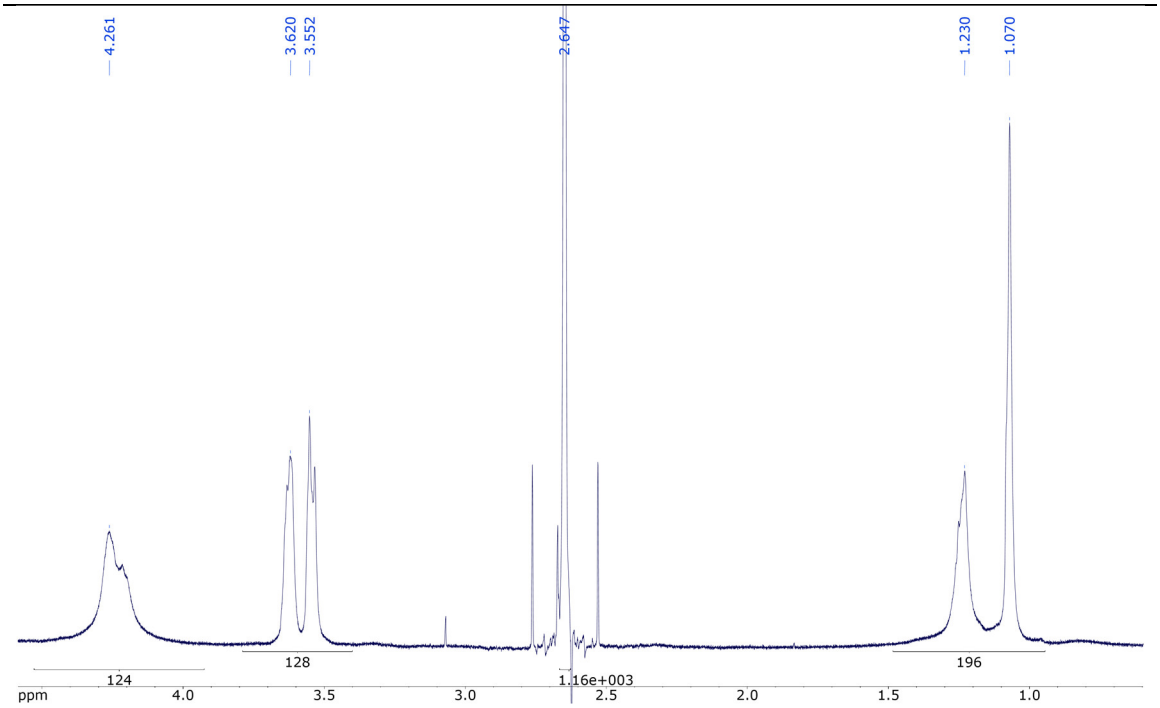

Figure 4.14. ^{1}H NMR spectrum for quantitation of dendron mass fraction of α-CT-G6-OH.

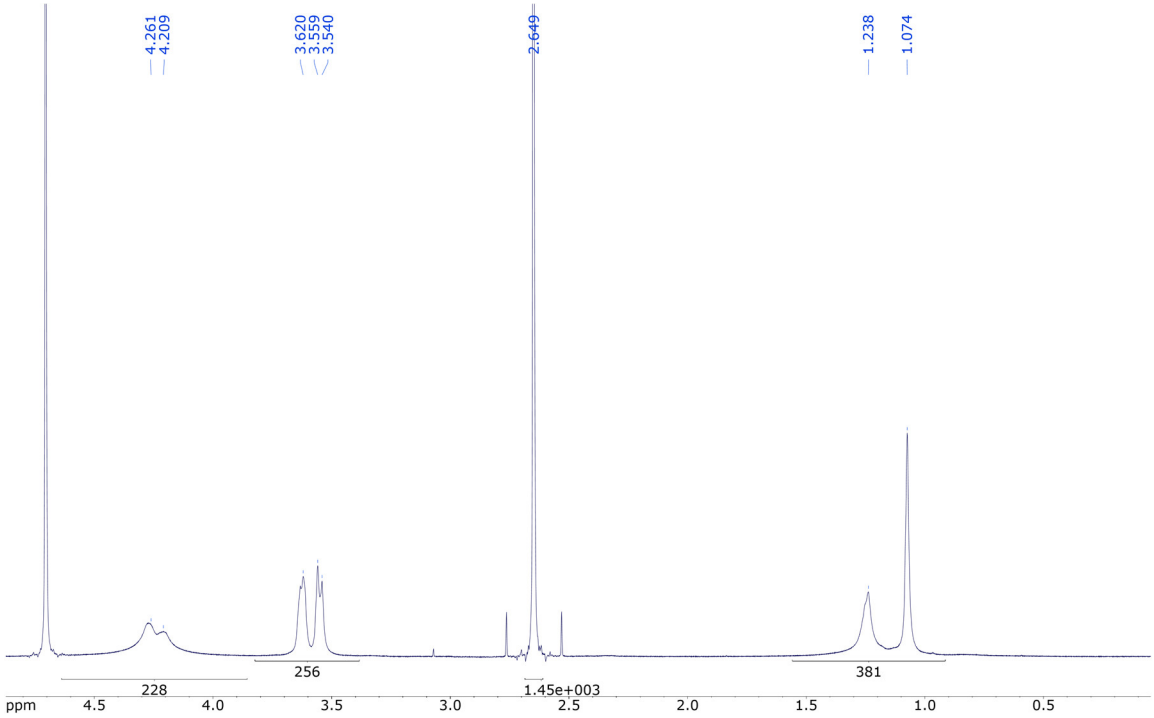

Figure 4.15. ^{1}H NMR spectrum for quantitation of dendron mass fraction of α-CT-G7-OH.

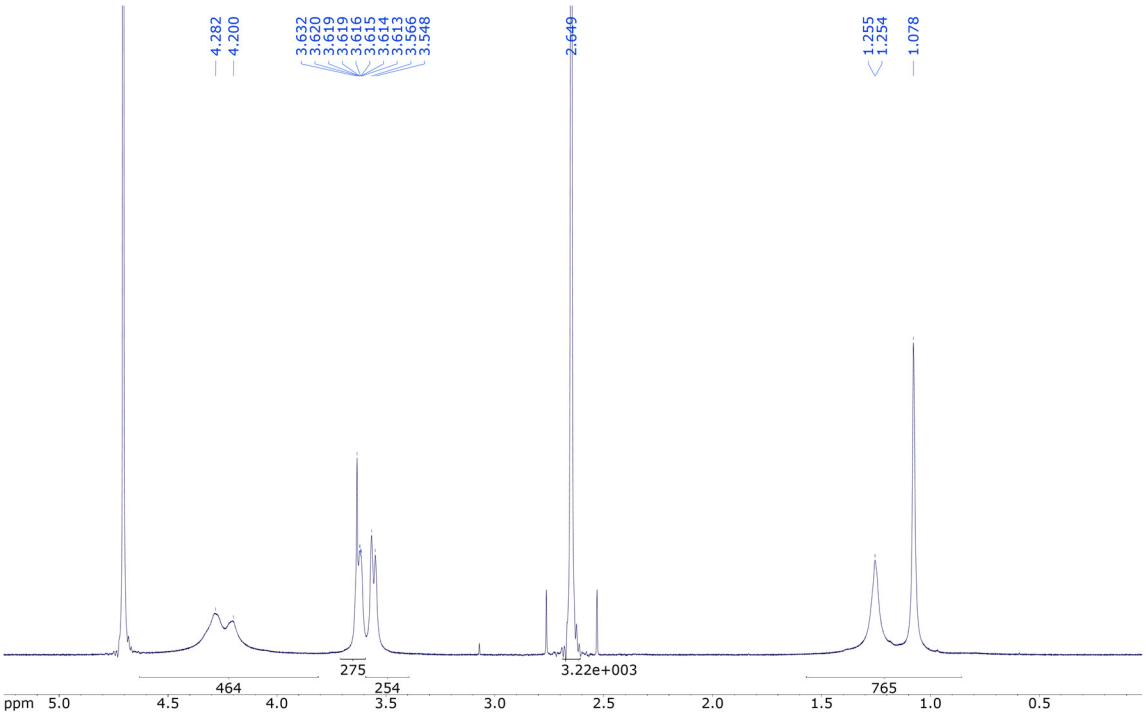

Figure 4.16.^{1}H NMR spectrum for quantitation of dendron mass fraction of α-CT-G8-OH.

Determination of Conjugate functionalization by FTIR

Since the starting α-CT-N_3 has an intensely absorbing IR band at ~2100 cm^{-1} due to the azide group, FTIR was used as an additional method for determining that complete conjugation had occurred. In each of the conjugates from G2-G8, no azide peak was observed by FTIR as seen in Figure 4.17 through Figure 4.23. To confirm that this was indicative of complete consumption of the azide, a sample of α-CT-G8-OH was spiked with 7 wt% α-CT-N_3 (based on mass of enzyme, not total mass of conjugate). This sample was dissolved in water and lyophilized to ensure full homogeneity, and then measured by DRIFTS FTIR (Figure 4.24). 7 wt% was chosen, as this corresponds to the amount of residual azide left if an average of 13/14 total azide groups were conjugated. Since the 7 wt% can be seen in the mixture of even the largest dendron, it is reasonable to conclude that all the conjugates must be fully converted, since no azide signal is observed for any of the conjugates.

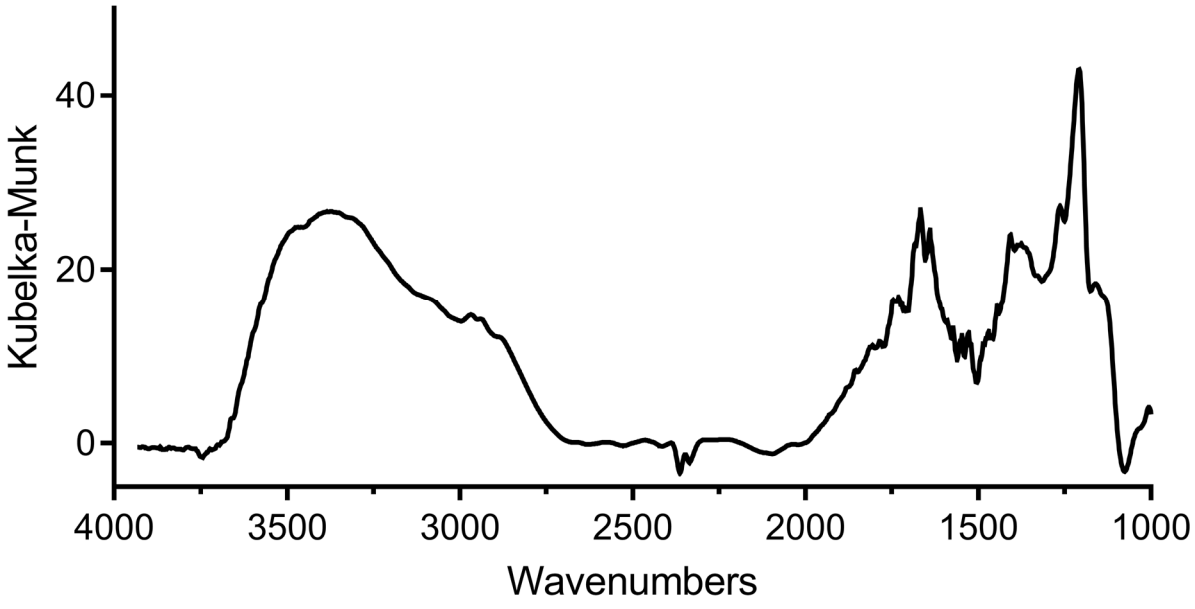

Figure 4.17. DRIFTS FTIR Spectrum of α-CT-G2-OH.

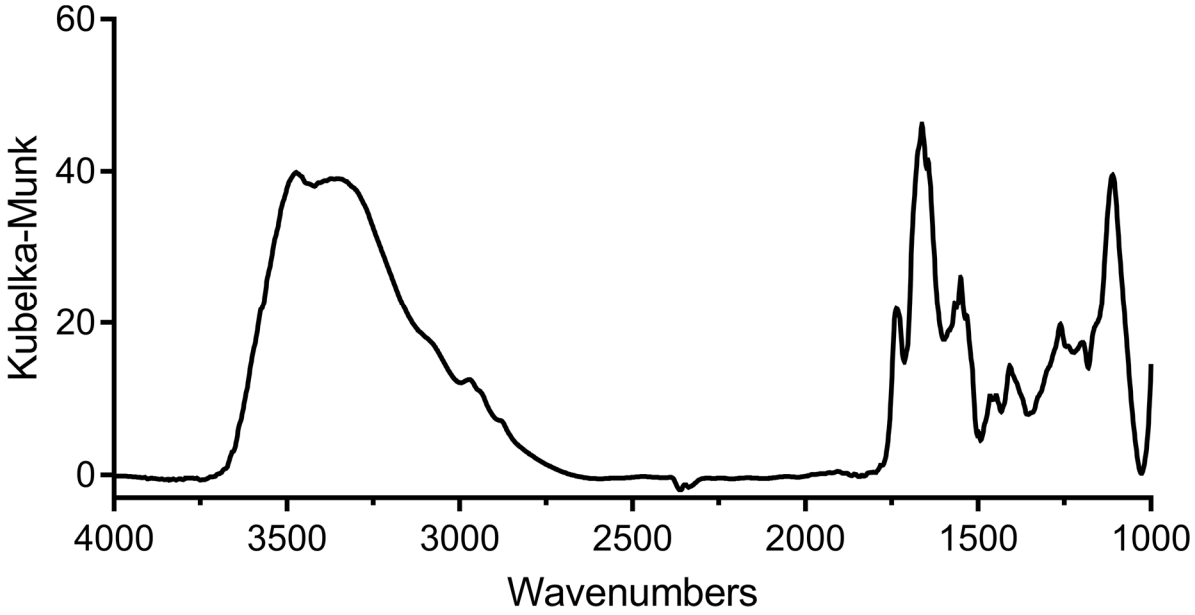

Figure 4.18. DRIFTS FTIR Spectrum of α-CT-G3-OH.

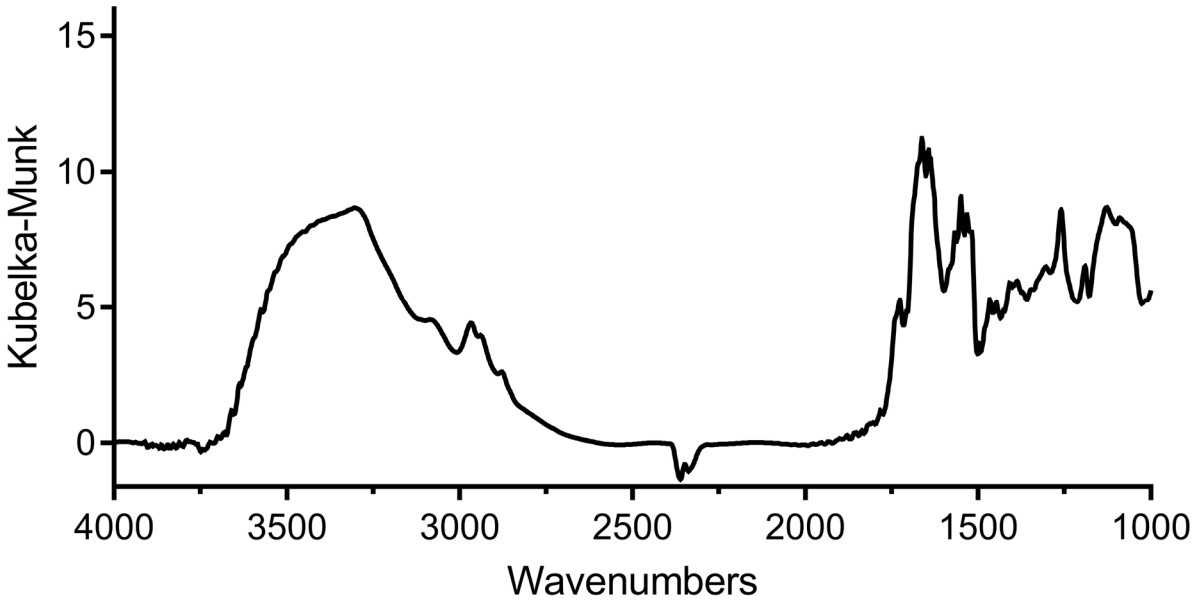

Figure 4.19. DRIFTS FTIR Spectrum of α-CT-G4-OH.

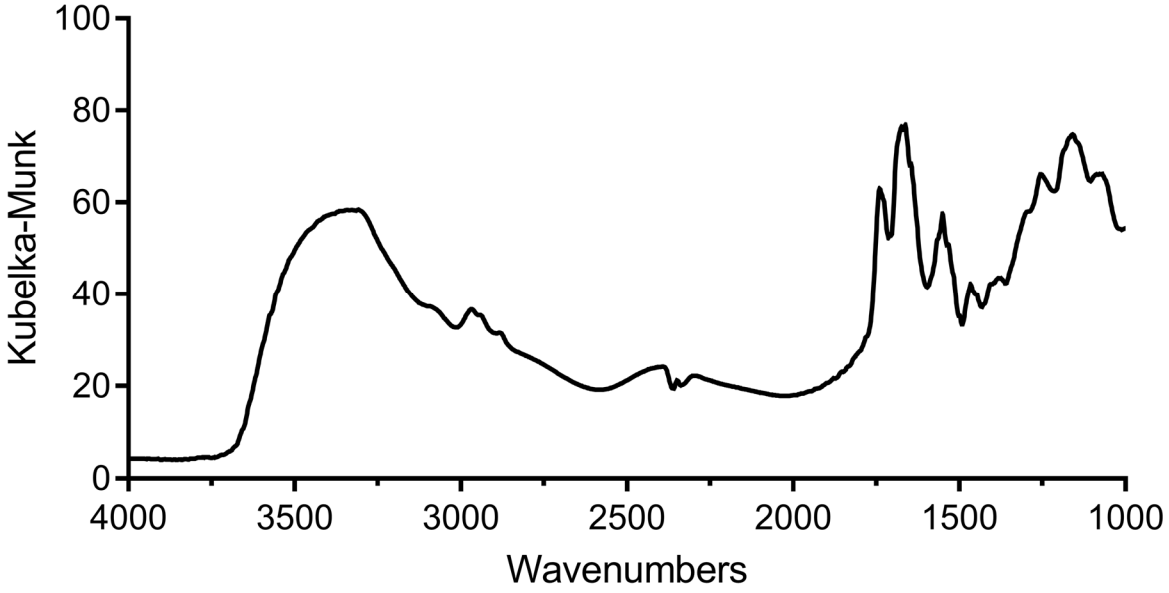

Figure 4.20. DRIFTS FTIR Spectrum of α-CT-G5-OH.

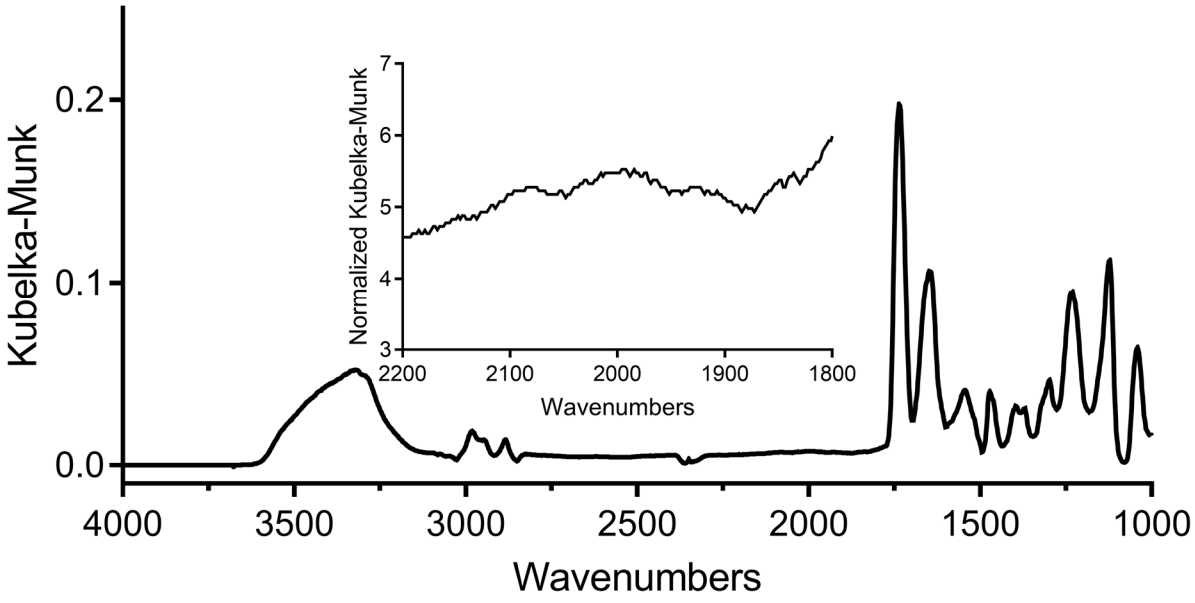

Figure 4.21. DRIFTS FTIR Spectrum of α-CT-G6-OH. Inset shows the region between 1800 and 2200 cm^{-1}, to magnify the region where any residual azide stretch would appear.

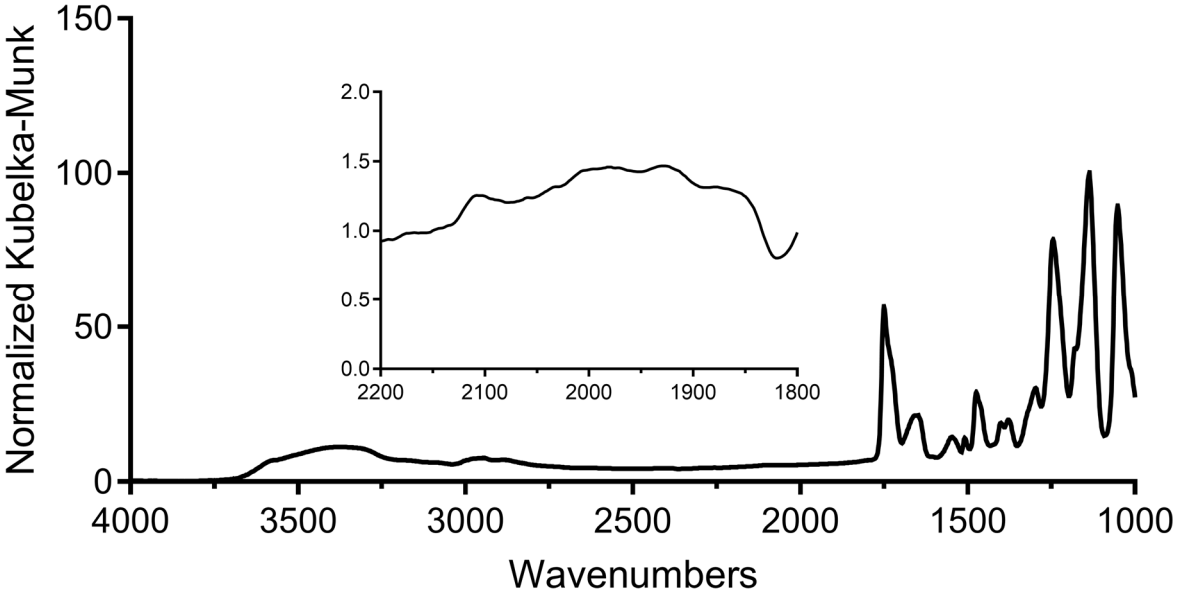

Figure 4.22. DRIFTS FTIR Spectrum of α-CT-G7-OH. Inset shows the region between 1800 and 2200 cm^{-1}, to magnify the region where any residual azide stretch would appear.

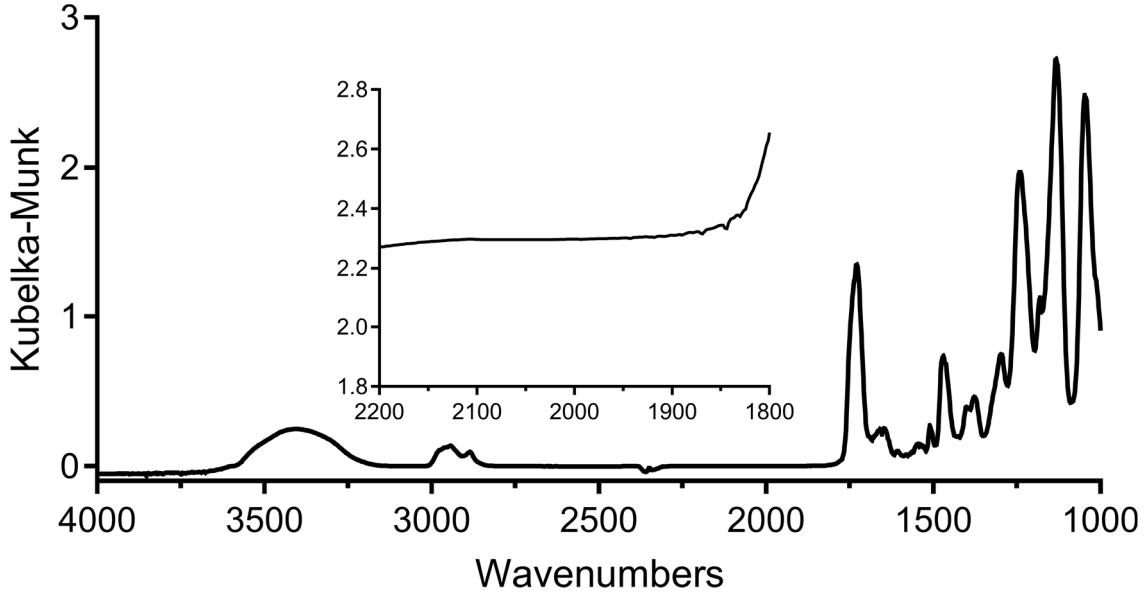

Figure 4.23. DRIFTS FTIR Spectrum of α-CT-G8-OH. Inset shows the region between 1800 and 2200 cm^{-1}, to magnify the region where any residual azide stretch would appear.

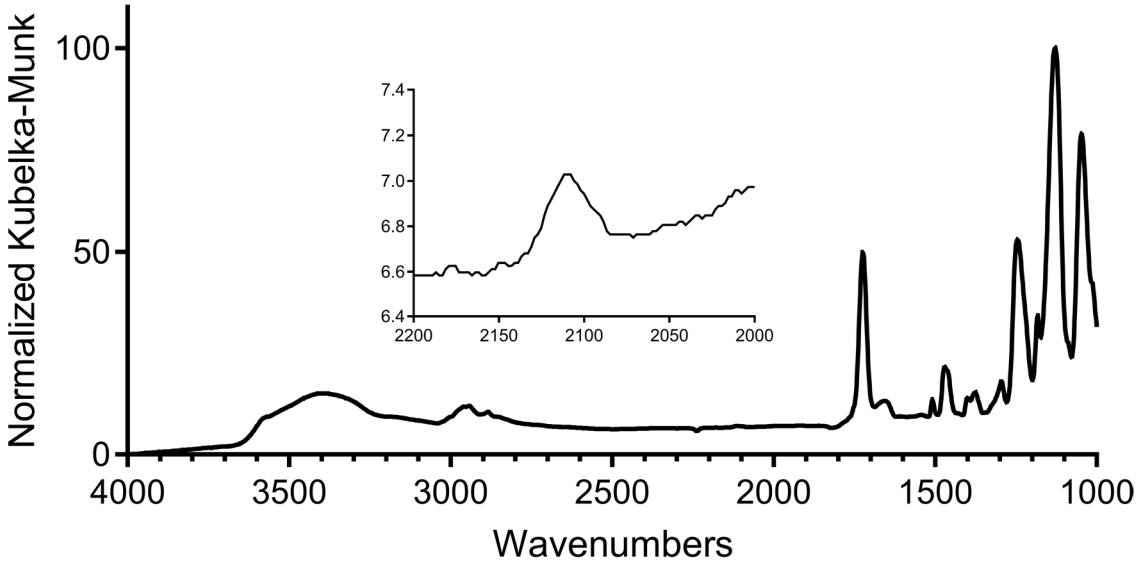

Figure 4.24. DRIFTS FTIR Spectrum of α-CT-G8-OH with 7 wt% (vs. enzyme mass) of α-CT-N_3 added, to mimic the possibility of 13 out of 14 sites being coupled on the enzyme. The azide peak can be seen in the inset at approximately 2100 cm^{-1}.

4.8 Chymotrypsin activity vs. BT*p*NA

Following the methods of Gauthier and coworkers,[35] the activity assays against BT*p*NA were performed as follows. First, a stock solution of native α-chymotrypsin or α-chymotrypsin-dendrimer conjugate was prepared in 0.1 M Tris buffer (pH 8) with an absorbance of approximately 0.2 AU, which allowed for the calculation of the precise concentration of enzyme in solution. 200 μL of this solution is added to 96 well plate, and this is incubated at 37 °C for 3 minutes. Separately, a stock solution of BT*p*NA was prepared at 1 mg/mL in DMF. 50 μL of this solution was then added to the well, and the absorbance at 412 nm was measured every 3 seconds for 3 minutes. The activity of the enzyme was taken from the initial slope of the absorbance line, which we chose as the first 30 seconds as this region had excellent linearity. Any absorbance at 412 nm measured at T = 0 was subtracted from the absorbance over time plots, so all plots have initially 0 absorbance at 412 nm.

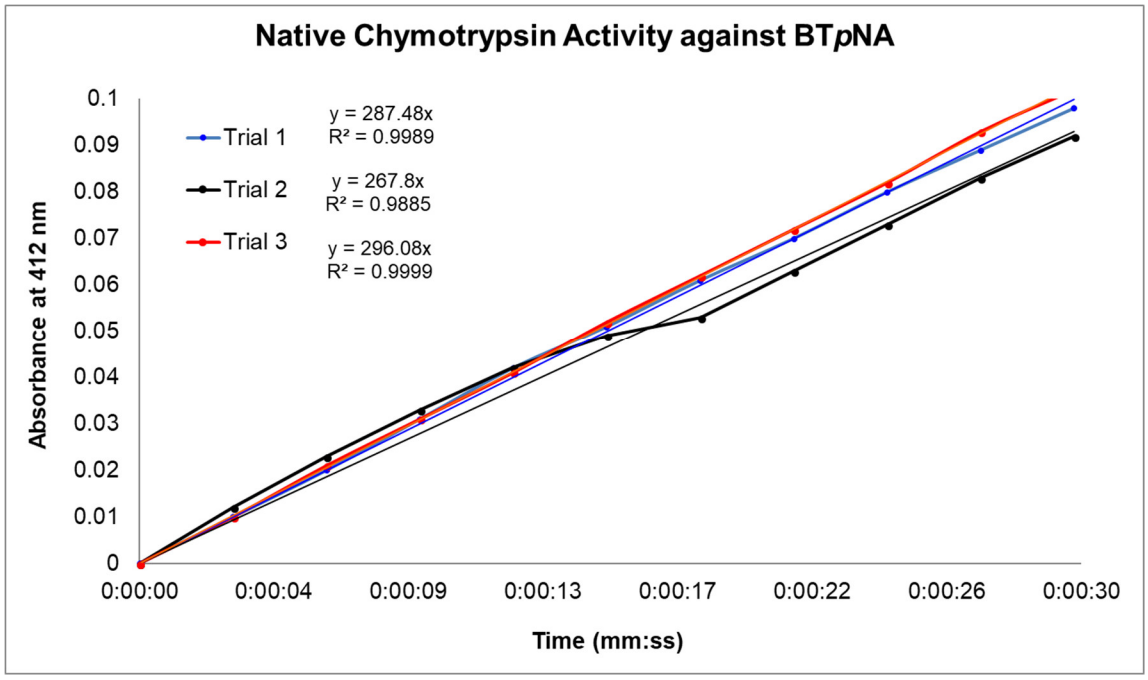

Figure 4.25. Absorbance over time of BT*p*NA cleavage by native chymotrypsin.

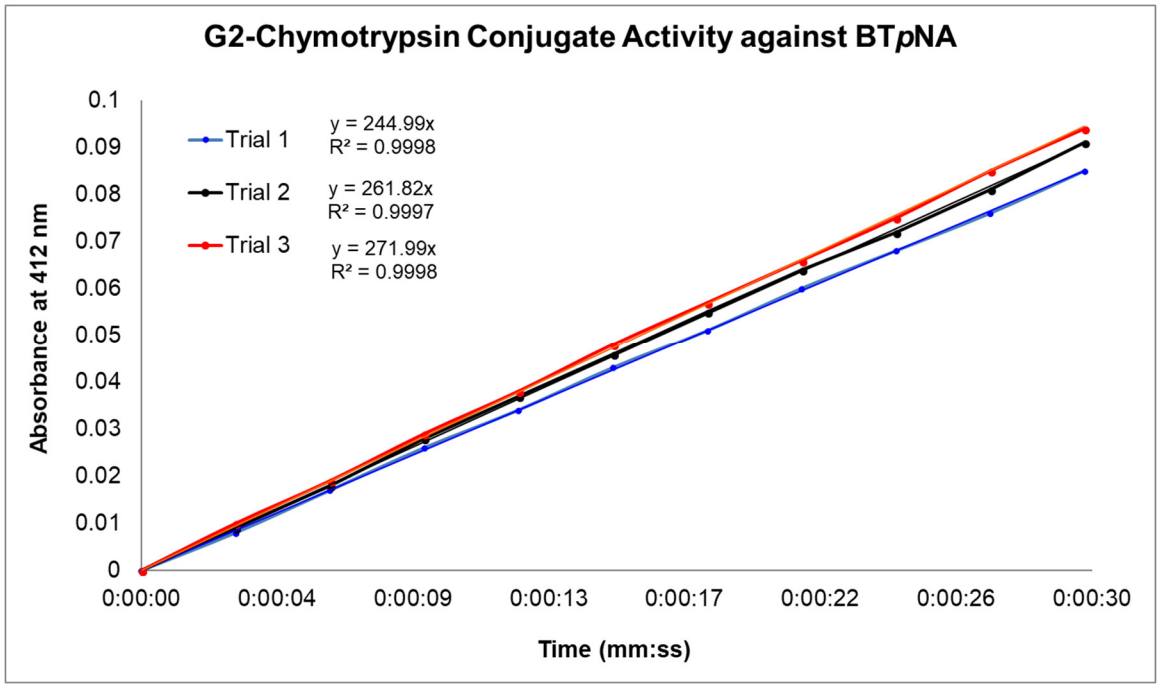

Figure 4.26. Absorbance over time of BT*p*NA cleavage by G2-CT conjugate.

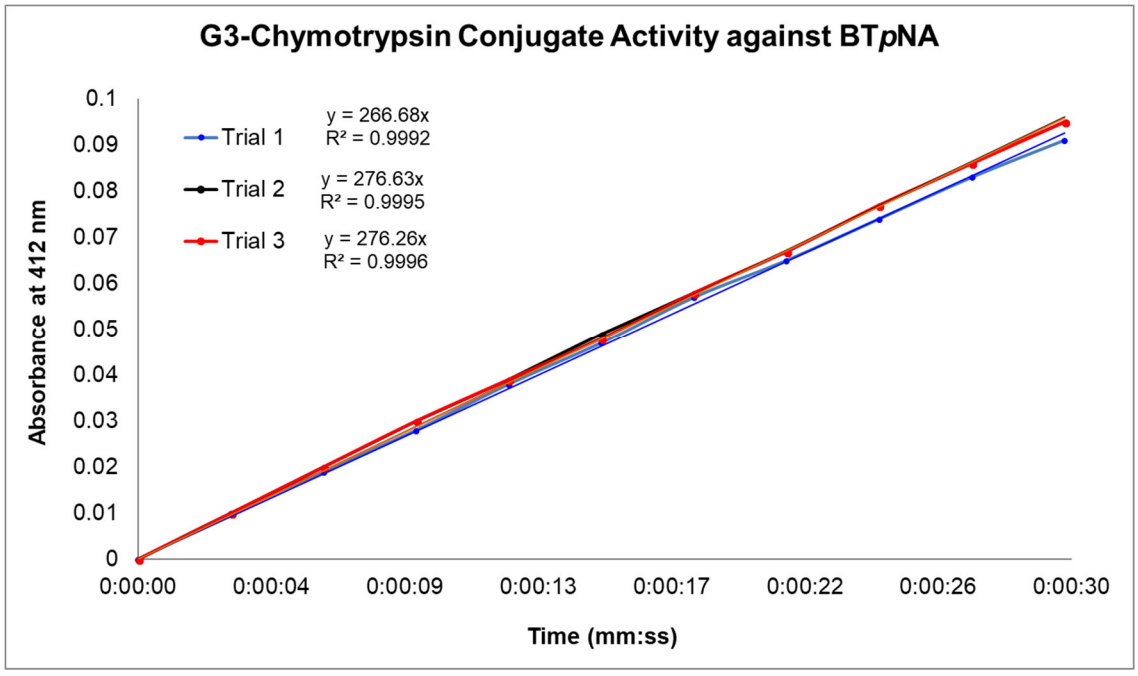

Figure 4.27. Absorbance over time of BT*p*NA cleavage by G3-CT conjugate.

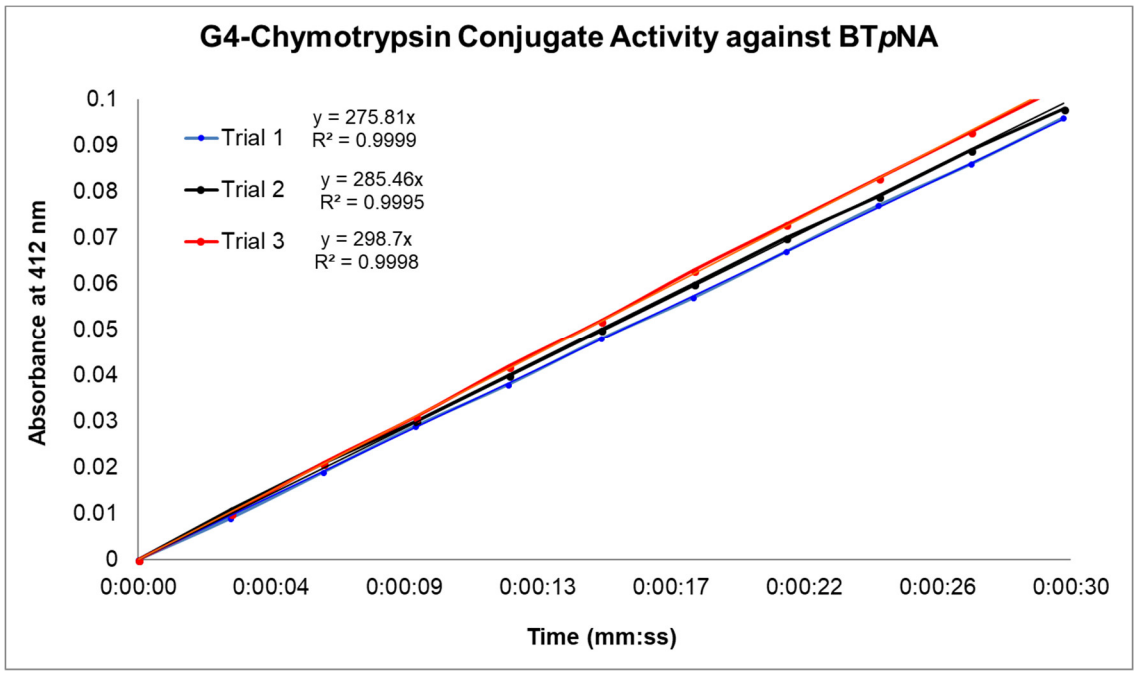

Figure 4.28. Absorbance over time of BT*p*NA cleavage by G4-CT conjugate.

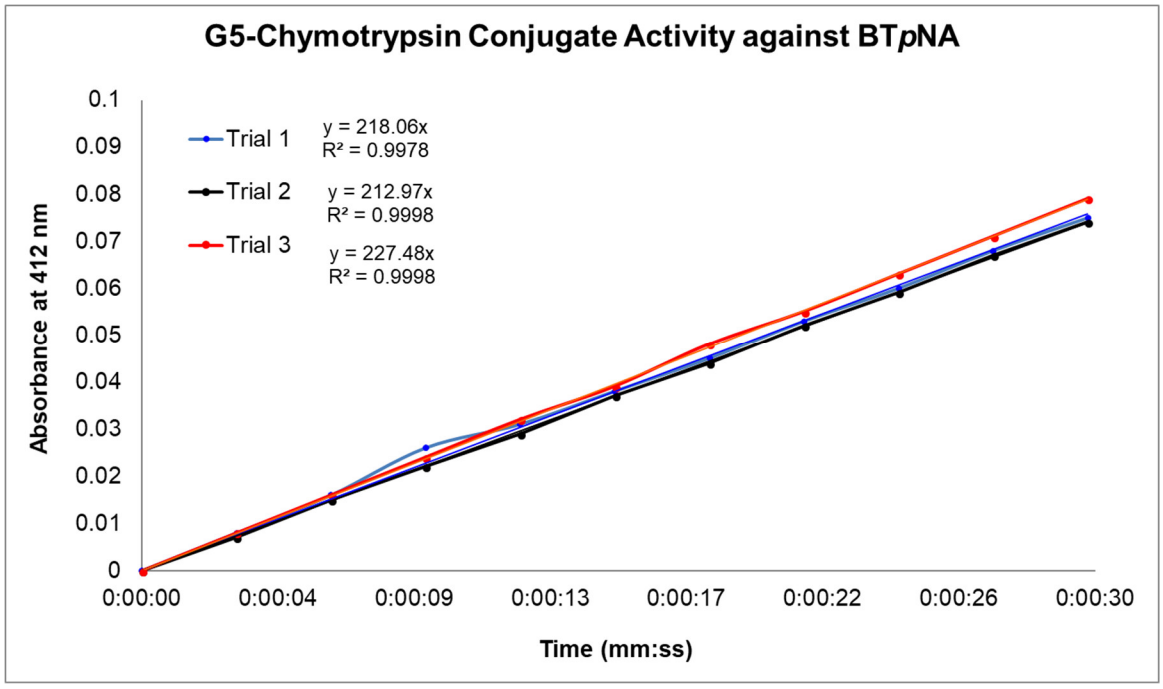

Figure 4.29. Absorbance over time of BT*p*NA cleavage by G5-CT conjugate.

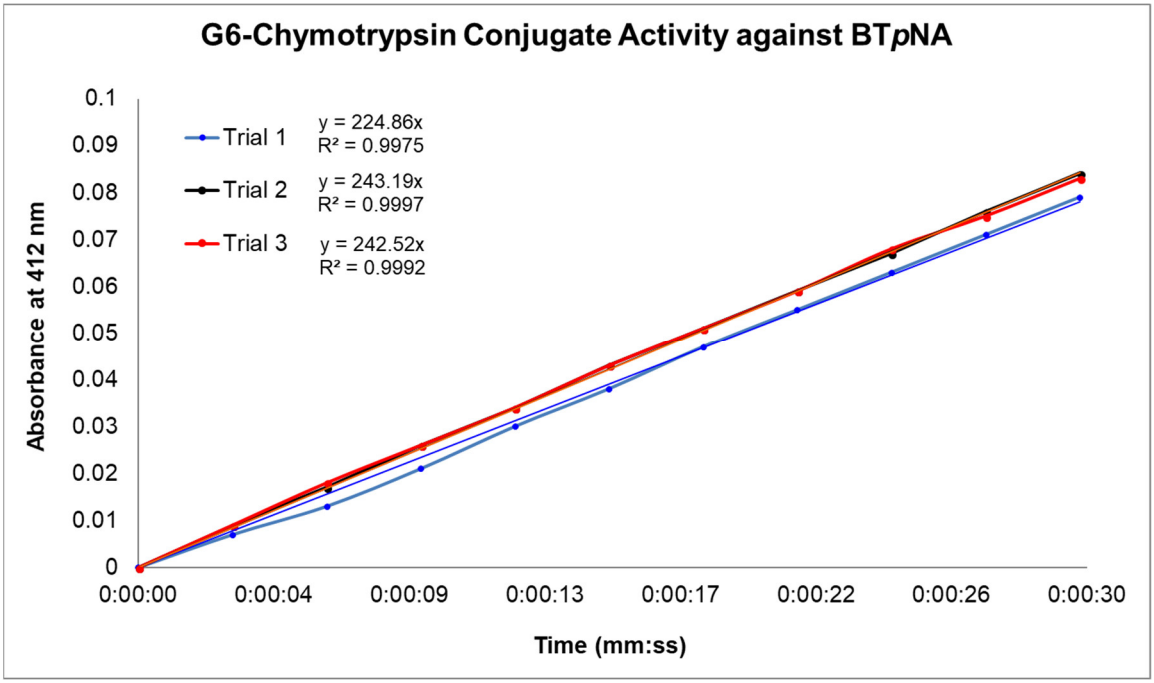

Figure 4.30. Absorbance over time of BT*p*NA cleavage by G6-CT conjugate.

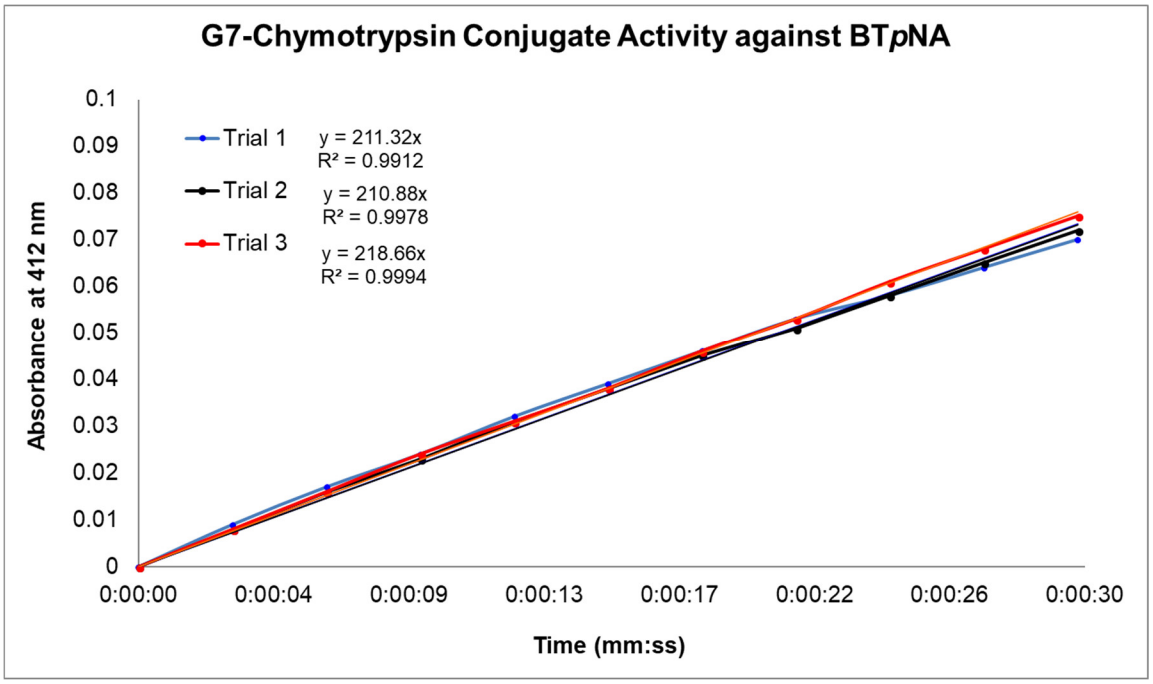

Figure 4.31. Absorbance over time of BT*p*NA cleavage by G7-CT conjugate.

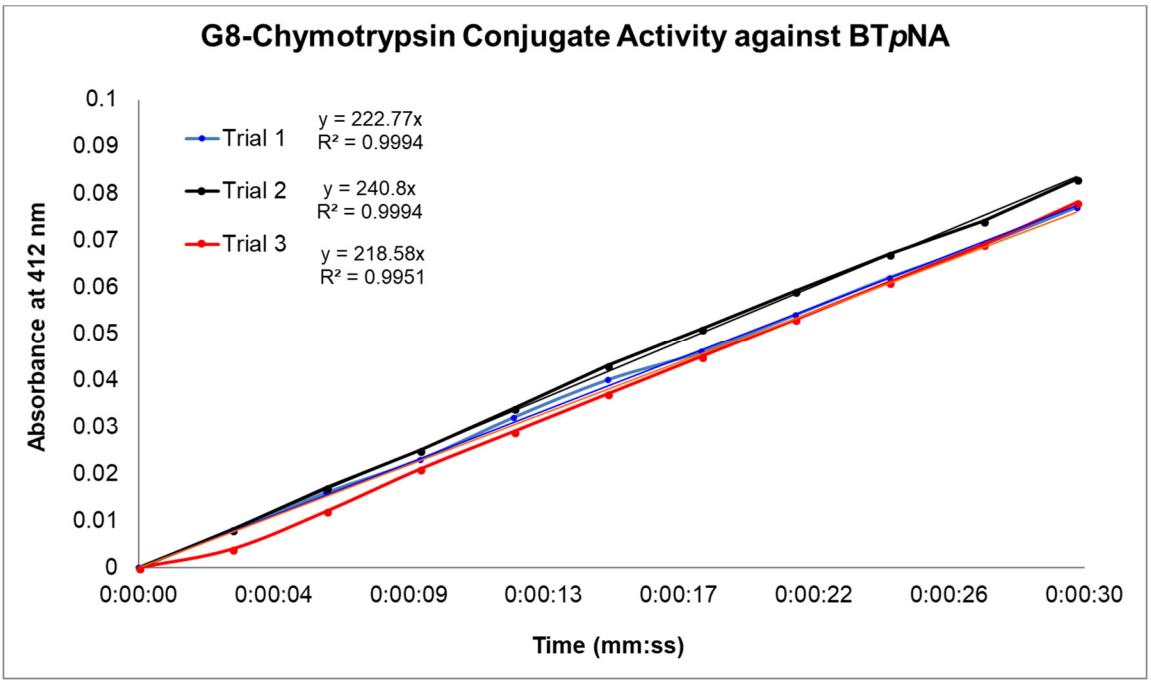

Figure 4.32. Absorbance over time of BT*p*NA cleavage by G8-CT conjugate.

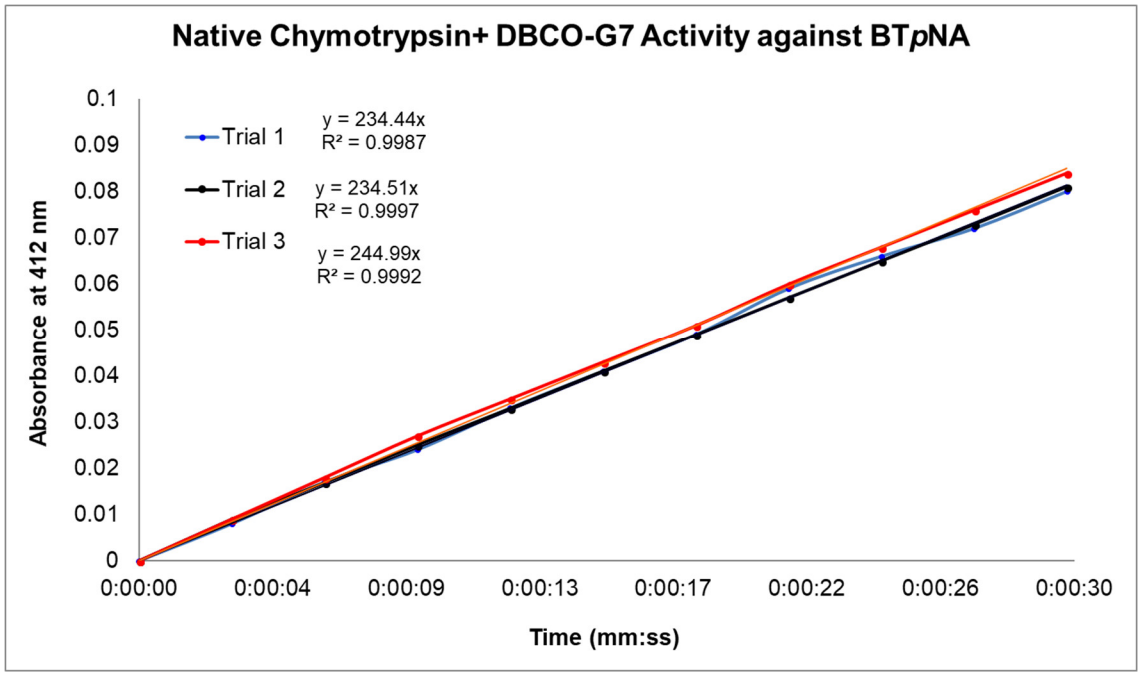

Figure 4.33. Absorbance over time of BT*p*NA cleavage by native CT with DBCO-G7.

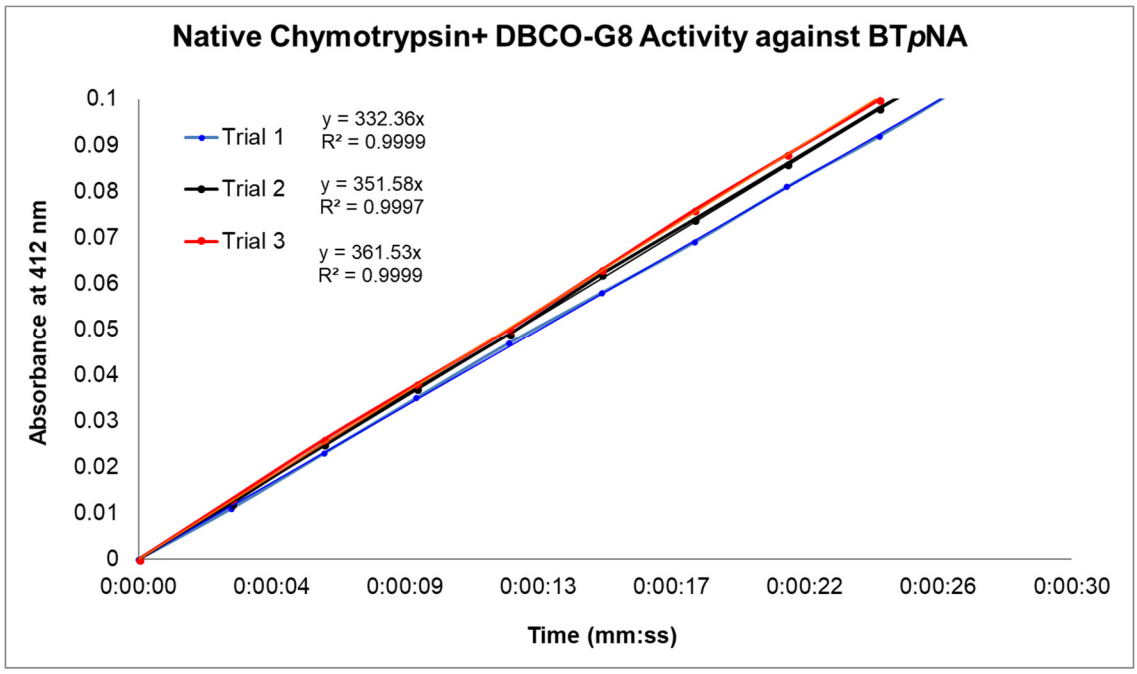

Figure 4.34. Absorbance over time of BT*p*NA cleavage by native CT with DBCO-G8

4.9 Chymotrypsin activity vs. Casein and Bovine Serum Albumin

Following the methods of Gauthier and co-workers,[35] the activity of chymotrypsin and chymotrypsin-dendron conjugates against Casein and BSA was determined as follows. A 10 mg/mL suspension of milk casein or BSA in 0.1 M Tris buffer (pH 8) was prepared and equilibrated at 37 °C for 1 minute with vigorous stirring. Separately, a stock solution of either the native chymotrypsin or chymotrypsin-dendron conjugate was dissolved in the same buffer solution to an absorbance at 280 nm of approximately 0.2 AU, to precisely determine the concentration of the conjugates. 100 μL of this stock was then added to the protein substrate suspensions and was left to stir at 37 °C for 20 minutes, at which point the reaction was quenched by the addition of 200 μL of 50% trichloroacetic acid in water. The precipitated protein was then removed by centrifugation at 4 °C at 10 000 *g* for 10 minutes. 600 μL of the supernatant was then transferred to a low volume 1 cm path length quartz cuvette and the absorbance was measured at 280 nm.

To account for incomplete precipitation of the protein substrate, a control experiment was run with all conditions the same as described above but without the addition of the chymotrypsin conjugate. This residual absorbance we denote as $\mathbf{A_{blank}}$**.** The average absorbance of this blank was then subtracted from the absorbances measured with the protein. An additional control was also performed, in which the assay was run without the addition of substrate to determine the precise amount of residual conjugate remaining after precipitation with trichloroacetic acid, which we denote $\mathbf{A_{conj}}$. The average value of this absorbance was also subtracted from the final absorbance of the assays to account for unprecipitated conjugate. When calculating the activity of the dendron-α-CT conjugates,

the “Corrected A280” value was used to denote the absorbance at 280 nm which bad been corrected for the difference in concentration vs. the native α-CT, and had $\mathbf{A_{blank}}$ and $\mathbf{A_{conj}}$ subtracted from it.

The molar absorptivity of the α-CT-dendron conjugates was calculated by preparing a stock solution of DBCO-G3-OH in 0.1 M phosphate buffer to an absorption at 309 nm of approximately 0.5 AU, and the molar concentration was then calculated from the known molar absorptivity of the DBCO moiety of ~12 000 cm^{-1} M^{-1}.[56] This was then reacted with 5 molar equivalents of azidoacetic acid, and after 1 hour the absorbance at 280 nm was measured and this was used to calculate the molar absorptivity of the clicked conjugate, with a value of 2 900 cm^{-1} M^{-1}. Since full functionalization of the α-CT-N_3 conjugate had already been verified, the molar absorptivity of the α-CT-dendron conjugates should be the sum of the native chymotrypsin absorptivity plus the absorptivity of the 14 clicked units, which gives an overall absorptivity of 93 000 cm^{-1} M^{-1}. This value is then used to determine the molar concentration of the α-CT-dendron conjugates in the assays.

Table 4.4. Raw data for determination of enzymatic activity of native chymotrypsin and chymotrypsin-dendron conjugates against BTpNA.

Generation Number	Initial Slopes	Concentration (μM)	Concentration Adjusted Slope	Activity Relative to Native	Mean	Relative St. Dev
2	244.99	2.77	88.6	1.38	**1.46**	0.05
	261.82	2.77	94.6	1.47		
	271.99	2.77	98.3	1.53		
3	266.68	2.62	101.7	1.58	**1.62**	0.02
	276.63	2.62	105.5	1.64		
	276.26	2.62	105.3	1.64		
4	275.81	2.81	98.1	1.52	**1.58**	0.04
	285.46	2.81	101.5	1.58		
	298.70	2.81	106.3	1.65		
5	218.06	2.38	91.6	1.42	**1.43**	0.03
	212.97	2.38	89.4	1.39		
	227.48	2.38	95.5	1.48		
6	224.86	2.30	97.7	1.52	**1.60**	0.04
	243.19	2.30	105.6	1.64		
	242.52	2.30	105.4	1.64		
7	211.32	2.58	81.9	1.27	**1.29**	0.02
	210.88	2.58	81.8	1.27		
	218.66	2.58	84.8	1.32		
8	222.77	2.27	98.0	1.52	**1.55**	0.08
	240.8	2.27	105.9	1.64		
	218.58	2.27	96.1	1.49		
Native	287.48	4.41	65.2	1.01	**1.00**	0.05
	267.80	4.41	60.8	0.94		
	296.08	4.41	67.2	1.04		
Native + DBCO G7	234.44	3.91	60.0	0.93	**0.95**	0.03
	234.51	3.91	60.0	0.93		
	244.99	3.91	62.7	0.97		
Native + DBCO G8	332.36	4.36	76.3	1.19	**1.24**	0.05
	351.58	4.36	80.7	1.25		
	361.53	4.36	83.0	1.29		
DBCO-G3-$(PEG_{15})_8$	232.05	2.73	84.9	1.32	**1.26**	0.07
	230.25	2.73	84.3	1.31		
	202.56	2.73	74.1	1.15		
mPEG-5500	228.89	2.37	96.6	1.50	**1.52**	0.04
	237.8	2.37	100.3	1.56		
	228.5	2.37	96.4	1.50		

Table 4.5. Raw data for determination of enzymatic activity of native chymotrypsin and chymotrypsin-dendron conjugates against casein.

Generation Number	A280	Concentration (μM)	Corrected A280	Casein Activity Relative to Native	Mean Activity Relative to Native	Mean Sieving	Relative St. Dev
2	0.4495 0.4505 0.4558	2.77 2.77 2.77	0.147 0.147 0.149	0.96 0.96 0.97	0.96	**1.04**	0.05
3	0.4715 0.4381 0.4657	2.62 2.62 2.62	0.164 0.151 0.162	1.07 0.99 1.06	1.04	**0.98**	0.05
4	0.5625 0.5651 0.5462	2.81 2.81 2.81	0.184 0.185 0.179	1.20 1.21 1.17	1.19	**0.83**	0.05
5	0.4110 0.4139 0.4380	2.38 2.38 2.38	0.157 0.158 0.168	1.02 1.03 1.10	1.05	**0.95**	0.05
6	0.3429 0.3285 0.3442	2.30 2.30 2.30	0.133 0.127 0.134	0.87 0.83 0.87	0.86	**1.20**	0.05
7	0.2541 0.2770 0.2936	2.58 2.58 2.58	0.083 0.092 0.098	0.54 0.60 0.64	0.59	**1.75**	0.09
8	0.2706 0.2359 0.2929	2.27 2.27 2.27	0.090 0.075 0.100	0.59 0.49 0.65	0.58	**1.73**	0.152
Native	0.8332 0.9437 0.8682	4.01 4.01 4.01	0.141 0.169 0.150	0.92 1.10 0.98	1.00	**1.00**	0.11
Native + DBCO G7	0.4340 0.4634 0.4995	4.36 4.36 4.36	0.083 0.090 0.099	0.54 0.59 0.64	0.59	**1.60**	0.09
Native + DBCO G8	0.4721 0.4507 0.5228	4.36 4.36 4.36	0.090 0.085 0.102	0.59 0.55 0.66	0.60	**2.06**	0.10
DBCO-G3-$(PEG_{15})_8$	0.3051 0.2930 0.2604	2.73 2.73 2.73	0.097 0.093 0.081	0.63 0.60 0.53	0.59	**2.14**	0.12
mPEG-5500	0.3444 0.3712 0.4447	2.37 2.37 2.37	0.128 0.140 0.171	0.84 0.91 1.11	0.95	**1.05**	0.15

Table 4.6. Raw data for determination of enzymatic activity of native chymotrypsin and chymotrypsin-dendron conjugates against bovine serum albumin.

Generation Number	A280	Concentration (μM)	Corrected A280	BSA Activity Relative to Native	Mean Activity Relative to Native	Sieving Ratio	Relative St. Dev
2	0.1150 0.1126 0.1068	2.38 2.38 2.38	0.033 0.032 0.029	0.95 0.92 0.85	0.907	**1.10**	0.07
3	0.0996 0.1064 0.0966	2.05 2.05 2.05	0.033 0.036 0.031	0.90 0.99 0.85	0.913	**1.09**	0.08
4	0.1076 0.1079 0.0949	2.39 2.39 2.39	0.029 0.029 0.024	0.89 0.89 0.74	0.840	**1.19**	0.11
5	0.0883 0.0900 0.1014	2.38 2.38 2.38	0.021 0.022 0.027	0.64 0.66 0.80	0.700	**1.43**	0.13
6	0.0813 0.0844 0.0775	2.30 2.30 2.30	0.020 0.021 0.018	0.47 0.51 0.42	0.467	**2.14**	0.11
7	0.0666 0.0516 0.0373 0.0593 0.0451	2.30 2.30 2.30 2.44 2.44	0.013 0.007 0.001 0.005 -0.001	0.29 0.10 -0.08 0.15 -0.01	0.090	**11.1**	1.61
8	0.0507 0.0770 0.0573	2.27 2.27 2.27	-0.006 0.005 -0.003	-0.18 0.15 -0.10	0.044	**23.0**	4.00
Native	0.2380 0.2043 0.2349	4.21 4.21 4.21	0.041 0.033 0.040	1.08 0.85 1.06	0.997	**1**	0.13
Native + DBCO G7	0.1894 0.1673 0.1670	3.91 3.91 3.91	0.032 0.027 0.027	0.85 0.70 0.70	0.750	**1.33**	0.11
Native + DBCO G8	0.2163 0.2535 0.2905	4.36 4.36 4.36	0.031 0.04 0.048	0.90 1.15 1.40	1.150	**0.87**	0.22
DBCO-G3-$(PEG_{15})_8$	0.0554 0.0468 0.0504	2.73211 2.73211 2.73211	0.006 0.003 0.004	0.16 0.07 0.11	0.116	**8.59**	0.40
mPEG-5500	0.0875 0.0671 0.0824	2.37 2.37 2.37	0.020 0.011 0.018	0.58 0.33 0.51	0.473	**2.11**	0.13

4.10 Chymotrypsin activity vs. BT*p*NA with Antichymotrypsin

Following the methods of Gauthier and coworkers,[35] the activity assays against BTpNA were performed as above in the presence of α-anti-CT. The conjugate solution was incubated for 3 minutes with 1.5 equivalents of α-anti-CT at 37 °C.

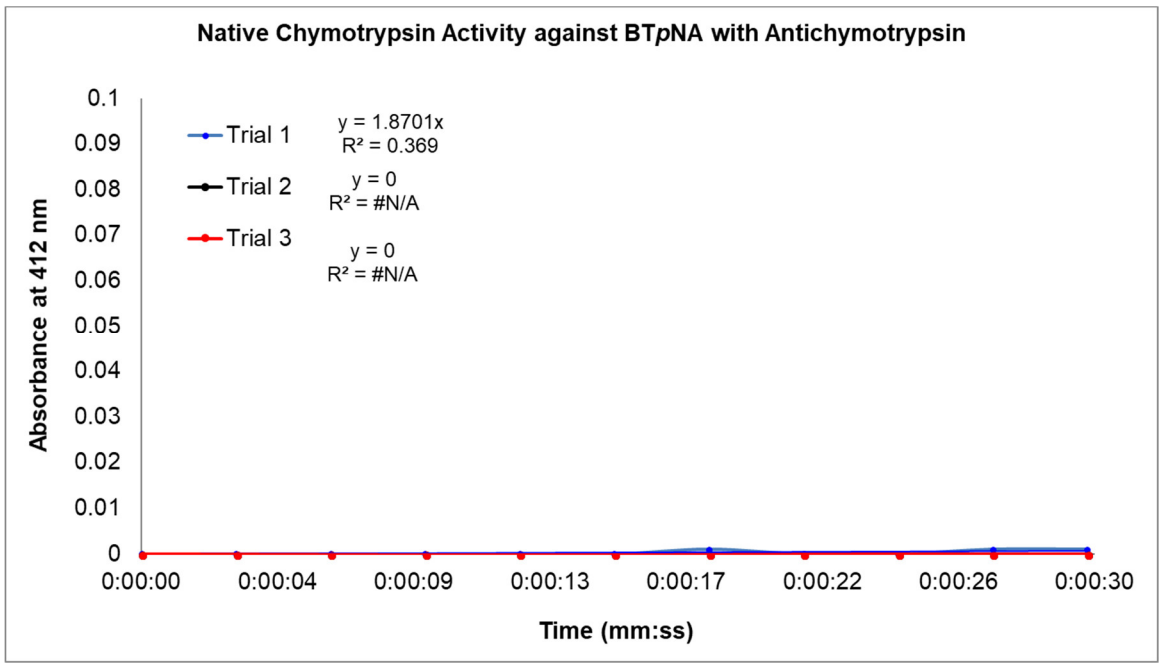

Figure 4.35. Absorbance over time of BT*p*NA cleavage by native CT with 1.5 equivalents of antichymotrypsin.

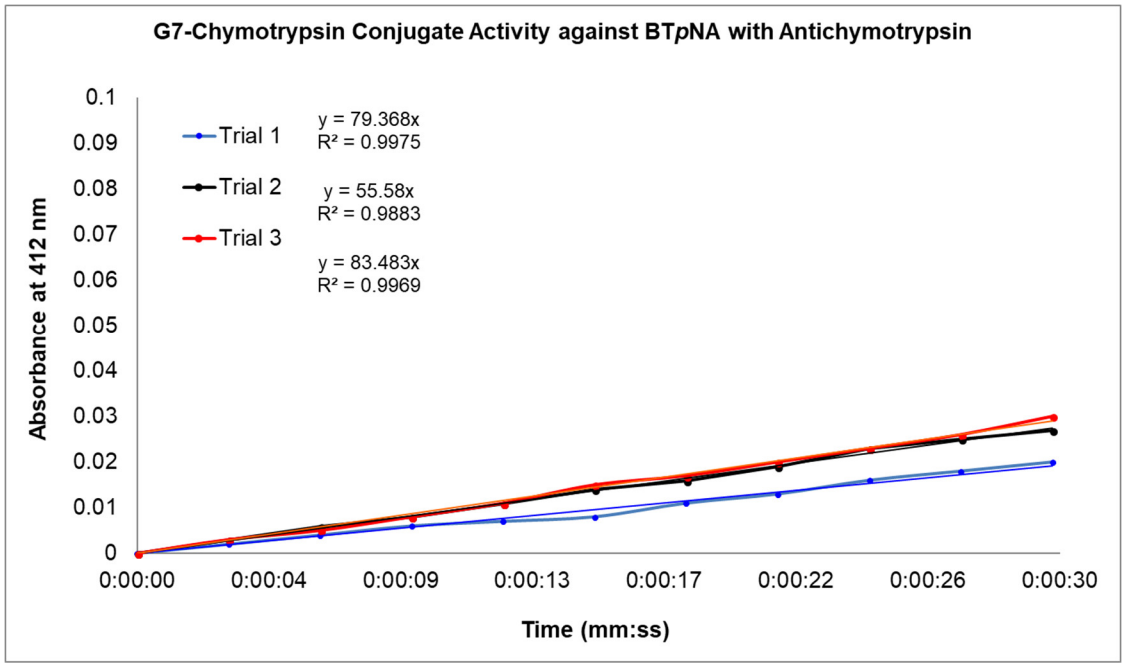

Figure 4.36. Absorbance over time of BT*p*NA cleavage by G7-CT with 1.5 equivalents of antichymotrypsin.

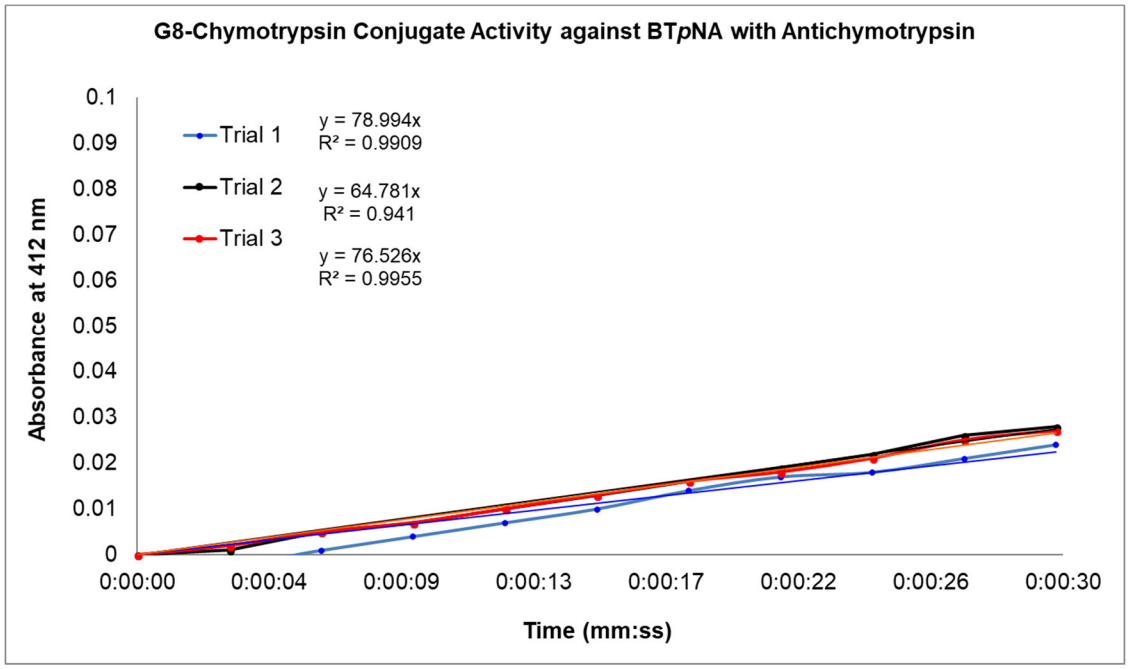

Figure 4.37. Absorbance over time of BT*p*NA cleavage by G8-CT with 1.5 equivalents of antichymotrypsin.

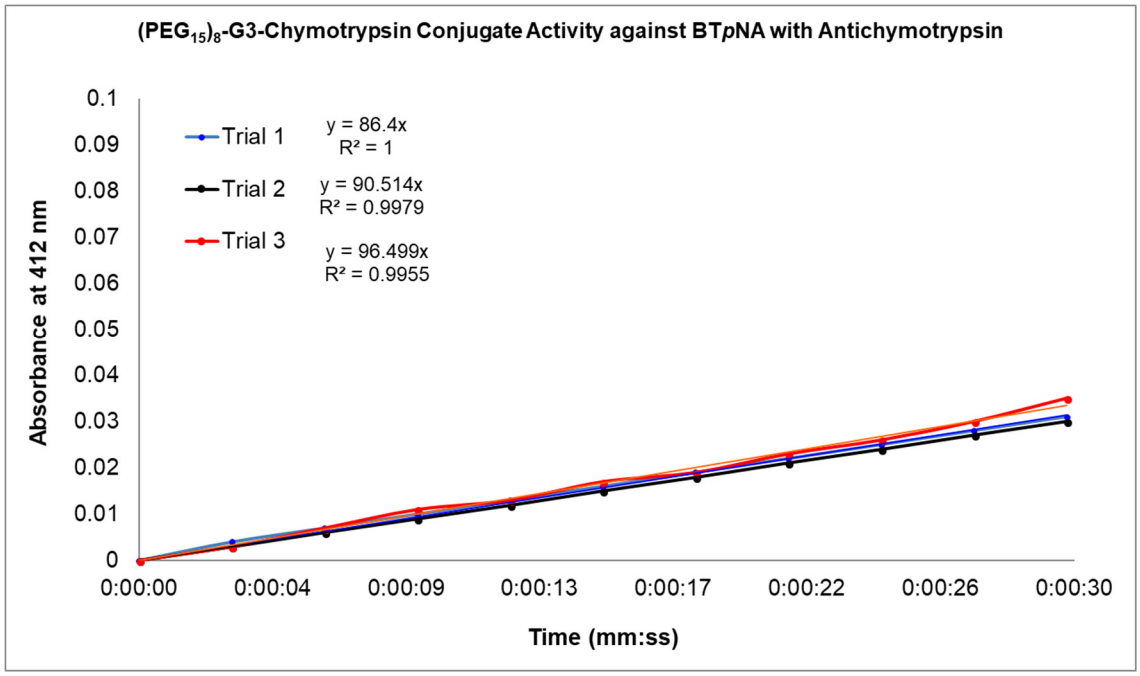

Figure 4.38. Absorbance over time of BT*p*NA cleavage by $(PEG_{15})_8$-G3-CT with 1.5 equivalents of α-antichymotrypsin.

4.11 Circular Dichroism Measurements

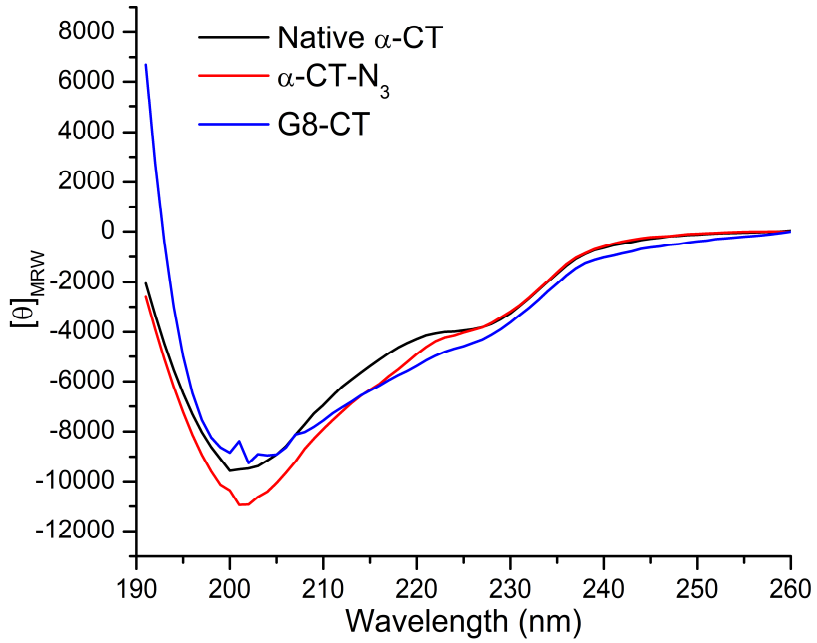

Figure 4.39.. Circular dichroism spectra of native α-CT, α-CT-N_3, and the G8-CT conjugate.

4.12 3-Dimensional Models of Dendrimer-CT Conjugates

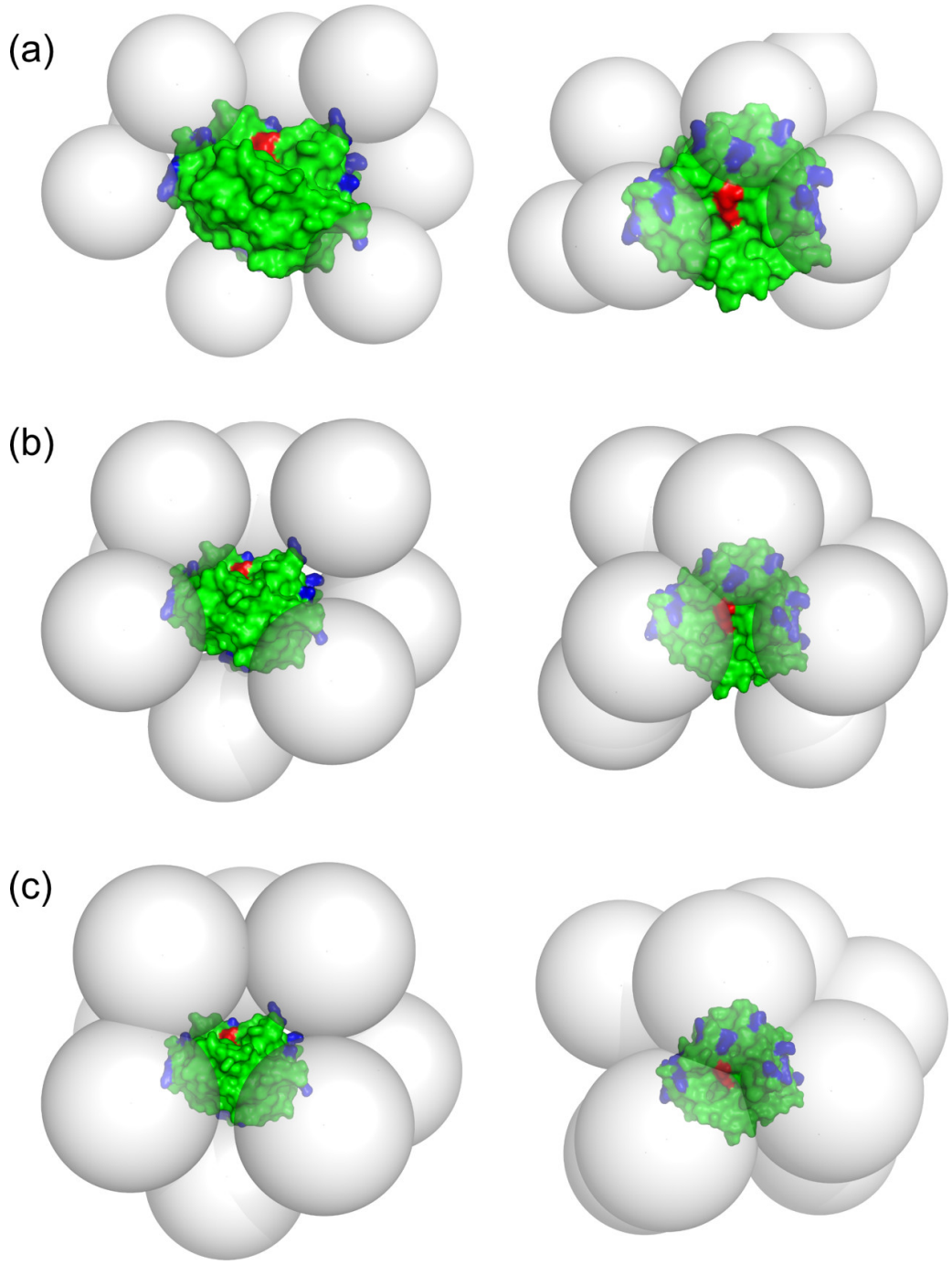

Figure 4.40. 3-D models of α-CT-G6 (a), α-CT-G7 (b), and α-CT-G8 (c) conjugates. Front view (left) and top view (right). Active site residues are colored red, while lysine residues are in blue.

4.13 References

[1] J. R. Kintzing, M. V. Filsinger Interrante, J. R. Cochran, *Trends Pharmacol. Sci.* **2016**, *37*, 993–1008.

[2] W. V. Moore, H. J. Nguyen, G. B. Kletter, B. S. Miller, D. Rogers, D. Ng, J. A. Moore, E. Humphriss, J. L. Cleland, G. M. Bright, *J. Clin. Endocrinol. Metab.* **2016**, *101*, 1091–1097.

[3] L. V. Gushchina, S. Bhattacharya, K. E. McElhanon, J. H. Choi, H. Manring, E. X. Beck, J. Alloush, N. Weisleder, *Mol. Ther.* **2017**, *25*, 2360–2371.

[4] M. J. Burke, S. R. Rheingold, *Leuk. Lymphoma* **2017**, *58*, 540–551.

[5] R. Shen, D. Ye, Q. Huang, J. Li, Q. Wang, J. Fei, *Acta Biochim. Biophys. Sin. (Shanghai).* **2018**, *50*, 391–398.

[6] M. L. Etheridge, S. A. Campbell, A. G. Erdman, C. L. Haynes, S. M. Wolf, J. McCullough, *Nanomedicine Nanotechnology, Biol. Med.* **2013**, *9*, 1–14.

[7] J. I. Hare, T. Lammers, M. B. Ashford, S. Puri, G. Storm, S. T. Barry, *Adv. Drug Deliv. Rev.* **2017**, *108*, 25–38.

[8] P. Bailon, A. Palleroni, C. A. Schaffer, C. L. Spence, W. J. Fung, J. E. Porter, G. K. Ehrlich, W. Pan, Z. X. Xu, M. W. Modi, et al., *Bioconjug. Chem.* **2001**, *12*, 195–202.

[9] P. Caliceti, O. Schiavon, F. M. Veronese, *Bioconjug. Chem.* **2001**, *12*, 515–522.

[10] A. Abuchowski, T. van Es, N. C. Palczuk, *J. Biol. Chem.* **1977**, *252*, 3578–81.

[11] Y. Kamisaki, H. Wada, T. Yagura, A. Matsushima, Y. Inada, *J. Pharmacol. Exp. Ther.* **1981**, *216*, 410–414.

[12] K. Knop, R. Hoogenboom, D. Fischer, U. S. Schubert, *Angew. Chemie - Int. Ed.* **2010**, *49*, 6288–6308.

[13] G. Pasut, F. M. Veronese, *J. Control. Release* **2012**, *161*, 461–472.

[14] J. M. Harris, R. B. Chess, *Nat. Rev. Drug Discov.* **2003**, *2*, 214–221.

[15] F. M. Veronese, *Biomaterials* **2001**, *22*, 405–417.

[16] J. K. Dozier, M. D. Distefano, *Int. J. Mol. Sci.* **2015**, *16*, 25831–25864.

[17] S. Asayama, K. Nagashima, H. Kawakami, *ACS Omega* **2017**, *2*, 2382–2386.

[18] L. A. G. van Leeuwen, E. C. Hinchy, M. P. Murphy, E. L. Robb, H. M. Cochemé, *Free Radic. Biol. Med.* **2017**, *108*, 374–382.

[19] F. Zhang, M. Liu, H. Wan, *Biol. Pharm. Bull.* **2014**, *37*, 335–339.

[20] S. Jevševar, M. Kunstelj, V. G. Porekar, *Biotechnol. J.* **2010**, *5*, 113–128.

[21] Z. Yang, J. Wang, Q. Lu, J. Xu, Y. Kobayashi, T. Takakura, A. Takimoto, T.

Yoshioka, C. Lian, C. Chen, et al., *Cancer Res.* **2004**, *64*, 6673–6678.

[22] F. M. Veronese, A. Mero, *Biodrugs* **2008**, *22*, 315–329.

[23] A. Grotzky, Y. Manaka, T. Kojima, P. Walde, *Biomacromolecules* **2011**, *12*, 134–144.

[24] Y. Hou, J. Yuan, Y. Zhou, J. Yu, H. Lu, *J. Am. Chem. Soc.* **2016**, *138*, 10995–11000.

[25] B. S. Lele, H. Murata, K. Matyjaszewski, A. J. Russell, *Biomacromolecules* **2005**, *6*, 3380–3387.

[26] D. Miyamoto, J. Watanabe, K. Ishihara, *Biomaterials* **2004**, *25*, 71–76.

[27] Z. R. Lu, P. Kopečková, Z. Wu, J. Kopeček, *Bioconjug. Chem.* **1998**, *9*, 793–804.

[28] L. Tao, J. Xu, D. Gell, T. P. Davis, *Macromolecules* **2010**, *43*, 3721–3727.

[29] Y. Hu, Y. Hou, H. Wang, H. Lu, *Bioconjug. Chem.* **2018**, *29*, 2232–2238.

[30] F. Wurm, C. Dingels, H. Frey, H. A. Klok, *Biomacromolecules* **2012**, *13*, 1161–1171.

[31] B. R. Spears, J. Waksal, C. McQuade, L. Lanier, E. Harth, *Chem. Commun.* **2013**, *49*, 2394–2396.

[32] F. Wurm, J. Klos, H. J. Räder, H. Frey, *J. Am. Chem. Soc.* **2009**, *131*, 7954–7955.

[33] M. A. Gauthier, H. A. Klok, *Polym. Chem.* **2010**, *1*, 1352–1373.

[34] A. J. Keefe, S. Jiang, *Nat. Chem.* **2012**, *4*, 59–63.

[35] M. Liu, P. Tirino, M. Radivojevic, D. J. Phillips, M. I. Gibson, J. C. Leroux, M. A. Gauthier, *Adv. Funct. Mater.* **2013**, *23*, 2007–2015.

[36] M. Liu, P. Johansen, F. Zabel, J. C. J. Leroux, M. A. A. Gauthier, P. Johansen, F. Zabel, J. C. J. Leroux, M. A. A. Gauthier, *Nat. Commun.* **2014**, *5*, 5526.

[37] E. R. Gillies, J. M. J. Fréchet, *Drug Discov. Today* **2005**, *10*, 35–43.

[38] C. C. Lee, J. A. MacKay, J. M. J. Fréchet, F. C. Szoka, *Nat. Biotechnol.* **2005**, *23*, 1517–1526.

[39] H. Ihre, A. Hult, E. Söderlind, *J. Am. Chem. Soc.* **1996**, *118*, 6388–6395.

[40] H. Ihre, A. Hult, J. M. J. Fréchet, I. Gitsov, *Macromolecules* **1998**, *31*, 4061–4068.

[41] M. V. Walter, M. Malkoch, *Chem. Soc. Rev.* **2012**, *41*, 4593–4609.

[42] A. Carlmark, E. Malmström, M. Malkoch, *Chem. Soc. Rev.* **2013**, *42*, 5858–5879.

[43] K. Jain, P. Kesharwani, U. Gupta, N. K. Jain, *Int. J. Pharm.* **2010**, *394*, 122–142.

[44] N. Feliu, M. V. Walter, M. I. Montañez, A. Kunzmann, A. Hult, A. Nyström, M. Malkoch, B. Fadeel, *Biomaterials* **2012**, *33*, 1970–1981.

[45] J. D. Schulz, M. Patt, S. Basler, H. Kries, D. Hilvert, M. A. Gauthier, J. C. Leroux,

Adv. Mater. **2016**, *28*, 1455–1460.

[46] N. J. Agard, J. a. Prescher, C. R. Bertozzi, Nicholas J. Agard, and Jennifer A. Prescher, C. R. Bertozzi*, *J. Am. Chem. Soc.* **2004**, *126*, 15046–15047.

[47] R. C. Chadwick, S. Van Gyzen, S. Liogier, A. Adronov, *Synth.* **2014**, *46*, 669–677.

[48] S. A. McNelles, A. Adronov, *Macromolecules* **2017**, *50*, 7993–8001.

[49] M. C. Parrott, S. R. Benhabbour, C. Saab, J. A. Lemon, S. Parker, J. F. Valliant, A. Adronov, *J. Am. Chem. Soc* **2009**, *131*, 2906–2916.

[50] A. Zaghmi, E. Mendez-villuendas, A. A. Greschner, J. Y. Liu, H. W. De Haan, M. A. Gauthier, *Mater. Today Chem.* **2019**, *12*, 121–131.

[51] L. Sawyer, C. Holt, *J. Dairy Sci.* **1993**, *76*, 3062–3078.

[52] V. Thilakarathne, V. A. Briand, Y. Zhou, R. M. Kasi, C. V. Kumar, *Langmuir* **2011**, *27*, 7663–7671.

[53] P. Krishna, D. Pandey, *Close-Packed Structures*, University College Cardiff Press, Cardiff, Wales, **1981**.

[54] L. Gráf, L. Szilágyi, I. Venekei, in *Handb. Proteolytic Enzym.* (Ed.: G.B.T.-H. of P.E. Salvesen), Academic Press, **2013**, pp. 2626–2633.

[55] M. Volini, P. Tobias, *J. Biol. Chem.* **1969**, *244*, 5105–5109.

[56] D. Liu, J. Yang, H. F. Wang, Z. Wang, X. Huang, Z. Wang, G. Niu, A. R. Hight Walker, X. Chen, *Anal. Chem.* **2014**, *86*, 5800–5806.

5 Zwitterion Dendrimers for Imaging

5.1 Abstract

A series of high generation polyester dendrimers functionalized at the periphery with sulfobetaine or carboxybetaine groups was prepared and characterized by NMR spectroscopy, DLS, zeta-potential, and SEC. The resulting dendrons were molecularly dispersed in buffer and were larger than the renal clearance threshold of 5 nm and had a near-zero zeta potential. Radiolabeling of the dendrimers was then attempted with $[^{99m}Tc(CO)_3(H_2O)_3]^+$, but all conditions tried resulted in either no labeling of the dipicolylamine group, or caused extensive decomposition of the dendron.

5.2 Introduction

The use of macromolecular therapeutics has seen extensive research in the past 40 years.[1–3] The conjugation of a wide variety of water-soluble polymers such as polyethylene glycol (PEG),[4,5] poly(sarcosine),[6] poly(oxazolines),[7–9] and others[10–12] have been used to improve drug solubility, reduce the immune response,[5,13,14] and increase the blood elimination half-life[15–17] of numerous pharmaceuticals. The conjugation of polyethylene glycol, known as PEGylation, is by far the most successful of these approaches, and has been used clinically for a number of therapeutics. However, the use of PEGylation has recently been questioned due to the detection of anti-PEG antibodies in humans, which can cause increased blood clearance rates and immune responses to the PEG conjugates.[18–22]

Zwitterionic polymers such as poly(sulfobetaines) and poly(carboxybetaines) have been the subject of intense research interest in recent years. They have been found to exhibit

extremely low biofouling[23], exceptional water solubility, have near-zero zeta potentials, and very low toxicity.[24] For these reasons, zwitterionic acrylate polymers have been conjugated to biologic drugs in a similar manner as previous PEGylation work, and this results in conjugates that have higher specific activity, lower protein binding, and much lower immunogenicity than their PEGylated counterparts.[25] These parameters indicate that zwitterionic polymers are excellent candidates to augment PEGylation as a macromolecular modification to improve pharmacokinetics.

While many macromolecular architectures have been investigated for biological applications, dendritic macromolecules are seen as particularly attractive for a variety of reasons.[26,27] Dendritic macromolecules are prepared through precise, stepwise synthesis methodologies that allow for precise control over the size, molecular weight, core, and periphery functionality of the resulting polymer. The globular nature of the resulting conjugate also differs substantially from the random-coil arrangement of typical linear polymers such as polyacrylates, and this can have profound effects on the blood half-life[28] and display of peripheral groups.[29]

Among the available dendrimer architectures, 2,2-bis(hydroxymethyl) propionic acid (bis-MPA) dendrimers are particularly attractive. They can be prepared through both convergent[30,31] and divergent[32,33] methodologies, exhibit low toxicity[31], and decompose *in vivo* over the course of several weeks,[34] which obviates the concern over accumulation often encountered with nanoparticles for biological applications.[35]

In our previous work we have prepared monodisperse bis-MPA dendrons with alcohol groups at the periphery and radiolabeled these with ^{99m}Tc to determine their biodistribution via Single Photon Emission Computed Tomography (SPECT) imaging.[36] We determined that these dendrons cleared the blood in under 15 minutes with nearly full excretion to the bladder, and so we undertook a further study to investigate the conjugation of high-generation dendrons with PEG to increase its hydrodynamic diameter.[37] While this methodology was effective in increasing the hydrodynamic diameter and blood circulation time, the use of thiol-ene chemistry did not allow for full functionalization of the dendron with PEG. This combined with the intrinsic dispersity of PEG resulted in conjugates that were not monodisperse, sacrificing one of the key aspects that make dendrimers attractive for biological applications.

Herein, we describe the synthesis of high-generation bis-MPA dendrons with sulfobetaine and carboxybetaine peripheries. The use of our previously-developed SPAAC dendrimer synthesis[38] has allowed for the preparation of perfectly defined zwitterionic dendrimers. Initial radiolabeling studies with ^{99m}Tc were attempted, but unfortunately the dendrimers could not be labeled using this isotope, and as such biodistribution studies could not be undertaken.

5.3 Results and Discussion

To prepare the desired dendrons, we employed our previously described Strain-Promoted Alkyne-Azide Cycloaddition (SPAAC) chemistry to prepare dendrimers by a convergent approach using a pair of “inner” and “outer” dendrons. The inner dendron required a dipicolylamine ligand at the core for co-ordination of $^{99m}Tc(CO)_3$, and azide groups at the

periphery for coupling to the "outer" dendron. The inner dendron was prepared with 2,2-dimethyl substituted ester linked azides as seen in Scheme 5.1.

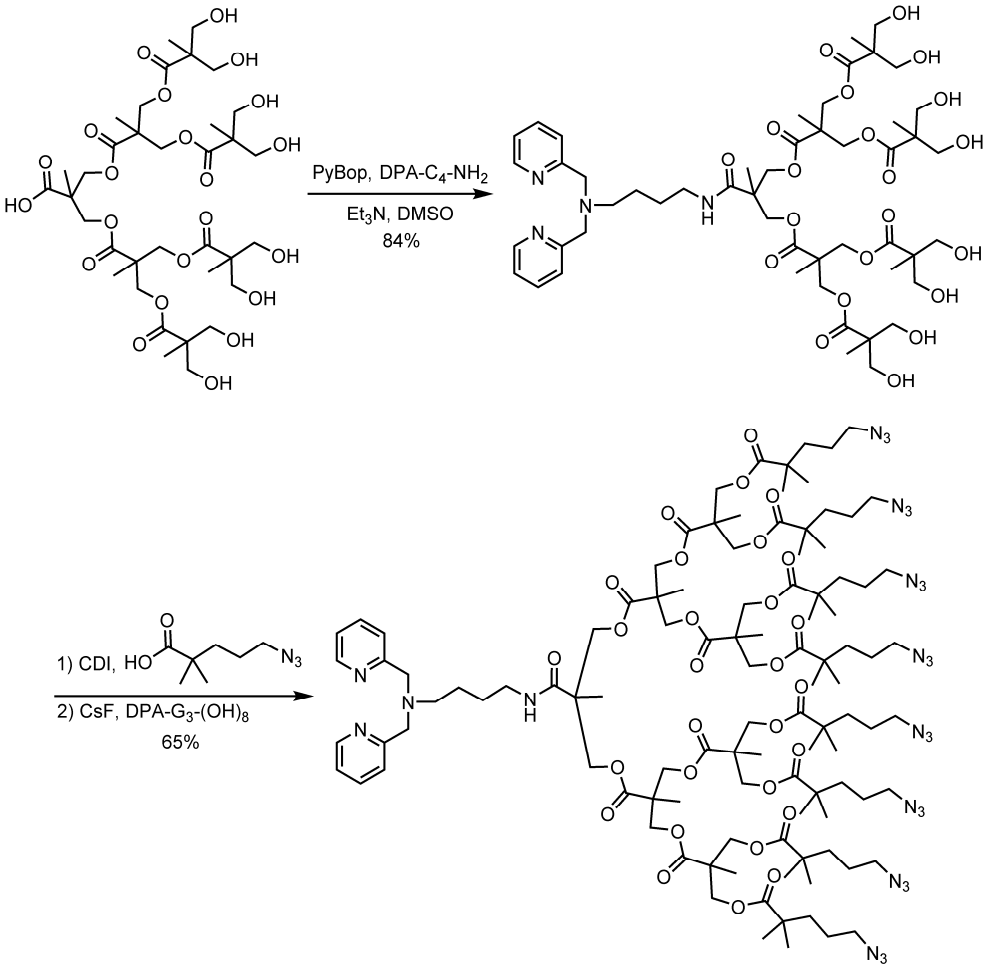

Scheme 5.1. Synthesis of DPA-G3-$(N_3)_8$ with azides appended by ester linkages

Starting from COOH-G3-$(OH)_8$ which was prepared according to modified literature procedures,[36] the core of the dendron was amidated with the dipicolylamine ligand using benzotriazol-1-yl-oxytripyrrolidinophosphonium hexafluorophosphate (PYBOP) coupling in good yield. This was then functionalized with azides using fluoride promoted esterification (FPE) by pre-activation of 5-azido-2,2-dimethylvaleric acid with carbonyl

diimidazole (CDI) for 1 hour at 50 °C, and subsequent addition of the DPA-G3-$(OH)_8$ dendron and 20 mol% of cesium fluoride.

With the "inner" dendrons in hand, corresponding "outer" dendrons with zwitterionic groups at the periphery and a strained cyclooctyne were then prepared. A Cbz protected amine core dendron was grown divergently from mono-Cbz protected butanediamine hydrochloride using FPE, as seen in Scheme 5.2

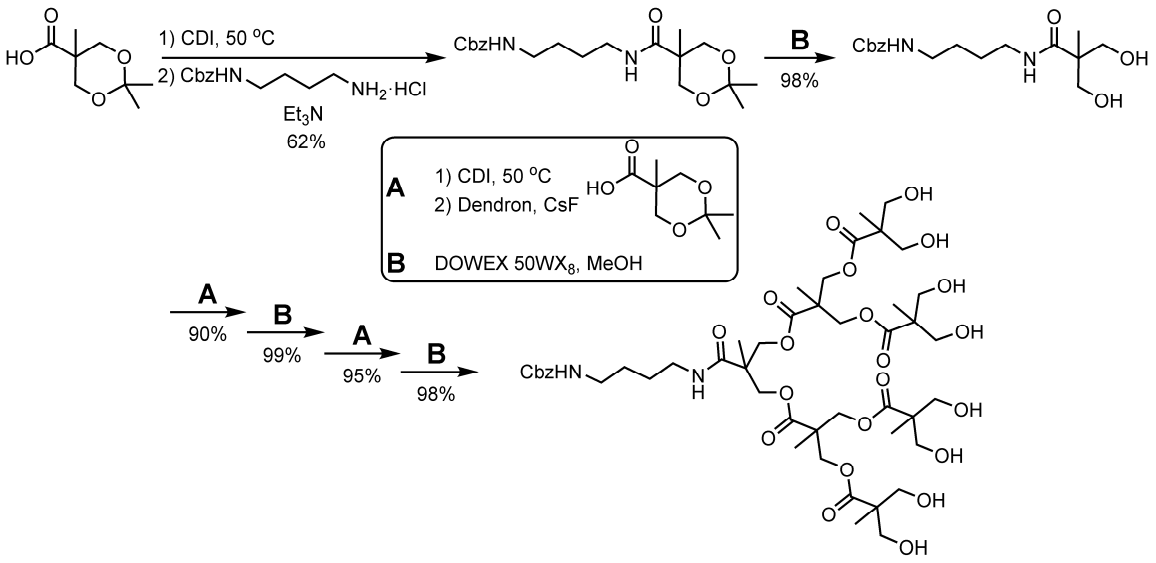

Scheme 5.2. Synthesis of CBz-G3-$(OH)_8$

CDI was used to activate acetonide-protected bis-MPA to the acyl imidazole, and this was then amidated with mono-Cbz butanediamine hydrochloride to give the Cbz-G1-(acet) dendron. The resulting acetonides were then deprotected using DOWEX 50WX2 in methanol to liberate the hydroxyl groups. The growth and deprotection steps were repeated up to the third generation, resulting in the CBz-G3-$(OH)_8$ dendron.

The Cbz-G3-$(OH)_8$ dendron was then activated with nitrophenyl chloroformate and substituted with *N*,*N*-dimethylaminopropylamine to give an intermediate that was suitable for preparing both sulfobetaine and carboxybetaine dendrons (Scheme 5.3). This tertiary amine periphery dendron was quaternized with either 1,3-propanesultone in THF (for the sulfobetaine) or with benzyl bromoacetate in acetonitrile (for the carboxybetaine). Both of these were then deprotected via hydrogenolysis with $Pd(OH)_2/C$ and H_2 gas. The core was then amidated with DBCO-NHS in a solvent of 1:1 phosphate buffer:THF, and the final DBCO-core dendron was isolated by size exclusion chromatography (Scheme 5.4)

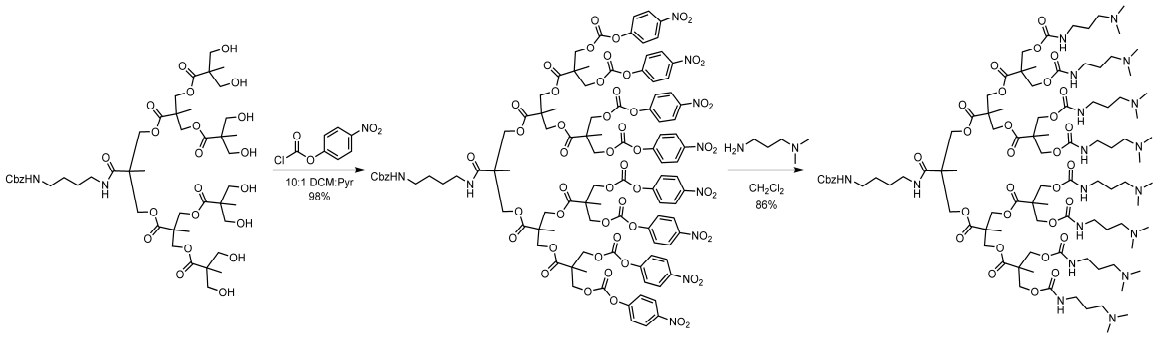

Scheme 5.3. Synthesis of Cbz-G3-$(amine)_8$ dendron

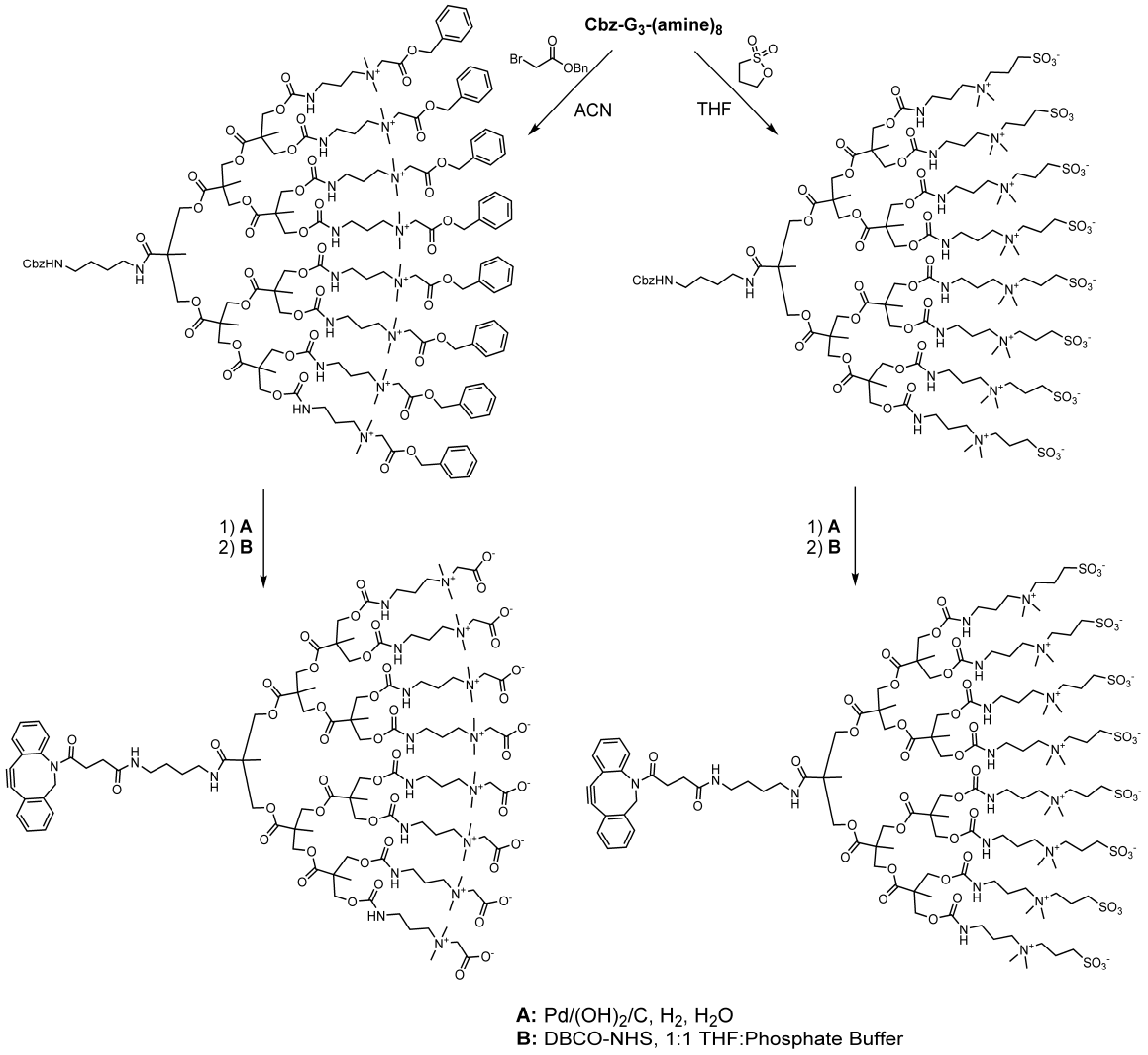

Scheme 5.4. Synthesis of dendrons with carboxybetaine and sulfobetaine groups at the periphery

With both an "inner" dendron functionalized with a DPA ligand, and the "outer" sulfobetaine dendron, preparation of the sixth generation DPA core dendrons was performed by simply mixing the inner and outer dendrons in 1:1 THF:water and letting this react overnight at room temperature, as seen in Scheme 5.5.

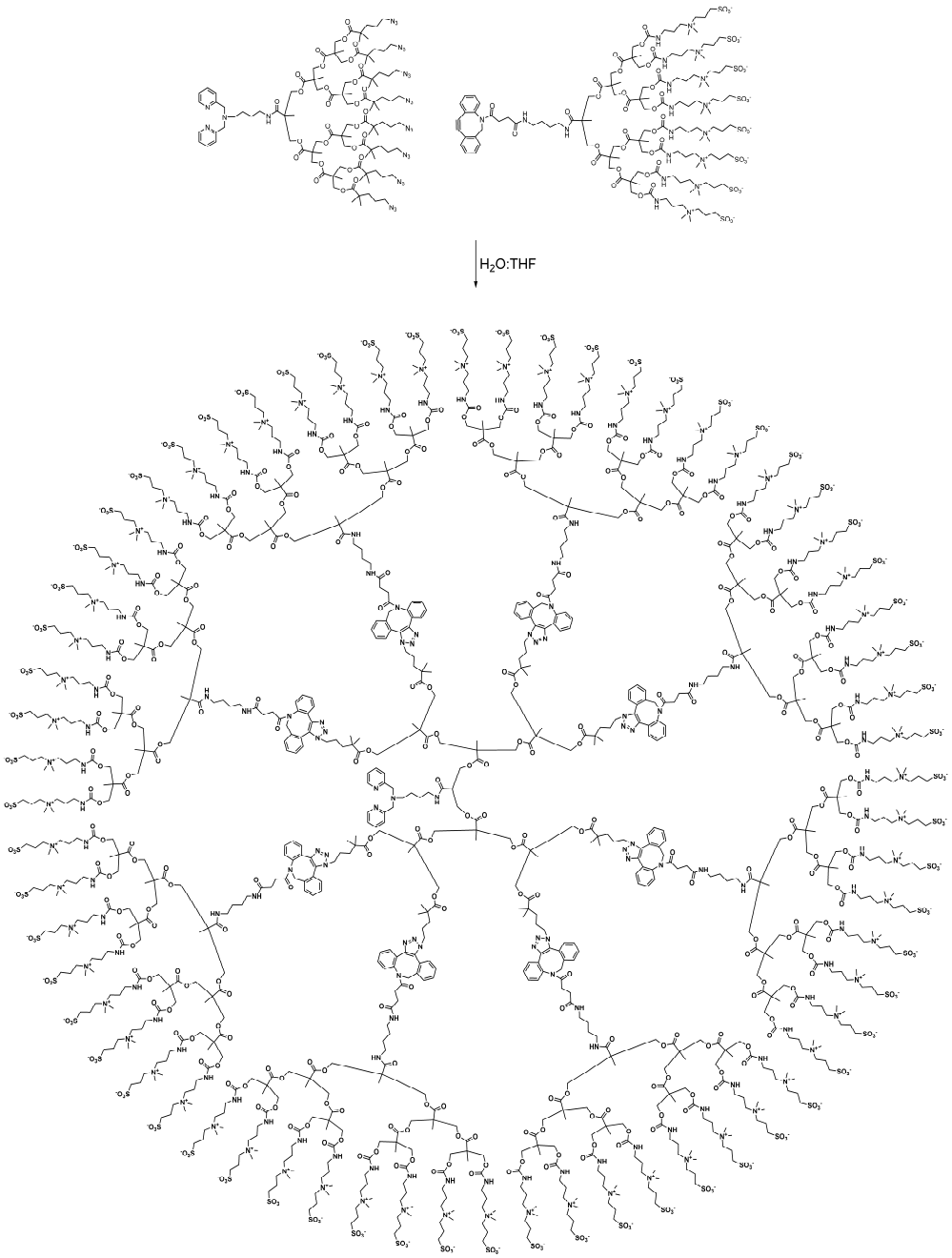

Scheme 5.5. Synthesis of DPA-G6-(sulfobetaine)$_{64}$ dendron

Dynamic light scattering was used to characterize the hydrodynamic diameter of the resulting clicked dendron, and it was found to have a hydrodynamic diameter of 6.2 nm, which is above the renal clearance of 5 nm.

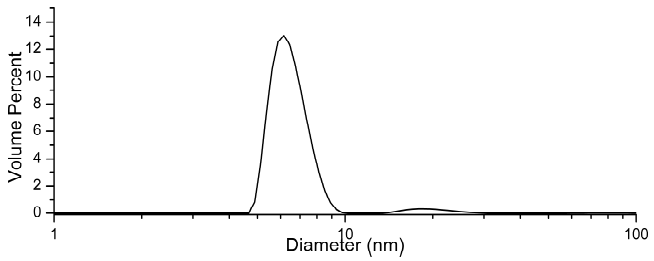

Figure 5.1 Volume-Average hydrodynamic plot of DPA-G6-(sulfobetaine)$_{64}$

The zwitterionic dendrons exhibited a small amount of aggregation in solution, though most of the material is molecularly dispersed. The zeta potential was assessed by electrophoretic mobility measurements and was found to be -3.53 mV. With two dendrons with sufficient size for extended circulation and suitable zeta potential, we proceeded with radiolabeling.

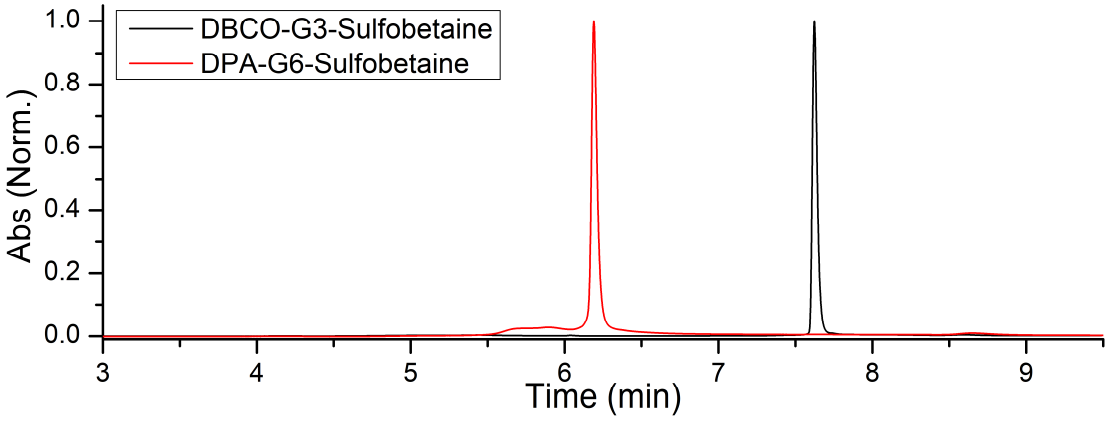

Figure 5.2. SEC Chromatograms of the sulfobetaine dendrons before and after clicking

Radiolabeling of the DPA-G6-(sulfobetaine)$_{64}$ was attempted using [^{99m}Tc(CO)$_3$(H$_2$O)$_3$]$^+$ that was prepared from the reduction of sodium pertechnetate (Na^{99m}TcO$_4$) according to modified procedures based on the work of Alberto and co-workers.[39–41] Initial attempts were made using the same conditions as had been done in our previous work, by labeling with [^{99m}Tc(CO)$_3$(H$_2$O)$_3$]$^+$ at 110 °C for 4 minutes at a pH of ~7. This was found to severely degrade the dendrimers, with no macromolecules being detected by SEC with either UV or γ detection. Since the labeling conditions appeared too harsh, the temperature was lowered first to 90 °C, then to 80 °C, and finally to 60 °C. At these reduced temperatures, labeling times were varied from 4 minutes up to 15 minutes, though neither changing temperature or labeling time resulted in labeling of the DPA-G6-(sulfobetaine)$_{64}$. Reducing temperature did prevent the complete decomposition of the dendrons, and at both 60 °C and 80 °C, a peak was visible in the UV chromatogram that had a very similar elution time to the DBCO-G3-(sulfobetaine)$_8$ dendron, though nothing (not even free [^{99m}Tc(CO)$_3$(H$_2$O)$_3$]$^+$) was visible in the γ chromatogram. Using the pancake meter, it was found that the first ~2-3 cm of the column had retained the majority of the injected activity, and so we postulate that the labeling of the DPA ligand occurs, though the resulting [^{99m}Tc(CO)$_3$DPA-G6-(sulfobetaine)$_{64}$]$^+$ is insoluble in water and thus is retained at the head of the SEC column. Since no methodology was found that would allow for the labeling of the dendron without decomposition, the project was discontinued.

The inability to radiolabel the DPA-G6-(sulfobetaine)$_{64}$ was surprising, considering the comparatively facile labeling that was performed on the PEGylated dendron in Chapter 2. I suspect that there are several distinct factors that prevented labeling of the zwitterionic

dendron. First, the $[^{99m}Tc(CO)_3(H_2O)_3]^+$ may interact with the sulfobetaine periphery, with coulombic interactions between the positively charged ^{99m}Tc complex and the negatively charged sulfonate groups at the periphery. This may be especially significant due to the steric congestion at the periphery of the high generation dendrons, which makes access to the core of the dendron particularly challenging. Depending on the strength of this interaction it could prevent the access of the $[^{99m}Tc(CO)_3(H_2O)_3]^+$ to the core of the dendron, and thus labeling could only occur once the dendron had been decomposed. This does not however explain the ease with which the decomposition occurred.

Based on the SEC results, it appears as though the dendron decomposes into fragments which are of nearly the same size as the "outer" DBCO-G3-(sulfobetaine)$_8$ dendron that was used to construct the DPA-G6-(sulfobetaine)$_{64}$. This is suggestive of a decomposition mechanism which relies on cleavage of a bond in the linker between the "inner" and "outer" dendrons. The conditions used (temperature of up to 110 °C, pH between 5 and 7 for up to 15 min) should not be capable of hydrolyzing the amide bonds which attach the DBCO to the rest of the outer dendron, nor should this be capable of cleaving the triazole ring or the rest of the DBCO moiety. The potential weakest bond of the linker is the ester which is used to attach the azide to the inner dendron. Despite testing of this ester for stability at pH of 4, 7, and 10 and finding it stable for at least 1 month at room temperature (data not shown), this would seem to be the functional group which would be most prone to decomposed under the reaction conditions to give degradation products the same size as the DBCO-G3-(sulfobetaine)$_8$. It is possible that the buffer in which the $^{99m}TcO_4^-$ is reduced has a unique synergistic effect which allows for facile

hydrolysis of this ester. Other possibilities such as radiological degradation from the ^{99m}Tc, while possible, again seem unlikely as the functional groups in the linker (SPAAC moieties, esters and amides) have been used in ^{99m}Tc labeled compounds without issue.[42] Radiolytic degradation of the sulfobetaine periphery may be possible due to a radical mediated Hoffmann elimination of the quaternary amines, though this degradation would not give fragments the same size as DBCO-G3-(sulfobetaine)$_8$.

Overall, the synthesis of bis-MPA dendrons with a zwitterionic periphery proved very challenging. Divergent methods were also attempted, but high conversion of the peripheral alcohols was never achieved using the divergent approach. The use of the convergent click methodology presented in Chapter 3 proved effective for the synthesis, though the radiolabeling challenges ultimately were insurmountable.

5.4 Experimental

All chemicals were purchased from either Sigma-Aldrich or Chem-Impex and used without further purification. ^{1}H NMR spectroscopy was performed on a Bruker Avance AV600 or AV700 spectrometer equipped with a cryoprobe, at 600 MHz and 700 MHz, respectively. ^{13}C NMR spectroscopy was performed on a Bruker Avance AV700 at 176 MHz. Residual non-deuterated solvent signals were used as internal chemical shift references for both ^{1}H and ^{13}C spectra. All chemical shifts are reported in ppm. MALDI mass spectra were collected on a Bruker UltraFlextreme spectrometer in positive ion mode using dithranol or dihydroxybenzoic acid as matrix. Electrospray MS was performed using a Micromass Quattro triple quadrupole instrument in positive mode. Exact masses were collected on either an Agilent 6210 TOF or a Bruker Maxis II Q-TOF. Flash chromatography was

performed using an AnaLogix Intelliflash 280 automated flash chromatography system, equipped with a variable wavelength (200-320 nm) UV detector. Empty Biotage SNAP columns packed with Silicycle R60 20-45 μm silica gel were used as chromatography media. Analytical size exclusion chromatography was performed using a Waters 2695 separations module equipped with a 2487 dual wavelength UV-Vis detector, using a 7.5 × 300 mm Agilent PL Aquagel-OH 20 column at a flow rate of 0.8 mL per minute using 1X PBS as eluent. Size exclusion chromatography for ^{99m}Tc labeled compounds was performed using a Waters 1525 binary solvent pump using a waters 2998 photodiode array detector and a Bio-Rad IN/US gamma detector using a 7.5 × 300 mm Agilent PL Aquagel-OH 20 column at a flow rate of 1 mL per minute deionized water as eluent.

Caution: ^{99m}Tc is radioactive and should only be handled in an appropriately licensed and equipped laboratory

COOH-G3-(OH)$_8$

BnO-G3-(OH)$_8$ (0.201 g. 0.218 mmol) was dissolved in 10 mL of methanol. To this, Pd(OH)$_2$/C (40 mg, 20 wt%) was added, and the reaction was vigorously stirred with a magnetic stirrer. The flask was purged and backfilled with H_2 gas three times and left to stir vigorously for 3 h. The reaction mixture was then filtered through a 0.22 um Teflon syringe filter, and solvent was removed by rotary evaporation. The resulting oil was dried *in vacuo* overnight to give the product as a white foam (177 mg, 99%)

^{1}H NMR (600 MHz; MeOD): δ 4.32-4.25 (m, 12H), 3.67 (dd, J = 10.9, 3.2, 8H), 3.60 (d, J = 10.9, 8H), 1.30 (s, 9H), 1.15 (s, 12H)

DPA-G3-(OH)$_8$

COOH-G3-(OH)$_8$ (100 mg, 0.120 mmol) was dissolved in 1 mL of 1:1 MeOH:iPrOH. To this, PyBOP (94 mg, 0.181 mmol) and N^1,N^1-Bis(pyridin-2-ylmethyl)butane-1,4-diamine (46 mg, 169 mmol) were added, then Et_3N (50 uL, 0.361 mmol). This was stirred overnight, at which point it had turned a pale brown colour. Solvent was removed by rotary evaporation and the crude reaction mixture was redissolved in 2 mL of water and filtered through a pipette filter and loaded directly onto a 10-gram C18 reversed phase Biotage Snap column equilibrated in 2% acetonitrile in 0.1% TFA: H2O solution. The product was purified by gradient elution from 2% to 35% acetonitrile over 20 column volumes, and the fractions containing product were pooled and solvent was removed by rotary evaporation. Residual TFA was removed by co-distillation with acetonitrile using 3 × 10 mL aliquots. The resulting oil was dried *in vacuo* overnight to give a slightly yellow oil. (109 mg, 84%)

^{1}H NMR (600 MHz; MeOD): δ 8.67 (d, J = 4.9, 2H), 7.92 (td, J = 7.7, 1.4, 2H), 7.52 (d, J = 7.8, 2H), 7.47 (dd, J = 7.2, 5.2, 2H), 4.62 (s, 4H), 4.29-4.21 (m, 12H), 3.67 (dd, J = 10.9, 3.0, 8H), 3.58 (d, J = 10.8, 8H), 3.36 (t, J = 8.0, 2H), 3.20 (t, J = 7.0, 2H), 1.84 (dt, J = 15.2, 7.7, 2H), 1.58 (quintet, J = 7.4, 2H), 1.29 (d, J = 10.7, 10H), 1.14 (d, J = 4.4, 12H)

^{13}C NMR (176 MHz; MeOD): δ 176.0, 174.7, 173.7, 151.8, 150.4, 139.5, 125.55, 125.42, 68.2, 66.3, 65.9, 58.6, 56.1, 51.9, 48.0, 47.7, 39.9, 27.7, 22.8, 18.24, 18.08, 17.3

DPA-G3-(N_3)$_8$

1,1'-carbonyldiimidazole (72 mg, 0.443 mmol) was added to 0.5 mL of EtOAc, then heated to 50 °C. To this, 2,2-dimethyl-5-azidovaleric acid (79 mg, 0.454 mmol) was added and

the reaction mixture was stirred for 1 hour. DPA-G3-$(OH)_8$ (20 mg, 0.018 mmol) was then added, along with cesium fluoride (8 mg, 0.055 mmol) and this was stirred overnight. The reaction mixture was then quenched with 0.1 mL of water for 1 hour, then solvent was removed by rotary evaporation and the crude material was redissolved in 0.5 mL of DMSO and loaded directly onto a 10 gram C18 reversed phase Biotage Snap column equilibrated in 5% acetonitrile in 0.1% TFA:H2O solution. The product was purified by gradient elution from 5% to 100% acetonitrile over 20 column volumes, and the fractions containing product were pooled and solvent was removed by rotary evaporation. Residual TFA was removed by co-distillation with acetonitrile using 3 × 10 mL aliquots. The resulting oil was dried *in vacuo* overnight to give a slightly yellow oil (28 mg, 65%)

^{1}H NMR (600 MHz; $CDCl_3$): δ 8.55 (d, J = 4.5, 2H), 7.68 (td, J = 7.7, 1.8, 2H), 7.52 (d, J = 7.7, 2H), 7.18 (dd, J = 6.6, 5.1, 2H), 6.54 (t, J = 5.8, 1H), 4.32-4.24 (m, 20H), 4.18-4.15 (m, 8H), 3.83 (s, 3H), 3.27 (q, J = 7.6, 16H), 3.23 (t, J = 6.9, 2H), 2.59 (t, J = 7.2, 2H), 1.60-1.58 (m, 18H), 1.55-1.51 (m, 18H), 1.27 (s, 24H), 1.19 (s, 48H)

Outer Dendrons

Cbz-G1-(Acet)

1,1’ carbonyldiimidazole (500 mg, 3.077 mmol) was added to 5 mL of EtOAc at 50 °C, forming a white suspension. To this, acetonide protected bis-MPA (0.535 g, 3.068 mmol) was added, and the reaction mixture was stirred for 1 hour. Benzyl *N*-(4-aminobutyl)carbamate hydrochloride (0.717 g, 2.769 mmol) was then added, along with Et_3N (1.287 mL, 9.231 mmol) and the reaction mixture was stirred for 2 hours, at which

point it was quenched by the addition of 0.5 mL of water for 1 hour. The reaction mixture was then diluted with 30 mL of EtOAc and extracted with 3 × 25 mL Na_2CO_3, 3 × 25 mL 1 M H_3PO_4, 1 × 50 mL brine, dried with $MgSO_4$, filtered, and then solvent was removed by rotary evaporation. The crude material was then purified by flash purification using a 25-gram Biotage Snap column using a gradient from 15% to 50% acetone in hexanes over 20 column volumes, with UV monitoring at 205 nm. The fractions containing product were pooled and solvent was removed by rotary evaporation. The product was then dried *in vacuo* overnight to give a clear, colourless oil (722 mg, 62%).

^{1}H NMR (600 MHz; CDCl3): δ 7.35 (d, J = 4.4, 4H), 7.30 (dq, J = 8.7, 4.3, 1H), 7.10 (s, 1H), 5.08 (s, 2H), 4.84 (d, J = 156.8, 1H), 3.89 (d, J = 12.3, 2H), 3.75 (dd, J = 11.3, 1.2, 2H), 3.32 (d, J = 5.7, 2H), 3.22 (d, J = 5.7, 2H), 1.57 (s, 4H), 1.46 (s, 3H), 1.40 (s, 3H), 0.99 (s, 3H)

^{13}C NMR (176 MHz; CDCl3): δ 176.7, 175.1, 156.75, 156.56, 136.75, 136.63, 128.6, 128.2, 98.6, 68.3, 67.3, 66.81, 66.70, 47.7, 40.8, 40.2, 39.1, 38.8, 31.1, 29.1, 27.37, 27.26, 27.07, 26.5, 18.5, 18.1, 17.9

Cbz-G1-(OH)$_2$

Cbz-G1-(acet) (0.700 g, 1.85 mmol) was dissolved in 70 mL of MeOH, to which 4 scoops of DOWEX beads was added. This was stirred at room temperature for 3 hours, at which point the reaction mixture was filtered through a glass frit. Solvent was removed by rotary evaporation, and the product was then dried *in vacuo* to give the product as a clear, colourless oil (613 mg, 98%).

^{1}H NMR (600 MHz; MeOD): δ 7.34-7.33 (m, 4H), 7.30-7.27 (m, 1H), 5.06 (s, 2H), 3.63 (q, J = 14.2, 4H), 3.21 (t, J = 5.8, 2H), 3.13 (t, J = 6.1, 2H), 1.52 (t, J = 3.2, 4H), 1.11 (s, 3H)

^{13}C NMR (176 MHz; MeOD): δ 178.1, 158.9, 138.5, 129.4, 128.92, 128.75, 67.3, 66.6, 41.4, 39.9, 28.2, 27.7, 17.7

Cbz-G2-(Acet)$_2$

1,1' carbonyldiimidazole (1.409 g, 8.688 mmol) was added to 5 mL of EtOAc at 50 °C, forming a white suspension. To this, acetonide protected bis-MPA (1.559g, 8.688 mmol) was added, and the reaction mixture was stirred for 1 hour. Cbz-G1-(OH)$_2$ (0.734 g, 2.172 mmol) was then added, along with CsF (0.165 g, 1.086 mmol) and the reaction mixture was stirred for 4 hours, at which point it was quenched by the addition of 0.5 mL of water for 1 hour. The reaction mixture was then diluted with 30 mL of EtOAc and extracted with 3 × 25 mL Na_2CO_3, 3 × 25 mL 1 M H_3PO_4, 1 × 50 mL brine, dried with $MgSO_4$, filtered, and then solvent was removed by rotary evaporation. The crude material was then purified by flash purification using a 25-gram Biotage Snap column using a gradient from 10% to 50% acetone in hexanes over 20 column volumes, with UV monitoring at 205 nm. The fractions containing product were pooled and solvent was removed by rotary evaporation. The product was then dried *in vacuo* overnight to give a clear, colourless oil (1.275 g, 90%).

^{1}H NMR (600 MHz; CDCl3): δ 7.35 (d, J = 4.2, 4H), 7.31 (dq, J = 8.8, 4.4, 1H), 6.53 (t, J = 4.9, 1H), 5.08 (s, 2H), 4.99 (t, J = 4.6, 1H), 4.35 (d, J = 11.2, 2H), 4.28 (d, J = 11.2, 2H),

4.15 (s, 4H), 3.64 (d, J = 11.9, 4H), 3.25 (q, J = 5.9, 2H), 3.20 (q, J = 5.9, 2H), 1.52 (t, J = 3.0, 4H), 1.41 (s, 6H), 1.35 (s, 6H), 1.26 (s, 3H), 1.09 (s, 6H)

^{13}C NMR (176 MHz; CDCl3): δ 174.00, 173.81, 172.5, 156.6, 136.7, 128.6, 128.28, 128.24, 98.4, 66.8, 66.53, 66.43, 66.40, 66.31, 66.27, 46.8, 42.4, 40.7, 39.4, 31.1, 27.3, 26.8, 26.5, 21.0, 18.4, 18.07, 17.93, 17.3

ESI-MS: Calc'd $[M+H]^+$ = 651.3487, Found $[M+H]^+$ 651.3490

Cbz-G2-(OH)$_4$

Cbz-G2-(acet)$_2$ (1.251 g, 1.92 mmol) was dissolved in 75 mL of MeOH, to which 4 scoops of DOWEX beads was added. This was stirred at room temperature for 3 hours, at which point the reaction mixture was filtered through a glass frit. Solvent was removed by rotary evaporation, and the product was then dried *in vacuo* to give the product as a clear, colourless oil (1.088 g, 99%).

^{1}H NMR (600 MHz; MeOD): δ 7.34-7.32 (m, 4H), 7.30-7.28 (m, 1H), 5.07 (d, J = 31.3, 2H), 4.25 (q, J = 9.3, 4H), 3.68 (d, J = 10.8, 4H), 3.59 (d, J = 10.9, 4H), 3.21 (t, J = 6.2, 2H), 3.13 (t, J = 6.4, 2H), 1.55-1.49 (m, 4H), 1.27 (s, 3H), 1.15 (s, 6H)

^{13}C NMR (176 MHz; MeOD): δ 176.0, 175.2, 158.9, 138.4, 129.4, 128.94, 128.77, 67.35, 67.21, 65.9, 51.9, 47.5, 41.4, 40.3, 28.3, 27.7, 18.3, 17.3

ESI-MS: Calc'd $[M+Na]^+$ = 593.2681, found $[M+Na]^+$ 593.2704

Cbz-G3-(Acet)$_4$

1,1’ carbonyldiimidazole (1.663 g, 10.254 mmol) was added to 5 mL of EtOAc at 50 °C, forming a white suspension. To this, acetonide protected bis-MPA (1.843g, 10.581 mmol) was added, and the reaction mixture was stirred for 1 hour. Cbz-G2-(OH)$_4$ (0.977 g, 1.712 mmol) was then added, along with CsF (0.248g, 1.633 mmol) and the reaction mixture was stirred overnight, at which point it was quenched by the addition of 0.5 mL of water for 1 hour. The reaction mixture was then diluted with 30 mL of EtOAc and extracted with 3 × 25 mL Na_2CO_3, 3 × 25 mL 1 M H_3PO_4, 1 × 50 mL brine, dried with $MgSO_4$, filtered, and then solvent was removed by rotary evaporation. The crude material was then purified by flash purification using a 25-gram Biotage Snap column using a gradient from 10% to 40% acetone in hexanes over 20 column volumes, with UV monitoring at 205 nm. The fractions containing product were pooled and solvent was removed by rotary evaporation. The product was then dried *in vacuo* overnight to give a clear, colourless oil (1.945 g, 95%).

^{1}H NMR (600 MHz; CDCl3): δ 7.34 (d, J = 4.3, 4H), 7.30 (dq, J = 8.4, 4.2, 1H), 6.31 (t, J = 5.5, 1H), 5.34 (t, J = 5.7, 1H), 5.08 (s, 2H), 4.35-4.27 (m, 8H), 4.22 (q, J = 10.8, 4H), 4.14 (d, J = 11.9, 8H), 3.60 (dd, J = 11.6, 1.9, 8H), 3.29 (q, J = 6.1, 2H), 3.21 (q, J = 6.0, 2H), 1.57-1.54 (m, 4H), 1.40 (s, 12H), 1.33 (s, 12H), 1.28 (s, 6H), 1.24 (s, 3H), 1.11 (d, J = 1.8, 12H)

^{13}C NMR (176 MHz; CDCl3): δ 173.88, 173.83, 172.0, 171.7, 156.7, 136.9, 128.6, 128.29, 128.17, 98.3, 67.4, 66.7, 66.13, 66.10, 65.2, 47.1, 46.5, 42.3, 40.7, 39.7, 27.5, 26.9, 25.77, 25.73, 21.79, 21.75, 18.6, 18.01, 17.84

ESI-MS: Calc'd [M+Na]+ = 1217.5827, found [M+Na]+ 1217.5879

Cbz-G3-$(OH)_8$

Cbz-G3-$(acet)_4$ (1.935 g, 1.619 mmol) was dissolved in 225 mL of MeOH, to which 4 scoops of DOWEX beads were added. This was stirred at room temperature for 3 hours, at which point the reaction mixture was filtered through a glass frit. Solvent was removed by rotary evaporation, and the product was then dried *in vacuo* to give the product as a clear, colourless oil (1.088 g, 99%).

^{1}H NMR (600 MHz; MeOD): δ 7.35-7.34 (m, 4H), 7.30-7.28 (m, 1H), 5.07 (s, 2H), 4.30-4.22 (m, 12H), 3.67 (ddd, J = 10.9, 2.2, 1.0, 8H), 3.59 (d, J = 10.8, 8H), 3.21 (t, J = 6.7, 2H), 3.15 (t, J = 6.4, 2H), 1.54-1.51 (m, 4H), 1.28 (s, 9H), 1.15 (s, 12H)

ESI-MS: Calc'd $[M+H]^+$ = 1035.4755, Found $[M+H]^+$ = 1035.4744

Cbz-G3-$(NO_2Ph)_8$

Cbz-G3-$(OH)_8$ (0.103 g, 0.99 mmol) was dissolved in 500 uL of pyridine, then diluted with 1 mL of DCM and cooled to 0 °C in an ice bath. Separately, *p*-nitrophenyl chloroformate (0.312 g, 1.540 mmol) was dissolved in 1 mL of DCM, and this was added in a single aliquot to the cooled reaction mixture. This was left to react at 0 °C for 4 hours, at which point MALDI-TOF MS indicated full conversion. The reaction was then diluted with 30 mL of DCM and extracted with 3 × 25 mL of 1 M H_3PO_4, 1 × 50 mL brine, dried with $MgSO_4$, filtered, and solvent was removed by rotary evaporation to give the crude product as a pale yellow oil. This was then purified using 300A pore size silica in a 10-gram Biotage Snap column equilibrated in dichloromethane. The product was eluted using 4 column

volumes of DCM, then 5 column volumes of EtOAc, with monitoring at 254 nm. The fractions containing product were pooled and solvent was removed by rotary evaporation and then dried *in vacuo* overnight to give the product as a white foam (0.230 g, quant)

^{1}H NMR (600 MHz; CDCl3): δ 8.25-8.22 (m, 16H), 7.38-7.29 (m, 21H), 6.21 (t, J = 5.0, 1H), 5.06 (s, 2H), 4.99 (t, J = 5.8, 1H), 4.49 (d, J = 11.0, 8H), 4.43 (d, J = 11.0, 8H), 4.37 (dd, J = 11.1, 8.7, 4H), 4.30 (dd, J = 11.2, 6.1, 4H), 4.21 (d, J = 11.1, 2H), 4.14 (s, 2H), 3.21 (d, J = 4.7, 2H), 3.15 (q, J = 6.1, 2H), 1.50-1.47 (m, 4H), 1.35 (s, 12H), 1.29 (s, 6H), 1.21 (d, J = 8.5, 3H)

^{13}C NMR (176 MHz; CDCl3): δ 171.6, 171.3, 156.8, 155.3, 152.2, 145.7, 136.5, 128.7, 128.4, 128.2, 125.5, 121.9, 69.3, 67.5, 66.8, 65.7, 60.5, 46.85, 46.78, 46.3, 40.5, 39.6, 27.7, 26.5, 21.2, 17.8, 14.3

MALDI-TOF MS: Calc'd $[M+Na]^+$ 2378.93, Found $[M+Na]^+$ 2381.11

Cbz-G3-(Amine)$_8$

Cbz-G3-(NO_2Ph)$_8$ (192 mg, 0.081 mmol) was dissolved in 2 ml of DCM, and dimethylaminopropylamine (0.328 ml, 2.608 mmol) and the reaction was stirred for 90 minutes, at which point MALDI indicated complete conversion. The reaction mixture was then diluted with 25 mL of DCM, then washed with 3 × 25 mL of Na_2CO_3, 1 × 50 mL brine, dried with $MgSO_4$, filtered, and solvent was removed by rotary evaporation then dried *in vacuo*, giving the product as a slightly yellow oil. (0.161 g, 96%)

^{1}H NMR (600 MHz; CDCl3): δ 7.33 (d, J = 4.1, 4H), 7.30 (dt, J = 8.6, 4.4, 1H), 7.00 (s, 1H), 5.95 (d, J = 47.2, 8H), 5.06 (s, 2H), 4.31-4.10 (m, 28H), 3.24 (q, J = 5.9, 2H), 3.18 (q,

J = 6.2, 17H), 2.30 (t, J = 6.9, 16H), 2.19 (s, 47H), 1.64 (quintet, J = 6.8, 16H), 1.56-1.50 (m, 4H), 1.27 (s, 3H), 1.25 (s, 7H), 1.21-1.15 (m, 12H)

^{13}C NMR (176 MHz; CDCl3): δ 173.14, 172.99, 172.2, 171.9, 156.9, 156.26, 156.08, 156.03, 136.9, 128.6, 128.20, 128.16, 67.2, 66.6, 66.0, 65.31, 65.14, 58.0, 57.7, 47.35, 47.31, 46.8, 46.5, 45.5, 41.1, 40.7, 40.1, 39.7, 29.8, 27.50, 27.30, 27.04, 26.91, 18.0, 17.75, 17.59

MALDI-TOF MS: Calc'd $[M+Na]^+$ 2082.17, Found $[M+Na]^+$ 2082.26

Cbz-G3-(Sulfobetaine)$_8$

Cbz-G3-(amine)$_8$ (0.160 g, 0.078 mmol) was dissolved in 3 mL of THF, and to this 1,3-propanesultone (0.068 mL, 0.77 mmol) was added and this was stirred vigorously. After 4 hours the reaction mixture had become cloudy and viscous, and after overnight reaction the reaction mixture was a cloudy very viscous solution. THF was removed under reduced pressure to give the crude material as a white powder, which was purified by SEC using 3 × 5 mL GE HiTrap desalting columns equilibrated in 20 mM phosphate buffer. The high molecular weight fractions were collected and were lyophilized without desalting to give the product as a fluffy white powder (173 mg, 73%)

^{1}H NMR (600 MHz; D2O): δ 7.47 (t, J = 7.2, 2H), 7.43 (t, J = 6.3, 3H), 5.12 (s, 2H), 4.35-4.20 (m, 28H), 3.48 (dt, J = 7.7, 4.2, 16H), 3.37 (dt, J = 7.8, 4.1, 15H), 3.23 (t, J = 6.2, 18H), 3.11 (s, 48H), 2.98 (t, J = 7.1, 16H), 2.22 (dt, J = 15.8, 7.8, 16H), 1.99 (dt, J = 15.6, 7.4, 16H), 1.57-1.52 (m, 4H), 1.30 (t, J = 35.0, 21H)

MALDI-TOF MS: Calc'd $[M+Na]^+$ 3060.6, Found $[M+Na]^+$ 3061.4

H_2N-G3-(Sulfobetaine)$_8$

Cbz-G3-(amine)$_8$ (0.050 g, 0.016 mmol) was dissolved in 3 mL of water, to which $Pd(OH)_2/C$ (10 mg) was added and the reaction mixture was purged and backfilled with H_2 three times, then stirred vigorously for 3 hours. The reaction mixture was then filtered through a 0.2 μm Teflon filtration membrane and lyophilized overnight to give the product as a fluffy white solid (38 mg, 79%)

^{1}H NMR (600 MHz; D2O): δ 4.34-4.21 (m, 28H), 3.50 (dt, J = 7.9, 4.2, 16H), 3.41-3.38 (m, 16H), 3.25 (t, J = 6.2, 18H), 3.14 (s, 47H), 3.05-3.03 (m, 2H), 2.99 (t, J = 7.1, 16H), 2.25-2.20 (m, 16H), 2.02 (dt, J = 15.0, 7.3, 15H), 1.71 (dt, J = 15.3, 7.7, 2H), 1.62 (quintet, J = 7.6, 2H), 1.31 (dd, J = 41.7, 27.1, 21H)

DBCO-G3-(Sulfobetaine)$_8$

H_2N-G3-(sulfobetaine)$_8$ (25 mg, 0.009 mmol) was dissolved in 1 mL of 0.1 M phosphate buffer at pH 8. Separately, DBCO-NHS (10 mg, 0.026 mmol) was dissolved in 1 mL of THF, and this was added to the dendron solution. The pH of the solution was then brought to ~8.5 by the dropwise addition of 1 M KOH, and let stir for 30 minutes, at which point the pH had dropped to ~7.5. The pH was again adjusted to ~8.5 by addition of 1 M KOH and stirred for a further 30 minutes, at which point the pH had stabilized. This was stirred for 3 hours, and then the THF was removed by rotary evaporation, giving a significant precipitate of excess DBCO-NHS. Mixture was centrifuged at 15 000 *g* for 5 minutes to sediment the solids, and the supernatant was collected and was purified by SEC using 3 × 5 mL GE HiTrap desalting columns equilibrated in 20 mM phosphate buffer. The high

molecular weight fractions were collected and were lyophilized without desalting to give the product as a fluffy white powder (23 mg, 85%)

^{1}H NMR (600 MHz; D2O): δ 7.62 (d, J = 7.6, 1H), 7.50 (dd, J = 7.4, 3.5, 1H), 7.47-7.45 (m, 2H), 7.41-7.34 (m, 3H), 7.29-7.27 (m, 1H), 5.11-5.07 (m, 1H), 5.04 (d, J = 14.5, 1H), 4.26-4.11 (m, 28H), 3.74 (d, J = 14.7, 1H), 3.62 (d, J = 8.0, 2H), 3.40 (dd, J = 9.8, 6.6, 16H), 3.28 (dt, J = 7.1, 3.9, 16H), 3.14 (s, 20H), 3.03 (s, 48H), 2.89 (t, J = 7.1, 16H), 2.77-2.75 (m, 1H), 2.49-2.45 (m, 1H), 2.15-2.11 (m, 18H), 1.91-1.89 (m, 16H), 1.37-1.33 (m, 2H), 1.28-1.14 (m, 24H)

DPA-G6-(sulfobetaine)$_{64}$

DPA-G3-$(N_3)_8$ (2.5 mg, 0.001 mmol) was dissolved in 500 uL of THF. Separately, DBCO-G3-(sulfobetaine)8 (31 mg, 0.010 mmol) was dissolved in 500 uL of deionized water, and this was transferred to the solution of DPA-G3-$(N_3)_8$. The reaction mixture was initially turbid, but after approximately 2 minutes of stirring the reaction mixture had clarified. This was left to stir overnight, at which point the THF was removed by rotary evaporation. The aqueous phase was then dialyzed with 12 kDa MWCO dialysis tubing against deionized water, and the resulting material was lyophilized to give the product as a fluffy white solid (27 mg, 90%)

^{1}H NMR (600 MHz; D2O): δ 8.41-8.34 (m, 2H), 7.58-7.19 (m, 75H), 6.95 (dt, J = 21.3, 11.4, 5H), 5.95-5.86 (m, 6H), 5.18-5.18 (m, 5H), 4.22 (d, J = 69.9, 1H), 3.74-3.59 (m, 17H), 3.49 (s, 128H), 3.37 (s, 128H), 3.22 (s, 164H), 3.12 (s, 1H), 2.97 (s, 130H), 2.83 (s,

37H), 2.22 (d, J = 0.6, 134H), 1.99 (s, 136H), 1.90 (s, 16H), 1.44 (s, 40H), 1.32-1.11 (m, 1H)

Cbz-G3-(benzyl)$_8$

Cbz-G3-(amine)$_8$ (0.202 g, 0.098 mmol) was dissolved in 1 mL of acetonitrile. To this, benzyl bromoacetate (0.246 mL, 1.553 mmol) was added, and the reaction mixture was heated to 60 °C, resulting in the formation of a fine white precipitate. After overnight heating, the reaction mixture was diluted with 5 mL of room temperature acetonitrile, then precipitated into ether at -78 °C. The ether layer was decanted and the precipitation was repeated three total times. The resulting oil was dried *in vacuo* overnight to give the product as a slightly yellow oil. (294 mg, 93%)

^{1}H NMR (600 MHz; MeOD): δ 7.90 (s, 1H), 7.42-7.37 (m, 45H), 7.06 (s, 2H), 5.35-5.23 (m, 16H), 5.05 (s, 2H), 4.91 (s, 3H), 4.55-4.49 (m, 16H), 4.22 (d, J = 58.4, 28H), 3.67 (s, 16H), 3.33 (s, 48H), 3.16 (d, J = 34.5, 20H), 1.99 (s, 16H), 1.53 (s, 4H), 1.34-1.23 (m, 21H)

H$_2$N-G3-(Carboxybetaine)$_8$

Cbz-G3-(benzyl)$_8$ (135 mg, 0.0415 mmol) was dissolved in 5 mL of methanol. To this, Pd(OH)2/C (27 mg, 20 wt% Pd) was added, and the reaction vessel was purged and backfilled with hydrogen three times. The reaction was then left to stir vigorously under a hydrogen atmosphere overnight. This was then taken up in a 10 mL syringe and filtered through a 0.22 micron PTFE syringe filter, and solvent was removed by rotary evaporation. The oil was then dried *in vacuo* overnight to give the product as a slightly yellow oil. (99mg, 99%)

^{1}H NMR (600 MHz; MeOD): δ 4.48 (s, 3H), 4.25 (q, J = 14.8, 28H), 4.13 (s, 16H), 3.63-3.60 (m, 16H), 3.32 (s, 8H), 3.27 (s, 32H), 3.17 (t, J = 6.2, 16H), 2.95 (t, J = 7.5, 2H), 1.98-1.94 (m, 16H), 1.67 (dt, J = 13.6, 7.5, 2H), 1.59 (dt, J = 14.1, 6.8, 2H), 1.31 (s, 3H), 1.26 (s, 6H), 1.19 (s, 12H)

DBCO-G3-(Carboxybetaine)$_8$

H_2N-G3-(Carboxybetaine)$_8$ (0.099 g, 0.0413 mmol) was dissolved in 1 mL of 0.1 M phosphate buffer at a pH of 7.4. Separately, DBCO-NHS (0.050 mg, 0.125 mmol) was dissolved in 1 mL of THF. The THF solution was added to the dendron solution and stirred vigorously. The pH of the reaction mixture was adjusted to 8 by the addition of Et_3N, and the reaction was left to stir overnight. The THF was then removed by rotary evaporation, resulting in the precipitation of a fine white solid. The aqueous phase was filtered through a 0.22-micron nylon syringe filter, and then desalted using 3 × 5 mL GE HiTrap desalting columns using water as eluent. The fractions containing high-molecular weight components were then lyophilized overnight to give the product as a fluffy white solid. (63 mg, 57%)

^{1}H NMR (600 MHz; D_2O): δ 7.70 (d, J = 7.5, 1H), 7.58 (q, J = 4.1, 1H), 7.56-7.52 (m, 3H), 7.47 (td, J = 7.5, 0.8, 1H), 7.45-7.42 (m, 1H), 7.37-7.35 (m, 1H), 5.12 (d, J = 14.3, 1H), 4.41-4.19 (m, 28H), 3.86-3.81 (m, 16H), 3.59-3.56 (m, 16H), 3.33-3.31 (m, 3H), 3.21 (q, J = 10.1, 60H), 2.99 (t, J = 6.7, 2H), 2.57-2.54 (m, 1H), 2.26-2.21 (m, 3H), 1.96 (t, J = 7.9, 16H), 1.44 (dt, J = 14.1, 7.1, 2H), 1.29 (dd, J = 49.2, 32.2, 21H)

5.5 References

[1] J. Yang, J. Kopeček, *J. Control. Release* **2014**, *190*, 288–303.

[2] R. Duncan, M. J. Vicent, *Adv. Drug Deliv. Rev.* **2013**, *65*, 60–70.

[3] R. Duncan, *Nat. Rev. Drug Discov.* **2003**, *2*, 347–360.

[4] A. Abuchowski, T. van Es, N. C. Palczuk, F. F. Davis, *J. Biol. Chem.* **1977**, *252*, 3579–3581.

[5] A. Abuchowski, J. R. McCoy, N. C. Palczuk, T. van Es, F. F. Davis, *J. Biol. Chem.* **1977**, *252*, 3582–3586.

[6] Y. Hu, Y. Hou, H. Wang, H. Lu, *Bioconjug. Chem.* **2018**, *29*, 2232–2238.

[7] R. Konradi, B. Pidhatika, A. Mühlebach, M. Textor, *Langmuir* **2008**, *24*, 613–616.

[8] A. Mero, Z. Fang, G. Pasut, F. M. Veronese, T. X. Viegas, *J. Control. Release* **2012**, *159*, 353–361.

[9] J. Tong, R. Luxenhofer, X. Yi, R. Jordan, A. V Kabanov, *Mol. Pharm.* **2010**, *7*, 984–992.

[10] J. Kopeček, P. Kopečková, T. Minko, Z. R. Lu, *Eur. J. Pharm. Biopharm.* **2000**, *50*, 61–81.

[11] Y. Liu, J. Lee, K. M. Mansfield, J. H. Ko, S. Sallam, C. Wesdemiotis, H. D. Maynard, *Bioconjug. Chem.* **2017**, *28*, 836–845.

[12] K. M. Mansfield, H. D. Maynard, *ACS Macro Lett.* **2018**, *7*, 324–329.

[13] Y. Kamisaki, H. Wada, T. Yagura, A. Matsushima, Y. Inada, *J. Pharmacol. Exp. Ther.* **1981**, *216*, 410–414.

[14] J.-F. Zhang, L.-Y. Shi, D.-Z. Wei, *Biotechnol. Lett.* **2004**, *26*, 753–756.

[15] D. Santi, E. Schneider, R. Reid, L. Robinson, G. Ashley, *Proc. Natl. Acad. Sci.* **2012**, *109*, 6211–6216.

[16] G. Molineux, *Anticancer. Drugs* **2003**, *14*, 259–264.

[17] P. Bailon, A. Palleroni, C. A. Schaffer, C. L. Spence, W. J. Fung, J. E. Porter, G. K. Ehrlich, W. Pan, Z. X. Xu, M. W. Modi, et al., *Bioconjug. Chem.* **2001**, *12*, 195–202.

[18] H. Schellekens, W. E. Hennink, V. Brinks, *Pharm. Res.* **2013**, *30*, 1729–1734.

[19] F. Zhang, M. Liu, H. Wan, *Biol. Pharm. Bull.* **2014**, *37*, 335–339.

[20] B. Li, Z. Yuan, H. C. Hung, J. Ma, P. Jain, C. Tsao, J. Xie, P. Zhang, X. Lin, K. Wu, et al., *Angew. Chemie - Int. Ed.* **2018**, *57*, 13873–13876.

[21] A. Abuchowski, J. R. Mccoy, N. C. Palczuk, *J. Biol. Chem.* **1976**, *252*, 3582–3586.

[22] Q. Yang, S. K. Lai, *Wiley Interdiscip. Rev. Nanomedicine Nanobiotechnology* **2015**, *7*, 655–677.

[23] W. K. Cho, B. Kong, I. S. Choi, *Langmuir* **2007**, *23*, 5678–5682.

[24] P. Zhang, P. Jain, C. Tsao, Z. Yuan, W. Li, B. Li, K. Wu, H. C. Hung, X. Lin, S. Jiang, *Angew. Chemie - Int. Ed.* **2018**, *57*, 7743–7747.

[25] Z. Cao, S. Jiang, *Nano Today* **2012**, *7*, 404–413.

[26] J. M. J. Fréchet, *Science* **1994**, *263*, 1710–1715.

[27] C. C. Lee, J. A. MacKay, J. M. J. Fréchet, F. C. Szoka, *Nat. Biotechnol.* **2005**, *23*, 1517–1526.

[28] M. E. Fox, F. C. Szoka, J. M. J. Fréchet, *Acc. Chem. Res.* **2009**, *42*, 1141–1151.

[29] A. L. Martin, B. Li, E. R. Gillies, *J. Am. Chem. Soc.* **2009**, *131*, 734–741.

[30] H. Ihre, A. Hult, J. M. J. Fréchet, I. Gitsov, *Macromolecules* **1998**, *31*, 4061–4068.

[31] O. L. Padilla De Jesús, H. R. Ihre, L. Gagne, J. M. J. Fréchet, F. C. Szoka, *Bioconjug. Chem.* **2002**, *13*, 453–461.

[32] H. Ihre, O. L. Padilla De Jesús, J. M. J. Fréchet, *J. Am. Chem. Soc.* **2001**, *123*, 5908–5917.

[33] S. García-Gallego, D. Hult, J. V Olsson, M. Malkoch, *Angew. Chemie - Int. Ed.* **2015**, *54*, 2416–2419.

[34] B. Fadeel, M. I. Montañez, M. Malkoch, A. Nyström, A. Kunzmann, N. Feliu, M. V Walter, A. Hult, *Biomaterials* **2012**, *33*, 1970–1981.

[35] M. Yu, J. Zheng, *ACS Nano* **2015**, *9*, 6655–6674.

[36] M. C. Parrott, S. R. Benhabbour, C. Saab, J. A. Lemon, S. Parker, J. F. Valliant, A. Adronov, *J. Am. Chem. Soc* **2009**, *131*, 2906–2916.

[37] S. A. McNelles, S. D. Knight, N. Janzen, J. F. Valliant, A. Adronov, *Biomacromolecules* **2015**, *16*, 3033–3041.

[38] S. A. McNelles, A. Adronov, *Macromolecules* **2017**, *50*, 7993–8001.

[39] R. Alberto, R. Schibli, A. Egli, A. P. Schubiger, U. Abram, T. A. Kaden, *J. Am. Chem. Soc.* **1998**, *120*, 7987–7988.

[40] R. Alberto, R. Schibli, A. P. Schubiger, U. Abram, H. J. Pietzsch, B. Johannsen, *J. Am. Chem. Soc.* **1999**, *121*, 6076–6077.

[41] R. Alberto, K. Ortner, N. Wheatley, R. Schibli, a. P. Schubiger, *J. Am. Chem. Soc.* **2001**, *123*, 3135–3136.

[42] N. A. Lodhi, J. Y. Park, K. Kim, Y. J. Kim, J. H. Shin, Y. S. Lee, H. J. Im, J. M. Jeong, M. Khalid, G. J. Cheon, et al., *Mol. Pharm.* **2019**, *16*, 1586–1595.

6 Conclusions & Future Work

6.1 Conclusions

This thesis focused on the preparation of dendrimers for imaging, as well as the development of dendrimers for conjugation to biomolecules.

PEGylated dendrimers as EPR effect imaging agents were investigated in chapter 2. The synthesis of bis-MPA dendrimers up to the fifth generation was detailed, as well as their functionalization with alkenes to allow for thiol-ene conjugation. Separately, a series of PEG thiol reagents with molecular weights from 150 Da to 750 Da with were prepared, and these were coupled to the dendron using thiol-ene chemistry. The resulting PEGylated dendrimers had molecular weights from 10 kDa to 18 kDa. Only the highest molecular weight PEGylated dendrimer was found to be molecularly dispersed by DLS, and this was radiolabeled with $[^{99m}Tc(CO)_3]^+$. The resulting labeled dendron was then used in SPECT imaging studies with healthy rats, which indicated that their circulation time was greater than 12 hours. Subsequent SPECT studies were then performed using tumour model mice using H520 xenograft tumours, and the labeled dendrimer was imaged at the tumour site after 6 hours, with the remainder of the activity primarily in the blood and the bladder.

In chapter 3, the SPAAC reaction was investigated as a functional handle to allow for the facile preparation of high-generation dendrons using a common “inner” dendron and an easily derivatized “outer” dendron. The “outer” dendrons were synthesized from a common intermediate dendron bearing a strained cyclooctyne at the core with acyl imidazole groups at the periphery that are readily substituted by primary amines. The final click reaction

between the inner azide periphery dendron and the outer strained-cyclooctyne core dendrons were remarkably quickly and could be prepared in minutes by simply dissolving both components in a volatile solvent such as dichloromethane, then gentle removal of the solvent by rotary evaporation. Overall, this approach enabled the facile preparation of high generation dendrons with peripheral functionalization, including challenging groups such as uniform molecular weight PEG grafts.

In chapter 4, the use of bis-MPA dendrimers for preparation of polymer-protein conjugates was explored. A model protein, α-chymotrypsin, was quantitatively modified with azide groups at each lysine. To couple to this, a series of bis-MPA dendrons from generation 2 through 8 with a strained cyclooctyne at the core were prepared. Conjugation of the dendrons to α-chymotrypsin was accomplished using SPAAC, and the resulting conjugates were found to be fully converted at all generations. All the conjugates were then investigated for their activity against a small molecule (BTpNA), a small flexible protein (milk casein), and a large, rigid protein (bovine serum albumin). All conjugates exhibited essentially unchanged activity against BTpNA and casein, though the highest generation conjugates (G7 and G8) were found to dramatically lower activity against BSA. This was then further confirmed using α-antichymotrypsin, a ~65 kDa protein which deactivates α-chymotrypsin. While native α-chymotrypsin was completely inactivated by the inhibitor, the dendrimers which exhibited sieving retained the majority of their activity, indicating that the active site of the enzyme was significantly shielded from proteins of this size. As a final confirmation that the size and geometry are the key parameters required for molecular sieving behavior, we prepared a PEGylated chymotrypsin using linear

$mPEG_{5500}$, and a third generation dendrimer with 8 smaller PEG chains. It was found that the linear $mPEG_{5500}$ did not exhibit any sieving effect, though the dendronized PEG had a sieving ratio which was approximately the same as the G7-OH dendron. The data from this study indicate that polymer architecture plays a key role in the function of polymer-protein conjugates.

6.2 Future Work

The conjugation of dendrimers to enzymes or other biomolecules as polymeric coatings has seen little attention in the literature, likely due to the very large size required before interesting properties become apparent. Because of this, there is a wide range of potential directions for future work.

Perhaps the most critical work in this direction would be elucidating the mechanism of sieving more thoroughly. While our current understanding is largely based on geometric intuition based on a relatively crude model, there are several other key factors that remain unknown. It is currently thought that PEGylated biomolecules lose activity through several mechanisms including: the polymer non-specifically associating to the active site, formation of a PEG layer into which substrates preferentially diffuse, and simple steric shielding. Since the high generation dendrimers do not exhibit these drawbacks, investigation into binding of the dendron to active sites on enzymes and ability of small molecules to be entrapped in the dendron would be a reasonable next step.

Since the goal of preparing polymer-protein conjugates is to enable new therapeutics, the preparation of dendrons with appropriate periphery functionality to allow for *in vivo* use (such as PEGylation or zwitterionic groups) also appears to be a logical next step. While

this could be initially done with the same model protein as the current studies, future work could extend to explore if the sieving effect is observed in more therapeutically relevant enzymes such as asparaginase and uricase, which are currently used to treat ALL and gout, respectively.